DOCTORAL THESIS

Materiales Biodegradables Mono y Multicapa con Capacidad Antimicrobiana Basados en Bioeconomia Circular de Interés en Envases Alimentarios

Biodegradable Mono and Multilayer Materials with Antimicrobial Capacity Based on Circular Bioeconomy of Application Interest in Food Packaging

Presented by:
Kelly Johana Figueroa López

Supervised by:
José María Lagarón Cabello
Sergio Torres Giner
Luis Cabedo Mas

Instituto de Agroquímica y Tecnología de Alimentos
Grupo de Nuevos Materiales y Nanotecnología para Aplicaciones Alimentarias

Universidad Politécnica de Valencia (UPV)
Doctorado en Ciencia, Tecnología y Gestión Alimentaria

Valencia (Spain) – Abril de 2021

Dr. José María Lagarón Cabello, Investigador Científico del Consejo Superior de Investigaciones Científicas (CSIC) en el Instituto de Agroquímica y Tecnología de Alimentos (IATA), Dr. Sergio Torres Giner, Investigador Ramón y Cajal en la Universidad Politécnica de Valencia (UPV) y Dr. Luis Cabedo Mas, Profesor titular de la Universidad Jaume I (UJI)

CERTIFICAN

Que la presente memoria titulada "*Materiales Biodegradables Mono y Multicapa con Capacidad Antimicrobiana Basados en Bioeconomia Circular de Interés en Envases Alimentarios*" constituye la tesis doctoral de Kelly Johana Figueroa López y reúne las condiciones adecuadas para su presentación. Asimismo, certifican haber dirigido y supervisado tanto los distintos aspectos del trabajo como la redacción.

Y para que así conste a los efectos oportunos, firmamos la presente en valencia a enero de 2021.

Fdo. José María Lagarón Cabello

Fdo. Sergio Torres Giner

Fdo. Luis Cabedo Mas

A mi Abuela, mi madre y mi hermano.
A ustedes va dedicado este gran logro
académico, porque son mi razón de ser y mi
fortaleza, donde encuentro motivación e
inspiración para alcanzar cada sueño y
objetivo que me propongo.

AGRADECIMIENTOS

Primero que todo agradezco al Universo y la Naturaleza por el privilegio de estar en este planeta y tener la capacidad y el entendimiento para apreciar y disfrutar cada una de sus maravillas y manifestaciones.

A todas las personas que han estado involucradas directamente con la realización de esta tesis doctoral. Así mismo, a todas las personas que indirectamente han contribuido, compartiendo parte de su tiempo conmigo, cargado de momentos alegres, divertidos, ocurrentes, emotivos y con un toque de "drama latino".

A mis directores de tesis, Jose María Lagarón, por la acogida en el grupo de investigación de Nuevos Materiales y Nanotecnología para Aplicaciones Alimentarias (IATA-CSIC), por la dirección, acompañamiento y apoyo en la realización del trabajo de investigación. A Sergio Torres Giner, por su dedicación, compromiso, apoyo y entrega en cada uno de los aspectos del trabajo de investigación. A Luis Cabedo Mas, por su asesoría y acompañamiento en algunos temas puntuales del trabajo de investigación.

A mis compañeros del grupo de investigación (cachondeo 502). Por su amistad, colaboración, amabilidad y compañía durante el desarrollo del trabajo de investigación. Sin ellos no habría sido igual mi estadía en el laboratorio y fuera de el.

Al Insituto de Agroquímica y Tecnología de Alimentos (IATA-CSIC), por abrirme las puertas y brindarme el servicio de su planta administrativa e instalaciones. A la Universidad de Valencia por su servicio de Microscopía. Al Laboratorio Ibérico Internacional de Nanotecnología (INL) y la Universitat Jaume I por su colaboración en el desarrollo de algunos experimentos. A la Universidad Politécnica de Valencia por ofrecerme las garantías para la culminación del programa de doctorado.

ABSTRACT

Active packaging is one of the most relevant emerging technologies in the food industry. It aims to interact with the packaging headspace to control the enzymatic, chemical, physical, and microbiological reactions that deteriorate food through scavenging or releasing means. The current PhD thesis originally deals with the development and characterization of mono and multilayer active and biodegradable food packaging structures based on electrospun polyhydroxyalkanoates (PHA) materials derived from circular bioeconomy strategies. In order to provide the packaging materials with active properties, essential oils, natural extracts, metallic nanoparticles or combinations thereof were incorporated into PHA by solution electrospinning. The resultant electrospun PHA mats were annealed to obtain continuous monolayers that were, thereafter, combined with cast-extruded, blown or solvent-casted biodegradable polymer films and/or barrier coatings of bacterial cellulose nanocrystals (CNCs) to develop novel multilayer systems with antimicrobial and barrier properties. These PHA-based multilayers systems presented good thermal and mechanical performance as well as high barrier properties to vapors and gases. The active films also showed improved antioxidant properties and high antimicrobial activity against food-borne bacteria in both open and, more importantly, closed systems, which can mimic real case use packaging conditions. Therefore, the here-developed materials and prototypes can be very promising as packaging materials, to constitute trays, flow packs and lids, being completely renewable and also biodegradable, with the final potential capacity to increase both quality and safety of food products in the new Circular Bioeconomy context.

RESUMEN

El envasado activo es una de las tecnologías emergentes más relevantes de la industria alimentaria. Su objetivo es interactuar con el espacio de cabeza del envase para controlar las reacciones enzimáticas, químicas, físicas y microbiológicas que deterioran los alimentos por medio de la absorción o liberación. La actual tesis doctoral trata originalmente del desarrollo y la caracterización de estructuras de envasado de alimentos activas y biodegradables mono y multicapa basadas en materiales de polihidroxialcanoatos (PHA) electroestirados derivados de estrategias de bioeconomía circular. Con el fin de dotar con propiedades activas los materiales de envasado, se incorporaron a los PHA aceites esenciales, extractos naturales, nanopartículas metálicas o combinaciones de los mismos mediante electrospinning de soluciones. Las fibras resultantes de PHA por electrospinning se recocieron para obtener monocapas continuas que, posteriormente, se combinaron con películas de polímeros biodegradables fundidas, sopladas o fundidas con disolventes y/o con revestimientos de barrera de nanocristales de celulosa bacteriana (CNC) para desarrollar novedosos sistemas multicapa con propiedades antimicrobianas y de barrera. Estos sistemas multicapas basados en PHA presentaron un buen rendimiento térmico y mecánico, así como altas propiedades de barrera a los vapores y gases. Las películas activas también mostraron mejores propiedades antioxidantes y una alta actividad antimicrobiana contra las bacterias transmitidas por los alimentos tanto en sistemas abiertos como, lo que es más importante, en sistemas cerrados, que pueden imitar las condiciones de envasado en casos reales. Por lo tanto, los materiales y prototipos desarrollados en este trabajo pueden ser muy prometedores como materiales de envasado, para constituir bandejas, flow packs y tapas, siendo completamente renovables y también biodegradables, con una potencial capacidad de aumentar tanto la calidad, como la seguridad de los productos alimenticios en el nuevo contexto de la Bioeconomía Circular.
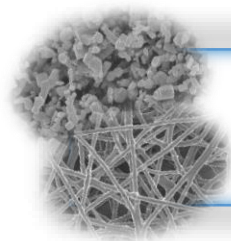
RESUM

L'envasament actiu és una de les tecnologies emergents més rellevants de la indústria alimentària. El seu objectiu és interactuar amb l'espai de cap de l'envàs per controlar les reaccions enzimàtiques, químiques, físiques i microbiològiques que deterioren els aliments per mitjà de l'absorció o alliberament. L'actual tesi doctoral tracta originalment de el desenvolupament i la caracterització d'estructures d'envasat d'aliments actives i biodegradables mono i multicapa basades en materials de polihidroxialcanoatos (PHA) electroestirados derivats d'estratègies de bioeconomia circular. Per tal de dotar amb propietats actives dels materials d'envasat, es van incorporar als PHA olis essencials, extractes naturals, nanopartícules metàl·liques o combinacions dels mateixos mitjançant electrospinning de solucions. Les fibres resultants de PHA per electrospinning es recocieron per obtenir monocapes contínues que, posteriorment, es van combinar amb pel·lícules de polímers biodegradables foses, bufades o foses amb dissolvents i / o amb revestiments de barrera de nanocristalls de cel·lulosa bacteriana (CNC) per desenvolupar nous sistemes multicapa amb propietats antimicrobianes i de barrera. Aquests sistemes multicapes basats en PHA van presentar un bon rendiment tèrmic i mecànic, així com altes propietats de barrera als vapors i gasos. Les pel·lícules actives també van mostrar millors propietats antioxidants i una alta activitat antimicrobiana contra bacteris transmeses pels aliments tant en sistemes oberts com, el que és més important, en sistemes tancats, que poden imitar les condicions d'envasament en casos reals. Per tant, els materials i prototips desenvolupats poden ser molt prometedors com materials d'envasat, per constituir safates, flow packs i tapes, sent completament renovables i també biodegradables, amb la capacitat potencial final d'augmentar tant la qualitat, com la seguretat de els productes alimentaris en el nou context de l'Bioeconomia Circular.

I. INTRODUCTION

1   Introduction

1.1   Biopolymers Based Food Packaging Materials

Global pollution, oil scarcity and new food safety and quality requirements have led to the study and development of different biopolymers to constitute packaging materials [1]. Packaging has a great impact on sustainability due to its direct or indirect use in the food chain and food waste, playing an important role in individual and social well-being [2]. Addressing these issues by using biopolymers in eco-friendly packaging design gives solutions which provide physical protection while creating proper physicochemical conditions to maintain food quality and safety as well as extending food shelf life [3].

1.1.1   Sustainability and Circular Bio-economy

Worldwide food systems are facing unprecedented challenges attributable to food demand by a growing population which are increasing the number of people suffering from hunger and malnutrition, the negative effects of climate change, the overexploitation of natural resources, and food loss and waste. Following the linear economy principle of "make, use and dispose" is unsustainable [4]. Therefore, a transition to a sustainable food system is needed to guarantee food security. To do this, it is necessary to follow the four pillars of food security based on: availability, access, utilization, and stability; as well as the three dimensions of sustainability: environment, economy, and society (Figure 1a). These parameters aim to conserve and protect ecosystems and resources while supporting equitable opportunities for economic development and providing people with adaptable, accessible, and connected places [5]. Likewise, implementing circular economy principles (rethink, redesign, remanufacture, repair, redistribute, reduce, reuse, recycle and recover energy) is a method of reducing production and the environmental impact of resource use. Restoring is also necessary to constantly keep products, components and materials at highest utility and value while distinguishing between technical and biological cycles (Figure 1b) [6]. These economic and productive strategies seek to reduce the use of raw materials as much as possible in the productive fabric and to minimize the generation of non-recyclable waste, since they cover the entire production cycle, including the efficient use of raw materials, the optimization of energy resources and the minimization of environmental risks [7]. In this context, circular bioeconomy has a systemic approach towards maintaining the value of any product contingent on simultaneous waste elimination, thus enabling the reuse of all byproducts in the value chain. Following circular economy principles, the breeding of higher value products (i.e., food and animal feed) must be ensured first, then the

sustainable reuse and recycling of byproducts, waste, and raw materials along with the bioproduct manufacturing, and finally, implementation of energy-yielding technologies to achieve a cleaner industrial production [8]. Further on recycling, the circular bioeconomy aims to convert the reserves and wastes into valuable goods such as bio-based products [9]. Shifting towards a new circular bioeconomy, a sustainable and bio-based market has a great opportunity to break through and overcome current petroleum-based market dependence [10]. Within this context, food packaging technology focuses on maximum efficiency with minimum environmental burden by using more environmentally friendly solutions, such as biomaterials production from wastes which do not compete with the production of food or animal feed and provide an abundance of raw material for the development of recyclable and compostable plastic packaging materials [11,12].
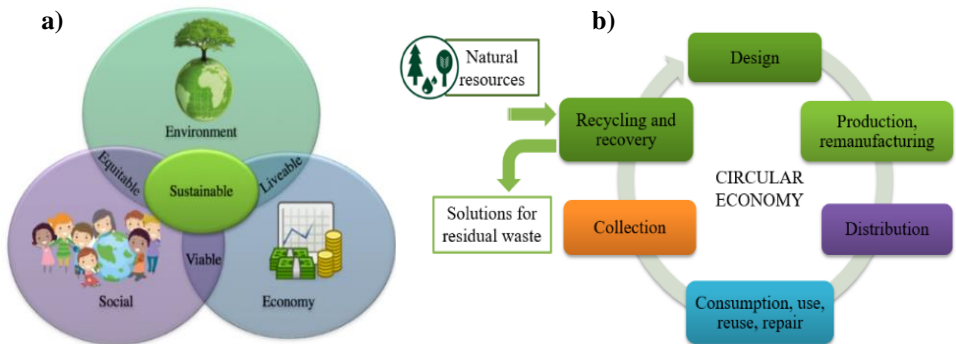
Figure 1. Sustainability (**a**) and Circular Economy principles (**b**).

1.1.2   *Classification of Biopolymers*

The above-described environmental and food safety issues are the main drivers behind the interest for the development of new materials for food packaging applications. Although bioplastics still represent under one percent of the approximately 350 million tons of plastics produced annually, mostly for packaging materials [13,14], including high-performance thermoplastic materials and foams, they also represent an important part of the bioeconomy and they will undoubtedly shape the future of the plastics industry [15]. Because of this, the use of biopolymers in packaging has increased considerably over the past few years due to their sustainable feedstock, biodegradability, and similar processing characteristics to existing thermoplastics [16].

Biopolymers comprise a whole family of materials with different properties and applications. They include polymers with a "bio-based" origin and "biodegradable"

polymers or polymers featuring both properties. Bio-based polymers correspond to any kind of polymer that is obtained from renewable resources, which include both naturally occurring polymers and synthetic polymers produced by means of monomers obtained from biological sources [17]. Naturally occurring polymers are biomacromolecules, that is, molecules of large molecular weight produced in nature by living organisms and plants. Biodegradable polymers are defined as those polymer materials whose physical and chemical properties undergo deterioration and completely degrade when exposed to the enzymatic action of microorganisms, carbon dioxide (aerobic process), methane (anaerobic process), water (aerobic and anaerobic processes), inorganic compounds, and biomass [18]. Bio-based polymers can be biodegradable but not all biodegradable polymers are bio-based. Additionally, in the near future, some synthetic biodegradable polymers could be partially or fully developed from bio-based monomers. Bio-based polymers offer the saving of fossil resources by using biomass that regenerates (annually) and the unique potential of carbon neutrality whereas biodegradability is an add-on property of certain types of polymers that offers additional means of recovery at the end of the product's life [19,20]. Figure 2 summarizes the classification of biopolymers grouped according to their origin and biodegradability characteristics. At the top right of the figure, bio-based and biodegradable polymers are grouped. Nature produces over 170 billion metric tons of biomass per year, yet only 3-4% of this material is being used by humans for food and non-food purposes [21]. Biomass carbohydrates are the most abundant renewable resources available, representing approximately 75% of this biomass, which are currently regarded as the basis for the green chemistry of the future. Most of these biopolymers are mainly made from carbohydrate rich plants such as corn or sugar cane, that is, the so-called food crops, which are also currently referred to as the "first generation feedstock of bioplastics". This currently represents the most efficient feedstock to produce bioplastics, as it requires the least amount of land to grow and produces the highest yields. Biomass-derived polyesters such as polylactide (PLA) and thermoplastic starch (TPS) are among the most promising biodegradable polymers and they comprise up to 65% of the family of bioplastics. Another promising biopolymer which has gained great interest in recent years due to its biodegradability and biocompatibility is Polyhydroxyalkanoate (PHA). The PHA is a carbon-based polymer which can be obtained from food waste (e.g., whey, starch, oils, lignocellulosic materials, legume, and sugar wastes) and is rich in simple sugars (e.g., glucose, lactose) and fatty acids (e.g., acetic or propionic acids) that are hydrolyzed to obtain precursor molecules to feed a specific microorganism culture. These bacteria can accumulate PHA granules of between 70%-85% of their weight [22].

Bio-based polyolefins:
Bio-based polyethylene (bio-PE)
Bio-based polypropylene (bio-PP)

Bio-based polyamides:
Polyamide 1010 (PA1010), polyamide 11 (PA11), polyamide 1012 (PA1012), etc.

Others:
Bio-based polyethylene terephatalate (bio-PET)
Poly(ethylene furanoate) (PEF)
Bio-based polyurethane (bio-PU)

Aliphatic polyesters:
Polylactide (PLA)
Poly(3-hydroxybutyrate) (PHB)
Poly(3-hydroxybutyrate-*co*-3-hydroxyvalerate) (PHBV)
Poly(3-hydroxybutyrate-*co*-4-hydroxybutyrate) [P(3HB-*co*-4HB)]

Proteins:
Wheat gluten (WG), soy protein (SP), keratin, casein, zein, etc.

Polysaccharides:
Thermoplastic starch (TPS), cellulose, chitin, chitosan, pectin, etc.

Renewable resources

Bioplastics
e.g.
bio-PE, PA1010, bio-PET

Bioplastics
e.g.
PLA, PHB, TPS, cellulose

Not biodegradable ⇐ ⇒ Biodegradable

Conventional plastics
e.g.
PE, PP, PAs, PET

Bioplastics
e.g.
PCL, PBS, PBAT, PVOH

Commodity plastics:
Polyethylene (PE), polypropylene (PP), polyvinyl chloride (PVC), polystyrene (PS), etc.

Engineering plastics:
Polyamides (PAs), polyethylene terephthalate (PET), polybutylene terephthalate (PBT), polycarbonate (PC), etc.

High-performance plastics:
Poly(ether ether ketone) (PEEK), etc.

Aliphatic polyesters:
Poly(ε-caprolactone) (PCL)
Polyglycolic acid (PGA)
Polybutylene succinate (PBS)
Poly(butylene succinate-*co*-adipate) (PBSA)

Aromatic polyesters:
Poly(butylene adipate-*co*-terephthalate) (PBAT)

Others:
Polyvinyl alcohol (PVOH)

Petrochemical resources

Figure 2. Classification of biopolymers widely used in packaging.

The same durability properties that have made traditional petroleum-derived plastics ideal for many applications, such as those found in packaging, are leading to terrible waste-disposal problems as these materials are resistant to microbial degradation, leading to plastics accumulation in the environment. For this reason, some biodegradable polymers, still based on petrochemical polymers, have been developed over the past years. The most frequently studied polymers are included in the bottom-right group, which are aliphatic or aliphatic-aromatic polyesters since neat aromatic polyesters based on terephthalic acid are generally insensitive to hydrolytic degradation and enzymatic or microbial attack due to their high stability. Indeed, the biodegradation rate increases rapidly when the concentration of terephthalic acid becomes lower than 55%. These petrochemical biodegradable polymers can find several uses in both flexible and rigid packaging applications.

Bio-based but not biodegradable polymers, which are shown at the top left of the figure, currently offer important contributions not only to the reduction of dependence on fossil fuels but also to the related positive environmental impact, such as the reduction of carbon dioxide emissions. New approaches move towards the complete or partial substitution of conventional plastics by renewable resources such as biomass [23]. Conventional polymers from feedstock routes are being explored for well-known applications, including the packaging industry [24]. These are generally based on monomers derived from agricultural and food-based resources such as corn,

potatoes, and other carbohydrate feedstock. The new branch of these "green polymers" reflects the "biorefinery" concept [25]. The monomers that produce these bio-based polymers can be obtained from natural resources, for example, catalytic dehydration of bioethanol obtained by microbial fermentation. Although these biopolymers are not biodegradable, they have the same processing and performance as conventional polymers made from natural gas or oil feedstock. Such developments have recently led to the new paradigm for sustainable food packaging: "Bio-based but not biodegradable" [26]. This is further evidenced by the development of fully bio-based polyethylene terephthalate (bio-PET) in which the ethylene glycol and the terephthalic acid are both derived from plant-based sugars and agricultural residues. The discussion about the use of biomass for industrial purposes is still often linked to the question of whether the conversion of potential food and feed into materials is ethically justifiable. Although, the surface required to grow sufficient feedstock for current bioplastics production is only about 0.01% of the global agricultural area of a total of 5 billion hectares. The bioplastics industry is also researching the use of non-food crops and agricultural residues, the so-called "second generation feedstock", with a view to its further use. Innovative technologies are focusing on non-edible by-products as the source for bioplastics, which include large amounts of cellulosic by-products and wastes such as straw, corn stover or bagasse. This leaves significant potential for using biotechnological processes to create platform chemicals for industrial purposes, amongst them is the production of bioplastics. Therefore, the trend for the development of the next generation of bioplastics is currently led by the emergence of conventional polymers made from renewable and non-food sources.

1.1.3   *Polyhydroxyalkanoates (PHAs)*

One of the most important alternatives to fossil-derived polymers in the frame of the Circular Economy are polyhydroxyalkanoates (PHAs) [27], showing the highest potential to replace polyolefins in packaging applications due to their biocompatibility and physical properties [28]. PHAs are a family of biopolyesters synthesized by more than 300 species of Gram-positive and Gram-negative bacteria, highlighting strains such as *Escherichia coli*, *Aeromonas sp.*, *Cupriavidus necator*, *Alcaligenes latus*, *Azotobacter sp.*, as well as a wide range of archaea, such as carbon storage material [29]. PHAs are accumulated in bacteria as a high-molecular-weight polymer which constitutes up to 85% of the weight of the total bacteria cell (Figure 3) [30] and they generate intracellular spherical granules with diameters between 0.2 – 0.3 μm. PHAs granules are formed by a hydrophobic core of spiral PHA chains and water acting as plasticizer; this core is covered by different types of hydrophilic

enzymes and structural proteins [31]. The PHAs productivity yield also depends on the type of fermentation and culture conditions; thus, many reports have indicated that the most efficient methods to produce PHAs are the fed-batch fermentations in bioreactor and mixed microbial cultures. In the case of the mixed microbial cultures, acidogenic fermentation of the carbon source is used to produce volatile fatty acids (VFA) as precursors to PHA biosynthesis, culture selection based on PHA storage ability, and PHA production in which the selected microorganisms are fed with the VFA produced, reaching a level of volumetric productivity around 4.60 g/L/h [32]. PHAs are homo-, co- and terpolymers, their molecules are principally constituted by (R)-hydroxy-fatty acid monomer units that mainly consist of 3-, 4-, 5-, and 6-hydroxycarboxylic acids [33]. The PHAs classification is based on the number of carbons in their repeating units, such as short-chain-length PHAs (scl- PHAs) with 3 to 5 carbon atoms, (e.g., poly-3-hydroxybutyrate (PHB) and poly-3-hydroxybutyrate-co-3-hydroxyvalerate (PHBV)); the medium-chain-length PHAs (mcl-PHAs) with 6 to 14 carbon atoms, (e.g., poly-3-hydroxyhexanoate (PHHx) and poly-3-hydroxyoctanoate (PHO)); and long-chain-length PHAs (lcl-PHAs) with more than 14 carbon atoms [34]. The resulting polymers have suitable characteristics: biodegradability, thermoplasticity, resistance to UV degradation, and similar water resistance and mechanical strength to polypropylene and polystyrene [35]. However, their production is expensive due to the high costs of the fermentation and downstream processes. The use of industrial by-products and waste, or mixed microbial cultures represents a viable option to reduce the production costs of PHAs [36].
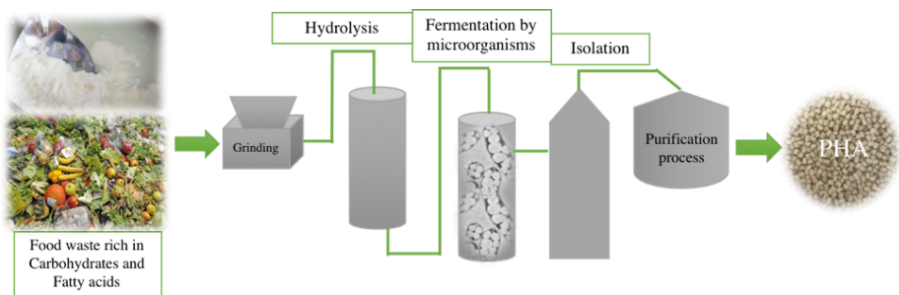
Figure 3. Polyhydroxyalkanoates (PHA) process.

Among PHAs, poly(3-hydroxybutyrate) (PHB) is the most widely studied and the first identified bacterial member of this family. This isotactic homopolyester is biodegradable not only in composting conditions but also in other environments such as marine water; it also presents similar thermal and mechanical properties to some petrochemical polymers. However, its use is limited due to its poor impact-strength

resistance, fragility, lack of hydrophilicity, and a narrow processing temperature window [37]. Incorporation of HV into the PHB homopolymer chain improves the mechanical and thermal properties depending on their chemical composition and fraction of HV co-units. The copolymer poly(3-hydroxybutyrate-co-3-hydroxyvalerate) (PHBV) has a significantly lower crystallinity and melting temperature (Tm) which decrease as the fraction of HV in the polymer increases; their T_g can vary from -40 to 5 °C and the Tm can vary from 50 to 180 °C [38]. Also, it exhibits lower stiffness and brittleness, higher ductility, and elongation at break, and increases tensile strength due to a decrease in the value of Young's modulus with an increase in the HV molar fraction in PHB-HV polymer chain reference [39]; likewise, this mechanical improvement has been attributed to the smaller dimensions of the crystallites as the hydroxyvalerate (HV) co-units act as defects in the PHB lattice [40].

PHAs can be processed with common methods such as extrusion, injection molding, thermoforming, film blowing, electrospinning, etc. [41]. These materials are suitable for very different areas of food and cosmetic packaging, for instance, blow-molded bottles, milk cartons, cosmetic containers, feminine hygiene products, adhesives, paper coating waxes and paints [42]. Figure 4 depicts, as an example, an injected tray made of PHA. Moreover, the use of nanofillers or active substances, such as antimicrobial and/or antioxidant substances, incorporated into a PHA-based packaging material can change the packed food condition, extending the shelf life and improving the protection and/or sensory properties [43,44].

Figure 4. Biodegradable food tray made of poly(3-hydroxybutyrate) (PHB) obtained by injection moulding.

1.2 Food Packaging for Food Preservation

According to the Food and Agriculture Organization of the United Nations (FAO), approximately one third of the food produced globally is either lost or wasted [45]. Food waste is produced throughout the whole food value chain, from manufacturing to distribution, retail, food service activities and households. Because of the limited natural resources available, it is more effective to reduce food waste than to increase

food production. For this reason, several efforts have been made to develop more effective food packaging strategies [46,47].

Packaging items have become essential to preserve food. They can be customized to prevent or inhibit microbial growth as well as food decomposition by blocking light, oxygen, and moisture entrance; they can even prevent spoilage caused by small insects. Additionally, novel packaging items can be monitored to give information about packaged food quality which, in turn, diminishes food waste during distribution and transportation [48]. Food products are normally classified into three basic categories depending on their characteristics and composition: perishable food (e.g., milk, meat, and fresh fruits and vegetables) which has a shorter shelf life and must be stored at refrigeration and freezing temperatures; semi-perishable food which can contain some natural inhibitors (e.g., some cheeses) or receive some kind of treatment (e.g., pasteurized milk); and nonperishable food which can either be stored at room temperatures because of its low water activity (e.g., honey, cereal grains, nuts) or preserved by heat sterilization (e.g., canned food) and preservative substances. However, these types of food stability and preservation depend on packaging integrity [49].

Process and storage systems considerably influence physicochemical, microbiological, and biochemical changes in food. According to different external conditions (e.g., humidity, temperature, light) these changes take action at different rates and extents [50]. Food is mainly formed by water, carbohydrates, protein, lipids, minerals, and vitamins. Each nutrient group requires special treatment to preserve their nutritional quality and to maintain food characteristics such as texture, color, and flavor. Humidity and water activity (a_w) are the principal medium for microorganism proliferation. For other nutrients, oxygen and UV light are the main external agents that promote molecule oxidation, resulting in quality loss, unsavory flavors, and color changes [51]. Moreover, the most popular method to extend food shelf life is packaging technology [52]. Therefore, food quality depends on packaging material because there is constant chemical and physical activity on the surfaces between packaging and food [53,54]. That is why food packaging materials must have specific characteristics depending on the product that will be stored inside. Figure 5 shows the principal functions of packaging in food protection which include: avoiding mechanical stress and controlling temperature, humidity, organic vapors, gases, microorganisms, light, and water vapor [55].
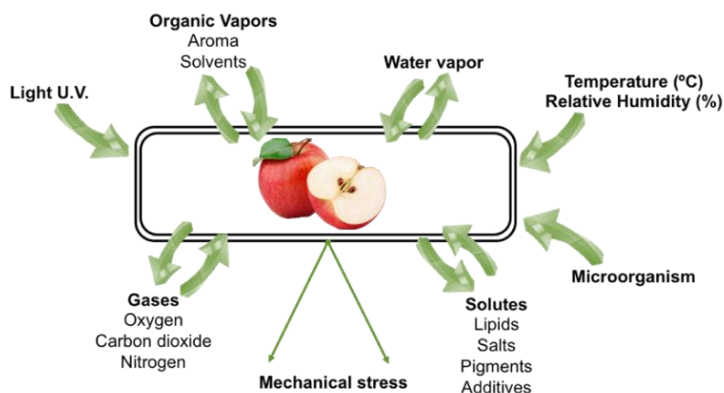
Figure 5. Food Packaging functions.

Since the middle twentieth century, the main materials used for food packaging have been developed from petroleum-based polymers given their high mechanical (strength, flexibility), thermal, water vapor barrier and gas barrier properties [56]. A report by Geyer et al. [57] indicated that out of 8.300 million tons of plastic generated since the start of its massive use, 30% of it is still in use, while everything else (approximately 6.000 million tons) has been turned into waste. Only 9% of it has been recycled and 12% has been incinerated whereas 79% has ended up in landfills or has been dumped into the environment. If this continues, by 2050 plastic will have reached an amount of approximately 13.000 million tons, generating irreversible damage in marine and terrestrial ecosystems. In accordance with Huang et al. [58], the most affected is the marine ecosystem (oceans, seas, rivers, lakes). Microplastic particles (<5 mm in size) can be ingested by a wide variety of aquatic organisms, altering their health, and diminishing their physiological functions. Plastic bioaccumulation generates a reduction in their feed capability and changes their behavior. Recently, there has been a major push for different research groups, industries, governments, and populations to find, develop and optimize new biodegradable materials from renewable sources [59]. As a result of their biodegradability, availability and low cost, biopolymers are considered a potential alternative to progressively replace synthetic plastics obtained from fossil fuels [60]. Packaging has changed throughout history, adjusting to social and environmental demands: Table 1 shows food packaging technology evolution throughout time. Next-generation food packaging must be biodegradable, eco-friendly, and intelligent with active properties (i.e., antimicrobial, antioxidant, scavengers) to extend food shelf life; it must also address consumers´ needs and their conformity to new circular economy politics and Sustainable Development Goals.

Table 1. Food packaging technology evolution [49]

Time	Packaging characteristics
1960s	Convenience and POP marketing
1970s	Lightweighting, source reduction, energy saving
1980s	Safety and tamper evidence
1990s	Environmental impact
2000s	Safety and security
2010s	Active properties and shelf life extension
2020s	Intelligent functionalities and active properties

1.3 Active Food Packaging

Food products are exposed to external conditions throughout the production chain, i.e., harvesting, post-processing, distribution, transportation, storage, and delivery to the final consumer. In this context, traditional food packaging was initially developed to contain food products and protect them from external conditions (e.g., moisture, oxygen, dust, light, microorganisms, and mechanical forces) [61]. During the last decade food packaging has been developing new active and smart materials that extend shelf life, maintain quality, safety, and integrity, and avoid microorganisms' proliferation and food oxidative reactions by incorporating active substances [62]. Along with protecting food products from environmental conditions and mechanical forces, active packaging plays an active role in quality and food preservation during the distribution process. Regulation (CE) No. 450/2009 (29/05/2009), defines active packaging as a material which is designed to incorporate the intentionality of active compounds to release and absorb substances into or from either the environment or packaged food [63]. Active packaging is mainly classified as either a scavenger (absorber) which removes undesired food compounds or active-releasing (emitter) which adds compounds to packaged food or into headspace (Figure 6), providing flavor, antioxidants, and long-term antimicrobial properties [49,64]. Therefore, the most studied active food packaging types are those containing antimicrobials and antioxidants. Different active compounds have been used to functionalize packaging materials and have been tested against a wide variety of foodborne associated organisms [65].
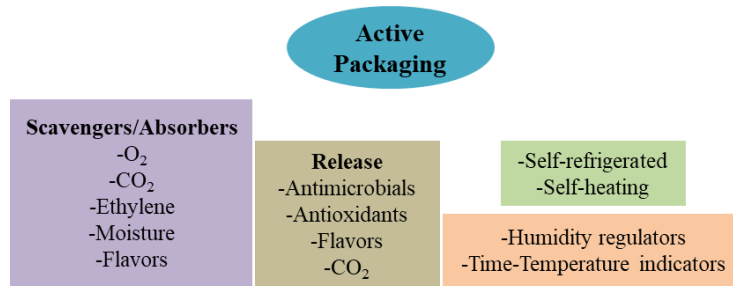
Figure 6. Active packaging classification.

1.3.1 Scavenging Technologies

Scavenger type active packaging includes oxygen scavengers, moisture scavengers, ethylene absorbers, and carbon dioxide emitters/scavengers. Scavengers are usually incorporated inside packaging like sachets, labels, films, and/or incorporated into the packaging structure as a coating or a layer during processing (Figure 7). Each one has a specific function in food preservation to maintain integrity, safety, and nutritional and microbiological quality of products. Oxygen scavengers/absorbers capture oxygen present within packaging material; they can also create an oxygen-free environment preventing food from oxidation and avoiding aerobic bacteria and fungi growth. One of the most common oxygen-scavengers is iron powder, whose action mechanism is mainly based on iron oxidation in the presence of humidity and metal-free oxygen absorbers, wherein ferrous oxide (Fe^{2+}) is converted to ferric oxide (Fe^{3+}), reducing O_2 levels inside package to less than 0.01 % [66,67]. Other systems that chemically scavenge oxygen include photosensitive dyes, ascorbic acid, Gallic acid, unsaturated hydrocarbon dienes, palladium; α-tocopherol, enzymes (e.g., oxalate oxidase and glucose oxidase along with catalase) [68] and oxygen scavenging based on microorganisms like dried yeast which are usually immobilized in a solid matrix [69,70]. In another example, moisture scavengers work by applying desiccant (e.g., silica gel, clays, zeolite, sodium, potassium, calcium alumina silicate, calcium oxide, others) that controls relative humidity and scavenge humidity in packaging headspace in addition to an absorber that removes moisture and absorbs liquids. Yet another common type of scavenger is an ethylene absorber that has capacity to remove the ethylene hormone from the product environment, thereby reducing the senescence rate of harvested vegetables and fruits by chemical reactions and physical adsorption generated by dispersed minerals, such as zeolite, active carbon, and nanoparticles; with potassium permanganate ($KMnO_4$) being the most used active component to oxidize/inactivate ethylene [67,71]. Finally, carbon dioxide emitters/scavengers based on ferrous carbonate or an ascorbic and acid mixture act

as inhibitors of microbial growth, that prevent packaging from inflating due to CO_2 formed after the packaging process [72].

1.3.2   Release Technologies

Active release packaging is designed to prevent food components from spoilage generated by pathogenic microorganisms' growth as well as lipids, proteins, and carbohydrates oxidation, making active packaging a preservation technology which maintains food quality and extends its shelf life [61]. Active substances with biocide and antioxidant capacity can be incorporated into the packaging atmosphere and packaged food in different ways, such as, coating or absorption into polymer surfaces, directly incorporating volatile and nonvolatile substances into packaging material to release and migrate progressively to food surface or remain at package/food interface and controlling migration issues. Similarly, sachets/pads use compounds containing volatile antimicrobials/antioxidants in packages and antimicrobial activity polymers (e.g., chitosan) [73,74] (see Figure 7) [75]. These strategies are alternatives to adding active substances directly into food, providing the possibility of controlling substance diffusion from packaging material toward food [76]. Active release antimicrobials/antioxidants include a wide range of substances such as organic acids, bacteriocins, enzymes, chelating agents, metals, essential oils, and natural extracts. The following items describe antimicrobial and antioxidant packaging.
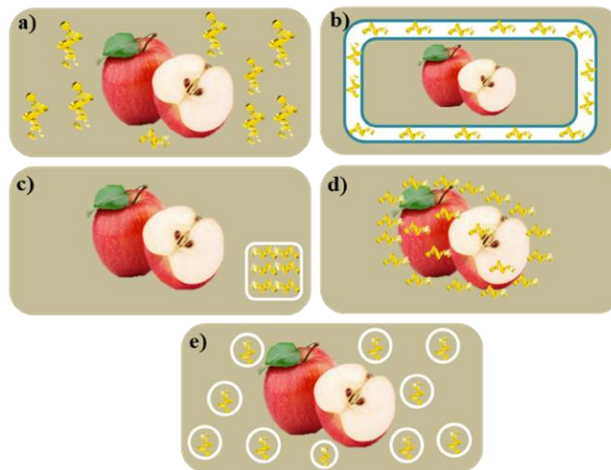

Figure 7. Active packaging methods: **a**) direct mixing into the packaging material, **b**) adsorption or coating of the packaging material, **c**) construction of small antimicrobial packaging, **d**) addition to packaging in gaseous form, and **e**) microencapsulation followed by packaging [71].

1.3.2.1 Antimicrobial Packaging

The goal of Antimicrobial packaging to minimize food loss and to provide safe and wholesome food products has taken on great importance in the food packaging industry. The principal food spoilage factor is foodborne microorganisms. The main functions of antimicrobial packaging are to reduce, inhibit or delay foodborne bacterial growth. Antimicrobial substances are classified as either organic or inorganic materials (Figure 8) [60]; both of which present high activity against Gram-negative and Gram-positive bacteria. However, most organic substances (e.g., essential oils, enzymes, and organic acids) are sensitive to high temperatures and pressures, while inorganic materials are more resistant [77,78]. Incorporating these sensitive substances into polymer matrixes improves their stability and maintains antimicrobial activity. Polymeric antimicrobial materials can be classified by their action mechanism such as contact-active antimicrobial polymers that possess a cationic charge which allows them to directly inhibit bacterial growth by interactions with negatively charged bacterial membranes. In addition, active release polymer materials activate bacteria by releasing a low molecular weight antimicrobial substance [79]. These antimicrobial substances are incorporated into different forms of packaging, as described in Figure 7. Active release polymer materials act as active compound carriers. An active molecule or ion is incorporated into the polymer matrix through either physical interaction or chemical bonding [80]. The antimicrobial agent´s action mechanism depends upon its structural components and bacterial outer membrane which interact through different mechanisms, such as damage or cell wall synthesis inhibition, cell membrane function inhibition, protein synthesis inhibition, nucleic acids (DNA and RNA) inhibition, and the inhibition of other metabolic processes [81]. The use of each one of them depends on the final application of food packaging to avoid loss during processing. Table 2 provides some studies on antimicrobial substances with polyhydroxyalkanoates for food packaging applications.
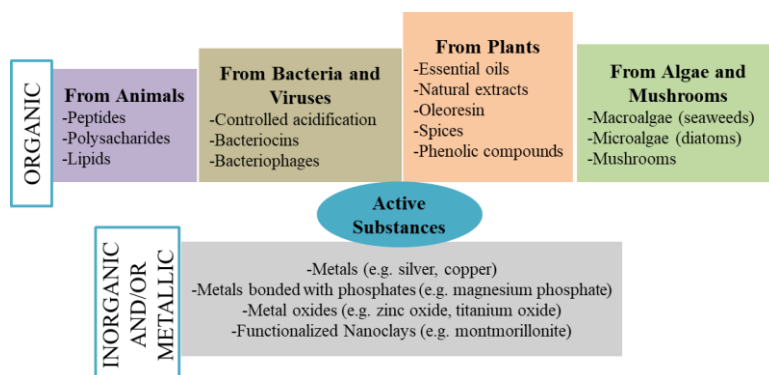
Figure 8. Antimicrobial/antioxidant substances classification.

Table 2. Research studies of antimicrobial substances within polyhydroxyalkanoates against food-borne bacteria for active food packaging

Polymer matrix	Antimicrobial substances	Bacterial strains	Highlighted result	Reference
Polyhydroxyalkanoate Chitosan	Molybdenum disulfide (MoS$_2$) nanoparticles	*Escherichia coli* *Staphylococcus aureus*	Effective antibacterial activity against both bacteria	Mukheem et al. [82]
Poly(3-hydroxybutyrate)	Silver nanoparticles (AgNPs)	*Salmonella enterica* *Listeria monocytogenes*	Presented a strong antimicrobial activity against both pathogens	Castro-Mayorga et al. [83]
Polyhydroxyalkanoate	Oregano Green tea Rosemary	*Escherichia coli* *Staphylococcus aureus*	OEO-containing PHBV films presented the highest antimicrobial activity against both strains respect to the other natural extracts	Figueroa-Lopez et al. [84]
Polyhydroxyalkanoate	Mesoporous silica nanoparticles containing eugenol	*Escherichia coli* *Staphylococcus aureus*	Successfully inhibited the bacterial growth after 15 days	Melendez-Rodriguez et al. [85]

1.3.2.2 Antioxidant active packaging

Antioxidant packaging materials have been developed to avoid oxidative reactions that decrease nutritional foodstuff value caused by essential fatty acids, proteins and lipid soluble vitamin degradation which generates off-flavors, odors, and color change. One of main reactions that affects food quality and safety is lipid oxidation

which is caused by reactive oxygen species production from fatty acids. The main mechanisms of lipid oxidation are based on hydrogen radical loss from an unsaturated fatty acid reacting with oxygen in a light or heat presence to form peroxyl radicals; another example of this occurs when peroxyl radicals react with more unsaturated fatty acids to form lipid hydroperoxides. Finally, the oxidation chain process concludes when two peroxyl radicals react to produce a non-radical species [86,87]. Antioxidant activity is defined as the capacity to prevent the oxidation of lipids or other substances by either inhibiting the initiation or propagation of oxidative chain reactions or forming stable radicals which are unreactive [88]. Antioxidant substances are classified primarily by action mechanism (or chain-braking) antioxidants, namely free-radical scavengers, and secondarily (or preventive) by antioxidants including metal chelators, UV absorbers, singlet oxygen ($^1O_2$) quenchers and oxygen scavengers. Secondary antioxidants have the capacity to reduce or prevent the occurrence of oxidation reactions, whereas primary antioxidants react with free radicals to convert them into stable substances [89]. The food packaging industry has been using different synthetic antioxidant substances to prevent lipid oxidation, such as butylated hydroxytoluene (BHT), butylated hydroxyanisole (BHA) and tert-butylhydroquinone (TBHQ). Synthetic substances are now suspected to be potentially harmful to human health. That is why natural antioxidants with lower toxicity and higher safety, such as polyphenols, tocopherols, carotenoids, caffeic acid, ferulic acid, ascorbic acid, plant, and fruit extracts, as well as essential oils from herbs and spices have gained great importance in antioxidant active food packaging [90]. However, natural substances can be sensitive to high temperatures. Therefore, the incorporation of biopolymers is a good option to protect antioxidant agents [91]. In this context, antioxidant compound and polymer packaging material should be compatible to achieve a homogeneous distribution, and to ease antioxidant agent release into food or headspace. Antioxidant effectiveness depends on its solubility. Therefore, antioxidant type should be selected in accordance with the food product [92]. Antioxidant packaging can act in two different ways: as an antioxidant releaser from package to food and as a scavenger that can react, modify, or trap substances responsible for the lipid oxidation process (e.g., oxygen, radical oxidative species, or metal ions from food product headspace). The main advantage of active packaging containing antioxidant agents is that the compound release is controlled, allowing the food active compound concentration to be maintained throughout the production and marketing chain [93,94]. Table 3 provides some studies on antioxidant substances with polyhydroxyalkanoates for food packaging applications.

Table 3. Some research studies of antioxidant substances within polyhydroxyalkanoates for active food packaging

Polymer matrix	Antioxidant substances	Antioxidant test	Highlighted result	Reference
Poly (3-hydroxybutyrate-co-3-hydroxyvalerate) (PHBV)	Fish scales (FS)	2,2-diphenyl-1-picrylhydrazyl (DPPH) radical assay	Free-radical scavenging rates of the PHBV/FS and PHBV-g-MA/FS samples increased with increasing FS content	Chin-San Wu [95]
Bacterial cellulose-based nanopapers coated with Polyhydroxyalkanoate	Apple extract	2,2-diphenyl-1-picrylhydrazyl (DPPH) radical and 2,2´-azino-bis(3-ethylbenzothiazoline-6-sulfonic acid (ABTS) assays	All the films showed DPPH and ABTS scavenging activity. Free radical scavenging activity increased with extract content in the films	Urbina et al. [96]
Poly(3-hydroxybutyrate-co-3-hydroxyvalerate) P(3HB-co-3HV) copolymer	Ascorbic acid	1,1-diphenyl-2-picryl-hydrazyl (DPPH) assay	Functionalized copolymer P(3HB-co-3HV)-ascorbic acid showed 14% free radical scavenging activity in 24 h with DPPH	Bathia et al. [97]

1.4 Active Substances

1.4.1 Essential oils

Essential oils (EOs) are the product of the secondary metabolism of the plant (roots, leaves, seed, bark), separated from the aqueous phase [98,99]. The composition depends on cultivation, geographical and environmental conditions, plant species and age. Chemically, essential oils are complex mixtures with approximately 7000 constituents where mono and sesquiterpene are predominant. The terpene is the volatile compound characteristic of the essential oils, such as the oxides, alcohols, aldehydes, ketones, acids, or reaction products (i.e., esters and ethers responsible for the strong biological activity as well as the antioxidant, antimicrobial, antifungal, and antiviral properties of plants) [100,101]. The oil can be obtained by dragging with water vapor, hydro distillation, organic solvents, cold pressure, and supercritical fluid, among other methods [99]. EOs are insoluble in water, but they are soluble in volatile compounds such as alcohol, ether, and fixed oils [102], they are also biologically safe and have a low risk of causing resistance in pathogens. In addition, they are classified as Generally Recognized as Safe (GRAS) by the U.S. Food and Drug Administration (FDA) [103]. EOs are an excellent alternative as food additives; they have interesting flavoring properties, aromatics, antimicrobial activity, and benefits to the human body due to its active principles. The study of antimicrobials obtained from natural sources has taken on great importance in the food industry in recent years, since most of the used antimicrobials are chemically synthesized, causing health problems in some cases. This is the reason why many synthesized

antimicrobials have been banned in different countries [104,105]. Antimicrobial effects of EOs are dependent on the chemical and architectural structure of the microorganism which varies among Gram-positive and Gram-negative bacteria presenting variations in the density of the bacterial cell wall [106]. The action mechanism consists primarily in destabilizing the cellular structure of bacteria, leading to the breakdown of membrane integrity. Due to the lipophilic nature, the EOs are taken up quickly within Gram-positive bacteria which have dense lipophilic phospholipid bilayer within cell walls. Therefore, EOs generate a quick antimicrobial effect at the junction of the cell wall as well as within the cell cytoplasm. Damage to the cell membrane increases permeability of the cell, this allows the avoidance of energy production, membrane transport, metabolic regulatory functions, increased leakage of cellular components and loss of ions. The effect of EOs in cell cytoplasm consist in disrupting proton pumps and depleting intracellular-ATP, generating cytoplasmic coagulation of inner cellular constituents which cause death to the cell (Figure 9) [107,108]. Many research studies have shown that the use of essential oils inhibit the growth of a wide variety of Gram-negative bacteria, such as *Escherichia coli* (*E. coli*), *Pseudomonas aeruginosa* (*P. aeruginosa*), and *Salmonella typhimurium* (*S. typhimurium*); as well as Gram-positive bacteria including *Staphylococcus aureus* (*S. aureus*), *Listeria monocytogenes* (*L. monocytogenes*), *Bacillus subtilis* (*B. subtilis*), *Streptococcus pyogenes* (*S. pyogenes*), and *Alicyclobacillus acidoterrestris* (*A. acidoterrestris*) [109-112]. Also, other reports have demonstrated the high antioxidant activity of essential oils, which ranges from 70% to 95% inhibition of free radicals of 2,2-diphenyl-1-picrylhydrazyl (DPPH) and 2,2′-azino-bis-(-3-ethylbenzothiazoline-6-sulfonic acid) (ABTS) [113,114], due to the presence of hydroxyl groups (–OH) in its chemical structure [115,116]. High activity attributes of the essential oils have motivated their incorporation in food active packaging to extend the shelf life of products [117].
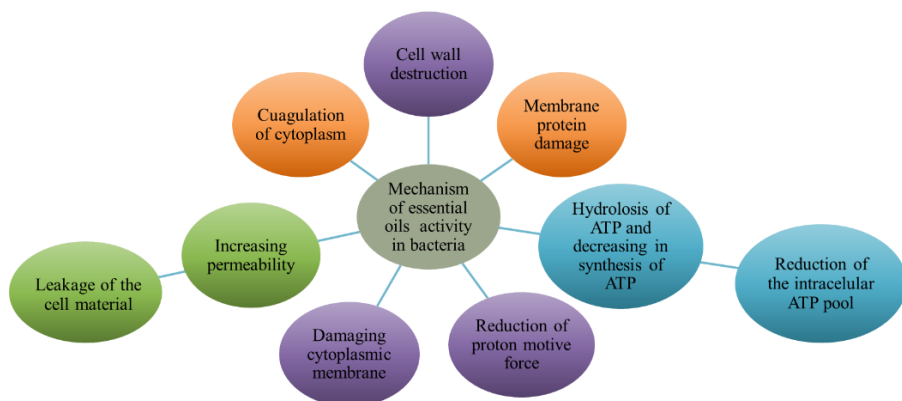
Figure 9. Action mechanism of essential oils against Gram-positive and Gram-negative bacteria.

1.4.1.1   *Oregano essential oil (OEO)*

Origanum species are important medicinal plants which belong to the Lamiaceae family. This group is comprised of 42 species and 18 hybrids that are widely distributed throughout Eurasia and North Africa [118]. They have been used for centuries as medicinal plants and traditionally consumed as a spice. Recently, they have been gaining more attention given the proven antimicrobial and antioxidant effects of their essential oils which contain high amounts of hydrocarbons, ketones, aldehydes, alcohols, ethers, phenols, and esters of phenolic and terpenic origins [119]. European oregano (*Origanum vulgare* L.) has been most studied essential oil (OEO) and is constituted by monoterpene hydrocarbons (3.44 %) and phenolic compounds (66.26 %) with 47 characterized compounds [120]. Carvacrol is the most predominant compound (36.46 %), followed by thymol (29.74 %), and a representation of up to 26 % of lesser abundant molecules including monoterpene hydrocarbons (ρ-cymene, γ-terpinene, α-pinene, β-pinene, camphene) and sesquiterpenes (α-copaene, α-humulene, β-bisabolene, β-caryophyllene oxide, and β-caryophyllene) which are responsible for antimicrobial, antifungal, and antioxidant properties (Figure 10) [84,121]. The antimicrobial activity of the OEO is attributed to phenolic monoterpenes (thymol and carvacrol) and oxygen-substituted derivatives. One of the possible main action mechanisms is based on the disruption of the bacterial cell wall and the cytoplasmic membrane for the action of phenolic compounds, this penetrates the phospholipids layer of the cell wall, blocking their normal functions [122]. Different research studies have reported the antimicrobial activity of the OEO against different Gram-positive (e.g., *Bacillus cereus*, *Bacillus subtilis*, *Staphylococcus aureus*, *Staphylococcus epidermidis*, *Streptococcus faecalis*) and Gram-negative bacteria (e.g., *Escherichia coli*, *Proteus mirabilis*, *Proteus vulgaris*,

Pseudomonas aeruginosa, *Salmonella typhi*), concluding that OEO is less effective against the Gram-positive bacteria [84,123]. However, the high antioxidant activity of OEO is attributed to the polyphenols and the degree of hydroxylation; its high reactivity to active free radicals provides effective protection in all phases of lipid oxidation and is considered the main mechanism. The scavenging capacities against DPPH radical and ABTS of the OEO have been reported by different authors, demonstrating strong antioxidant activity [84,124]. Given the high antimicrobial and antioxidant activity of the secondary metabolites, the OEO have potential applications in many industrial fields. Nowadays, the food industry is one of the most interested in active substances for foodstuff preservation and active food packaging design.
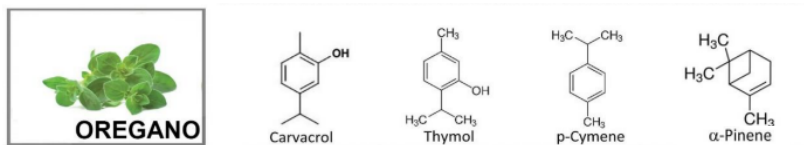
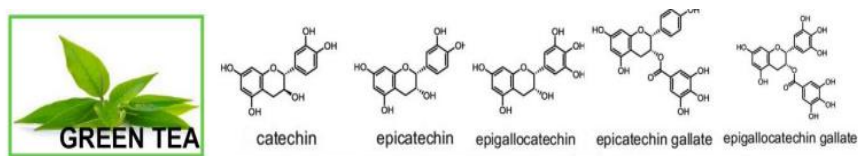**Figure 10.** Chemical structure of oregano main components.

1.4.2 Natural Extracts

Natural extracts (NEs) are composed of biologically active substances, such as polyphenols, quinones, flavanols/flavanoids, alkaloids, and lectins present in plant tissues (e.g., flower, seed, leaves, fruits, stems, and others) that tend to present greater stability and activity [125]. NEs are classified as generally recognized as safe (GRAS) food additives by the Food and Drug Administration (FDA). Active substance quantities and composition may widely vary depending on plant edaphoclimatic characteristics [84] and extraction methods by solvents (e.g., alcohol, water, propylene glycol and organic solvents), maceration, percolation, Soxhlet, and CO_2 column. NEs present high antimicrobial activity against foodborne pathogens as well as the capacity to retard lipid, protein, and sugar oxidation. A study on antioxidant and antimicrobial activity has shown a high inhibition of different microorganisms (e.g., *Bacillus cereus*, *Staphylococcus aureus*, *Escherichia coli*, *Listeria monocytogenes* and *Pseudomonas aeruginosa*, others) [126]. These activities have been attributed to polyphenolic compounds, bound to plant sugars as glycosides, and include flavonoids [127].

1.4.2.1 Green Tea Extract

Originated in China, the chemical composition of green tea (*Camellia sinensis* L) mainly consists of caffeine (~3.5 % of total dry weight), theobromine (0.15 – 0.2 %),

theophylline (0.02 – 0.04 %), organic acids (1.5 %), chlorophyll (0.5 %), theanine (4 %) and free amino acids (1 – 5.5 %) [128], volatile compounds, flavones, polyphenols (catechins and flavonoids), flavonols (quercetin, kaempferol, myricetin, and their glycosides), all of which are catalogued as strong antioxidant and antimicrobial agents [129]. The most important components of green tea are catechins (~15 – 30 % of dry weight of green tea leaves), which are water-soluble compounds. Its six primary catechins are (−)-epicatechin (EC), (−)-epicatechin gallate (ECG), (−)-epigallocatechin (EGC), and (−)-epigallocatechin gallate (EGCG) (Figure 11). According to its high content (up to 50%), the most important and studied tea catechin is EGCG which has greater physiological properties (high scavenging activity of free radicals), while (+) –GC and (+) –C are usually present in trace components. These polyphenolic compounds (hydroxyl groups) have high antioxidant properties as a result of their redox mechanism based on hydrogen donors, reactive oxygen species including superoxide anions, peroxyl radicals, and singlet oxygen, reducing agents, nascent oxygen quenchers, and chelating redox active transition-metal ions. Other antioxidant mechanisms are based on metal ion transition to initiate free radical chain oxidations by decomposing lipid hydroperoxides, and antioxidant activity by inhibiting pro-oxidant enzymes and inducing antioxidant enzymes [128]. Also, these polyphenols have shown inhibitory effects on Gram-positive as well as Gram-negative bacteria, where green tea extract susceptibility against bacterial strains can be related to differences in cell membranes [84]. Green tea extract inclusion into bio-based polymers has been studied by different researchers for antioxidant and antimicrobial food packaging design [84,129,130].

Figure 11. Chemical structure of green tea main components.

1.4.2.2   Rosemary Extract

Rosemary (*Rosmarinus officinalis* L.) is an aromatic plant belonging to Lamiaceae family which has interesting biological activities conferred by phenolic and volatile compounds [131]. Given its health benefits, rosemary has been used for food preservation, cosmetics, pharmaceutic, aromatherapy, and in folk medicine [132]. Rosemary antioxidant activity is mainly contributed to phenolic compounds, such as carnosol, carnosoic acid, rosmanol, rosmadial, epirosmanol, rosmadiphenol, and rosmarinic acid [133]. While antimicrobial activity is mainly attributed to α-pinene

(2 – 25% of composition), (−)-bornyl acetate (0 – 17 %), camphor (2 – 14 %), and 1,8-cineole (3 – 89 %) compounds (Figure 12) [134]. Antimicrobial activity has been tested against Gram-positive bacteria, such as *Staphylococcus epidermidis*, *Staphylococcus aureus*, *Bacillus subtilis* [135]; and Gram-negative bacteria, such as *Escherichia coli*, *Proteus vulgari*, *Pseudomonas aeruginosa* [136]. It has also been tested against fungi strains, such as *Candida albicans* and *Aspergillus niger* [137]. By virtue of its active properties, rosemary has been widely used as additive in active packaging systems to extend food shelf life, preventing lipid, sugar, and protein oxidation, as well as delaying or inhibiting spoilage and pathogenic bacterial growth [138].
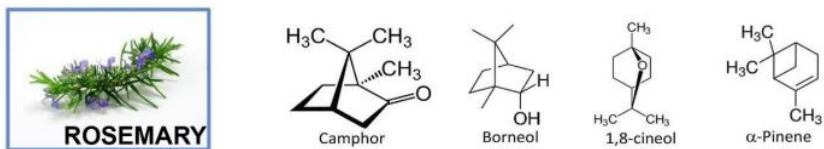
Figure 12. Chemical structure of rosemary main components.

1.4.3 Metallic Nanoparticles

Metallic nanoparticles (MNs) sized 1-100 nm have gained considerable application in biomedicine, biotechnology, chemical sensing, agriculture, and active food packaging. They show more effective physicochemical and biological properties compared to particles (>100 nm) [139,140]. Some of its properties are high surface area and a good distribution due to their charge, shape, surface properties, resistance to high temperature and pressures, and high mechanical stability. Furthermore, some of them are biocompatible, have low cost and toxicity, and even contain mineral elements essential to human health [141-143]. The most common antibacterial inorganic/metallic nanoparticles and metal oxide nanoparticles are silver (Ag), copper (Cu), gold (Au), titanium oxide (TiO_2), zinc oxide (ZnO), silicium oxide (SiO_2), magnesium oxide (MgO) and calcium oxide (CaO). Some of them are categorized as GRAS by U.S. FDA [144-146]. Metallic nanoparticles can be synthesized by mechanochemical processing, sol-gel methods, spray pyrolysis, green chemistry, photochemical methods, chemical reduction, electron irradiation, gamma irradiation, and laser ablation [147-149]. Antimicrobial effects of the Ag, Cu, Au and ZnO are performed by different mechanisms of action such as ion release, where ions interact and disintegrate both the bacterial cell wall and membrane, affecting amines and carboxyl groups in N-acetylglucosamine and N-acetylmuramic acid in the peptidoglycan layer and sulfhydryl groups. There are other action mechanisms such as reactive oxygen species (ROS) that lead to bacterial death; nanoparticle release

which bind to bacterial cell surfaces through electrostatic forces and molecular interactions; transmembrane electron transport interruption and blockage; and direct cell wall or membrane penetration by endocytosis [150-152]. A broad spectrum of metallic nanoparticle bactericide has been reported in most Gram-negative and Gram-positive bacteria by numerous investigations [153-155]. Therefore, high thermal stability, antimicrobial and physical MN properties have driven their inclusion in biopolymer matrices to food active packaging design. Their use in food can be classified as free if incorporated directly as additives or embedded if incorporated into food contact materials [156,157]. The principal MNs used in food packaging have been photocatalysts with antimicrobial and ethylene-scavenging properties. Also, the MNs have shown an improvement in tensile strength, gas, and UV barrier material properties. These are useful properties for safety, quality, and food conservation. Nevertheless, possible MN toxicological properties in food packaging are concerning to consumers; hence MNs migration from packaging into food must be determined to ensure safety of packaging containing MNs [158,159]. However, nanoparticle regulation in food packaging is not clear. This way, materials containing nanoparticles must be assessed to ascertain whether nanoparticles migrate from packaging material into food. If there is no migration or values are within limits, food packaging material should follow the food contact materials regulation directive. MNs migration from packaging into food is caused by diffusion, dissolution, and abrasion of the packaging surface. Therefore, it is necessary to establish toxicological characteristics of MNs used to determine their optimal concentration in packaging when in contact with food products. European Commission (EC) has established regulations specifying conditions in which migration tests must be conducted. Most migration studies and research on nanoparticle migration into food packaging materials have used food simulants depending on the food product type that is in contact with packaging, such as water, ethanol (10 % – 50 % v/v), acetic acid (3 % v/v), and vegetable oil [159]. If nanoparticles migrate to the food product, it will be considered a novel food and, according to EU Regulation on Novel Food (EU) No. 2015/2283, it will require an authorization [117].

1.4.3.1   Zinc oxide (ZnO)

Zinc oxide (ZnO) is a common inorganic material generated in the mineral zincite, but the most common commercial product is made by high-temperature oxidation of metallic zinc or zinc ores. ZnO can have up to three crystal structures including hexagonal wurtzite, cubic zinc-blende structure (Figure 13), and a rarely observed cubic rock-salt (NaCl-type) [103]. The wurtzite form is the most thermodynamically

stable structure in environmental conditions. The zinc-blende structure is metastable while the cubic rock-salt structure is stable under extreme pressure. ZnO has a great number of applications in rubber, ceramics, medicine, food, pharmaceuticals, and cosmetics (e.g., sunscreens) due to their high mechanical and thermal stability with a melting point around 1975 ºC, biocompatibility, low cost and toxicity, and UV-blocking properties. ZnO is also among the five zinc compounds categorized as GRAS by the U.S. FDA (21CFR182.8991). Zinc oxide nanoparticles (ZnONPs) can be synthesized by mechanochemical processing, sol-gel methods, and spray pyrolysis [160]. ZnONPs have biocidal action and strong antibacterial activity; the crystallite size and the nanoparticle shape have an effect on the antibacterial activity where the smaller ZnONPs are the ones with higher antibacterial activity. Also, low concentrations of ZnONPs are nontoxic to eukaryotic, human colorectal carcinoma (HCT-116 cells), human mesenchymal stem (hMS) and fibroblast cells [159,161,162]. The antimicrobial effect of ZnONPs is exerted by different action mechanisms, such as reactive oxygen species (ROS), ion release (Zn^{2+}), membrane dysfunction, nanoparticle penetration, interruption, and blockage of transmembrane electron transport. ZnONPs cause irreversible damage disintegrating the membrane and increasing its permeability. Several reports have shown a broad spectrum of ZnONPs bactericide in most Gram-negative and Gram-positive bacteria, such as *Escherichia coli*, *Salmonella enteritidis*, *Salmonella typhimurium*, *Proteus vulgaris*, *Klebsiella pneumonia*, *Streptococcus pyogenes*, *Aeromonas hydrophila*, *Bacillus subtilis*, *Staphylococcus aureus*, *Listeria monocytogenes*, *Pseudomonas aeruginosa*, *Enterococcus faecalis*, *Sarcina lutea*, *Enterobacter aerogenes*, *Klebsiella pneumonia*, and others [161]. Likewise, they present activity against fungi strains (e.g., *Candida glabrata*, *Candida albicans*, *Pyricularia oryzae*, *Glomus macrocarpum* and *Cryptococcus neoformans*) [163]. Those effects are preserved when ZnONPs are included into polymers, contributing to the control of bacterial growth. Also, they can improve tensile strength, water vapor and oxygen barrier properties, and UV light of the materials [158,164-166].
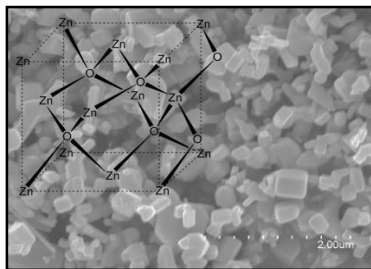
Figure 13. Zinc oxide particles and typical zinc-blende structure.

### 1.4.4 *Active Substances Encapsulation and Protection*

Most active substances such as essential oils, extracts and oleoresins are very sensitive to high temperature/pressure, present high volatility, and oxidation and polymerization susceptibility during storage, losing their bioactivity [167]. Consequently, sensitive substances have been widely encapsulated in polymeric and organic/inorganic materials to protect and maintain their bioactivity in active food packaging. Encapsulation is an attractive technique to entrap and protect unstable active substances (termed core material or active agent) within another substance (coating, shell, or carrier/wall material) from different factors such as light, heat, water, pH, enzymes, and oxygen which affect its stability [168]. Oil encapsulation has many benefits such as oxidation protection, active substances, flavors, vitamin protection from external factors, solubility and mixing property improvement, volatile compound release control to attain a suitable delay for desirable stimulus, prevention of volatile compounds evaporation, making undesirable aroma and tastes, and oil interaction with food component optimization [169,170]. Encapsulation benefits of active food packaging are associated with protection from bioactive compound degradation, volatilization, or undesirable interaction with packaging materials, packaging polymer and bioactive substance compatibility improvement, which increase bioactive substance availability [171]. Encapsulation techniques are usually classified as chemical (e.g., in situ polymerization and liposomes entrapment), physical (e.g., spray-drying, spray chilling, extrusion, fluidized bed coating), and physicochemical (e.g., coacervation process and sol–gel) [168]. There are different delivery systems or carrier systems to encapsulate bioactive compounds, such as cyclodextrins, liposomes, emulsions, halloysites nanotubes, nanofibers by electrospinning (electro-hydrodynamic), nanoparticles (e.g., silica) or microcapsules [117,172,173]. Electro-hydrodynamic (electrospinning and electrospraying) is an active encapsulation emergent technique which has different advantages over other encapsulation technologies, such as not needing to use high temperatures, capability of reducing substance amount on the surface of the structure (non-encapsulated substance); high encapsulation efficiency, sustained encapsulated material release, greater thermal and storage stability, light protection ability, and enhanced chemical degradation bioactive protection [174,175]. In other words, this versatile technique allows a wide variety of synthetic and food-grade polymer processes which, by applying a high-voltage electrostatic field, generate electrospun fibers to obtain nano and microstructures that can be controlled in terms of morphology, size, and porosity, due to process parameter adjustment. These advantages allow a wide range of active substance incorporation into polymer materials to develop active food packaging

systems with bacterial growth control and oxidative degradation reaction inhibition capability [174,176].

1.4.4.1 *Cyclodextrins (CDs)*

Cyclodextrins (CDs) are cyclic oligosaccharides formed by α-1,4 glycosidic linkages, wherein this cyclic structure, glycoside oxygen and hydrogen atoms are oriented toward the cavity, making it hydrophobic [177]. CDs are obtained from starch by the action of the cyclodextrin glycosyltransferase (CDTGase) enzyme that is produced by various bacteria; in this sense, the final ratio of cyclodextrins depends on the enzyme, and the conditions and duration of the reaction. The most used CDs are α-CD (6 glucose molecules), β-CD (7 glucose molecules) and γ-CD (8 glucose molecules) with an inside diameter of 0.57 nm, 0.78 nm and 0.95 nm, respectively (Figure 14a). CDs are conformed by a hydrophobic cavity and a hydrophilic exterior (Figure 14b) which allow the inclusion of guest molecules and form host-guest inclusion complexes due to the fixation capacity of substances of high volatility (e.g., essential oils) and enhancing the solubility of poorly water-soluble compounds, stability, and bioavailability [178-180]. Complexation is a phenomenon in which a cyclodextrin molecule embraces a guest molecule. Some factors that influence the process are the solvent acting on both the cyclodextrin and the guest, the speed rate of dissolution and complexation, and temperature. High temperatures increase the solubility of the CDs and guest; therefore, the optimum temperature to generate complexes also depends on the guest type [181,182]. However, the hydrophobic cavity of the CD molecule gives a more thermodynamically stable environment for the hydrophobic guest than the aqueous environment. CDs stabilize the encapsulated compound against the degradation mechanisms triggered by environmental conditions, reduce the sensory changes by masking strong flavors, and control and delay the release of aromatic substances. CDs are inert and do not interfere with the biological properties of essential oils. Several procedures have been developed to prepare inclusion complexes (e.g., kneading (KM), co-precipitation, heating in a sealed container, freeze drying (FD), spray drying and supercritical fluid technology). KM and FD methods are the most used: (i) Kneading method, also known as slurry complexation, is a method that requires a small amount of solvent in the preparation and gives a very high yield of inclusion. Consequently, it leads to an easier scale-up process and lowers production costs. (ii) Freeze drying is another method that produces a powdered sample in a very good yield of inclusion formation. The low temperature minimizes the loss of extremely volatile guests. This method is especially useful for heat labile compounds [178]. The CDs have been included into polymeric solutions to develop active food packaging [183] which control the release

of the active substances in the inner cavity and act as preservatives, and hence reducing the use of food additives or, in the outer surface of the package, providing protection against environmental factors and increasing the shelf life of the food products given the antimicrobial and antioxidant properties [184]. One of the most employed techniques to develop active food packaging is electrospinning; despite the CD solutions having aggregates that may be electrospun into ultrafine nanofibers. The success of electrospinning of the CD nanofibers could rely on the presence of substantial aggregates and the sufficient intermolecular interactions between the CD molecules, that act as chain entanglements in the CD solution inclusion complexes. In this regard, electrospinning has been used to successfully develop polymer nanofibers containing different types of cyclodextrin (e.g., α-CD, β-CD, and γ-CD), allowing the selective inclusion complex (IC) formation with molecules of different size or differences in affinity of IC formation with one type of molecule [178,185-187].
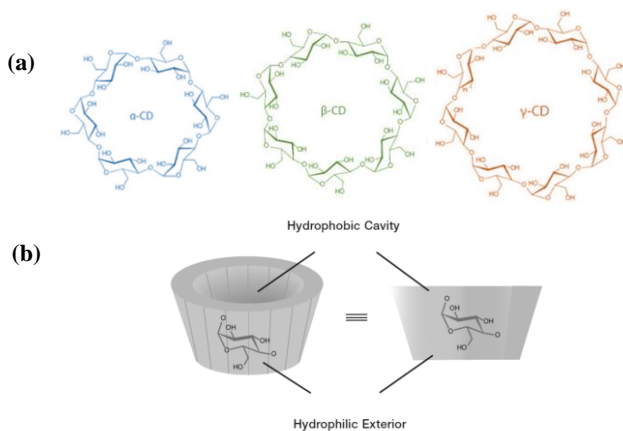

Figure 14. (**a**) Chemical structure and dimensions of α-, β-, and γ-cyclodextrins (CDs) and (**b**) the toroidal shape of α-, β- and γ-cyclodextrins (CDs).

1.5 Electrospinning for Food Packaging

1.5.1 Principles

Electrospinning is a simple and versatile technique for generating ultrathin fibers from a wide variety of polymers that allows material and structural design with improved properties because of its ability to create nano and micro-scale structures with variable fiber diameters and porosity [188]. Electrospinning equipment is essentially formed by a capillary tube with a needle where polymer solution is contained, a power voltage supply which provides electrical forces that exceed the surface tension of viscoelastic polymer solutions, and a collector (e.g., copper plate

aluminum foil or plates, and rotating drums) to collect fibers during the electrospinning process [189]. A typical electrospinning system is schematically illustrated in Figure 15. A polymer solution with optimal molecular entanglement direction forms a droplet at the needle tip by the syringe pump. Then, an electric field is applied to the needle tip and the droplet surface takes on a conical shape due to electrostatic repulsion action and external force; Finally, an electrically charged polymer jet is ejected from the tip of the Taylor cone and directed towards the opposite charge collector. Distance between needle and collector allows solvent evaporation and forms randomly oriented polymer nanofibers which are deposited on collector [174]. Principal parameters that must be controlled during electrospinning process are molecular weight, solvent type, and polymer solution properties (i.e., viscosity, conductivity, dielectric constant, and surface tension) and process parameters, such as electric potential, flow rate, distance between syringe needle and collector plate, and environmental conditions (e.g., temperature, humidity, and air flow). Fiber morphology, diameter distribution, and structure depend on polymer solution; therefore, high concentration allows obtaining thick fibers whereas low concentration produces thin fibers with a variety of cross-sectional shapes. In addition, voltage and distance between syringe needle and collector plate affects fiber morphology [190]. Electrospinning presents several advantages over other techniques since it runs at room temperature, leads to an efficient encapsulation, which avoids antimicrobial loss and antioxidant activity of encapsulated compounds, sustained and controlled release, reduced denaturation, and enhanced bioactive compound stability. Easy bioactive compound incorporation into nanofibers allows their incorporation into polymer matrices for active food packaging systems. Also, the produced nanofibers exhibit structural and functional properties, such as submicron to nanoscale diameters, high surface to volume ratio, suitable porosity, and uniform fiber diameters. These advantages have turned electrospinning into a potential technique for active food packaging design [188,191,192].
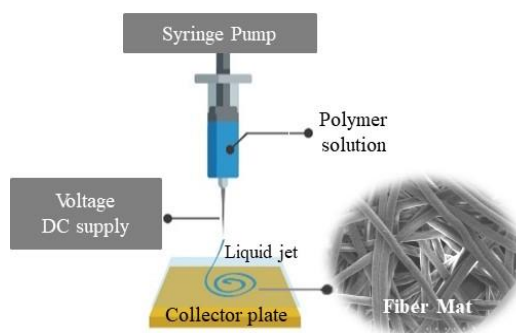
Figure 15. Scheme of a laboratory scale electrospinning equipment.

1.5.2   Electrospun Biopapers

Biopapers, in our context, refers to electrospun fiber-based materials made of very functional biopolymers in terms of physicochemical properties which are biobased and biodegradable, compared to conventional paper based on cellulose that is processed with several chemicals and contains petrochemical additives and/or hydrophobizing coatings [193]. Electrospun PHA biopapers are an alternative for use in developing food industry packaging materials, given that their structures are processed with minimal thermal exposure to obtain continuous, homogeneous, and flexible films with improved mechanical strength, optic, gas, water, and oxygen barrier properties. Furthermore, metallic nanoparticles and bioactive substance incorporation into biopapers by electrospinning allows the formation of coatings, interlayers, bilayers, and multilayers with functional properties to develop scavenger (oxygen-scavenging) and release (antioxidant and antimicrobial) active food packaging types [193,194].

1.5.3   Advantages over Conventional Film Manufacturing Techniques

Main polymer processing techniques to develop food packaging films and sheets are solvent casting, cast extrusion, injection molding, blow molding, and compression molding [195]. The most commonly used method for a laboratory biopolymer film formation is solvent casting that largely depends on polymer solubility. This method consists of three basic steps; first, biopolymer solubilization in a solvent, which is chosen according to biopolymer chemical structure; second, the solution is poured into mold, which are usually Teflon-coated glass plates; and third, the casted solution is heat dried where solvent is evaporated to obtain a polymer film adhered to mold with a homogeneous and continuous microstructure [196,197]. Lastly, physical and chemical properties of the film are dependent on casting solution composition, wet casting thickness and drying conditions (e.g., temperature and relative humidity) [198].

The extrusion process is extensively used for commercial edible film/packaging material production with good mechanical, barrier, and optical properties. Extrusion essentially consists in a complex physical-chemical process that takes place under mechanical forces, high temperature and/or humidity influences. This process follows different steps, such as polymer heating and melting, pumping polymer into a shaping unit, forming the melt into required shape and dimensions, and cooling and solidification. Extrusion can be continuous (theoretically producing an indefinitely long piece) or semi-continuous (producing many pieces). This process allows obtaining materials with a fixed cross-section profile where a material is pushed or pulled through a die with desired cross-section and has many advantages, such as a

simple forming process, high production efficiency, good surface quality, and near-net-shape forming. Post-extrusion procedures will depend mostly on extrudate geometry and dimensions [199,200].

In the cast film extrusion process, film dimensions are primarily controlled by die geometry, extrusion speed and take-off speed. In this process molten polymer is conducted through a flat head system (co-extrusion block and head, for co-extrusion processes, or head only, when it is a single extrusion) where it comes tangentially into contact with a first cooling roll, which forces melt against cooling roll, increasing contact angle between them; then, it passes through a second cooling roll which removes trapped air between film and roll, decreasing cooling rates; after that, film is longitudinally pulled by rubber coated nip rolls and winded up [200].

Injection molding is a cyclical process that consists in melting in a mold cavity, followed by cooling and extraction. Melting, mixing, and pumping are carried out by a plasticizing unit with an axial back and forth movement screw. Material fed by a vertical hopper is melted and accumulated between nozzle and screw tip. Then, the mold is completely filled as a result of material displacement generated by screw through nozzle using pressure. Once the material solidifies, the mold opens, and the part is removed. The machine is usually composed of four systems assembled on a common base, such as an injection system containing plasticizing unit; a hydraulic, electric, or combined power system that controls screw movements; a mold clamping system (it can be a two-plate mold, a three-plate mold, or a hot-runner mold); and a process parameters control system (e.g., pressure, time, and temperature). This process presents precision, reproducibility, and control capacity, as well as versatility to produce parts with different characteristics [200].

Blow molding has two process stages. In the first step, plastic is injected into a cavity where the preform is molded. Then, the preform is transferred to a blow mold for inflation. Essentially, blow molding is a process where materials are formed by the inflation of a molten polymer to fill a mold cavity with a specific shape and dimensions. An extruder pumps polymer through an annular die to form a molten parison with exact and controlled dimensions. The parison is clamped between both mold halves and inflated by internal air pressure to take the mold cavity shape, which is usually cooled. After that, the material solidifies due to cooling, which is optimal to extract vessel from mold. This process has advantages, such as precise dimensional control, waste elimination, and thread molding before blowing. Likewise, it is simple and economical, and is widely used to produce different sized containers and with significant thickness distribution [200].

Compression molding is another two-step manufacturing process, first one preheating and pressurizing. The process essentially consists in introducing polymer

into an open, heated mold cavity with a specific shape, where polymer is pressed into the mold by the heated plates of a hydraulic press, producing compression while heat and pressure are maintained until molding material has cured and takes mold shape [201]. The process is divided in two types: cold compression and hot compression molding. It is mainly used for thermoset materials [202]. In cold compression molding, pressure is applied, and the curing process takes place at room temperature; in hot compression, the molding pressure and temperature are applied, then molding preforms are placed in a mold cavity where the curing process takes place by applying heat to mold which is, in turn, transferred to composites [44]. With this process it is possible to produce parts with a wide array of lengths, thicknesses, complexities which are also high in strength. It is, as well, an interesting way of producing rigid polymer-based materials since it is fast and requires no solvent [203], providing a water vapor permeability reduction while helping to overcome some implicit drawbacks that biopolymers present, mainly poor mechanical properties [204].

Regarding the process methods mentioned above, the electrospinning technique is a broadly used and efficient technology for micro- and nano-fiber mat formation (see section 1.5.1 and 1.5.2). This technique has great versatility to produce ultrathin structures with controlled size, diameters, and porosity that cannot be achieved using other conventional technologies. Additionally, the capability to work at room temperature allows thermal sensitive substance processing. Cherpinski et al. [205] reported that electrospinning obtained poly(3-hydroxybutyrate) (PHB) films and showed similar rigidity to conventional compression-molded films, but with enhanced elongation at break and toughness. Moreover, in terms of oxygen, water vapor, and limonene permeability, electrospun PHB films showed better results. In this regard, biopapers have potential applications in the development of barrier and active layers, adhesive interlayers, and coatings for food packaging materials [84,103,193,194].

1.6   Multilayer Packaging

Multilayer systems are composed of materials created from the combination of different layers typically based on polymers with dissimilar properties glued together, achieving functions that monomaterials do not offer [206,207]. Multilayers are composed of "structural" layers, usually on the outside, and "barrier" layers on the inside. An "active" layer can also be added, either on the outside or inside, depending on the application. Layers of adhesive polymers, named "tie layers," are used as glue between the different layers if needed. The purpose of using multilayer systems is to improve the properties of the food packaging. The majority of polymers, particularly biopolymers, present a low barrier to water vapor and/or oxygen as well as poor

mechanical performance [208-210]. Likewise, the inclusion of the active substances (e.g., essential oils and metallic nanoparticles) in one of the layers can confer antimicrobial and antioxidant properties [211]. Active packaging (active layer) can be developed in two ways: an active layer containing the antimicrobial/antioxidant agents that migrate to the surface of the food or active agents bounded to the surface layer of the films (active coating) [212], and the mechanism of the antimicrobial substances consists in the releasing of the active agents from the active layer to the food surface controlled by the food contact layer. The multilayer systems are obtained by different methods (e.g., extrusion, lamination, electrospinning, co-extrusion, and extrusion coating), followed by lamination treatment, where each layer is usually made by adhesives, compression molding, atmospheric air cold plasma and thermal treatments. In this context, electrospinning technology can be considered very effective in preparing active packaging materials with sustained released capacity through coatings or interlayers containing entrapped substances with functionality. Moreover, the electrospun interlayers have the capacity of layers' adhesion, which avoids the use of adhesive substances that usually are employed in the conventional process to develop multilayer systems [213,214]. A typical multilayer system with antimicrobial and barrier properties, shown in Figure 16, consists of four layers, including the structural layer, the barrier layer, the active layer, and the food contact layer; additionally, in Table 4, some examples of multilayer systems developed by electrospinning are enounced.
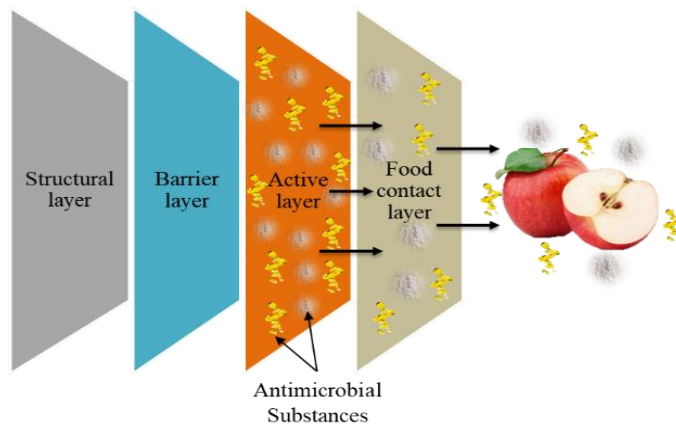
Figure 16. Active multilayer system structure [212].

Table 4. Some multilayer structures based on annealed electrospun biopolymer coatings

Multilayer structure	Active substances	Highlighted result	Reference
PLA/Electrospun PLA+GA film/PLA	Gallic Acid (GA)	Multilayers presented sufficient adhesion between layers and high transparency. The incorporation of GA delayed the thermal degradation of PLA. Also, it had a sustained release of the natural antioxidant (GA) for extended periods	Quiles-Carrillo et al. [213]
-Paper/PVOH/PHB film -Paper/PLA/PHB film	---	The developed annealed electrospun coatings resulted in a significant improvement of the paper barrier properties to water and limonene vapors, being the Paper/PVOH/PHB film the best performing multilayer packaging structure	Cherpinski et al. [215]
-PHBV + zein/CNMA + PHBV -PHBV8 + zein/CNMA + alginate	Cinnamaldehyde (CNMA)	The active multilayer systems improved stability, efficiency and release of CNMA and showed antibacterial activity against *Listeria monocytogenes*, being the PHBV + zein/CNMA + PHBV multilayer the one that showed the greater antibacterial activity	Cerqueira et al. [192]
PCL/OR+GEL+PCL/OR	Black pepper oleoresin (OR)	The multilayer system improved the thermal resistance, the permeance to water vapor and showed strong antimicrobial activity after 10 days against *S. aureus* strains	Figueroa-Lopez et al. [216]

1.7   Overview of European Projects Dealing with PHAs for Food Packaging

The feasibility of PHA production using waste and other carbon feedstocks to develop food packaging materials has been demonstrated by several recent European projects. In this regard, the VOLATILE project aimed at the development of an innovative Volatile Fatty Acids Platform for the bioconversion of municipal solid biowaste fraction and sludgy biowaste from other industries [217]. The PAPER-P (2016) project showed a novel technology to synthetize high quality PHA bioplastics (98% purity) from on-site paper waste [218]. Through an extremely cost-effective process, it was demonstrated that PAPER-P can be seen as a unique technology able to use rough material printed waste and/or waste solvent and ink, with an approximate price of €0.1/Kg, to transform them into PHA. This results in a 60 times more valuable product worth, that is, €6/Kg, thus quadruplicating printers' Return on Investment (ROI), from current 2-8% up to 30%. The YPACK (2017) project, to which this PhD thesis has been contributing, aimed at optimizing the performance of cheese whey and almond shell bioproducts to derive PHA-based thermoformed trays and high barrier multilayers blown films for food packaging applications [219]. The BioBarr (2017) project also proposed the development of new bio-based and biodegradable food packaging materials by enhancing barrier functionalities of PHAs, and validating the new material in a food industry environment [220]. The RES URBIS (REsources from URban BIo-waSte, 2017) project aimed at making it possible to convert several types of urban bio-waste into valuable bio-based products, including PHAs, in an integrated single biowaste biorefinery and by using one main technology chain [221]. In the same topic, the POLIPO (2018) project aimed at developing the first chemical route (not based on bacterial fermentation) to produce PHA from vegetal oils and fats [222]. POLIPO's chemical route to PHAs can potentially represent a game-changing technology in the field of bioplastics, making it possible to produce a biodegradable plastic with some cost reduction advantages with respect to current conventional fermentative routes. More recently, the VEnvirotech (2019) project proposed a solution based on biotechnology, with the use of bacteria, to transform organic waste into biodegradable PHA bioplastics at significantly lower costs [223]. The innovative technology envisages reducing waste management costs by 30 %, as well as bioplastics price by 50 %. Similarly, the BterBioPlastics (2019) project aimed at creating biodegradable materials to reduce global environment pollution, examining pilot fermentations and metabolic modulation strategies to raise the level of bioplastics production [224]. The USABLE Packaging (2019) project also aimed at developing high-performance PHA based packaging through a sustainable and fully circular value chain, where the biomass

raw material sourcing derives from food processing side streams [225]. Finally, the NENU2PHAR (2020) project aimed at taking a holistic approach that includes raw materials production with microalgae and bacteria, the formulation and processing of biopolymers, and the production of eight different PHA-based products [226].

References

1. Sorrentino, A.; Gorrasi, G.; Vittoria, V. Potential perspectives of bio-nanocomposites for food packaging applications. *Trends in Food Science & Technology* **2007**, *18*, 84-95.
2. Zeng, T.; Deschênes, J.; Durif, F. Eco-design packaging: An epistemological analysis and transformative research agenda. *Journal of Cleaner Production* **2020**, *276*, 123361.
3. Rhim, J.-W.; Park, H.-M.; Ha, C.-S. Bio-nanocomposites for food packaging applications. *Progress in Polymer Science* **2013**, *38*, 1629-1652.
4. Yadav, B.; Chavan, S.; Atmakuri, A.; Tyagi, R.D.; Drogui, P. A review on recovery of proteins from industrial wastewaters with special emphasis on PHA production process: Sustainable circular bioeconomy process development. *Bioresource Technology* **2020**, *317*, 124006.
5. Food and Agriculture Organization of The United Nations (FAO). Global food losses and food waste. **2011**. Availabe online: (accessed on http://www.fao.org/3/mb060e/mb060e00.pdf).
6. Jubinville, D.; Esmizadeh, E.; Saikrishnan, S.; Tzoganakis, C.; Mekonnen, T. A comprehensive review of global production and recycling methods of polyolefin (PO) based products and their post-recycling applications. *Sustainable Materials and Technologies* **2020**, *25*, e00188.
7. Mesa, J.; González-Quiroga, A.; Maury, H. Developing an indicator for material selection based on durability and environmental footprint: A Circular Economy perspective. *Resources, Conservation and Recycling* **2020**, *160*, 104887.
8. Kaszycki, P.; Głodniok, M.; Petryszak, P. Towards a bio-based circular economy in organic waste management and wastewater treatment – The Polish perspective. *New Biotechnology* **2021**, *61*, 80-89.
9. Talan, A.; Kaur, R.; Tyagi, R.D.; Drogui, P. Bioconversion of oily waste to polyhydroxyalkanoates: Sustainable technology with circular bioeconomy approach and multidimensional impacts. *Bioresource Technology Reports* **2020**, *11*, 100496.
10. Jõgi, K.; Bhat, R. Valorization of food processing wastes and by-products for bioplastic production. *Sustainable Chemistry and Pharmacy* **2020**, *18*, 100326.
11. Taoukis, P.; Smolander, M. 18 - Biobased intelligent food packaging. In *Environmentally Compatible Food Packaging*, Chiellini, E., Ed. Woodhead Publishing: **2008**, 439-458.
12. Sirohi, R.; Prakash Pandey, J.; Kumar Gaur, V.; Gnansounou, E.; Sindhu, R. Critical overview of biomass feedstocks as sustainable substrates for the production of polyhydroxybutyrate (PHB). *Bioresource Technology* **2020**, *311*, 123536.
13. Williams, C.K.; Hillmyer, M.A. Polymers from Renewable Resources: A Perspective for a Special Issue of Polymer Reviews. *Polymer Reviews* **2008**, *48*, 1-10.
14. Xie, Y.; Kohls, D.; Noda, I.; Schaefer, D.W.; Akpalu, Y.A. Poly(3-hydroxybutyrate-co-3-hydroxyhexanoate) nanocomposites with optimal mechanical properties. *Polymer* **2009**, *50*, 4656-4670.
15. Payne, J.; McKeown, P.; Jones, M.D. A circular economy approach to plastic waste. *Polymer Degradation and Stability* **2019**, *165*, 170-181.
16. Tharanathan, R.N. Biodegradable films and composite coatings: past, present and future. *Trends in Food Science & Technology* **2003**, *14*, 71-78.
17. Ashter, S.A. 5 - Types of Biodegradable Polymers. In *Introduction to Bioplastics Engineering*, Ashter, S.A., Ed. William Andrew Publishing: Oxford, **2016**, 81-151.
18. Laycock, B.; Nikolić, M.; Colwell, J.M.; Gauthier, E.; Halley, P.; Bottle, S.; George, G. Lifetime prediction of biodegradable polymers. *Progress in Polymer Science* **2017**, *71*, 144-189.
19. Thakur, S.; Chaudhary, J.; Sharma, B.; Verma, A.; Tamulevicius, S.; Thakur, V.K. Sustainability of bioplastics: Opportunities and challenges. *Current Opinion in Green and Sustainable Chemistry* **2018**, *13*, 68-75.
20. Tsang, Y.F.; Kumar, V.; Samadar, P.; Yang, Y.; Lee, J.; Ok, Y.S.; Song, H.; Kim, K.-H.; Kwon, E.E.; Jeon, Y.J. Production of bioplastic through food waste valorization. *Environment International* **2019**, *127*, 625-644.
21. Balan, V. Current Challenges in Commercially Producing Biofuels from Lignocellulosic Biomass. *ISRN Biotechnology* **2014**, *2014*, 463074.
22. Nielsen, C.; Rahman, A.; Rehman, A.U.; Walsh, M.K.; Miller, C.D. Food waste conversion to microbial polyhydroxyalkanoates. *Microbial biotechnology* **2017**, *10*, 1338-1352.
23. Braunegg, G.; Lefebvre, G.; Genser, K.F. Polyhydroxyalkanoates, biopolyesters from renewable resources: Physiological and engineering aspects. *Journal of Biotechnology* **1998**, *65*, 127-161.

24. Cui, S.; Borgemenke, J.; Liu, Z.; Li, Y. Recent advances of "soft" bio-polycarbonate plastics from carbon dioxide and renewable bio-feedstocks via straightforward and innovative routes. *Journal of CO2 Utilization* **2019**, *34*, 40-52.

25. Höfer, R.; Selig, M. 10.02 - Green Chemistry and Green Polymer Chemistry. In *Polymer Science: A Comprehensive Reference*, Matyjaszewski, K., Möller, M., Eds. Elsevier: Amsterdam, 2012, 5-14.

26. Hatti-Kaul, R.; Nilsson, L.J.; Zhang, B.; Rehnberg, N.; Lundmark, S. Designing Biobased Recyclable Polymers for Plastics. *Trends in Biotechnology* **2020**, *38*, 50-67.

27. Torres-Giner, S.; Montanes, N.; Fombuena, V.; Boronat, T.; Sanchez-Nacher, L. Preparation and characterization of compression-molded green composite sheets made of poly(3-hydroxybutyrate) reinforced with long pita fibers. *Advances in Polymer Technology* **2018**, *37*, 1305-1315.

28. Mutlu, G.; Calamak, S.; Ulubayram, K.; Guven, E. Curcumin-loaded electrospun PHBV nanofibers as potential wound-dressing material. *Journal of Drug Delivery Science and Technology* **2018**, *43*, 185-193.

29. Laycock, B.; Halley, P.; Pratt, S.; Werker, A.; Lant, P. The chemomechanical properties of microbial polyhydroxyalkanoates. *Progress in Polymer Science* **2014**, *39*, 397-442.

30. Colombo, B.; Favini, F.; Scaglia, B.; Sciarria, T.P.; D'Imporzano, G.; Pognani, M.; Alekseeva, A.; Eisele, G.; Cosentino, C.; Adani, F. Enhanced polyhydroxyalkanoate (PHA) production from the organic fraction of municipal solid waste by using mixed microbial culture. *Biotechnology for biofuels* **2017**, *10*, 201.

31. Koller, M. A Review on Established and Emerging Fermentation Schemes for Microbial Production of Polyhydroxyalkanoate (PHA) Biopolyesters. *Fermentation* **2018**, *4*, 30.

32. Zikmanis, P.; Kolesovs, S.; Semjonovs, P. Production of biodegradable microbial polymers from whey. *Bioresources and Bioprocessing* **2020**, *7*, 36.

33. Park, S.J.; Kim, T.W.; Kim, M.K.; Lee, S.Y.; Lim, S.C. Advanced bacterial polyhydroxyalkanoates: towards a versatile and sustainable platform for unnatural tailor-made polyesters. *Biotechnology advances* **2012**, *30*, 1196-1206.

34. Poltronieri, P.; Kumar, P. Polyhydroxyalcanoates (PHAs) in Industrial Applications. In *Handbook of Ecomaterials*, Martínez, L.M.T., Kharissova, O.V., Kharisov, B.I., Eds. Springer International Publishing: Cham, **2017**, 1-30.

35. Reddy, C.S.K.; Ghai, R.; Rashmi; Kalia, V.C. Polyhydroxyalkanoates: an overview. *Bioresource Technology* **2003**, *87*, 137-146.

36. Choi, J.-i.; Lee, S.Y. Process analysis and economic evaluation for Poly(3-hydroxybutyrate) production by fermentation. *Bioprocess Engineering* **1997**, *17*, 335-342.

37. Yeo, J.C.C.; Muiruri, J.K.; Thitsartarn, W.; Li, Z.; He, C. Recent advances in the development of biodegradable PHB-based toughening materials: Approaches, advantages and applications. *Materials Science and Engineering: C* **2018**, *92*, 1092-1116.

38. McChalicher, C.W.; Srienc, F. Investigating the structure-property relationship of bacterial PHA block copolymers. *J Biotechnol* **2007**, *132*, 296-302.

39. Zhuikov, V.A.; Zhuikova, Y.V.; Makhina, T.K.; Myshkina, V.L.; Rusakov, A.; Useinov, A.; Voinova, V.V.; Bonartseva, G.A.; Berlin, A.A.; Bonartsev, A.P., et al. Comparative Structure-Property Characterization of Poly(3-Hydroxybutyrate-Co-3-Hydroxyvalerate)s Films under Hydrolytic and Enzymatic Degradation: Finding a Transition Point in 3-Hydroxyvalerate Content. *Polymers (Basel)* **2020**, *12*, 728.

40. Righetti, M.C.; Aliotta, L.; Mallegni, N.; Gazzano, M.; Passaglia, E.; Cinelli, P.; Lazzeri, A. Constrained Amorphous Interphase and Mechanical Properties of Poly(3-Hydroxybutyrate-co-3-Hydroxyvalerate). *Front Chem* **2019**, *7*, 790-790.

41. Keshavarz, T.; Roy, I. Polyhydroxyalkanoates: bioplastics with a green agenda. *Current Opinion in Microbiology* **2010**, *13*, 321-326.

42. Ragaert, P.; Buntinx, M.; Maes, C.; Vanheusden, C.; Peeters, R.; Wang, S.; D'Hooge, D.R.; Cardon, L. Polyhydroxyalkanoates for Food Packaging Applications. In *Reference Module in Food Science*, Elsevier: **2019**.

43. Requena, R.; Vargas, M.; Chiralt, A. Release kinetics of carvacrol and eugenol from poly(hydroxybutyrate-co-hydroxyvalerate) (PHBV) films for food packaging applications. *European Polymer Journal* **2017**, *92*, 185-193.

44. Torres-Giner, S.; Hilliou, L.; Melendez-Rodriguez, B.; Figueroa-Lopez, K.J.; Madalena, D.; Cabedo, L.; Covas, J.A.; Vicente, A.A.; Lagaron, J.M. Melt processability, characterization, and antibacterial activity of compression-molded green composite sheets made of poly(3-hydroxybutyrate-co-3-hydroxyvalerate) reinforced with coconut fibers impregnated with oregano essential oil. *Food Packaging and Shelf Life* **2018**, *17*, 39-49.

45. FAO. The Food and Agriculture Organization of The United Nations. Availabe online: (accessed on

46. Ahvenainen, R. 1 - Introduction. In *Novel Food Packaging Techniques*, Ahvenainen, R., Ed. Woodhead Publishing: 200, 1-2.

47. Wunderlich, S.M.; Martinez, N.M. Conserving natural resources through food loss reduction: Production and consumption stages of the food supply chain. *International Soil and Water Conservation Research* **2018**, *6*, 331-339.

48. Majid, I.; Ahmad Nayik, G.; Mohammad Dar, S.; Nanda, V. Novel food packaging technologies: Innovations and future prospective. *Journal of the Saudi Society of Agricultural Sciences* **2018**, *17*, 454-462.

49. Torres-Giner, S., Luis Gil, Pascual-Ramírez, Leonor, and Garde-Belza, José A. Packaging: Food Waste Reduction; In book: *Encyclopedia of Polymer Applications*, Publisher: CRC Press, **2018**.

50. Ma, M.; Sun, Q.J.; Li, M.; Zhu, K.X. Deterioration mechanisms of high-moisture wheat-based food - A review from physicochemical, structural, and molecular perspectives. *Food chemistry* **2020**, *318*, 126495.

51. Santagata, G.; Mallardo, S.; Fasulo, G.; Lavermicocca, P.; Valerio, F.; Di Biase, M.; Di Stasio, M.; Malinconico, M.; Volpe, M.G. Pectin-honey coating as novel dehydrating bioactive agent for cut fruit: Enhancement of the functional properties of coated dried fruits. *Food chemistry* **2018**, *258*, 104-110.

52. Soliva-Fortuny, R.C.; Martín-Belloso, O. New advances in extending the shelf-life of fresh-cut fruits: a review. *Trends in Food Science & Technology* **2003**, *14*, 341-353.

53. Sharma, C.; Dhiman, R.; Rokana, N.; Panwar, H. Nanotechnology: An Untapped Resource for Food Packaging. *Front Microbiol* **2017**, *8*, 1735-1735.

54. Lau, O.-W.; Wong, S.-K. Contamination in food from packaging material. *Journal of Chromatography A* **2000**, *882*, 255-270.

55. Guilbert, S.; Gontard, N.; Cuq, B. Technology and applications of edible protective films. *Packaging Technology and Science* **1995**, *8*, 339-346.

56. Genovese, L.; Lotti, N.; Gazzano, M.; Siracusa, V.; Dalla Rosa, M.; Munari, A. Novel biodegradable aliphatic copolyesters based on poly(butylene succinate) containing thioether-linkages for sustainable food packaging applications. *Polymer Degradation and Stability* **2016**, *132*, 191-201.

57. Geyer, R.; Jambeck, J.R.; Law, K.L. Production, use, and fate of all plastics ever made. *Science Advances* **2017**, *3*, e1700782.

58. Huang, Q.; Lin, Y.; Zhong, Q.; Ma, F.; Zhang, Y. The Impact of Microplastic Particles on Population Dynamics of Predator and Prey: Implication of the Lotka-Volterra Model. *Scientific Reports* **2020**, *10*, 4500.

59. La Mantia, F.P.; Morreale, M. Green composites: A brief review. *Composites Part A: Applied Science and Manufacturing* **2011**, *42*, 579-588.

60. Sharma, R.; Jafari, S.M.; Sharma, S. Antimicrobial bio-nanocomposites and their potential applications in food packaging. *Food Control* **2020**, *112*, 107086.

61. Zhang, C.; Li, Y.; Wang, P.; Zhang, H. Electrospinning of nanofibers: Potentials and perspectives for active food packaging. *Comprehensive Reviews in Food Science and Food Safety* **2020**, *19*, 479-502.

62. Byun, Y.; Darby, D.; Cooksey, K.; Dawson, P.; Whiteside, S. Development of oxygen scavenging system containing a natural free radical scavenger and a transition metal. *Food chemistry* **2011**, *124*, 615-619.

63. Ozdemir, M.; Floros, J.D. Active food packaging technologies. *Critical reviews in food science and nutrition* **2004**, *44*, 185-193.

64. Torres-Giner, S.; Prieto, C.; Lagaron, J.M. Nanomaterials to Enhance Food Quality, Safety, and Health Impact. *Nanomaterials* **2020**, *10*, 941.

65. Appendini, P.; Hotchkiss, J.H. Review of antimicrobial food packaging. *Innovative Food Science & Emerging Technologies* **2002**, *3*, 113-126.

66. *Code Fed. Regul. (Cfr). Title 21 Food Drugs. Chapter I—Food Drug Adm. Dep. Heal. Hum. Serv. Subchapter b—Food Hum. Consum. (Continued), Part 182—Subst. Gen. Recognized as Safe (Gras)* **2016**.

67. Yildirim, S.; Röcker, B.; Pettersen, M.K.; Nilsen-Nygaard, J.; Ayhan, Z.; Rutkaite, R.; Radusin, T.; Suminska, P.; Marcos, B.; Coma, V. Active Packaging Applications for Food. *Comprehensive Reviews in Food Science and Food Safety* **2018**, *17*, 165-199.

68. Gaikwad, K.K.; Singh, S.; Lee, Y.S. Oxygen scavenging films in food packaging. *Environmental Chemistry Letters* **2018**, *16*, 523-538.

69. Biji, K.B.; Ravishankar, C.N.; Mohan, C.O.; Srinivasa Gopal, T.K. Smart packaging systems for food applications: a review. *Journal of Food Science and Technology* **2015**, *52*, 6125-6135.

70. Dey, A.; Neogi, S. Oxygen scavengers for food packaging applications: A review. *Trends in Food Science & Technology* **2019**, *90*, 26-34.

71. Rai, M.; Ingle, A.P.; Gupta, I.; Pandit, R.; Paralikar, P.; Gade, A.; Chaud, M.V.; dos Santos, C.A. Smart nanopackaging for the enhancement of food shelf life. *Environmental Chemistry Letters* **2019**, *17*, 277-290, doi:10.1007/s10311-018-0794-8.

72. Lee, D.S. Carbon dioxide absorbers for food packaging applications. *Trends in Food Science & Technology* **2016**, *57*, 146-155.

73. Al-Tayyar, N.A.; Youssef, A.M.; Al-hindi, R. Antimicrobial food packaging based on sustainable Bio-based materials for reducing foodborne Pathogens: A review. *Food chemistry* **2020**, *310*, 125915.

74. Tyuftin, A.A.; Kerry, J.P. Review of surface treatment methods for polyamide films for potential application as smart packaging materials: surface structure, antimicrobial and spectral properties. *Food Packaging and Shelf Life* **2020**, *24*, 100475.

75. Ju, J.; Chen, X.; Xie, Y.; Yu, H.; Guo, Y.; Cheng, Y.; Qian, H.; Yao, W. Application of essential oil as a sustained release preparation in food packaging. *Trends in Food Science & Technology* **2019**, *92*, 22-32.

76. Benbettaïeb, N.; Debeaufort, F.; Karbowiak, T. Bioactive edible films for food applications: mechanisms of antimicrobial and antioxidant activity. *Critical reviews in food science and nutrition* **2019**, *59*, 3431-3455.

77. Huang, T.; Qian, Y.; Wei, J.; Zhou, C. Polymeric Antimicrobial Food Packaging and Its Applications. *Polymers (Basel)* **2019**, *11*, 560.

78. Joerger, R.D. Antimicrobial films for food applications: a quantitative analysis of their effectiveness. *Packaging Technology and Science* **2007**, *20*, 231-273.

79. Kyzioł, A.; Khan, W.; Sebastian, V.; Kyzioł, K. Tackling microbial infections and increasing resistance involving formulations based on antimicrobial polymers. *Chemical Engineering Journal* **2020**, *385*, 123888.

80. Chen, A.; Peng, H.; Blakey, I.; Whittaker, A.K. Biocidal Polymers: A Mechanistic Overview. *Polymer Reviews* **2017**, *57*, 276-310.

81. Ren, W.; Cheng, W.; Wang, G.; Liu, Y. Developments in antimicrobial polymers. *Journal of Polymer Science Part A: Polymer Chemistry* **2017**, *55*, 632-639.

82. Mukheem, A.; Shahabuddin, S.; Akbar, N.; Anwar, A.; Sarih, N.M.; Sudesh, K.; Khan, N.A.; Sridewi, N. Fabrication of biopolymer polyhydroxyalkanoate/chitosan and 2D molybdenum disulfide-doped scaffolds for antibacterial and biomedical applications. *Applied microbiology and biotechnology* **2020**, *104*, 3121-3131.

83. Castro-Mayorga, J.L.; Freitas, F.; Reis, M.A.M.; Prieto, M.A.; Lagaron, J.M. Biosynthesis of silver nanoparticles and polyhydroxybutyrate nanocomposites of interest in antimicrobial applications. *International Journal of Biological Macromolecules* **2018**, *108*, 426-435.

84. Figueroa-Lopez, K.J.; Vicente, A.A.; Reis, M.A.M.; Torres-Giner, S.; Lagaron, J.M. Antimicrobial and Antioxidant Performance of Various Essential Oils and Natural Extracts and Their Incorporation into Biowaste Derived Poly(3-hydroxybutyrate-co-3-hydroxyvalerate) Layers Made from Electrospun Ultrathin Fibers. *Nanomaterials (Basel, Switzerland)* **2019**, *9*.

85. Melendez-Rodriguez, B.; Figueroa-Lopez, K.J.; Bernardos, A.; Martínez-Máñez, R.; Cabedo, L.; Torres-Giner, S.; Lagaron, J.M. Electrospun Antimicrobial Films of Poly(3-hydroxybutyrate-co-3-hydroxyvalerate) Containing Eugenol Essential Oil Encapsulated in Mesoporous Silica Nanoparticles. *Nanomaterials (Basel, Switzerland)* **2019**, *9*.

86. Ayala, A.; Muñoz, M.F.; Argüelles, S. Lipid peroxidation: production, metabolism, and signaling mechanisms of malondialdehyde and 4-hydroxy-2-nonenal. *Oxid Med Cell Longev* **2014**, *2014*, 360438.

87. Domínguez, R.; Pateiro, M.; Gagaoua, M.; Barba, F.J.; Zhang, W.; Lorenzo, J.M. A Comprehensive Review on Lipid Oxidation in Meat and Meat Products. *Antioxidants (Basel)* **2019**, *8*, 429.

88. Perumalla, A.V.S.; Hettiarachchy, N.S. Green tea and grape seed extracts — Potential applications in food safety and quality. *Food Research International* **2011**, *44*, 827-839.

89. Islam, R.U.; Khan, M.A.; Islam, S.U. Plant Derivatives as Promising Materials for Processing and Packaging of Meat-Based Products — Focus on Antioxidant and Antimicrobial Effects. *Journal of Food Processing and Preservation* **2017**, *41*, e12862.

90. Vilela, C.; Kurek, M.; Hayouka, Z.; Röcker, B.; Yildirim, S.; Antunes, M.D.C.; Nilsen-Nygaard, J.; Pettersen, M.K.; Freire, C.S.R. A concise guide to active agents for active food packaging. *Trends in Food Science & Technology* **2018**, *80*, 212-222.

91. Gómez-Estaca, J.; López-de-Dicastillo, C.; Hernández-Muñoz, P.; Catalá, R.; Gavara, R. Advances in antioxidant active food packaging. *Trends in Food Science & Technology* **2014**, *35*, 42-51.

92. López-de-Dicastillo, C.; Gómez-Estaca, J.; Catalá, R.; Gavara, R.; Hernández-Muñoz, P. Active antioxidant packaging films: Development and effect on lipid stability of brined sardines. *Food chemistry* **2012**, *131*, 1376-1384.

93. Lobo, V.; Patil, A.; Phatak, A.; Chandra, N. Free radicals, antioxidants and functional foods: Impact on human health. *Pharmacogn Rev* **2010**, *4*, 118-126, doi:10.4103/0973-7847.70902.
94. Kurutas, E.B. The importance of antioxidants which play the role in cellular response against oxidative/nitrosative stress: current state. *Nutrition journal* **2016**, *15*, 71.
95. Wu, C.-S. Comparative assessment of the interface between poly(3-hydroxybutyrate-co-3-hydroxyvalerate) and fish scales in composites: Preparation, characterization, and applications. *Materials Science and Engineering: C* **2019**, *104*, 109878.
96. Urbina, L.; Eceiza, A.; Gabilondo, N.; Corcuera, M.Á.; Retegi, A. Valorization of apple waste for active packaging: multicomponent polyhydroxyalkanoate coated nanopapers with improved hydrophobicity and antioxidant capacity. *Food Packaging and Shelf Life* **2019**, *21*, 100356.
97. Bhatia, S.K.; Wadhwa, P.; Hong, J.W.; Hong, Y.G.; Jeon, J.M.; Lee, E.S.; Yang, Y.H. Lipase mediated functionalization of poly(3-hydroxybutyrate-co-3-hydroxyvalerate) with ascorbic acid into an antioxidant active biomaterial. *Int J Biol Macromol* **2019**, *123*, 117-123.
98. Gendy, A.N.E.; Leonardi, M.; Mugnaini, L.; Bertelloni, F.; Ebani, V.V.; Nardoni, S.; Mancianti, F.; Hendawy, S.; Omer, E.; Pistelli, L. Chemical composition and antimicrobial activity of essential oil of wild and cultivated Origanum syriacum plants grown in Sinai, Egypt. *Industrial Crops and Products* **2015**, *67*, 201-207.
99. Asbahani, A.E.; Miladi, K.; Badri, W.; Sala, M.; Addi, E.H.A.; Casabianca, H.; Mousadik, A.E.; Hartmann, D.; Jilale, A.; Renaud, F.N.R., et al. Essential oils: From extraction to encapsulation. *International Journal of Pharmaceutics* **2015**, *483*, 220-243.
100. Calo, J.R.; Crandall, P.G.; O'Bryan, C.A.; Ricke, S.C. Essential oils as antimicrobials in food systems – A review. *Food Control* **2015**, *54*, 111-119.
101. Chávez-González, M.L.; Rodríguez-Herrera, R.; Aguilar, C.N. Chapter 11 - Essential Oils: A Natural Alternative to Combat Antibiotics Resistance. In *Antibiotic Resistance*, Kon, K., Rai, M., Eds. Academic Press: **2016**, 227-237.
102. Bhavaniramya, S.; Vishnupriya, S.; Al-Aboody, M.S.; Vijayakumar, R.; Baskaran, D. Role of essential oils in food safety: Antimicrobial and antioxidant applications. *Grain & Oil Science and Technology* **2019**, *2*, 49-55.
103. Figueroa-Lopez, K.J.; Torres-Giner, S.; Enescu, D.; Cabedo, L.; Cerqueira, M.A.; Pastrana, L.M.; Lagaron, J.M. Electrospun Active Biopapers of Food Waste Derived Poly(3-hydroxybutyrate-co-3-hydroxyvalerate) with Short-Term and Long-Term Antimicrobial Performance. *Nanomaterials* **2020**, *10*, 506.
104. Hayashi, M.A.; Bizerra, F.C.; Da Silva, P.I., Jr. Antimicrobial compounds from natural sources. *Front Microbiol* **2013**, *4*, 195-195.
105. Cowan, M.M. Plant products as antimicrobial agents. *Clin Microbiol Rev* **1999**, *12*, 564-582.
106. Gavahian, M.; Chu, Y.-H.; Lorenzo, J.M.; Mousavi Khaneghah, A.; Barba, F.J. Essential oils as natural preservatives for bakery products: Understanding the mechanisms of action, recent findings, and applications. *Critical reviews in food science and nutrition* **2020**, *60*, 310-321.
107. Cosentino, S.; Tuberoso, C.I.; Pisano, B.; Satta, M.; Mascia, V.; Arzedi, E.; Palmas, F. In-vitro antimicrobial activity and chemical composition of Sardinian Thymus essential oils. *Letters in applied microbiology* **1999**, *29*, 130-135.
108. Leigh-de Rapper, S.; van Vuuren, S.F. Odoriferous Therapy: A Review Identifying Essential Oils against Pathogens of the Respiratory Tract. *Chemistry & Biodiversity* **2020**, *17*, e2000062.
109. Dutra, T.V.; Castro, J.C.; Menezes, J.L.; Ramos, T.R.; do Prado, I.N.; Machinski, M.; Mikcha, J.M.G.; Filho, B.A.d.A. Bioactivity of oregano (Origanum vulgare) essential oil against Alicyclobacillus spp. *Industrial Crops and Products* **2019**, *129*, 345-349.
110. Reyes-Jurado, F.; Cervantes-Rincón, T.; Bach, H.; López-Malo, A.; Palou, E. Antimicrobial activity of Mexican oregano (Lippia berlandieri), thyme (Thymus vulgaris), and mustard (Brassica nigra) essential oils in gaseous phase. *Industrial Crops and Products* **2019**, *131*, 90-95.
111. Burt, S. Essential oils: their antibacterial properties and potential applications in foods—a review. *International Journal of Food Microbiology* **2004**, *94*, 223-253.
112. Deans, S.G.; Ritchie, G. Antibacterial properties of plant essential oils. *International Journal of Food Microbiology* **1987**, *5*, 165-180.
113. Rodríguez-Meizoso, I.; Marin, F.R.; Herrero, M.; Señorans, F.J.; Reglero, G.; Cifuentes, A.; Ibáñez, E. Subcritical water extraction of nutraceuticals with antioxidant activity from oregano. Chemical and functional characterization. *Journal of Pharmaceutical and Biomedical Analysis* **2006**, *41*, 1560-1565.

114. Mechergui, K.; Coelho, J.A.; Serra, M.C.; Lamine, S.B.; Boukhchina, S.; Khouja, M.L. Essential oils of Origanum vulgare L. subsp. glandulosum (Desf.) Ietswaart from Tunisia: chemical composition and antioxidant activity. *Journal of the Science of Food and Agriculture* **2010**, *90*, 1745-1749.

115. Kulisic, T.; Radonic, A.; Katalinic, V.; Milos, M. Use of different methods for testing antioxidative activity of oregano essential oil. *Food chemistry* **2004**, *85*, 633-640.

116. Atarés, L.; Chiralt, A. Essential oils as additives in biodegradable films and coatings for active food packaging. *Trends in Food Science & Technology* **2016**, *48*, 51-62.

117. Becerril, R.; Nerín, C.; Silva, F. Encapsulation Systems for Antimicrobial Food Packaging Components: An Update. *Molecules* **2020**, *25*, 1134.

118. Alagawany, M.; Farag, M.R.; Salah, A.S.; Mahmoud, M.A. The role of oregano herb and its derivatives as immunomodulators in fish. *Reviews in Aquaculture* **2020**, *12*, 2481–2492.

119. Davidenco, V.; Pelissero, P.J.; Argüello, J.A.; Vega, C.R.C. Ecophysiological determinants of Oregano productivity: Effects of plant's canopy architecture on radiation capture and use, biomass partitioning and essential oil yield. *Scientia Horticulturae* **2020**, *272*, 109553.

120. Babili, F.E.; Bouajila, J.; Souchard, J.P.; Bertrand, C.; Bellvert, F.; Fouraste, I.; Moulis, C.; Valentin, A. Oregano: Chemical Analysis and Evaluation of Its Antimalarial, Antioxidant, and Cytotoxic Activities. *Journal of Food Science* **2011**, *76*, C512-C518.

121. Rocha-Guzmán, N.E.; Gallegos-Infante, J.A.; González-Laredo, R.F.; Ramos-Gómez, M.; Rodríguez-Muñoz, M.E.; Reynoso-Camacho, R.; Rocha-Uribe, A.; Roque-Rosales, M.R. Antioxidant effect of oregano (Lippia berlandieri v. Shauer) essential oil and mother liquors. *Food chemistry* **2007**, *102*, 330-335.

122. Marrelli, M.; Statti, G.A.; Conforti, F. Origanum spp.: an update of their chemical and biological profiles. *Phytochemistry Reviews* **2018**, *17*, 873-888.

123. De Martino, L.; De Feo, V.; Formisano, C.; Mignola, E.; Senatore, F. Chemical Composition and Antimicrobial Activity of the Essential Oils from Three Chemotypes of Origanum vulgare L. ssp. hirtum (Link) Ietswaart Growing Wild in Campania (Southern Italy). *Molecules* **2009**, *14*, 2735-2746.

124. Marrelli, M.; Conforti, F.; Formisano, C.; Rigano, D.; Arnold, N.A.; Menichini, F.; Senatore, F. Composition, antibacterial, antioxidant and antiproliferative activities of essential oils from three Origanum species growing wild in Lebanon and Greece. *Natural Product Research* **2016**, *30*, 735-739, doi:10.1080/14786419.2015.1040993.

125. Cowan, M.M. Plant Products as Antimicrobial Agents. *Clin Microbiol Rev* **1999**, *12*, 564, doi:10.1128/CMR.12.4.564.

126. Quinto, E.J.; Caro, I.; Villalobos-Delgado, L.H.; Mateo, J.; De-Mateo-Silleras, B.; Redondo-Del-Río, M.P. Food Safety through Natural Antimicrobials. *Antibiotics* **2019**, *8*, 208.

127. AHN, J.; GRÜN, I.U.; MUSTAPHA, A. Antimicrobial and Antioxidant Activities of Natural Extracts In Vitro and in Ground Beef. *Journal of Food Protection* **2004**, *67*, 148-155.

128. Namal Senanayake, S.P.J. Green tea extract: Chemistry, antioxidant properties and food applications – A review. *Journal of Functional Foods* **2013**, *5*, 1529-1541.

129. Yavari Maroufi, L.; Ghorbani, M.; Tabibiazar, M. A Gelatin-Based Film Reinforced by Covalent Interaction with Oxidized Guar Gum Containing Green Tea Extract as an Active Food Packaging System. *Food and Bioprocess Technology* **2020**, *13*, 1633-1644.

130. Jamróz, E.; Kulawik, P.; Kopel, P.; Balková, R.; Hynek, D.; Bytesnikova, Z.; Gagic, M.; Milosavljevic, V.; Adam, V. Intelligent and active composite films based on furcellaran: Structural characterization, antioxidant and antimicrobial activities. *Food Packaging and Shelf Life* **2019**, *22*, 100405.

131. Nouri, A.; Tavakkoli Yaraki, M.; Ghorbanpour, M.; Wang, S. Biodegradable κ-carrageenan/nanoclay nanocomposite films containing Rosmarinus officinalis L. extract for improved strength and antibacterial performance. *International Journal of Biological Macromolecules* **2018**, *115*, 227-235.

132. Ribeiro-Santos, R.; Carvalho-Costa, D.; Cavaleiro, C.; Costa, H.S.; Albuquerque, T.G.; Castilho, M.C.; Ramos, F.; Melo, N.R.; Sanches-Silva, A. A novel insight on an ancient aromatic plant: The rosemary (Rosmarinus officinalis L.). *Trends in Food Science & Technology* **2015**, *45*, 355-368.

133. Li, P.; Yang, X.; Lee, W.J.; Huang, F.; Wang, Y.; Li, Y. Comparison between synthetic and rosemary-based antioxidants for the deep frying of French fries in refined soybean oils evaluated by chemical and non-destructive rapid methods. *Food chemistry* **2021**, *335*, 127638.

134. Abdollahi, M.; Rezaei, M.; Farzi, G. A novel active bionanocomposite film incorporating rosemary essential oil and nanoclay into chitosan. *Journal of Food Engineering* **2012**, *111*, 343-350.

135. Turasan, H.; Sahin, S.; Sumnu, G. Encapsulation of rosemary essential oil. *LWT - Food Science and Technology* **2015**, *64*, 112-119.

136. Abu El-Wafa, W.M.; Ahmed, R.H.; Ramadan, M.A.-H. Synergistic effects of pomegranate and rosemary extracts in combination with antibiotics against antibiotic resistance and biofilm formation of Pseudomonas aeruginosa. *Brazilian Journal of Microbiology* **2020**, *51*, 1079-1092.

137. Jiang, Y.; Wu, N.; Fu, Y.-J.; Wang, W.; Luo, M.; Zhao, C.-J.; Zu, Y.-G.; Liu, X.-L. Chemical composition and antimicrobial activity of the essential oil of Rosemary. *Environmental Toxicology and Pharmacology* **2011**, *32*, 63-68.

138. Estevez-Areco, S.; Guz, L.; Candal, R.; Goyanes, S. Active bilayer films based on cassava starch incorporating ZnO nanorods and PVA electrospun mats containing rosemary extract. *Food Hydrocolloids* **2020**, *108*, 106054.

139. Razavi, R.; Molaei, R.; Moradi, M.; Tajik, H.; Ezati, P.; Shafipour Yordshahi, A. Biosynthesis of metallic nanoparticles using mulberry fruit (Morus alba L.) extract for the preparation of antimicrobial nanocellulose film. *Applied Nanoscience* **2020**, *10*, 465-476.

140. Hajizadeh, H.; Peighambardoust, S.J.; Peighambardoust, S.H.; Peressini, D. Physical, mechanical, and antibacterial characteristics of bio-nanocomposite films loaded with Ag-modified SiO2 and TiO2 nanoparticles. *Journal of Food Science* **2020**, *85*, 1193-1202.

141. Vaid, P.; Raizada, P.; Saini, A.K.; Saini, R.V. Biogenic silver, gold and copper nanoparticles - A sustainable green chemistry approach for cancer therapy. *Sustainable Chemistry and Pharmacy* **2020**, *16*, 100247.

142. Moezzi, A.; McDonagh, A.M.; Cortie, M.B. Zinc oxide particles: Synthesis, properties and applications. *Chemical Engineering Journal* **2012**, *185-186*, 1-22.

143. Jones, N.; Ray, B.; Ranjit, K.T.; Manna, A.C. Antibacterial activity of ZnO nanoparticle suspensions on a broad spectrum of microorganisms. *FEMS Microbiology Letters* **2008**, *279*, 71-76.

144. Bradley, E.L.; Castle, L.; Chaudhry, Q. Applications of nanomaterials in food packaging with a consideration of opportunities for developing countries. *Trends in Food Science & Technology* **2011**, *22*, 604-610.

145. Emamifar, A.; Kadivar, M.; Shahedi, M.; Soleimanian-Zad, S. Effect of nanocomposite packaging containing Ag and ZnO on inactivation of Lactobacillus plantarum in orange juice. *Food Control* **2011**, *22*, 408-413.

146. Espitia, P.J.P.; Soares, N.d.F.F.; Coimbra, J.S.d.R.; de Andrade, N.J.; Cruz, R.S.; Medeiros, E.A.A. Zinc Oxide Nanoparticles: Synthesis, Antimicrobial Activity and Food Packaging Applications. *Food and Bioprocess Technology* **2012**, *5*, 1447-1464.

147. Turner, S.; Tavernier, S.M.F.; Huyberechts, G.; Biermans, E.; Bals, S.; Batenburg, K.J.; Van Tendeloo, G. Assisted spray pyrolysis production and characterisation of ZnO nanoparticles with narrow size distribution. *Journal of Nanoparticle Research* **2010**, *12*, 615-622.

148. Mahmud, S.; Johar Abdullah, M.; Putrus, G.A.; Chong, J.; Karim Mohamad, A. Nanostructure of ZnO Fabricated via French Process and its Correlation to Electrical Properties of Semiconducting Varistors. *Synthesis and Reactivity in Inorganic, Metal-Organic, and Nano-Metal Chemistry* **2006**, *36*, 155-159.

149. Mavaei, M.; Chahardoli, A.; Shokoohinia, Y.; Khoshroo, A.; Fattahi, A. One-step Synthesized Silver Nanoparticles Using Isoimperatorin: Evaluation of Photocatalytic, and Electrochemical Activities. *Scientific Reports* **2020**, *10*, 1762.

150. Dos Santos, C.A.; Ingle, A.P.; Rai, M. The emerging role of metallic nanoparticles in food. *Applied microbiology and biotechnology* **2020**, *104*, 2373-2383.

151. Eskandari, M.; Haghighi, N.; Ahmadi, V.; Haghighi, F.; Mohammadi, S.R. Growth and investigation of antifungal properties of ZnO nanorod arrays on the glass. *Physica B: Condensed Matter* **2011**, *406*, 112-114.

152. Zhang, L.; Jiang, Y.; Ding, Y.; Daskalakis, N.; Jeuken, L.; Povey, M.; O'Neill, A.J.; York, D.W. Mechanistic investigation into antibacterial behaviour of suspensions of ZnO nanoparticles against E. coli. *Journal of Nanoparticle Research* **2010**, *12*, 1625-1636.

153. Kumar, R.; Umar, A.; Kumar, G.; Nalwa, H.S. Antimicrobial properties of ZnO nanomaterials: A review. *Ceramics International* **2017**, *43*, 3940-3961.

154. Ramani, M.; Ponnusamy, S.; Muthamizhchelvan, C.; Cullen, J.; Krishnamurthy, S.; Marsili, E. Morphology-directed synthesis of ZnO nanostructures and their antibacterial activity. *Colloids and Surfaces B: Biointerfaces* **2013**, *105*, 24-30.

155. Stanković, A.; Dimitrijević, S.; Uskoković, D. Influence of size scale and morphology on antibacterial properties of ZnO powders hydrothemally synthesized using different surface stabilizing agents. *Colloids and Surfaces B: Biointerfaces* **2013**, *102*, 21-28.

156. Peighambardoust, S.J.; Peighambardoust, S.H.; Pournasir, N.; Mohammadzadeh Pakdel, P. Properties of active starch-based films incorporating a combination of Ag, ZnO and CuO nanoparticles for potential use in food packaging applications. *Food Packaging and Shelf Life* **2019**, *22*, 100420.

157. Ebrahimi, Y.; Peighambardoust, S.J.; Peighambardoust, S.H.; Karkaj, S.Z. Development of Antibacterial Carboxymethyl Cellulose-Based Nanobiocomposite Films Containing Various Metallic Nanoparticles for Food Packaging Applications. *Journal of Food Science* **2019**, *84*, 2537-2548.

158. Azeredo, H.M.C.; Otoni, C.G.; Corrêa, D.S.; Assis, O.B.G.; de Moura, M.R.; Mattoso, L.H.C. Nanostructured Antimicrobials in Food Packaging—Recent Advances. *Biotechnology Journal* **2019**, *14*, 1900068.

159. Yusof, N.A.A.; Zain, N.M.; Pauzi, N. Synthesis of ZnO nanoparticles with chitosan as stabilizing agent and their antibacterial properties against Gram-positive and Gram-negative bacteria. *International Journal of Biological Macromolecules* **2019**, *124*, 1132-1136.

160. Taheri, M.; Bernardo, I.D.; Lowe, A.; Nisbet, D.R.; Tsuzuki, T. Green Full Conversion of ZnO Nanopowders to Well-Dispersed Zeolitic Imidazolate Framework-8 (ZIF-8) Nanopowders via a Stoichiometric Mechanochemical Reaction for Fast Dye Adsorption. *Crystal Growth & Design* **2020**, *20*, 2761-2773.

161. Saravanan, M.; Gopinath, V.; Chaurasia, M.K.; Syed, A.; Ameen, F.; Purushothaman, N. Green synthesis of anisotropic zinc oxide nanoparticles with antibacterial and cytofriendly properties. *Microbial Pathogenesis* **2018**, *115*, 57-63.

162. Akhtar, S.; Rehman, S.; Asiri, S.M.; Khan, F.A.; Baig, U.; Hakeem, A.S.; Gondal, M.A. Evaluation of bioactivities of zinc oxide, cadmium sulfide and cadmium sulfide loaded zinc oxide nanostructured materials prepared by nanosecond pulsed laser. *Materials Science and Engineering: C* **2020**, *116*, 111156.

163. Ranjbar, M.; Kiani, M.; Khakdan, F. Mentha mozaffarianii mediated biogenic zinc nanoparticles target selected cancer cell lines and microbial pathogens. *Journal of Drug Delivery Science and Technology* **2020**, *60*, 102042.

164. Guo, X.; Chen, B.; Wu, X.; Li, J.; Sun, Q. Utilization of cinnamaldehyde and zinc oxide nanoparticles in a carboxymethylcellulose-based composite coating to improve the postharvest quality of cherry tomatoes. *International Journal of Biological Macromolecules* **2020**, *160*, 175-182.

165. Guan, G.; Zhang, L.; Zhu, J.; Wu, H.; Li, W.; Sun, Q. Antibacterial properties and mechanism of biopolymer-based films functionalized by CuO/ZnO nanoparticles against Escherichia coli and Staphylococcus aureus. *Journal of Hazardous Materials* **2021**, *402*, 123542.

166. Wang, C.; Chang, T.; Dong, S.; Zhang, D.; Ma, C.; Chen, S.; Li, H. Biopolymer films based on chitosan/potato protein/linseed oil/ZnO NPs to maintain the storage quality of raw meat. *Food chemistry* **2020**, *332*, 127375.

167. Esmaeili, H.; Cheraghi, N.; Khanjari, A.; Rezaeigolestani, M.; Basti, A.A.; Kamkar, A.; Aghaee, E.M. Incorporation of nanoencapsulated garlic essential oil into edible films: A novel approach for extending shelf life of vacuum-packed sausages. *Meat Science* **2020**, *166*, 108135.

168. Castro Coelho, S.; Nogueiro Estevinho, B.; Rocha, F. Encapsulation in food industry with emerging electrohydrodynamic techniques: Electrospinning and electrospraying – A review. *Food chemistry* **2021**, *339*, 127850.

169. Ghaderi-Ghahfarokhi, M.; Barzegar, M.; Sahari, M.A.; Azizi, M.H. Nanoencapsulation Approach to Improve Antimicrobial and Antioxidant Activity of Thyme Essential Oil in Beef Burgers During Refrigerated Storage. *Food and Bioprocess Technology* **2016**, *9*, 1187-1201.

170. Mohammed, N.K.; Tan, C.P.; Manap, Y.A.; Muhialdin, B.J.; Hussin, A.S.M. Spray Drying for the Encapsulation of Oils—A Review. *Molecules* **2020**, *25*, 3873.

171. Akbari-Alavijeh, S.; Shaddel, R.; Jafari, S.M. Encapsulation of food bioactives and nutraceuticals by various chitosan-based nanocarriers. *Food Hydrocolloids* **2020**, *105*, 105774.

172. Bahrami, A.; Delshadi, R.; Jafari, S.M.; Williams, L. Nanoencapsulated nisin: An engineered natural antimicrobial system for the food industry. *Trends in Food Science & Technology* **2019**, *94*, 20-31.

173. Yang, S.; Liu, L.; Han, J.; Tang, Y. Encapsulating plant ingredients for dermocosmetic application: an updated review of delivery systems and characterization techniques. *International Journal of Cosmetic Science* **2020**, *42*, 16-28.

174. Wen, P.; Zong, M.-H.; Linhardt, R.J.; Feng, K.; Wu, H. Electrospinning: A novel nano-encapsulation approach for bioactive compounds. *Trends in Food Science & Technology* **2017**, *70*, 56-68.

175. Geranpour, M.; Assadpour, E.; Jafari, S.M. Recent advances in the spray drying encapsulation of essential fatty acids and functional oils. *Trends in Food Science & Technology* **2020**, *102*, 71-90.

176. Echegoyen, Y.; Fabra, M.J.; Castro-Mayorga, J.L.; Cherpinski, A.; Lagaron, J.M. High throughput electro-hydrodynamic processing in food encapsulation and food packaging applications: Viewpoint. *Trends in Food Science & Technology* **2017**, *60*, 71-79.

177. Mahjoubin-Tehran, M.; Kovanen, P.T.; Xu, S.; Jamialahmadi, T.; Sahebkar, A. Cyclodextrins: Potential therapeutics against atherosclerosis. *Pharmacology & Therapeutics* **2020**, *214*, 107620.

178. Figueroa-Lopez, K.J.; Enescu, D.; Torres-Giner, S.; Cabedo, L.; Cerqueira, M.A.; Pastrana, L.; Fuciños, P.; Lagaron, J.M. Development of electrospun active films of poly(3-hydroxybutyrate-co-3-hydroxyvalerate) by the incorporation of cyclodextrin inclusion complexes containing oregano essential oil. *Food Hydrocolloids* **2020**, *108*, 106013.

179. Tian, B.; Liu, Y.; Liu, J. Cyclodextrin as a magic switch in covalent and non-covalent anticancer drug release systems. *Carbohydrate Polymers* **2020**, *242*, 116401.

180. Bakshi, P.R.; Londhe, V.Y. Widespread applications of host-guest interactive cyclodextrin functionalized polymer nanocomposites: Its meta-analysis and review. *Carbohydrate Polymers* **2020**, *242*, 116430.

181. Hedges, A. Chapter 22 - Cyclodextrins: Properties and Applications. In *Starch (Third Edition)*, BeMiller, J., Whistler, R., Eds. Academic Press: San Diego, **2009**, 833-851.

182. Marques, H.M.C. A review on cyclodextrin encapsulation of essential oils and volatiles. *Flavour and Fragrance Journal* **2010**, *25*, 313-326.

183. do Nascimento, E.G.; de Azevedo, E.P.; Alves-Silva, M.F.; Aragão, C.F.S.; Fernandes-Pedrosa, M.F.; da Silva-Junior, A.A. Supramolecular aggregates of cyclodextrins with co-solvent modulate drug dispersion and release behavior of poorly soluble corticosteroid from chitosan membranes. *Carbohydrate Polymers* **2020**, *248*, 116724.

184. Matencio, A.; Navarro-Orcajada, S.; García-Carmona, F.; López-Nicolás, J.M. Applications of cyclodextrins in food science. A review. *Trends in Food Science & Technology* **2020**, *104*, 132-143.

185. Pan, J.; Ai, F.; Shao, P.; Chen, H.; Gao, H. Development of polyvinyl alcohol/β-cyclodextrin antimicrobial nanofibers for fresh mushroom packaging. *Food chemistry* **2019**, *300*, 125249.

186. Kayaci, F.; Uyar, T. Encapsulation of vanillin/cyclodextrin inclusion complex in electrospun polyvinyl alcohol (PVA) nanowebs: Prolonged shelf-life and high temperature stability of vanillin. *Food chemistry* **2012**, *133*, 641-649.

187. Uyar, T.; Havelund, R.; Hacaloglu, J.; Besenbacher, F.; Kingshott, P. Functional Electrospun Polystyrene Nanofibers Incorporating α-, β-, and γ-Cyclodextrins: Comparison of Molecular Filter Performance. *ACS Nano* **2010**, *4*, 5121-5130.

188. Bognitzki, M.; Czado, W.; Frese, T.; Schaper, A.; Hellwig, M.; Steinhart, M.; Greiner, A.; Wendorff, J.H. Nanostructured Fibers via Electrospinning. *Advanced Materials* **2001**, *13*, 70-72.

189. Schiffman, J.D.; Schauer, C.L. A Review: Electrospinning of Biopolymer Nanofibers and their Applications. *Polymer Reviews* **2008**, *48*, 317-352.

190. Chronakis, I.S. Novel nanocomposites and nanoceramics based on polymer nanofibers using electrospinning process—A review. *Journal of Materials Processing Technology* **2005**, *167*, 283-293.

191. Pérez-Masiá, R.; Lagaron, J.M.; López-Rubio, A. Development and Optimization of Novel Encapsulation Structures of Interest in Functional Foods Through Electrospraying. *Food and Bioprocess Technology* **2014**, *7*, 3236-3245.

192. Cerqueira, M.A.; Fabra, M.J.; Castro-Mayorga, J.L.; Bourbon, A.I.; Pastrana, L.M.; Vicente, A.A.; Lagaron, J.M. Use of Electrospinning to Develop Antimicrobial Biodegradable Multilayer Systems: Encapsulation of Cinnamaldehyde and Their Physicochemical Characterization. *Food and Bioprocess Technology* **2016**, *9*, 1874-1884.

193. Melendez-Rodriguez, B.; Torres-Giner, S.; Lorini, L.; Valentino, F.; Sammon, C.; Cabedo, L.; Lagaron, J.M. Valorization of Municipal Biowaste into Electrospun Poly(3-hydroxybutyrate-co-3-hydroxyvalerate) Biopapers for Food Packaging Applications. *ACS Applied Bio Materials* **2020**, *3*, 6110-6123.

194. Cherpinski, A.; Szewczyk, P.K.; Gruszczyński, A.; Stachewicz, U.; Lagaron, J.M. Oxygen-Scavenging Multilayered Biopapers Containing Palladium Nanoparticles Obtained by the Electrospinning Coating Technique. *Nanomaterials* **2019**, *9*, 262.

195. Vlachopoulos, J.; Strutt, D. Polymer processing. *Materials Science and Technology* **2003**, *19*, 1161-1169.

196. Suhag, R.; Kumar, N.; Petkoska, A.T.; Upadhyay, A. Film formation and deposition methods of edible coating on food products: A review. *Food Research International* **2020**, *136*, 109582.

197. Rhim, J.-W.; Mohanty, A.K.; Singh, S.P.; Ng, P.K.W. Effect of the processing methods on the performance of polylactide films: Thermocompression versus solvent casting. *Journal of Applied Polymer Science* **2006**, *101*, 3736-3742.

198. Ribeiro, A.M.; Estevinho, B.N.; Rocha, F. Preparation and Incorporation of Functional Ingredients in Edible Films and Coatings. *Food and Bioprocess Technology* **2020**, 10.1007/s11947-020-02528-4.

199. Wang, Y.; Zhao, G. Hot Extrusion Processing of Al–Li Alloy Profiles and Related Issues: A Review. *Chinese Journal of Mechanical Engineering* **2020**, *33*, 64.

200. Hilliou, L.; Covas, J.A. Chapter 5 - Production and Processing of Polymer-Based Nanocomposites. In *Nanomaterials for Food Packaging*, Cerqueira, M.Â.P.R., Lagaron, J.M., Pastrana Castro, L.M., de Oliveira Soares Vicente, A.A.M., Eds. Elsevier: 2018; 111-146.

201. Jaafar, J.; Siregar, J.P.; Tezara, C.; Hamdan, M.H.M.; Rihayat, T. A review of important considerations in the compression molding process of short natural fiber composites. *The International Journal of Advanced Manufacturing Technology* **2019**, *105*, 3437-3450.

202. Valencia-Sullca, C.; Atarés, L.; Vargas, M.; Chiralt, A. Physical and Antimicrobial Properties of Compression-Molded Cassava Starch-Chitosan Films for Meat Preservation. *Food and Bioprocess Technology* **2018**, *11*, 1339-1349.

203. Zubeldía, F.; Ansorena, M.R.; Marcovich, N.E. Wheat gluten films obtained by compression molding. *Polymer Testing* **2015**, *43*, 68-77.

204. Guerrero, P.; Muxika, A.; Zarandona, I.; de la Caba, K. Crosslinking of chitosan films processed by compression molding. *Carbohydrate Polymers* **2019**, *206*, 820-826.

205. Cherpinski, A.; Torres-Giner, S.; Cabedo, L.; Lagaron, J.M. Post-processing optimization of electrospun submicron poly(3-hydroxybutyrate) fibers to obtain continuous films of interest in food packaging applications. *Food Additives & Contaminants: Part A* **2017**, *34*, 1817-1830.

206. Marangoni Júnior, L.; Oliveira, L.M.d.; Bócoli, P.F.J.; Cristianini, M.; Padula, M.; Anjos, C.A.R. Morphological, thermal and mechanical properties of polyamide and ethylene vinyl alcohol multilayer flexible packaging after high-pressure processing. *Journal of Food Engineering* **2020**, *276*, 109913.

207. Gómez Ramos, M.J.; Lozano, A.; Fernández-Alba, A.R. High-resolution mass spectrometry with data independent acquisition for the comprehensive non-targeted analysis of migrating chemicals coming from multilayer plastic packaging materials used for fruit purée and juice. *Talanta* **2019**, *191*, 180-192.

208. Wang, L.; Chen, C.; Wang, J.; Gardner, D.J.; Tajvidi, M. Cellulose nanofibrils versus cellulose nanocrystals: Comparison of performance in flexible multilayer films for packaging applications. *Food Packaging and Shelf Life* **2020**, *23*, 100464.

209. Úbeda, S.; Aznar, M.; Vera, P.; Nerín, C.; Henríquez, L.; Taborda, L.; Restrepo, C. Overall and specific migration from multilayer high barrier food contact materials - kinetic study of cyclic polyester oligomers migration. *Food additives & contaminants. Part A, Chemistry, analysis, control, exposure & risk assessment* **2017**, *34*, 1784-1794.

210. Fang, J.M.; Fowler, P.A.; Escrig, C.; Gonzalez, R.; Costa, J.A.; Chamudis, L. Development of biodegradable laminate films derived from naturally occurring carbohydrate polymers. *Carbohydrate Polymers* **2005**, *60*, 39-42.

211. Song, W.; Du, Y.; Yang, C.; Li, L.; Wang, S.; Liu, Y.; Wang, W. Development of PVA/EVA-based bilayer active film and its application to mutton. *LWT* **2020**, *133*, 110109.

212. Ozdemir, M.; Floros, J. Active Food Packaging Technologies. *Critical reviews in food science and nutrition* **2004**, *44*, 185-193.

213. Quiles-Carrillo, L.; Montanes, N.; Lagaron, J.M.; Balart, R.; Torres-Giner, S. Bioactive Multilayer Polylactide Films with Controlled Release Capacity of Gallic Acid Accomplished by Incorporating Electrospun Nanostructured Coatings and Interlayers. *Applied Sciences* **2019**, *9*, 533, doi:10.3390/app9030533.

214. Cerqueira, M.A.; Torres-Giner, S.; Lagaron, J.M. Chapter 6 - Nanostructured Multilayer Films. In *Nanomaterials for Food Packaging*, Cerqueira, M.Â.P.R., Lagaron, J.M., Pastrana Castro, L.M., de Oliveira Soares Vicente, A.A.M., Eds. Elsevier: 2018; 147-171.

215. Cherpinski, A.; Torres-Giner, S.; Cabedo, L.; Méndez, J.A.; Lagaron, J.M. Multilayer structures based on annealed electrospun biopolymer coatings of interest in water and aroma barrier fiber-based food packaging applications. *Journal of Applied Polymer Science* **2018**, *135*, 45501, doi:10.1002/app.45501.

216. Figueroa-Lopez, K.J.; Castro-Mayorga, J.L.; Andrade-Mahecha, M.M.; Cabedo, L.; Lagaron, J.M. Antibacterial and Barrier Properties of Gelatin Coated by Electrospun Polycaprolactone Ultrathin Fibers Containing Black Pepper Oleoresin of Interest in Active Food Biopackaging Applications. *Nanomaterials* **2018**, *8*, 199.

217. Biowaste derived volatile fatty acid platform for biopolymers, bioactive compounds and chemical building blocks. VOLATILE, Grant agreement ID: 720777. **2016**. http://www.volatile-h2020.eu/theproject.html [Accessed April 26, 2021].

218. Unique technology to turn on-site paper waste from the printing industry into high-quality PHA bioplastic. PAPER-P, Grant agreement ID: 735158. **2016**. https://www.bio-pro.it/wordpress/ [Accessed April 26, 2021].

219. High Performance Polyhydroxyalkanoates Based Packaging to Minimise Food Waste. YPACK, Grant agreement ID: 773872. **2017**. https://www.ypack.eu/ [Accessed April 26, 2021].

220. New bio-based food packaging materials with enhanced barrier properties. BioBarr, Grant agreement ID: 745586. **2017**. https://www.biobarr.eu/ [Accessed April 26, 2021].

221. Resources from Urban Bio-waste. RESURBIS, Grant agreement ID: 730349. **2017**. http://www.resurbis.eu/ [Accessed April 26, 2021].

222. The first non-fermentative production process for low cost synthesis of biodegradable PHAs bioplastic from vegetal oils and fats. POLIPO, Grant agreement ID: 812602. **2018**. http://www.polipo.eu/ [Accessed April 26, 2021].

223. From waste to value: Transforming organic waste into biodegradable bioplastics. VEnvirotech, Grant agreement ID: 888704. **2019**. https://www.venvirotech.com/ [Accessed April 26, 2021].

224. Turning Bacteria into factories of Biodegradable Plastics. BterBioPlastics, Grant agreement ID: 867437. **2019**. [Accessed April 26, 2021].

225. Unlocking the potential of Sustainable BiodegradabLe Packaging. USABLE PACKAGING, Grant agreement ID: 836884. **2019**. [Accessed April 26, 2021].

226. For a sustainable and european value chain of PHA-based materials for high-volume consumer products. NENU2PHAR, Grant agreement ID: 887474. **2020**. [Accessed April 26, 2021].
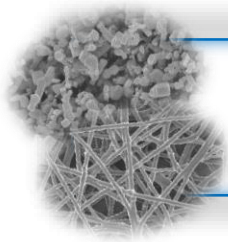
II.   OBJECTIVES

General and Specific Objectives

The development of biodegradable packaging materials with active properties for food preservation applications derived from food processing by-products and industrial waste is a topic of great interest. This new trend arises from the consumer demand for safer and more nutritious foods as well as current environmental issues related to the extensive use of plastics for food packaging applications. In this regard, polyhydroxyalkanoates (PHAs) are biopolymers of great industrial interest for their bio-based origin and inherent biodegradability, good properties, non-toxicity, and full compatibility with Circular Bioeconomy strategies. Furthremore, natural substances with antimicrobial and/or antioxidant activities, such as essential oils and metallic nanoparticles, are nowadays considered as great canditates to replace synthetic additives to develop active food packaging materials. In this way, the general objective of this PhD thesis was:

"The development and characterization of active mono and multilayer systems based on polyhydroxyalkanoates containing essential oils and metallic nanoparticles processed by the solution electrospinning technique with application interest in food packaging".

This goal was achieved by the accomplishment of the following specific objectives, which were developed sequentially:

1. Selection and optimization of active compounds based on essential oils (EOs), natural extracts (NEs), metallic nanoparticles (MNPs), and their combinations thereof with optimal antimicrobial and antioxidant properties with the aim of being incorporated into PHAs by electrospinning.

2. Development of melt-compounded monolayers films made of PHAs containing the selected active compounds and their characterization in terms of morphological, antioxidant, antimicrobial, thermal, mechanical, and barrier properties.

3. Evaluation of the short- and long-term antimicrobial performance of monolayer films of PHA containing mixtures of the selected active compounds in an open and closed system.

4. Incorporation of the selected essential oils into cyclodextrins inclusion complexes to protect and improve their antioxidant and antimicrobial activity, with the aim of being incorporated into PHAs by electrospinning.

5. Development and characterization of multilayer films based on the active electrospun monolayers developed to attain an antimicrobial packaging film.

6. Development and characterization of active and barrier multilayer systems based on monolayers containing the active compounds developed to attain a high-barrier packaging film.

7. Assessment of the migration of metallic nanoparticles from the developed mono and multilayers films in food simulants.

8. Analysis of cytotoxicity of developed multilayers films containing the active compounds using Caco-2 cells.
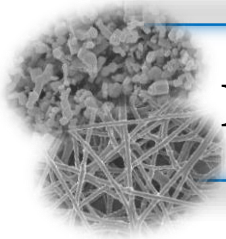
III. RESULTS AND DISCUSSION

Results and Discussions

This PhD thesis is a compilation of works focused on the development of monolayer and multilayer systems based on polyhydroxyalkanoates (PHAs) and active compounds, such as essential oils and metallic nanoparticles for antimicrobial active food packaging applications. Each chapter deals with one of the specific aims defined above and correspond to journal papers already published.

BLOCK I

Assesment of the Antioxidant and Antimicrobial Performance af Essential Oils and Natural Extracts for Active Packaging

Chapter I

Kelly J. Figueroa-Lopez, António A. Vicente, Maria A.M. Reis, Sergio Torres-Giner and Jose M. Lagaron. **Antimicrobial and Antioxidant Performance of Various Essential Oils and Natural Extracts and Their Incorporation into Biowaste Derived Poly(3-hydroxybutyrate-co-3-hydroxyvalerate) Layers Made from Electrospun Ultrathin Fibers**. *Nanomaterials* 2019, 9(2), 144; https://doi.org/10.3390/nano9020144

BLOCK II

Development and Characterization of Active Monolayers based on Polyhydroxyalkanoates containing the Selected Essential Oils and Metallic Nanoparticles

Chapter II

S. Torres-Giner, L. Hilliou, B. Melendez-Rodriguez, K.J. Figueroa-Lopez, D. Madalena, L. Cabedo, J.A. Covas, A.A. Vicente, J.M. Lagaron. **Melt processability, characterization, and antibacterial activity of compression-molded green composite sheets made of poly(3-hydroxybutyrate-co-3-hydroxyvalerate) reinforced with coconut fibers impregnated with oregano essential oil**. *Food Packaging and Shelf Life* 2018, 17, 39-49; https://doi.org/10.1016/j.fpsl.2018.05.002

Chapter III

Kelly J. Figueroa-Lopez, Sergio Torres-Giner, Daniela Enescu, Luis Cabedo, Miguel A. Cerqueira, Lorenzo M. Pastrana, Jose M. Lagaron. **Electrospun Active Biopapers of Food Waste Derived Poly(3-hydroxybutyrate-co-3-hydroxyvalerate) with Short-Term and Long-Term Antimicrobial Performance**. *Nanomaterials* 2020, 10(3), 506; https://doi.org/10.3390/nano10030506

Chapter IV

K. J. Figueroa-Lopez, D. Enescu, S. Torres-Giner, L. Cabedo, M.A. Cerqueira, L. Pastrana, P. Fuciños, J.M. Lagaron. **Development of electrospun active films of poly(3-hydroxybutyrate-co-3-hydroxyvalerate) by the incorporation of cyclodextrin inclusion complexes containing oregano essential oil**. *Food Hydrocolloids* 2020, 108; https://doi.org/10.1016/j.foodhyd.2020.106013

BLOCK III
Development and Characterization of Active Multilayers based on Polyhydroxyalkanoates containing the Selected Essential Oils and Metallic Nanoparticles

Chapter V

Kelly J. Figueroa-Lopez, S. Torres-Giner, Luis Cabedo, and J. M. Lagaron. **Development of electrospun poly(3-hydroxybutyrate-co-3-hydroxyvalerate) monolayers containing eugenol and their application in multilayer antimicrobial food packaging**. *Frontiers in Nutririon* 2020, 7:140; https://doi.org/10.3389/fnut.2020.00140

Chapter VI

Kelly J. Figueroa-Lopez, S. Torres-Giner, Inmaculada Angulo, Maria Pardo-Figuerez, Jose Manuel Escuin, Ana Isabel Bourbon, Luis Cabedo, Yuval Nevo, Miguel A. Cerqueira, and Jose M. Lagaron. **Development of Active Barrier Multilayer Films Based on Antimicrobial Hot-Tack Electrospun Food Waste Derived Poly(3-hydroxybutyrate-co-3-hydroxyvalerate) and Cellulose Nanocrystals Interlayers**. *Nanomaterials* 2020, 10(12), 2356; https://doi.org/10.3390/nano10122356

CHAPTER I

Various Essential Oils and Natural Extracts and Their Incorporation into Biowaste Derived Poly(3-hydroxybutyrate-co-3-hydroxyvalerate) Layers Made from Electrospun Ultrathin Fibers

Kelly J. Figueroa-Lopez, António A. Vicente, Maria A.M. Reis, Luis Cabedo, Sergio Torres-Giner, Jose M. Lagaron

Antimicrobial and Antioxidant Performance of Various Essential Oils and Natural Extracts and Their Incorporation into Biowaste Derived Poly(3-hydroxybutyrate-co-3-hydroxyvalerate) Layers Made from Electrospun Ultrathin Fibers

Abstract

In this research, the antibacterial and antioxidant properties of oregano essential oil (OEO), rosemary extract (RE), and green tea extract (GTE) were evaluated. These active substances were encapsulated into ultrathin fibers of poly(3-hydroxybutyrate-co-3-hydroxyvalerate) (PHBV) derived from fruit waste using solution electrospinning, and the resultant electrospun mats were annealed to produce continuous films. The incorporation of the active substances resulted in PHBV films with a relatively high contact transparency, but it also induced a slightly yellow appearance and increased the films opacity. Whereas OEO significantly reduced the onset of thermal degradation of PHBV, both the RE and GTE-containing PHBV films showed a thermal stability profile that was similar to the neat PHBV film. In any case, all the active PHBV films were stable up to approximately 200 °C. The incorporation of the active substances also resulted in a significant decrease in hydrophobicity. The antimicrobial and antioxidant activity of the films were finally evaluated in both open and closed systems for up to 15 days in order to anticipate the real packaging conditions. The results showed that the electrospun OEO-containing PHBV films presented the highest antimicrobial activity against two strains of food-borne bacteria, as well as the most significant antioxidant performance, ascribed to the films high content in carvacrol and thymol. Therefore, the PHBV films developed in this study presented high antimicrobial and antioxidant properties, and they can be applied as active layers to prolong the shelf life of the foods in biopackaging applications.

Keywords: PHBV; oregano; rosemary; green tea; electrospun nanofibers; antibacterial; antioxidant

1   Introduction

The packaging industry requires the development of new plastic materials with active properties, based on the demand by consumers for safer and more nutritive food [1]. Moreover, the growing concern over the environmental problems caused by petroleum-derived materials has led to the search for new renewable raw materials for the development of compostable packaging [2,3]. Polyhydroxyalkanoates (PHAs) are amongst the most promising biopolymers, being a group of totally renewable, biodegradable, and biocompatible aliphatic polyesters. PHAs are synthesized in the cytoplasm of a wide range of bacteria from glucose-rich substrates [4,5]. Some PHAs, such as poly(3-hydroxybutyrate) (PHB), poly(3-hydroxybutyrate-co-3-hydroxyvalerate) (PHBV), poly(3-hydroxybutyrate-co-4-hydroxybutyrate) (P(3HB-co-4HB)), and poly(3-hydroxybutyrate-co-3-hydroxyhexanoate) (PHBH) are currently being employed to develop bioplastic packaging articles, such as injection-molded pieces, compression-molded sheets, and films [6-9].

Active packaging technology is mostly related to materials and articles that are intended to extend food shelf life, and also to improve packaged food conditions by interacting with the food product and/or with its internal packaging environment. Active packaging materials are usually designed to deliberately incorporate components, which would then release and/or absorb substances into or from the packaged food or the environment surrounding the food [10]. Active packaging systems can therefore extend the shelf life of food products and reduce food waste by maintaining the quality of food products for longer, increasing product safety by securing the foods against pathogens, and enhancing the convenience of food processing, distribution, retailing, and consumption [11]. Concerning the active packaging materials, these are classified as either active scavenging types (e.g., oxygen scavengers) [12] or active releasing types (e.g., antioxidants) [13]. Active releasing-type packaging can provide novel "extra" functions, such as aromatic, antioxidant, and long-term antimicrobial properties [14]. In particular, active-releasing antimicrobial packaging applications are directly related to food microbial safety, as well as to shelf life extension, by preventing the growth of spoilage and/or pathogenic microorganisms [15,16]. The growth of spoilage microorganisms can not only reduce the food shelf life, but it can also endanger public health (particularly in the case of pathogenic microorganisms).

Active properties can be conferred by the incorporation into the packaging materials of substances with inherent antioxidant and antimicrobial properties, such as essential oils (EOs) [17], natural extracts (NEs) [18], and/or inorganic and metal nanoparticles [19]. EOs are volatile compounds obtained from aromatic plants that produced them naturally as secondary metabolites [20]. EOs and NEs are mainly composed of

terpenoids, phenolic, and aromatic compounds, and their composition can widely vary depending on the edaphoclimatic characteristics of the plant, the part of the plant (i.e., flower, seed, leaves, fruits, stems, and others), and the extraction procedure [21]. There is great interest in the use of these natural products because they are classified as generally recognized as safe (GRAS) food additives by the Food and Drug Administration (FDA) [22].

In line with this, over the last few years, different EOs and NEs have been proposed as alternative sources of antimicrobials in packaging materials. Within the great variety of EOs, oregano essential oil (OEO) from *Origanum vulgare* is well known for its antioxidative and antimicrobial activities [23]. The EO content in the oregano plant fluctuates from 0.5 – 2 % [24] up to 7 % [25]. Its main constituents are the isomer phenols, carvacrol and thymol, which represent up to 80 % and 64 %, respectively [26]. In addition, up to 52 % of each of their precursor monoterpenes, p-cymene and γ-terpinene, as well as terpinen-4-ol, linalool, β-myrcene, trans-sabinene hydrate, and β-caryophyllene, are also present [27]. Rosemary extract (RE), which is obtained from *Rosmarinus officinalis*, is an aromatic plant belonging to the Lamiaceae family [28], and it also presents strong antimicrobial and antifungal properties [29]. The active properties of RE are primarily conferred by its phenolic, and the volatile constituents carnosol, carnosic acid, and rosmarinic acid [30]. Its minor components may have a potential influence on biological activity due to the possibility of synergistic effects amongst their components [31]. Finally, green tea tree extract (GTE) obtained from *Camellia sinensis* has gained significant attention in recent years. GTE is mainly composed of gallic acid, theobromine, chlorogenic acid, and caffeic acid [32]. In view of the potential uses of these natural products as effective antimicrobial and antioxidants for food preservation, they can be great candidates for incorporation into PHA films to generate active packaging articles.

Since most EOs and NEs are volatile compounds, they require the use of manufacturing methods that are carried out at room temperature to preserve their original properties. In this sense, the electrospinning technique is an emerging technology in the food packaging field [33,34], which is based on the application of electrostatic forces to polymer solutions to generate polymer fibers with diameters ranging from below 100 nm to several micrometers. Owing to the high surface-to-volume ratio of the electrospun fibers and the controllable pore size of the electrospun mats, several active and bioactive applications have been proposed in recent years [35], including the development of novel antimicrobial systems [36]. Since the electrospinning technique is frequently performed at room temperature, it facilitates the processing of thermolabile substances [37]. In addition, in a packaging application context, the ultrathin electrospun PHA fiber mats can be further converted

into continuous films through the application of a thermal post-treatment below the polymer's melting temperature (T_m), i.e., the so-called annealing [38,39].

The objective of this research was to develop, for the first time, electrospun PHBV films containing OEO, RE, and GTE, in order to obtain active packaging layers with antioxidant and antimicrobial properties. Likewise, the morphological, optical, and thermal properties of the electrospun biopolymer films were also evaluated.

2 Materials and Methods

2.1 Materials

PHBV copolyester was produced at a pilot-plant scale at the Universidade NOVA de Lisboa (Lisboa, Portugal). This biopolymer was obtained using mixed microbial cultures fed with fermented fruit waste derived from the manufacturing of fruit juice, supplied by SumolCompal S.A. (Lisbon, Portugal). The molar fraction of the 3-hydroxyvalerate (HV) in the copolyester used was 20 %. The synthesis, purification, and characterization details of this biopolymer was thoroughly described in Reference [39].

Chloroform, reagent grade with 99.8 % purity, and methanol, HPLC grade with 99.9% purity, were purchased from Panreac S.A. (Barcelona, Spain). Additionally, 1-Butanol, reagent grade with 99.5 % purity, and 2,2-diphenyl-1-picrylhydrazyl radical (DPPH) were purchased from Sigma Aldrich S.A. (Madrid, Spain).

OEO had a purity >99 % and a relative density of 0.925 – 0.955 g/mL. RE presented a relative density of 0.915 – 0.926 g/mL, an acidity index of $\leq$1 mg KOH/g, an iodine index of 80.0 – 145.0 %, a saponification index of 180–200 mg KOH/g, and a peroxide index of $\leq$5.0 meqO$_2$/kg. GTE showed a relative density of 0.915 – 0.925 g/mL, an acidity index of $\leq$1 mg KOH/g, an iodine index of 80 – 145 %, a saponification index of 188 – 195 mg KOH/g, and a peroxide index of $\leq$5.0 meq O$_2$/Kg. All natural products were obtained from Gran Velada S.L. (Zaragoza, Spain) and were processed as received.

2.2 Preparation of the Solutions

The PHBV solution was prepared by dissolving 10 % (wt./vol.) of biopolymer in a chloroform/1-butanol 75:25 (vol./vol.) mixture, both reagent grades, at room temperature. The OEO, RE, and GTE, were all added to the solution at 10 wt.% in relation to the PHBV and stirred for 24 h until a single-phase solution was obtained.

2.3 Characterization of the Solution Properties

All the PHBV solutions were analyzed in terms of their viscosity, surface tension, and conductivity. The apparent viscosity (ηa) was determined at 100 s^{-1} using a rotational viscosity meter Visco BasicPlus L from Fungilab S.A. (San Feliu de Llobregat, Spain). The surface tension was measured following the Wilhemy plate method using an EasyDyne K20 tensiometer from Krüss GmbH (Hamburg, Germany). The conductivity was evaluated using a conductivity meter HI9819X from

Hanna Instruments (Woonsocket, Rhode Island, USA). All the measurements were carried out at room temperature and in triplicate.

2.4 Electrospinning

The PHBV solutions containing OEO, RE, and GTE were each electrospun for 3 h onto an aluminum foil using a high-throughput electrospinning/electrospraying pilot line Fluidnatek® LE-500 with temperature and relative humidity (RH) control, which was manufactured and commercialized by Bioinicia S.L. (Valencia, Spain). The solutions were then processed at 25 °C and 40 % RH under a constant flow using a 24 emitter multi-nozzle injector, scanning vertically onto the metallic plate. A dual polarization added voltage of 38 kV, and a flow-rate of 4 mL/h per single emitter and a tip-to-collector distance of 20 cm were used. A neat PHBV solution was electrospun in identical conditions as the control.

Thereafter, an annealing treatment was applied to the resultant electrospun mats. This process was performed in a 4122-model press from Carver, Inc. (Wabash, IN, USA) at 125 °C, for 5 s, without pressure. The resultant film samples had an average thickness in the 60 – 80 µm range.

2.5 Characterization of the Electrospun Materials

2.5.1 Film Thickness

Before testing, the thickness of the PHBV films containing the natural products was measured using a digital micrometer (S00014, Mitutoyo, Corp., Kawasaki, Japan) with ± 0.001 mm accuracy. Measurements were performed and averaged at five different points, one in each corner and one in the middle.

2.5.2 Morphology

The morphology of the electrospun PHBV fibers and their films containing the OEO, RE, and GTE were examined by scanning electron microscopy (SEM). The micrographs were taken using a Hitachi S-4800 electron microscope (Tokyo, Japan), at an accelerating voltage of 10 kV and a working distance of 8 – 10 mm. The samples were previously sputtered with a gold-palladium mixture for 3 min under vacuum. The average fiber diameter was determined via the ImageJ software v 1.41 using at least 20 SEM images.

2.5.3 Transparency

The light transmission of the PHBV films was determined in specimens of 50 × 30 mm^2 by quantifying the absorption of light at wavelengths between 200 and 700 nm, using an ultraviolet–visible (UV–Vis) spectrophotometer VIS3000 from Dinko Instruments (Barcelona, Spain). The transparency value (T) of the films was calculated using Equation (1) [1], whereas their opacity value (O) was determined using Equation (2) [40]:

$$T = \frac{A_{600}}{L} \tag{1}$$

$$O = A_{500}\, L \tag{2}$$

where A_{500} and A_{600} are the absorbance values at 500 and 600 nm, respectively, and L is the film thickness (mm).

2.5.4 Color

The PHBV films color was determined using a chroma meter CR-400 (Konica Minolta, Tokyo, Japan). The color difference (ΔE*) was calculated using the following Equation (3) [1], as defined by the Commission Internationale de l'Eclairage (CIE):

$$\Delta E^* = [(\Delta L^*)^2 + (\Delta a^*)^2 + (\Delta b^*)^2]^{0.5} \tag{3}$$

where ΔE*, ΔL*, Δa*, and Δb* correspond to the differences between the color parameters of the sample films and the values of the control film (a* = 0.87, b* = – 0.38, L* = 89.82).

2.5.5 Thermal Analysis

Thermogravimetric analysis (TGA) of the neat OEO, RE, and GTE in their liquid form, and the PHBV films, was performed under a nitrogen atmosphere in a Thermobalance TG-STDA Mettler Toledo model TGA/STDA851e/LF/1600 analyzer (Greifensee, Switzerland). The TGA curves were obtained after conditioning the samples in the sensor for 5 min at 30 °C. The samples were then heated from 25 °C to 700 °C, at a heating rate of 10 °C/min. All tests were carried out in triplicate.

2.5.6 *Water Contact Angle Measurements*

The PHBV films surface wettability was evaluated using dynamic water contact angle (WCA) measurements in an optical tensiometer (Theta Lite, Staffordshire, UK). Five droplets were seeded at 5 µL/s on the film surfaces of each studied material sizing of 2×5 cm^2, in triplicate, and the resulting average contact angle was calculated.

2.5.7 *Antimicrobial Activity*

Staphylococcus aureus (*S. aureus*) CECT240 (ATCC 6538p) and *Escherichia coli* (*E. coli*) CECT434 (ATCC 25922) strains were obtained from the Spanish Type Culture Collection (CECT, Valencia, Spain) and stored in phosphate buffered saline (PBS), with 10 wt.% tryptic soy broth (TSB, Conda Laboratories, Madrid, Spain) and 10 wt.% glycerol (99.5 % purity, Sigma Aldrich S.A. Madrid, Spain) at –80 °C. Prior to each study, a loopful of bacteria was transferred to 10 mL of TSB and incubated at 37 °C for 24 h. A 100 µL aliquot from the culture was again transferred to the TSB and grown at 37 °C to the mid-exponential phase of growth. The approximate count of 5×10^5 CFU/mL of culture had an absorbance value of 0.20, as determined by the optical density at 600 nm (UV 4000 spectrophotometer, Dinko Instruments, Barcelona, Spain).

The minimum inhibitory concentration (MIC) and minimum bactericide concentration (MBC) of the OEO, RE, and GTE against the selected food-borne bacteria was tested following the plate micro-dilution protocol, as described in the Methods for Dilution Antimicrobial. Susceptibility Tests for Bacteria That Grow Aerobically; Approved Standard Tenth. Edition (M07-A10) by the Clinical and Laboratory Standards Institute (CLSI). For this, a 96-well plate with an alpha numeric coordination system (columns 12 and rows A-H) was used, where 10 µl of the tested samples were introduced into the wells with 90 µl of the bacteria medium. In the wells corresponding to A, B, C, E, F, and G columns, different concentrations of the natural products, that is, 0.312, 0.625, 1.25, 2.5, 5, 10, 20, 40, 80, 160 µl/ml, were tested, in triplicate, from rows 1 to 10. Columns D and H were used as control of the natural extracts in the TSB without bacteria. Row 11 was taken as a positive control, that is, only the TSB, and row 12 was used as a negative control, that is, *S. aureus* and *E. coli* in the TSB. The plates were incubated at 37 °C for 24 h. Thereafter, 10 µl of resazurin sodium salt (MP biologicals, Illkirch, France), a metabolic indicator, was added to each well and incubated again at 37 °C for 2 h. Upon obtaining the resazurin change, the wells were read through the color difference. The MIC and MBC values were determined as the lowest concentration of the natural products presenting bacteriostatic and bactericide effects, respectively [41].

The antimicrobial performance of the electrospun PHBV films was evaluated using a modification of the Japanese Industrial Standard (JIS) Z2801 (ISO 22196:2007) [42]. To this end, a microorganism suspension of S. aureus and E. coli was applied onto the test films, that is, containing the natural extracts, and the negative control film, that is, without the natural extracts, all sizing 1.5×1.5 cm^2. Tests were performed in either hermetically closed or open vials with a volume of 20 mL. After incubation at 24 °C and at a relative humidity (RH) of, at least, 95 % for 24 h, the bacteria were recovered with PBS, 10-fold serially diluted, and incubated at 37 °C for 24 h in order to quantify the number of viable bacteria by a conventional plate count. The antimicrobial activity was evaluated after 1 (initial day), 8, and 15 days. The value of the antimicrobial reduction (R) was calculated following Equation (4):

$$R = \left[log\left(\frac{B}{A}\right) - log\left(\frac{C}{A}\right) \right] = log\left(\frac{B}{C}\right) \tag{4}$$

where A is the average of the number of viable bacteria on the control film sample immediately after inoculation, B is the average of the number of viable bacteria on the control film sample after 24 h, and C is the average of the number of viable bacteria on the test film sample after 24 h. Three replicate experiments were performed for each sample and the following assessment was conducted: Nonsignificant (R < 0.5), slight (R ≥ 0.5 and <1), significant (R ≥ 1 and <3), and strong (R ≥ 3) as in Reference [43].

2.5.8   Antioxidant Activity

The DPPH inhibition assay was used to evaluate the free radical scavenging activity of the neat OEO, RE, GTE in their oil forms, in the electrospun PHBV fibers (at day 1) and their corresponding films (at 1, 8, and 15 days). Samples were weighed in triplicate in cap vials and then an aliquot of the DPPH solution (0.05 g/L in methanol) was added to each one. Vials without samples were also prepared as controls. All the samples were prepared and immediately stored at room temperature for 2 h in darkness. After this, the absorbance of the solution was measured at 517 nm in the UV 4000 spectrophotometer from Dinko Instruments. Results were expressed as the percentage of inhibition to DPPH following Equation (5) [44] and μg equivalent of trolox per gram of sample, employing a previously prepared calibration curve of Trolox.

$$Inhibition\ DPPH\ (\%) = \frac{A_{Control} - (A_{sample} - A_{blank})}{A_{control}} * 100 \tag{5}$$

where $A_{control}$, A_{blank}, and A_{sample} are the absorbance values of the DPPH solution, methanol with the test sample, and the test sample, respectively.

2.5.9   Statistical Analysis

The solution properties, color, transparency, and opacity values, and contact angle values were evaluated through analysis of variance (ANOVA) using STATGRAPHICS Centurion XVI v 16.1.03 from StatPoint Technologies, Inc. (Warrenton, VA, USA). Fisher's least significant difference (LSD) was used at the 95 % confidence level ($p < 0.05$). Mean values and standard deviations were also calculated.

3 Results and Discussions

3.1 Solution Properties

The use of polymer solution with the adequate properties is a key parameter to obtain uniform fibers during electrospinning [45]. In Table 1, the viscosity, surface tension, and conductivity of the PHBV solutions containing OEO, RE, and GTE at 10 wt.% are shown. The neat PHBV solution, without OEO and NEs, showed the highest viscosity value, that is, 212.4 cP. This value was relatively similar to that reported by Melendez-Rodriguez et al. [39], who obtained a value of viscosity of 296.8 cP for a PHBV solution in 2,2,2-trifluoroethanol (TFE) at 2 wt%. This difference could be mainly ascribed to the solvent type and, more likely, to the use of a biopolymer with a higher molecular weight (MW). When OEO, RE, and GTE were added, the viscosity of the PHBV solution slightly decreased. This effect could be ascribed to a reduction of the molecular cohesion forces in the biopolymer due to the presence of the active substances. This result was in agreement with, for instance, previous research works reported by Arfa et al. [46] and Jouki et al. [47], showing that the addition of either OEO or its active components decreased the apparent viscosity of polymer solutions of mucilage and soy protein (SP). In any case, for all the here-prepared PHBV solutions, the viscosity values were within the range of values reported by other authors, that is, from 1 to 20 poise (P), for the formation of homogeneous fibers during electrospinning [48].

Table 1. Solution properties of poly(3-hydroxybutyrate-co-3-hydroxyvalerate) (PHBV) containing oregano essential oil (OEO), rosemary extract (RE), and green tea tree extract (GTE)

Sample	Apparent Viscosity (cP)	Surface Tension (mN/m)	Conductivity (μs)
PHBV	212.4 ± 0.04^a	25.3 ± 0.05^a	0.40 ± 0.00^a
PHBV + OEO	205.5 ± 0.01^b	25.5 ± 0.07^a	0.42 ± 0.00^a
PHBV + RE	208.1 ± 0.03^c	25.4 ± 0.09^a	0.41 ± 0.00^a
PHBV + GTE	206.9 ± 0.05^d	25.5 ± 0.06^a	0.39 ± 0.00^a

[a–d] Different letters in the same column indicate a significant difference (p < 0.05).

The surface tension and conductivity of the solutions showed no significant differences (p > 0.05). However, it is worthy to mention that other authors have observed changes in the latter parameters when homogenization treatments (e.g., ultrasound, sonication, etc.) were applied to polymer solutions containing different EOs and NEs [49,50]. Moreover, in the case of polymer emulsions, the incorporation of these natural extracts into the oil or water phases resulted in an increasing drop size that destabilized the emulsion [51]. Therefore, the similar values observed for

the neat PHBV solution and the PHBV solutions containing the OEO, RE, and GTE suggested that a high homogenization was achieved in all cases. Therefore, it was considered that the resulting solutions presented the adequate values for being processed by electrospinning.

3.2   Morphology

The morphology of the electrospun ultrathin neat PHBV fibers and the PHBV fibers containing the OEO, RE, and GTE was analyzed by SEM and the images are shown in Figure 1. The neat PHBV fibers, without EOs and NEs, were relatively uniform and presented a mean diameter of approximately 1 μm, as seen in Figure 1a. The morphology of the here-obtained electrospun ultrathin PHBV fibers was similar to those fibers reported by Melendez-Rodriguez et al [39], showing diameters of ~1.32 μm. The PHBV fibers containing 10 wt% OEO, RE, and GTE are presented in Figure 1b–d, respectively. The diameters of the fibers were relatively similar, with a mean size of approximately 0.8 μm. The reduction achieved in the fiber diameter could be related to the slightly lower viscosities observed for the PHBV solutions containing the active substances. It was also evident that all the electrospun fibers were uniform and smooth, without any superficial and structural defects, which indicated that the addition of both EOs and NEs did not alter the fiber formation during electrospinning.
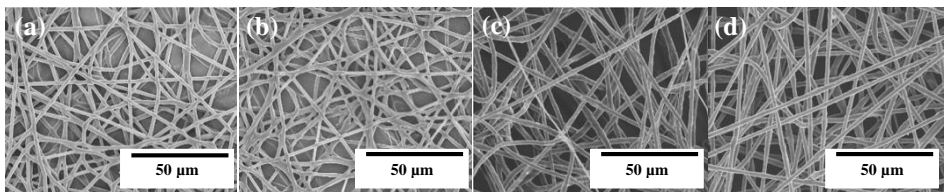
Figure 1. Scanning electron microscopy (SEM) micrographs of the electrospun fibers of: (**a**) Neat poly(3-hydroxybutyrate-co-3-hydroxyvalerate) (PHBV); (**b**) Oregano essential oil (OEO)-containing PHBV; (**c**) Rosemary extract (RE)-containing PHBV; (**d**) Green tea tree extract (GTE)-containing PHBV. Scale markers of 50 μm.

Figure 2 shows the SEM images of the electrospun materials, after annealing at 125 °C, in their cross-section and top views. In all cases, one can observe that the thermal post-treatment on the electrospun mats resulted in the formation of a continuous film. Figure 2a corresponds to the cross-section of the neat PHBV film, that is, without OEO and NEs, which presented an average thickness of ~80 μm. In Figure 2b, one can observe that the film sample also exhibited a homogeneous surface without cracks and/or pores. Similar morphologies were reported, for instance, by Cherpinski et al. [38] for electrospun PHB fibers thermally post-treated at 160 °C. The particular

change from fiber-based to film-like morphology was ascribed to a process of fibers coalescence during annealing. Figure 2c,e,g show the cross-sections of the electrospun PHBV films containing OEO, RE, and GTE, respectively. The thicknesses of all the film samples were kept at ~80 μm. The presence of a certain number of pores can be related to the partial evaporation of the oily materials enclosed in the PHBV film during the thermal post-treatment. Similar voids were observed in the electrospun PHBV films derived from biowaste by Melendez-Rodriguez et al. [39], when temperatures close to Tm were applied, which was ascribed to the partial material melting and/or degradation. However, in Figure 2d,f,h, showing the top view of the film samples containing the active substances, it can be seen that the PHBV films still showed a smooth and homogeneous surface without pores and cracks. Therefore, despite the fact that the active substances were partially released during the film-forming process, a good compatibility and then a high solubility of OEO and the NEs with the PHBV matrix was attained.
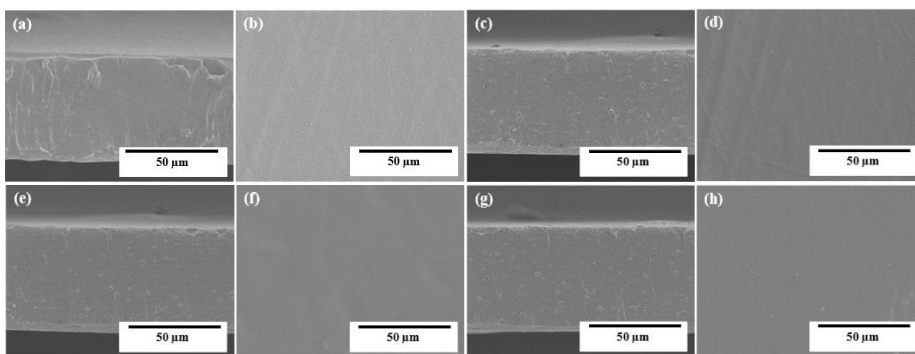
Figure 2. Scanning electron microscopy (SEM) micrographs of the electrospun films in their cross-section (left column) and top view (right column) of: (**a,b**) Neat poly(3-hydroxybutyrate-co-3-hydroxyvalerate) (PHBV); (**c,d**) Oregano essential oil (OEO)-containing PHBV; (**e,f**) Rosemary extract (RE)-containing PHBV; (**g,h**) Green tea tree extract (GTE)-containing PHBV. Scale markers of 50 μm.

3.3 Optical Properties

Figure 3 shows the visual aspect of the electrospun PHBV films to evaluate their contact transparency. The effects of the addition of OEO and the NEs on the color coordinates (L*, a*, b*) and the values of ΔE, T, and O of the electrospun PHBV films are shown in Table 2. One can observe that all the here-prepared PHBV films presented a high contact transparency, but they also developed a slightly yellow appearance when the active substances were incorporated. The ΔE values of the active PHBV films with respect to the neat PHBV film were 8.36, 7.52, and 15.82

for the films with OEO, RE, and GTE, respectively. Therefore, the highest color change was observed for the GTE-containing PHBV film. The main changes observed were based on a decrease in brightness (L*) and an increase in the b* coordinate, that is, a yellower material, which was related to the intrinsic color of the added active substances.
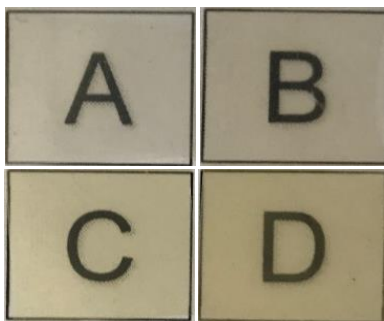
Figure 3. Visual aspect of the electrospun films of: (**a**) Neat poly(3-hydroxybutyrate-co-3-hydroxyvalerate) (PHBV); (**b**) Oregano essential oil (OEO)-containing PHBV; (**c**) Rosemary extract (RE)-containing PHBV; (**d**) Green tea tree extract (GTE)-containing PHBV. Films are 1.5 × 1.5 cm².

Table 2. Color parameters (ΔE*, a*, b*, and L*) and transparency characteristics of the electrospun films of poly(3-hydroxybutyrate-co-3-hydroxyvalerate) (PHBV) containing oregano essential oil (OEO), rosemary extract (RE), and green tea tree extract (GTE)

Sample	a*	b*	L*	ΔE*	T	O
PHBV	0.87 ± 0.07^a	-0.38 ± 0.02^a	89.82 ± 0.06^a	---	3.13 ± 0.02^a	0.016 ± 0.06^a
PHBV + OEO	1.13 ± 0.05^b	6.67 ± 0.03^b	85.35 ± 0.07^b	8.36 ± 0.08^a	3.55 ± 0.03^b	0.019 ± 0.08^b
PHBV + RE	0.04 ± 0.01^c	6.67 ± 0.08^b	87.33 ± 0.01^c	7.52 ± 0.06^b	6.44 ± 0.02^c	0.026 ± 0.05^c
PHBV + GTE	0.07 ± 0.09^c	14.45 ± 0.05^c	84.38 ± 0.03^d	15.82 ± 0.05^c	16.42 ± 0.06^d	0.067 ± 0.04^d

One can also observe that the OEO-containing PHBV film presented a transparency similar to that of the neat PHBV film, both having T values in the range of 3 – 4, which indicated a greater passage of visible light through the material. However, the incorporation of RE and, particularly, of GTE resulted in an increase of T up to values of 6.4 and 16.4, respectively. Therefore, the capacity of transmission of visible and UV light of the films was significantly reduced by the addition of RE and GTE ($p < 0.05$), causing a phenomenon of light scattering due to the characteristic tones of the active substances. Similarly, whereas opacity was kept relatively low for the neat PHBV film and the OEO-containing PHBV films, which both had O values in the 0.015 – 0.02 range, these values increased up to 0.026 and 0.067 for the RE- and GTE-containing PHBV films, respectively. Then, the presence of the latter active substances, particularly GTE, reduced the transparency properties by blocking the passage of UV-Vis light and it increased the opacity of the films, caused by the scattering of light. However, as other authors have previously stated, this property can be also a desired characteristic in some packaging materials for the protection of foodstuff from light, especially UV radiation, which can cause lipid oxidation in the food products [1,40]. In this sense, the work reported by Gómez-Estaca et al. [52] also concluded that the addition of certain NEs to fish gelatin films decreased the transparency of the films and increased the opacity of the final material.

3.4   Thermal Properties

Figure 4 includes the weight loss curves of the free active substances and of the electrospun PHBV films obtained by TGA. The curves for the neat OEO, RE, and GTE are shown in Figure 4A, while the values of the onset degradation temperature, that is, the temperature at 5 % weight loss ($T_{5\%}$), degradation temperature (T_{deg}), and residual mass at 700 °C are gathered in Table 3. One can observe that OEO presented the lowest thermal stability, showing values of $T_{5\%}$ and T_{deg} of 101.5 °C and 178.4 °C, respectively, with a respective weight loss of 74.16 % at T_{deg}, corresponding to the volatilization and/or degradation of low-MW volatile compounds present in the OEO (e.g., carvacrol, thymol, and pinene). In this sense, other authors have also reported that the EOs and NEs of oregano are among the most thermally unstable active substances. For instance, Barbieri et al. [53] reported that 96 – 97 % of the OEO's weight was lost between 200 °C and 216 °C, attributed to its volatilization. In another work, Yang et al. [54] determined a significant degradation of all terpenes extracted oregano leaves in the 200 – 250 °C range. Similarly, Gibara Guimarães et al. [55] reported the fully thermal decomposition of carvacrol, the most representative active compound of oregano, at 168 °C. Opposite to OEO, both RE and GTE showed a high thermal stability with a similar mass loss profile. In particular, both active

substances presented $T_{5\%}$ values over 350 °C, with Tdeg values of 412.7 °C (52.45 %) and 411.5 °C (49.89 %) for RE and and GTE, respectively. Similar results, though slighlty lower, were reported for RE by Piñeros-Hernandez et al. [56], showing a significant mass loss at 300 °C, corresponding to the decomposition of phenolic diterpenes, that is, carnosic acid, carnosol, and rosmarinic acid. Likewise, Cordeiro et al. [57] obtained a mass loss as low as 6 % up to 190 °C. In the case of GTE, López de Dicastillo et al. [58] determined that it remained stable up to the range of 200 – 400 °C, where the thermal degradation of partially glycosylated catechins occurs. Furthermore, all active substances produced a residual mass below 1 %.
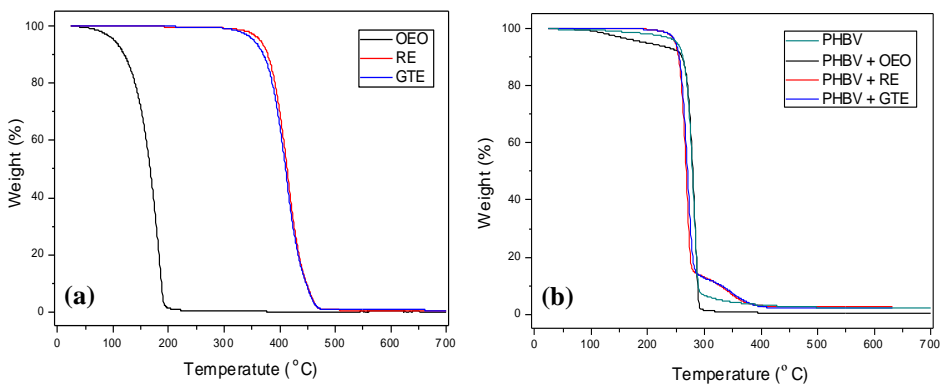
Figure 4. Weight loss as a function of temperature for: (**a**) Oregano essential oil (OEO), rosemary extract (RE), and green tea tree extract (GTE); (**b**) Electrospun films of neat poly(3-hydroxybutyrate-co-3-hydroxyvalerate) (PHBV) and PHBV containing OEO, RE, and GTE.

Table 3. Thermal properties of oregano essential oil (OEO), rosemary extract (RE), and green tea tree extract (GTE) and of the electrospun films of poly(3-hydroxybutyrate-co-3-hydroxyvalerate) (PHBV) containing OEO, RE, and GTE in terms of temperature at 5 % weight loss ($T_{5\%}$), degradation temperature (T_{deg}), and residual mass at 700 °C

| Sample	$T_{5\%}$ (°C)	T_{deg} (°C)	Mass loss (%)	Residual mass (%)
OEO	101.5	178.4	74.16	0.14
RE	364.0	412.7	52.45	0.48
GTE	352.7	411.5	49.89	0.56
PHBV	251.5	278.7	47.74	2.10
PHBV + OEO	197.5	283.6	69.58	0.16
PHBV + RE	248.5	270.8	60.94	2.49
PHBV + GTE	249.3	273.8	61.65	2.21

In Figure 4b, the weight loss curves of the electrospun PHBV films containing OEO, RE, and GTE are gathered. The neat PHBV film was thermally stable up to 251.5 °C,

showing a T_{deg} value of 278.7 °C (47.74 %) and a residual mass of 2.10 %. While the incorporation of RE and GTE slightly reduced the thermal stability by 5 – 10 °C, the presence of OEO considerably reduced the onset of degradation, showing a $T_{5\%}$ value of 197.5 °C. It is also worthy to mention, however, that all active substances increased the thermally decomposed mass at T_{deg}, that is, the weight values decreased to the 60 – 70 % range. Therefore, the here-produced active PHBV films were stable up to 200 °C, which certainly opened up their application as an active food packaging interlayer and/or coating.

3.5 Water Contact Angle

The water contact angle refers to the degree of affinity of water with a surface, which defines the degree of hydrophilicity/hydrophobicity of a given polymer material [59]. In Figure 5, the water drop images on the films, as well as the values of their contact angles, are shown for the electrospun PHBV films. In Figure 5a, one can observe that the neat PHBV film presented an angle of 103.61°, which is characteristic of hydrophobic materials [60]. In all cases, the incorporation of the active substances resulted in a significant decrease in hydrophobicity ($p < 0.05$). Figure 5b shows that the OEO-containing PHBV film presented a water contact angle of 82.23°, whilst these values were even lower for both the films containing RE (Figure 5c), that is, 73.86°, and GTE (Figure 5d), that is, 71.26°. The reduction achieved could be related to the presence of the oily molecules on the surfaces of the PHBV films, which decreased the surface tension. A similar decrease in the water contact angles was observed by Galus and Kadzińska [61] in whey protein isolate (WPI) edible films when almond and walnut oils were added. In any case, following the terms "hydrophobic" and "hydrophilic", defined for $\theta > 65$ ° and ≤ 65 °, respectively [62], the angles for each of the films studied were still within the hydrophobic range.
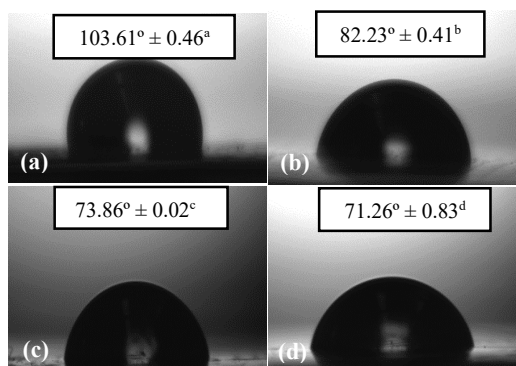
Figure 5. Water contact angle of the electrospun films of: (**a**) Neat poly(3-hydroxybutyrate-co-3-hydroxyvalerate) (PHBV); (**b**) Oregano essential oil (OEO)-containing PHBV; (**c**) Rosemary extract (RE)-containing PHBV; (**d**) Green tea tree extract (GTE)-containing PHBV.

3.6   Active properties

3.6.1   *Antimicrobial Activity*

The EOs and NEs obtained from aromatic plants are constituted by a wide range of active compounds that are responsible for antimicrobial and antioxidant activity, which has promoted their application in active food packaging [1,41,42]. Table 4 shows the MIC and MBC values of the neat OEO, RE, and GTE against strains of *S. aureus* (Gram positive, G+) and *E. coli* (Gram negative, G-). The results showed that the OEO presented the highest antibacterial effect against both bacterial strains, having achieved identical MIC and MBC values, that is, 0.625 µL/mL, against *E. coli*, and 0.312 µL/mL, against *S. aureus*. The fact that the MIC and MBC values were identical can be related to the high effectivity of the natural compounds that were achieved, at the same time, the inhibition of microbial growth and the elimination of 99.9% of the microorganisms [63]. The antimicrobial activity of the OEO has been mainly ascribed to its high content in carvacrol and thymol [64,65]. RE presented MIC values of 10 µL/mL and 5 µL/mL against *E. coli* and *S. aureus*, respectively, whereas its MBC values were 20 µL/mL, against *E. coli*, and 10 µL/mL, against *S. aureus*. The main compounds responsible for the antimicrobial activity of RE were α-pinene, myrcene, camphor, 1,8-cineole, and camphene [29,66,67]. Likewise, GTE showed the lowest antimicrobial performance. This NE presented MIC values of 160 µL/mL, against *E. coli*, and 80 µL/mL, against *S. aureus*. Its MBC values were 160 µL/mL, against *E. coli*, and 40 µL/mL, against *S. aureus*. Gallic acid (GA), theobromine, chlorogenic acid, and caffeic acid are known to be responsible for its antimicrobial activity [32,68]. Most research related to MIC and MBC

determination has been conducted with these EOs and NEs, finding that these compounds have a broad inhibition spectrum against G+ bacteria, but they are not as efficient against some G- bacteria [69,70]. The values of the MBC and MIC for OEO were the same, while for RE and GTE, the MBC values were higher than the MIC values. This fact is related to the effectiveness of the active compounds, the susceptibility of the microorganisms, and the variation in the penetration rate of the extracts through the cell wall and the structures of the cell membrane [71,72].

Table 4. Minimum inhibitory concentration (MIC) and minimum bactericidal concentration (MBC) of oregano essential oil (OEO), rosemary extract (RE), and green tea tree extract (GTE) against *S. aureus* and *E. Coli*

Sample	Bacteria	MIC	MBC
OEO	*E. coli*	0.625 µL/mL	0.625 µL/mL
	S. aureus	0.312 µL/mL	0.312 µL/mL
RE	*E. coli*	10 µL/mL	20 µL/mL
	S. aureus	5 µL/mL	10 µL/mL
GTE	*E. coli*	160 µL/mL	160 µL/mL
	S. aureus	40 µL/mL	80 µL/mL

The antimicrobial properties of the electrospun PHBV films containing OEO, RE, and GTE were also evaluated using the JIS Z2801 against *S. aureus* and *E. coli* bacteria, in both an open and closed system, for 1, 8, and 15 days. In relation to the open system, as shown in Table 5, one can observe that the films containing OEO showed the strongest inhibition. These films provided a strong reduction (R ≥ 3), that is, with a reduction of 3 log units, against *S. aureus*, and also a high antimicrobial effect, though slightly lower, presenting R values of 2.7–2.9 against *E. coli*. In the case of the films containing RE and GTE, the films yielded a bacteriostatic effect (1 ≤ R < 3) against both bacteria. The antimicrobial effect of RE was also approximately 1 log units higher than that observed for GTE. These results agreed with the MIC and MBC described above, where OEO inhibited the growth of *E. coli* and *S. aureus* at lower contents, whilst RE and GTE showed higher MIC and MBC values. It is also worthy to mention that in all cases, the bacterial reduction slightly increased over the days, which can be related to the slow release of the active compounds to the surface of the films. In comparison to the previous results of electrospun antimicrobial films reported by Jeong-Ann Parka and Song-Bae Kim [73] in open systems, it was observed that the inhibition of *S. aureus* increased from a 0.6 log of reduction, at the initial time, to a 1.2 log of reduction, after 120 min. In another study, Figueroa et al. [42] also reported an increase in the bacterial inhibition with the passage of storage days, showing a 3.9 log of reduction after 10 days against *S. aureus*.

Table 5. Antibacterial activity against *S. aureus* and *E. coli* of the electrospun poly(3-hydroxybutyrate-co-3-hydroxyvalerate) (PHBV) films containing oregano essential oil (OEO), rosemary extract (RE), and green tea tree extract (GTE) in the open system for up to 15 days

Bacteria	Sample	Day	Control sample log (CFU/mL)	Test sample log (CFU/mL)	R
S. aureus	PHBV + OEO	1	6.91 ± 0.06	3.78 ± 0.08	3.13 ± 0.06
		8	6.88 ± 0.50	3.68 ± 0.03	3.20 ± 0.04
		15	6.89 ± 0.20	3.65 ± 0.10	3.24 ± 0.15
	PHBV + RE	1	6.87 ± 0.03	4.07 ± 0.07	2.80 ± 0.06
		8	6.88 ± 0.09	4.01 ± 0.03	2.87 ± 0.03
		15	6.87 ± 0.02	3.95 ± 0.01	2.92 ± 0.02
	PHBV + GTE	1	6.91 ± 0.10	5.00 ± 0.32	1.91 ± 0.20
		8	6.89 ± 0.23	4.94 ± 0.18	1.95 ± 0.13
		15	6.92 ± 0.11	4.93 ± 0.22	1.99 ± 0.19
E. coli	PHBV + OEO	1	6.95 ± 0.30	4.24 ± 0.09	2.71 ± 0.10
		8	6.90 ± 0.08	4.09 ± 0.10	2.81 ± 0.20
		15	6.87 ± 0.07	4.01 ± 0.03	2.86 ± 0.05
	PHBV + RE	1	6.89 ± 0.03	5.00 ± 0.06	1.89 ± 0.05
		8	6.90 ± 0.09	4.96 ± 0.07	1.94 ± 0.07
		15	6.88 ± 0.08	4.91 ± 0.09	1.97 ± 0.07
	PHBV + GTE	1	6.89 ± 0.15	5.70 ± 0.19	1.19 ± 0.17
		8	6.87 ± 0.33	5.63 ± 0.21	1.24 ± 0.23
		15	6.90 ± 0.46	5.62 ± 0.27	1.28 ± 0.31

As shown in Table 6, for all the samples, the reduction was slightly higher in the closed system than in the open one. While the films containing OEO presented the strongest inhibition (R ≥ 3) after 15 days of storage in the closed system against the two bacterial strains, the films that contained RE and GTE showed a significant inhibition (1 ≤ R < 3). This result could be attributed to the accumulation of volatile active compounds in the headspace of the closed chamber. There are a limited number of studies reporting the antimicrobial performance of the active films in closed systems, which indeed are more practical from the point of view of packaging and the design of containers to avoid deterioration of food products during storage. For instance, Torres-Giner et al. [74] developed a multilayer system, based on an electrospun coating of zein composite nanofibers containing thymol on a polylactide (PLA) film, that was evaluated against *Listeria monocytogenes* in a closed atmosphere in desiccators. It was reported that a concentration as low as 1.6 ppm was able to produce a decrease in the CFU of about 3 log units, whereas above 6.1 ppm, no CFU were detected. The high antimicrobial performance achieved was ascribed to the capacity of the electrospun material to release the bioactive in a sustained manner. The results are of potential interest in packaging applications, since the antimicrobial effect was not only successfully achieved in open packaging systems,

but it also prolonged and improved over time in closed packaging systems, thereby extending the shelf life of perishable foods [75,76].

Table 6. Antibacterial activity against *S. aureus* and *E. coli* of the electrospun poly(3-hydroxybutyrate-co-3-hydroxyvalerate) (PHBV) films containing oregano essential oil (OEO), rosemary extract (RE), and green tea tree extract (GTE) in the closed system for up to 15 days

Bacteria	Sample	Day	Control sample log (CFU/mL)	Test sample log (CFU/mL)	R
S. aureus	PHBV + OEO	1	6.91 ± 0.06	3.78 ± 0.08	3.13 ± 0.06
		8	6.93 ± 0.30	3.52 ± 0.90	3.41 ± 0.30
		15	6.92 ± 0.20	3.33 ± 0.08	3.59 ± 0.07
	PHBV + RE	1	6.87 ± 0.03	4.07 ± 0.07	2.80 ± 0.06
		8	6.89 ± 0.07	3.92 ± 0.05	2.91 ± 0.04
		15	6.88 ± 0.12	3.86 ± 0.15	3.02 ± 0.11
	PHBV + GTE	1	6.91 ± 0.10	5.00 ± 0.32	1.91 ± 0.20
		8	6.89 ± 0.15	4.89 ± 0.17	2.00 ± 0.11
		15	6.86 ± 0.20	4.78 ± 0.19	2.08 ± 0.21
E. coli	PHBV + OEO	1	6.95 ± 0.30	4.24 ± 0.09	2.71 ± 0.10
		8	6.90 ± 0.08	3.96 ± 0.10	2.94 ± 0.30
		15	6.92 ± 0.09	3.91 ± 0.07	3.01 ± 0.06
	PHBV + RE	1	6.89 ± 0.03	5.00 ± 0.06	1.89 ± 0.05
		8	6.87 ± 0.05	4.88 ± 0.08	1.99 ± 0.09
		15	6.88 ± 0.07	4.79 ± 0.03	2.09 ± 0.05
	PHBV + GTE	1	6.89 ± 0.15	5.70 ± 0.19	1.19 ± 0.17
		8	6.91 ± 0.11	5.62 ± 0.13	1.29 ± 0.15
		15	6.90 ± 0.28	5.53 ± 0.21	1.37 ± 0.19

3.6.2 *Antioxidant Activity*

The antioxidant activity of the EOs and NEs, obtained from aromatic plants, is conferred by their phenolic compounds. The DPPH free radical method is an antioxidant assay based on an electron-transfer that produces a violet solution in methanol. This free radical, stable at room temperature, is reduced in the presence of an antioxidant molecule (active compound), giving rise to a colorless solution [77]. The use of the DPPH assay provides an easy and rapid way to evaluate antioxidants using spectrophotometry. In the conservation of foods, substances with character antioxidants are of great interest because the main cause of food deterioration results from enzymatic reactions that trigger the oxidation of lipids and carbohydrates [78,79].

The percent inhibition and the equivalent concentration in micrograms of trolox per gram of sample of the neat OEO, RE, GTE, and of the electrospun fibers and films of the PHBV containing the active substances are shown in Table 7. One can observe that all the EOs and NEs showed DPPH radical scavenging activity. OEO presented

the highest percentage of inhibition (91.96 %) attributed to its main active compounds (e.g., carvacrol, thymol, p-cymene, γ-terpinene) [64]. Similarly, Chun et al. [80] reported an inhibition percentage of DPPH of 82% for oregano extracts. RE presented a percentage of inhibition of 75.24 %, which was in agreement with, for instance, Bajalan et al. [81] who reported an inhibition percentage of DPPH of 73.69 %. GTE showed an inhibition of 71.77 %, conferred by the relative amount of catechins and GA [82]. Afroz Bakht et al. [83] studied the antioxidant activity from DPPH of five commercial teas, finding percentages of inhibition in the 24 – 71 % range. In addition, Lu and Chen [84] reported percentages of inhibition between 33 % and 62 %. In this sense, it is important to highlight that antioxidant activity is dependent on the quantity of secondary metabolites that the plant manages to synthesize in its development stage, which is influenced by the variety of the plant, the environmental conditions [85,86,87], and the extraction method used [83].

Table 7. Inhibition percentage (%) of 2,2-diphenyl-1-picrylhydrazyl radical (DPPH) and concentration (eq. trolox/g sample) of DPPH for oregano essential oil (OEO), rosemary extract (RE), and green tea tree extract (GTE) and the electrospun fibers of poly(3-hydroxybutyrate-co-3-hydroxyvalerate) (PHBV) containing OEO, RE, and GTE

Sample	Inhibition (%)	Concentration (µg eq Trolox/g sample)
OEO	91.96 ± 0.03	84.34 ± 0.03
RE	75.24 ± 0.04	62.34 ± 0.03
GTE	71.77 ± 0.08	61.95 ± 0.07
PHBV + OEO	43.14 ± 0.07	28.56 ± 0.05
PHBV + RE	25.82 ± 0.07	18.31 ± 0.05
PHBV + GTE	22.12 ± 0.06	13.14 ± 0.04

One can observe that the antioxidant activity decreased in the electrospun PHBV fibers containing OEO, RE, and GTE. After the electrospinning process, the fibers with OEO showed a percentage of inhibition of 43.14 %, whereas the fibers containing RE and GTE showed values of 25.82 % and 22.12 %, respectively. In all cases, there was a decrease in the antioxidant activity of between 20 % and 30 % compared to the pure OEO, RE, and GTE. The lower antioxidant inhibition of the active compounds inside the fibers could be related to polarity differences between the solvent and the polymer, the stirring process applied to the active solution prior to electrospinning, and the loss of volatiles compounds during the electrospinning process [44].

Table 8 shows the percentages of inhibition and the equivalent concentration in micrograms of trolox per gram of sample of the electrospun PHBV films containing OEO, RE, and GTE, evaluated in the so-called open and closed systems on days 1, 8, and 15. Films containing OEO exhibited the highest inhibition of DPPH at day 1

(24.54 %), followed by films with the RE (15.59 %) and films with the GTE (11.14 %). Over time, all the films decreased their antioxidant activity, obtaining no significant differences in the results between each storage system. Thus, after 15 days, an inhibition percentage in the range of 8.83 – 10.55 % was obtained for the films containing OEO. At this time, the inhibition percentage ranges for the films containing RE and GTE were 6.91 – 7.31 % and 5.45 – 6.68 %, respectively. As can be observed, the antioxidant activity decreased when the EOs and NEs were included in the PHBV fibers and, more intensively, when the films were formed. Likewise, during the days of storage, a continuous release of the characteristic volatile compounds of each EOs and NEs was produced, which was evidenced by the low percentage of DPPH inhibition at day 15 for all the samples. Previous reports have indicated that the degree of antioxidant power of biodegradable films is generally proportional to the amount of added antioxidant additives, while the thermal process for obtaining the films also affects the bioactivity, since most of the bioactive compounds are sensitive to temperatures above 80 °C [47,88]. Regardless of this, all the films presented antioxidant performance and they can, therefore, be applied in antioxidant active packaging systems to extend the shelf life of packaged food products, thus minimizing the development of off-flavors, color and flavor changes, and nutritional losses [89,90].

Table 8. Inhibition percentage (%) of 2,2-diphenyl-1-picrylhydrazyl radical (DPPH) and concentration (µg eq. trolox/g sample) of DPPH for the electrospun poly(3-hydroxybutyrate-co-3-hydroxyvalerate) (PHBV) films containing oregano essential oil (OEO), rosemary extract (RE), and green tea tree extract (GTE)

Sample	Day	Open system		Closed system	
		Inhibition (%)	Concentration (µg eq Trolox/g sample)	Inhibition (%)	Concentration (µg eq Trolox/g sample)
PHBV+ OEO	1	24.54 ± 0.04	26.48 ± 0.04	24.54 ± 0.04	26.48 ± 0.04
	8	16.08 ± 0.08	16.82 ± 0.09	17.43 ± 0.04	17.57 ± 0.04
	15	14.90 ± 0.06	15.75 ± 0.06	15.24 ± 0.01	16.47 ± 0.01
PHBV+ RE	1	15.59 ± 0.02	16.31 ± 0.02	15.59 ± 0.02	16.31 ± 0.02
	8	10.42 ± 0.08	10.27 ± 0.08	13.50 ± 0.01	13.97 ± 0.01
	15	7.310 ± 0.04	7.710 ± 0.04	8.200 ± 0.15	8.120 ± 0.02
PHBV+ GTE	1	11.14 ± 0.04	11.79 ± 0.04	11.14 ± 0.04	11.79 ± 0.04
	8	8.910 ± 0.10	8.760 ± 0.10	9.960 ± 0.02	9.820 ± 0.02
	15	6.680 ± 0.11	6.540 ± 0.11	7.800 ± 0.02	8.250 ± 0.02

4   Conclusions

The evaluation of the active properties, that is, antimicrobial and antioxidant properties, of OEO, RE, and GTE showed that OEO was the active substance that presented the highest antimicrobial activity against *S. aureus* and *E. coli*. This effect was mainly attributed to the effectiveness of its most representative active compounds, that is, carvacrol and thymol, showing identical MIC and MBC values of 0.312 and 0.625 µL/mL, respectively. The antioxidant activity of OEO was also higher than that for the RE and GTE. In particular, the percentage of inhibition of the DPPH was 91.96%. Thereafter, these active substances were incorporated at 10 wt.% into fruit waste derived PHBV by electrospinning. To this end, the solution properties of the PHBV containing OEO, RE, and GTE were first evaluated to determine the optimal conditions to obtain homogenous fibers. The diameters of the fibers were relatively similar, with a mean size of approximately ~0.8 µm, being uniform and smooth, without any superficial and structural defects. It was observed that the addition of the OEO and the NEs did not alter the fiber formation during electrospinning or the morphology of the electrospun ultrathin PHBV fibers. A good compatibility and, then, high solubility of the OEO and NEs with the PHBV matrix was considered.

In order to obtain an interesting active continuous layer to be applied in the design of biopackaging, the electrospun mats of the PHBV fibers containing the active substances were subjected to a thermal post-treatment at 125 °C. Continuous PHBV films of ~80 µm, with a smooth surface were obtained, though the presence of the active substances induced a slight porosity in their cross-section. The optical properties of the PHBV films were slightly impaired by the addition of the active substances, particularly GTE, reducing their transparency from 3.13 up to 16.42 through blocking the passage of UV-Vis light and increasing their opacity, which was caused by the scattering of light. In any case, all the PHBV films were contact transparent. All active substances also decreased the values of the Tonset by 54 °C for OEO, 3 °C for RE, and 2.2 °C for GTE, and the thermally decomposed mass at Tdeg decreased to the 60–70% range. However, all the active PHBV films were stable up to 200 °C. Referring to the hydrophobicity of the films, the addition of active substances decreased the superficial tension of the PHBV films with respect to the control, but the angles for each of the films studied were still within the hydrophobic range. The PHBV films containing OEO, RE, and GTE showed antimicrobial activity against strains of *S. aureus* and *E. coli* in both the here-studied open and closed systems, where the bacterial reduction improved over time due to the release and accumulation of the active compounds on the film surface. The antimicrobial activity was higher in the case of the closed system due to the presence

of volatiles stored in the headspace. The films containing OEO presented the highest reduction values against the two bacterial strains (R ≥ 3), while the films containing RE and GTE showed lower reduction values (1 ≤ R < 3), which agreed with the MIC and MBC values of the pure active substances. The antioxidant activity of the fibers and films was much lower than that of the neat active substances, which was related to entrapment and loss during electrospinning and film processing, and which was also reduced with the passage of days due to the continuous release of the active compounds.

The here-developed electrospun PHBV layers with OEO, RE, and GTE are potential candidates for use in the design of sustainable active multilayer biopackaging. The antimicrobial and antioxidant performance of these materials is advantageous to prolonging the shelf life of foods, delaying the proliferation of microorganisms, and the enzymatic oxidation of foodstuffs.

5 References

1. Figueroa-Lopez, K.J.; Andrade-Mahecha, M.M.; Torres-Varga, O.L. Development of antimicrobial biocomposite films to preserve the quality of bread. *Molecules* **2018**, *23*, 212.
2. Atarés, L.; Chiralt, A. Essential oils as additives in biodegradable films and coatings for active food packaging. *Trends Food Sci. Technol.* **2016**, *48*, 51–62.
3. Requena, R.; Vargas, M.; Chiralt, A. Obtaining antimicrobial bilayer starch and polyester-blend films with carvacrol. *Food Hydrocoll.* **2018**, *83*, 118–133.
4. Lenz, R.W.; Marchessault, R.H. Bacterial polyesters: Biosynthesis, biodegradable plastics and biotechnology. *Biomacromolecules* **2005**, *6*, 1–8.
5. Sudesh, K.; Abe, H.; Do, Y. Synthesis, structure and properties of polyhydroxyalkanoates: Biological polyesters. *Prog. Polym. Sci.* **2000**, *25*, 1503–1555.
6. Torres-Giner, S.; Montanes, N.; Boronat, T.; Quiles-Carrillo, L.; Balart, R. Melt grafting of sepiolite nanoclay onto poly(3-hydroxybutyrate-co-4-hydroxybutyrate) by reactive extrusion with multi-functional epoxy-based styrene-acrylic oligomer. *Eur. Polym. J.* **2016**, *84*, 693–707.
7. Torres-Giner, S.; Montanes, N.; Fombuena, V.; Boronat, T.; Sanchez-Nacher, L. Preparation and characterization of compression-molded green composite sheets made of poly(3-hydroxybutyrate) reinforced with long pita fibers. *Adv. Polym. Technol.* **2018**, *37*, 1305–1315.
8. Arifin, W.; Kuboki, T. Effects of thermoplastic elastomers on mechanical and thermal properties of glass fiber reinforced poly(3-hydroxybutyrate-co-3-hydroxyhexanoate) composites. *Polym. Compos.* **2018**, *39*, E1331–E1345.
9. Torres-Giner, S.; Hilliou, L.; Melendez-Rodriguez, B.; Figueroa-Lopez, K.J.; Madalena, D.; Cabedo, L.; Covas, J.A.; Vicente, A.A.; Lagaron, J.M. Melt processability, characterization, and antibacterial activity of compression-molded green composite sheets made of poly(3-hydroxybutyrate-co-3-hydroxyvalerate) reinforced with coconut fibers impregnated with oregano essential oil. *Food Packag. Shelf Life* **2018**, *17*, 39–49.
10. López-Rubio, A.; Almenar, E.; Hernandez-Muñoz, P.; Lagarón, J.M.; Catalá, R.; Gavara, R. Overview of active polymer-based packaging technologies for food applications. *Food Rev. Int.* **2004**, *20*, 357–387.
11. Torres-Giner, S.; Gil, L.; Pascual-Ramírez, L.; Garde-Belza, J.A. Packaging: Food waste reduction. In *Encyclopedia of Polymer Applications, 3 Volume Set*; Mishra, M., Ed.; CRC Press, Taylor and Francis Group: Boca Raton, FL, USA, 2018; pp. 1990–2009.
12. Cherpinski, A.; Gozutok, M.; Sasmazel, H.T.; Torres-Giner, S.; Lagaron, J.M. Electrospun oxygen scavenging films of poly(3-hydroxybutyrate) containing palladium nanoparticles for active packaging applications. *Nanomaterials* **2018**, *8*, 469.
13. Domínguez, R.; Barba, F.J.; Gómez, B.; Putnik, P.; Bursać Kovačevićc, D.; Pateiro, M.; Santos, E.M.; Lorenzo, J.M. Active packaging films with natural antioxidants to be used in meat industry: A review. *Food Res. Int.* **2018**, *113*, 93–101.
14. Ge, L.; Zhu, M.; Li, X.; Xu, Y.; Ma, X.; Shi, R.; Li, D.; Mu, C. Development of active rosmarinic acid-gelatin biodegradable films with antioxidant and long-term antibacterial activities. *Food Hydrocoll.* **2018**, *83*, 308–316.
15. Irkin, R.; Esmer, O.K. Novel food packaging systems with natural antimicrobial agents. *J. Food Sci. Technol.* **2015**, *52*, 6095–6111.
16. Appendini, P.; Hotchkiss, J.H. Review of antimicrobial food packaging. *Innov. Food Sci. Emerg. Technol.* **2002**, *3*, 113–126.
17. Ribeiro-Santos, R.; Andrade, M.; Sanches-Silva, A. Application of encapsulated essential oils as antimicrobial agents in food packaging. *Curr. Opin. Food Sci.* **2017**, *14*, 78–84.
18. Nguimjeu, C.; Moundanga, S.; Sadaka, F.; Dony, P.; Plasseraud, L.; Boni, G.; Brachais, L.; Vroman, I.; Brachais, C.H.; Tighzert, L.; et al. Suitability and effectiveness of active packaging for food contact: A study of sorption/desorption and antimicrobial performances of some natural extracts in packaging. In *18th IAPRI World Packaging Conference*; DEStech Publications, Inc.: Lancaster, PA, USA, 2012; pp. 15–22.
19. Hoseinnejad, M.; Jafari, S.M.; Katouzian, I. Inorganic and metal nanoparticles and their antimicrobial activity in food packaging applications. *Crit. Rev. Microbiol.* **2018**, *44*, 161–181.
20. Teixeira, B.; Marques, A.; Ramos, C.; Neng, N.R.; Nogueira, J.M.F.; Saraiva, J.A.; Nunes, M.L. Chemical composition and antibacterial and antioxidant properties of commercial essential oils. *Ind. Crop. Prod.* **2013**, *43*, 587–595.

21. Raut, J.S.; Karuppayil, S.M. A status review on the medicinal properties of essential oils. *Ind. Crop. Prod.* **2014**, *62*, 250–264.

22. FDA. *Code of Federal Regulations—Title 21—Food Drugs. Chapter I—Food Drug Adm. Dep. Heal. Hum. Serv. Subchapter b—Food Hum. Consum. (Continued), Part 182—Subst. Gen. Recognized as Safe (Gras)*; FDA: Silver Spring, MD, USA, 2016.

23. Leyva-López, N.; Gutiérrez-Grijalva, E.; Vazquez-Olivo, G.; Heredia, J. Essential oils of oregano: Biological activity beyond their antimicrobial properties. *Molecules* **2017**, *22*, 989.

24. Kokkini, S.; Karousou, R.; Dardioti, A.; Krigas, N.; Lanaras, T. Autumn essential oils of greek oregano. *Phytochemistry* **1997**, *44*, 883–886.

25. Gounaris, Y.; Skoula, M.; Fournaraki, C.; Drakakaki, G.; Makris, A. Comparison of essential oils and genetic relationship of origanum x intercedens to its parental taxa in the island of crete. *Biochem. Syst. Ecol.* **2002**, *30*, 249–258.

26. Shang, X.; Wang, Y.; Zhou, X.; Guo, X.; Donga, S.; Wang, D.; Zhang, J.; Pan, H.; Zhang, Y.; Miao, X. Acaricidal activity of oregano oil and its major component, carvacrol, thymol and p-cymene against psoroptes cuniculi in vitro and in vivo. *Vet. Parasitol.* **2016**, *226*, 93–96.

27. Burt, S.A.; Vlielander, R.; Haagsman, H.P.; Veldhuizen, E.J.A. Increase in activity of essential oil components carvacrol and thymol against *Escherichia coli* o157:H7 by addition of food stabilizers. *J. Food Prot.* **2005**, *68*, 919–926.

28. Begum, A.; Sandhya, S.; Ali, S.S.; Vinod, K.R.; Reddy, S.; Banji, D. An in-depth review on the medicinal flora rosmarinus officinalis (lamiaceae). *Acta Sci. Pol. Technol. Aliment.* **2013**, *12*, 61–73.

29. Jiang, Y.; Wu, N.; Fu, Y.-J.; Wang, W.; Luo, M.; Zhao, C.-J.; Zu, Y.-G.; Liu, X.-L. Chemical composition and antimicrobial activity of the essential oil of rosemary. *Environ. Toxicol. Pharmacol.* **2011**, *32*, 63–68.

30. Arranz, E.; Mes, J.; Wichers, H.J.; Jaime, L.; Mendiola, J.A.; Reglero, G.; Santoyo, S. Anti-inflammatory activity of the basolateral fraction of caco-2 cells exposed to a rosemary supercritical extract. *J. Funct. Foods* **2015**, *13*, 384–390.

31. Hussain, A.I.; Anwar, F.; Chatha, S.A.S.; Jabbar, A.; Mahboob, S.; Nigam, P.S. Rosmarinus officinalis essential oil: Antiproliferative, antioxidant and antibacterial activities. *Braz. J. Microbiol.* **2010**, *41*, 1070–1078.

32. Fournier-Larente, J.; Morin, M.-P.; Grenier, D. Green tea catechins potentiate the effect of antibiotics and modulate adherence and gene expression in porphyromonas gingivalis. *Arch. Oral Biol.* **2016**, *65*, 35–43.

33. Torres-Giner, S. Electrospun nanofibers for food packaging applications. In *Multifunctional and Nanoreinforced Polymers for Food Packaging*; Lagaron, J.M., Ed.; Woodhead Publishing Ltd.: Cambridge, UK, 2011; pp. 108–125.

34. Torres-Giner, S.; Busolo, M.; Cherpinski, A.; Lagaron, J.M. Electrospinning in the packaging industry. In *Electrospinning: From Basic Research to Commercialization*; Kny, E., Ghosal, K., Thomas, S., Eds.; The Royal Society of Chemistry: Cambridge, UK, 2018; pp. 238–260.

35. Torres-Giner, S.; Lagaron, J.M. Zein-based ultrathin fibers containing ceramic nanofillers obtained by electrospinning. I. Morphology and thermal properties. *J. Appl. Polym. Sci.* **2010**, *118*, 778–789.

36. Torres-Giner, S. Novel antimicrobials obtained by electrospinning methods. In *Antimicrobial Polymers*; Lagaron, J.M., Ocio, M.J., López-Rubio, A., Eds.; John Wiley & Sons, Inc.: Hoboken, NJ, USA; pp. 261–285.

37. Altan, A.; Aytac, Z.; Uyar, T. Carvacrol loaded electrospun fibrous films from zein and poly(lactic acid) for active food packaging. *Food Hydrocoll.* **2018**, *81*, 48–59.

38. Cherpinski, A.; Torres-Giner, S.; Cabedo, L.; Lagaron, J.M. Post-processing optimization of electrospun submicron poly(3-hydroxybutyrate) fibers to obtain continuous films of interest in food packaging applications. *Food Addit. Contam. Part A* **2017**, *34*, 1817–1830.

39. Melendez-Rodriguez, B.; Castro-Mayorga, J.L.; Reis, M.A.M.; Sammon, C.; Cabedo, L.; Torres-Giner, S.; Lagaron, J.M. Preparation and characterization of electrospun food biopackaging films of poly(3-hydroxybutyrate-co-3-hydroxyvalerate) derived from fruit pulp biowaste. *Front. Sustain. Food Syst.* **2018**, *2*, 1–16.

40. Kanatt, S.R.; Rao, M.S.; Chawla, S.P.; Sharma, A. Active chitosan–polyvinyl alcohol films with natural extracts. *Food Hydrocoll.* **2012**, *29*, 290–297.

41. Figueroa-Lopez, K.J.; Andrade-Mahecha, M.M.; Torres-Vargas, O.L. Spice oleoresins containing antimicrobial agents improve the potential use of bio-composite films based on gelatin. *Food Packag. Shelf Life* **2018**, *17*, 50–56.

42. Figueroa-López, K.J.; Castro-Mayorga, J.L.; Andrade-Mahecha, M.M.; Cabedo, L.; Lagaron, J.M. Antibacterial and barrier properties of gelatin coated by electrospun polycaprolactone ultrathin fibers

containing black pepper oleoresin of interest in active food biopackaging applications. *Nanomaterials* **2018**, *8*, 199.

43. Torres-Giner, S.; Torres, A.; Ferrándiz, M.; Fombuena, V.; Balart, R. Antimicrobial activity of metal cation-exchanged zeolites and their evaluation on injection-molded pieces of bio-based high-density polyethylene. *J. Food Saf.* **2017**, *37*, 1–12.

44. Busolo, M.A.; Lagaron, J.M. Antioxidant polyethylene films based on a resveratrol containing clay of interest in food packaging applications. *Food Packag. Shelf Life* **2015**, *6*, 30–41.

45. Rošic, R.; Pelipenko, J.; Kocbek, P.; Baumgartner, S.; Bešter-Rogač, M.; Kristl, J. The role of rheology of polymer solutions in predicting nanofiber formation by electrospinning. *Eur. Polym. J.* **2012**, *48*, 1374–1384.

46. Arfa, A.B.; Chrakabandhu, Y.; Preziosi-Belloy, L.; Chalie, P.; Gontard, N. Coating papers with soy protein isolates as inclusion matrix of carvacrol. *Food Res. Int.* **2007**, *40*, 22–32.

47. Jouki, M.; Yazdi, F.T.; Mortazavi, S.A.; Koocheki, A. Quince seed mucilage films incorporated with oregano essential oil: Physical, thermal, barrier, antioxidant and antibacterial properties. *Food Hydrocoll.* **2014**, *36*, 9–19.

48. Bhardwaj, N.; Kundu, S.C. Electrospinning: A fascinating fiber fabrication technique. *Biotechnol. Adv.* **2010**, *28*, 325–347.

49. Kaltsa, O.; Yanniotis, S.; Mandala, I. Stability properties of different fenugreek galactomannans in emulsions prepared by high-shear and ultrasonic method. *Food Hydrocoll.* **2016**, *52*, 487–496.

50. Mahdi Jafari, S.; He, Y.; Bhandari, B. Production of sub-micron emulsions by ultrasound and microfluidization techniques. *J. Food Eng.* **2007**, *82*, 478–488.

51. Paximada, P.; Echegoyen, Y.; Koutinas, A.A.; Mandala, I.G.; Lagaron, J.M. Encapsulation of hydrophilic and lipophilized catechin into nanoparticles through emulsion electrospraying. *Food Hydrocoll.* **2017**, *64*, 123–132.

52. Gómez-Estaca, J.; Montero, P.; Fernández-Martín, F.; Alemán, A.; Gómez-Guillén, M.C. Physical and chemical properties of tuna-skin and bovine-hide gelatin films with added aqueous oregano and rosemary extracts. *Food Hydrocoll.* **2009**, *23*, 1334–1341.

53. Barbieri, N.; Sanchez-Contreras, A.; Canto, A.; Cauich-Rodriguez, J.V.; Vargas-Coronado, R.; Calvo-Irabien, L.M. Effect of cyclodextrins and mexican oregano (lippia graveolens kunth) chemotypes on the microencapsulation of essential oil. *Ind. Crop. Prod.* **2018**, *121*, 114–123.

54. Yang, Y.; Kayan, B.; Bozer, N.; Pate, B.; Baker, C.; Gizir, A.M. Terpene degradation and extraction from basil and oregano leaves using subcritical water. *J. Chromatogr. A* **2007**, *1152*, 262–267.

55. Gibara Guimarães, A.; Almeida Oliveira, M.; dos Santos Alves, R.; dos Passos Menezes, P.; Russo Serafini, M.; Antunes de Souza Araújo, A.; Pereira Bezerra, D.; Quintans Júnior, L.J. Encapsulation of carvacrol, a monoterpene presents in the essential oil of oregano, with β-cyclodextrin, improves the pharmacological response on cancer pain experimental protocols. *Chem. Biol. Interact.* **2015**, *227*, 69–76.

56. Pineros-Hernandez, D.; Medina-Jaramillo, C.; López-Córdoba, A.; Goyanes, S. Edible cassava starch films carrying rosemary antioxidant extracts for potential use as active food packaging. *Food Hydrocoll.* **2017**, *63*, 488–495.

57. Cordeiro, A.M.T.M.; Medeiros, M.L.; Santos, N.A.; Soledade, L.E.B.; Pontes, L.F.B.L.; Souz, A.L.; Queiroz, N.; Souza, A.G. Rosemary (*Rosmarinus officinalis* L.) extract. *J. Therm. Anal. Calorim.* **2013**, *113*, 889–895.

58. López de Dicastillo, C.; Castro-López, M.d.M.; López-Vilariño, J.M.; González-Rodríguez, M.V. Immobilization of green tea extract on polypropylene films to control the antioxidant activity in food packaging. *Food Res. Int.* **2013**, *53*, 522–528.

59. Cherpinski, A.; Torres-Giner, S.; Vartiainen, J.; Peresin, M.S.; Lahtinen, P.; Lagaron, J.M. Improving the water resistance of nanocellulose-based films with polyhydroxyalkanoates processed by the electrospinning coating technique. *Cellulose* **2018**, *25*, 1291–1307.

60. Zou, P.; Liu, H.; Li, Y.; Huang, J.; Yao, D. Surface dextran modified electrospun poly (3-hydroxybutyrate-co-3-hydroxyvalerate) (phbv) fibrous scaffold promotes the proliferation of bone marrow-derived mesenchymal stem cells. *Mater. Lett.* **2016**, *179*, 109–113.

61. Galus, S.; Kadzińska, J. Whey protein edible films modified with almond and walnut oils. *Food Hydrocoll.* **2016**, *52*, 78–86.

62. Medina-Jaramillo, C.; Ochoa-Yepes, O.; Bernal, C.; Famá, L. Active and smart biodegradable packaging based on starch and natural extracts. *Carbohydr. Polym.* **2017**, *176*, 187–194.

63. Bravo Cadena, M.; Preston, G.M.; Van der Hoorn, R.A.L.; Townley, H.E.; Thompson, I.P. Species-specific antimicrobial activity of essential oils and enhancement by encapsulation in mesoporous silica nanoparticles. *Ind. Crop. Prod.* **2018**, *122*, 582–590.

64. Castilho, P.C.; Savluchinske-Feio, S.; Weinhold, T.S.; Gouveia, S.C. Evaluation of the antimicrobial and antioxidant activities of essential oils, extracts and their main components from oregano from madeira island, portugal. *Food Control* **2012**, *23*, 552–558.

65. Stefanakis, M.K.; Touloupakis, E.; Anastasopoulos, E.; Ghanotakis, D.; Katerinopoulos, H.E.; Makridis, P. Antibacterial activity of essential oils from plants of the genus origanum. *Food Control* **2013**, *34*, 539–546.

66. Mohsenabadi, N.; Rajaei, A.; Tabatabaei, M.; Mohsenifar, A. Physical and antimicrobial properties of starch-carboxy methyl cellulose film containing rosemary essential oils encapsulated in chitosan nanogel. *Int. J. Biol. Macromol.* **2018**, *112*, 148–155.

67. Okoh, O.O.; Sadimenko, A.P.; Afolayan, A.J. Comparative evaluation of the antibacterial activities of the essential oils of rosmarinus officinalis l. Obtained by hydrodistillation and solvent free microwave extraction methods. *Food Chem.* **2010**, *120*, 308–312.

68. Saeed, M.; Naveed, M.; Arif, M.; Kakar, M.U.; Manzoor, R.; El-Hack, M.E.A.; Alagawany, M.; Tiwari, R.; Khandia, R.; Munjal, A.; et al. Green tea (camellia sinensis) and l-theanine: Medicinal values and beneficial applications in humans—A comprehensive review. *Biomed. Pharmacother.* **2017**, *95*, 1260–1275.

69. Clarke, D.; Molinaro, S.; Tyuftin, A.; Bolton, D.; Fanning, S.; Kerry, J.P. Incorporation of commercially-derived antimicrobials into gelatin based films and assessment of their antimicrobial activity and impact. *Food Control* **2016**, *64*, 202–211.

70. Rakmai, J.; Cheirsilp, B.; Mejuto, J.C.; Torrado-Agrasar, A.; Simal-Gandara, J. Physico-chemical characterization and evaluation of bio-efficacies of black pepper essential oil encapsulated in hydroxypropyl-beta-cyclodextrin. *Food Hydrocoll.* **2017**, *65*, 157–164.

71. Cox, S.D.; Mann, C.M.; Markham, J.L.; Bell, H.C.; Gustafson, J.E.; Warmington, J.R.; Wyllie, S.G. The mode of antimicrobial action of the essential oil of melaleuca alternifolia (tea tree oil). *J. Appl. Microbiol.* **2000**, *88*, 170–175.

72. Yong, A.-L.; Ooh, K.-F.; Ong, H.-C.; Chai, T.-T.; Wong, F.-C. Investigation of antibacterial mechanism and identification of bacterial protein targets mediated by antibacterial medicinal plant extracts. *Food Chem.* **2015**, *186*, 32–36.

73. Park, J.-A.; Kim, S.-B. Preparation and characterization of antimicrobial electrospun poly (vinyl alcohol) nanofibers containing benzyl triethylammonium chloride. *React. Funct. Polym.* **2015**, *93*, 30–37.

74. Torres-Giner, S.; Martinez-Abad, A.; Lagaron, J.M. Zein-based ultrathin fibers containing ceramic nanofillers obtained by electrospinning. Ii. Mechanical properties, gas barrier, and sustained release capacity of biocide thymol in multilayer polylactide films. *J. Appl. Polym. Sci.* **2014**, *131*, 9270–9276.

75. Cruz-Gálvez, A.M.; Castro-Rosas, J.; Rodríguez-Marín, M.L.; Cadena-Ramírez, A.; Tellez-Jurado, A.; Tovar-Jiménez, X.; Chavez-Urbiola, E.A.; Abreu-Corona, A.; Gómez-Aldapa, C.A. Antimicrobial activity and physicochemical characterization of a potato starch-based film containing acetonic and methanolic extracts of hibiscus sabdariffa for use in sausage. *LWT* **2018**, *93*, 300–305.

76. Khaneghah, A.M.; Bagher Hashemi, S.M.; Limbo, S. Antimicrobial agents and packaging systems in antimicrobial active food packaging: An overview of approaches and interactions. *Food Bioprod. Process.* **2018**, *111*, 1–19.

77. Sentkowska, A.; Pyrzynska, K. Investigation of antioxidant interaction between green tea polyphenols and acetaminophen using isobolographic analysis. *J. Pharm. Biomed. Anal.* **2018**, *159*, 393–397.

78. Lorenzo, J.M.; Sichetti Munekata, P.E. Phenolic compounds of green tea: Health benefits and technological application in food. *Asian Pac. J. Trop. Biomed.* **2016**, *6*, 709–719.

79. Shahidi, F.; Zhong, Y. Novel antioxidants in food quality preservation and health promotion. *Eur. J. Lipid Sci. Technol.* **2010**, *112*, 930–940.

80. Chun, S.-S.; Vattem, D.A.; Lin, Y.-T.; Shetty, K. Phenolic antioxidants from clonal oregano (origanum vulgare) with antimicrobial activity against helicobacter pylori. *Process Biochem.* **2005**, *40*, 809–816.

81. Bajalan, I.; Rouzbahani, R.; Pirbalouti, A.G.; Maggi, F. Antioxidant and antibacterial activities of the essential oils obtained from seven iranian populations of rosmarinus officinalis. *Ind. Crop. Prod.* **2017**, *107*, 305–311.

82. Hongjun Shao, S.Y.; Qi Wang, Z.Z.; Xingbin Yang, L.Z. Non-extractable polyphenols of green tea and their antioxidant, anti-α-glucosidase capacity, and release during in vitro digestion. *J. Funct. Foods* **2018**, *42*, 129–136.

83. Afroz Bakht, M.; Geesi, M.H.; Riadi, Y.; Imran, M.; Imtiyaz Ali, M.; Jawed Ahsan, M.; Ajmal, N. Ultrasound-assisted extraction of some branded tea: Optimization based on polyphenol content, antioxidant potential and thermodynamic study. *Saudi J. Biol. Sci.* **2018**, in press.

84. Lu, M.-J.; Chen, C. Enzymatic modification by tannase increases the antioxidant activity of green tea. *Food Res. Int.* **2008**, *41*, 130–137.

85. Asensio, C.M.; Grosso, N.R.; Juliani, H.R. Quality characters, chemical composition and biological activities of oregano (*Origanum* spp.) essential oils from central and southern argentina. *Ind. Crop. Prod.* **2015**, *63*, 203–213.

86. Mechergui, K.; Jaouadi, W.; Coelho, J.P.; Larbi Khouja, M. Effect of harvest year on production, chemical composition and antioxidant activities of essential oil of oregano (*Origanum vulgare* subsp *glandulosum* (desf.) ietswaart) growing in north africa. *Ind. Crop. Prod.* **2016**, *90*, 32–37.

87. Yan, F.; Azizi, A.; Janke, S.; Schwarz, M.; Zeller, S.; Honermeier, B. Antioxidant capacity variation in the oregano (*Origanum vulgare* L.) collection of the german national genebank. *Ind. Crop. Prod.* **2016**, *92*, 19–25.

88. Shojaee-Aliabadi, S.; Hosseini, H.; Mohammadifar, M.A.; Mohammadi, A.; Ghasemlou, M.; Ojagh, S.M.; Hosseini, S.M.; Khaksar, R. Characterization of antioxidant-antimicrobial κ-carrageenan films containing satureja hortensis essential oil. *Int. J. Biol. Macromol.* **2013**, *52*, 116–124.

89. Gómez-Estaca, J.; López-de-Dicastillo, C.; Hernández-Muñoz, P.; Catalá, R.; Gavara, R. Advances in antioxidant active food packaging. *Trends Food Sci. Technol.* **2014**, *35*, 42–51.

90. Robertson, G.L. *Food Packaging: Principles and Practice*; CRC Press, Taylor and Francis Group: Boca Raton, FL, USA, **1998**; Volume 6.

CHAPTER II

Melt processability, characterization, and antibacterial activity of compression-molded green composite sheets made of poly(3-hydroxybutyrate-co-3-hydroxyvalerate) reinforced with coconut fibers impregnated with oregano essential oil

S. Torres-Giner, L. Hilliou, B. Melendez-Rodriguez, **K.J. Figueroa-Lopez**, D. Madalena, L. Cabedo, J.A. Covas, A.A. Vicente, J.M. Lagaron

Melt processability, characterization, and antibacterial activity of compression-molded green composite sheets made of poly(3-hydroxybutyrate-co-3-hydroxyvalerate) reinforced with coconut fibers impregnated with oregano essential oil

Abstract

New packaging materials based on green composite sheets consisting of poly(3-hydroxybutyrate-co-3-hydroxyvalerate) (PHBV) and coconut fibers (CFs) were obtained by twin-screw extrusion (TSE) followed by compression molding. The effect of varying the CF weight content, i.e. 1, 3, 5, and 10 wt.-%, and the screw speed during melt processing, i.e. 75, 150, and 225 rpm, on both the aspect ratio and dispersion of the fibers was analyzed and related to the properties of the compression-molded sheets. Finally, the CFs were impregnated with oregano essential oil (OEO) by an innovative spray coating methodology and then incorporated into PHBV at the optimal processing conditions. The functionalized green composite sheets presented bacteriostatic effect against *Staphylococcus aureus* from fiber contents as low as 3 wt.-%. Therefore, the here-prepared CFs can be successfully applied as natural vehicles to entrap extracts and develop green composites of high interest in active food packaging to provide protection and shelf life extension.

1   Introduction

The use of agro-food residues for the preparation of polymer composites is gaining a significant attention due to their huge availability and low price, being at the same time a highly sustainable strategy for waste valorization. Natural fibers (NFs), particularly those obtained from plants, represent an environmentally friendly and unique choice to reinforce bioplastic matrices due to their relative high strength and stiffness [1]. The substitution of oil-derived polymers with bio-based polymers as the matrix component results in the term "green composites" [2], which indicates that the composite as a whole, i.e. both matrix and reinforcement, originates from renewable resources. In this regard, the incorporation of NFs such as jute, sisal, flax, hemp, and bamboo fibers into biopolymers has been recently intensified [3]. Resultant green composites do not only offer environmental advantages over traditional polymer composites, such as reduced dependence on non-renewable energy/material sources, lower greenhouse gas and pollutant emissions, improved energy recovery, and end-of-life biodegradability of components [4], but also a potential reduction of both product density and energy requirements for processing [5].

Polyhydroxyalkanoates (PHAs) comprise a family of biodegradable aliphatic polyesters produced by microorganisms. PHAs show the highest potential to replace polyolefins in a wide range of applications, including packaging, due to their high mechanical strength and water resistance [6]. Among PHAs, poly(3-hydroxybutyrate) (PHB) and its copolymer with 3-hydroxyvalerate (HV), i.e. poly(3-hydroxybutyrate-co-3-hydroxyvalerate) (PHBV), have so far received the greatest attention in terms of pathway characterization and industrial-scale production. The use of PHA copolymers presents certain advantages since they have a lower melting point and higher flexibility than their homopolymers, which improves melt stability and broadens their processing window [7]. Furthermore, the introduction of comonomer units induces defects in the crystal lattice, reducing both the degree of crystallinity and crystallization rate [8].

Several plant-derived NFs, such as regenerated and/or recycled cellulose, pineapple leaf fibers (PALF), wheat straw fibers, wood floor, jute fibers, flax fibers, banana, sisal, and coir fibers, hemp fibers, abaca fibers, bamboo fibers, sugarcane bagasse fibers, kenaf and lyocell fibers, wood powder, and pita (agave) fibers, have been so far studied as sustainable reinforcements to produce PHA-based composite materials [9]. Recently, cellulose fibers from wheat straw and other by-products have been used in the European Projects ECOBIOCAP and YPACK as a cheap source of fillers to reduce the cost of a PHA matrix for packaging applications, where up to 20 % of cellulose fibers were allowed in the final composition. Some previous research studies have also suggested that the incorporation of NFs can definitely strengthen

the mechanical performance of both PHB and PHBV and, in some cases, also improve biodegradability [10-12]. However, the narrow processing window and the poor melt strength of PHAs are certainly responsible for the rather small number of studies involving extruded composites with potential for being converted into packaging articles such as films and sheets [13]. The most promising PHA-based composite manufacturing techniques are extrusion and compression molding, particularly the latter, given the relatively low shear-rates and thermomechanical stresses involved.

Coconut shells represent a good example of agro-industrial non-food feedstock that is still considered as waste, for which relevant industrial new end uses are being currently pursued [14]. In particular, it is estimated that around 55 billion coconuts are produced annually worldwide. Most of their husks are abandoned, creating a waste of natural resources and a cause of environmental pollution [15]. The coconut fibers (CFs), also referred as coir when completely ground up, are plant-derived NFs of the coconut fruit obtained from the palm tree (Cocos nucifera L.). The CFs are present in the mesocarp, which constitutes 30 – 35 wt.-% of the coconut [16]. Individual CFs show a length of 0.3–1.0 mm and a diameter of 0.01 – 0.02 mm, resulting in an average aspect ratio of approximately 35 [17]. The CFs are also characterized by a high toughness and durability as well as improved thermal stability due to their high lignin content (~40 %) and relatively low cellulose content (~32%) [18]. These lignocellulosic fibers are not only abundant in tropical countries but also versatile, renewable, cheap, and biodegradable. Therefore, they could become potential substitutes for energy-intensive synthetic fibers in many applications where high strength and modulus are not required [19].

The CFs have been tested as reinforcing fillers upon the formulation of different thermoplastic materials, such as low-density polyethylene (LDPE) [20,21] and linear low-density polyethylene (LLDPE) [20], polypropylene (PP) [15,17,21-23], poly(vinyl chloride) (PVC) [21], starch–gluten [24], natural rubber (NR) [25], among others. These previous studies have demonstrated that the incorporation of both untreated and chemically modified CFs into polymer formulations can represent a feasible route to produce low-cost composites with a moderate improvement of the mechanical properties. Interestingly, the CFs are exceptionally hydrophilic as they contain strongly polarized hydroxyl groups on their surface [26]. CFs are thus inherently capable to adsorb and hold moisture up to 7 – 9 times their weight, being proposed as biosorbents for water treatment [27]. The outstanding capacity of the CFs to retain water and other polar components certainly opens up new attractive opportunities for potential uses as vehicle of functional and bioactive substances.

The particular chemical and morphological characteristics of the CFs can be explored to adsorb essential oils (EOs), i.e. aromatic and volatile oily liquids obtained from herbs and spices. Most EOs and their constituents are categorized as Generally Recognized as Safe (GRAS) by the U.S. Food and Drug Administration [28]. Among EOs, oregano essential oil (OEO), extracted from Origanum vulgare L., is well-recognized for its antioxidative and antimicrobial action in the food industry [29]. The biocide performance of OEO has been mainly attributed to its rich composition in phenolic compounds, namely carvacrol (up to 80 %), thymol (up to 64 %), and the monoterpene hydrocarbons γ-terpinene and p-cymene (both up to 52 %) [30]. The incorporation of OEO in plastic films to avoid microbial food spoilage currently represents an attractive option for packaging manufacturers. Several studies have demonstrated its efficacy in inhibiting microbial development and synthesis of microbial metabolites, including pathogenic bacteria, yeasts, and molds [31-36]. Besides imparting antimicrobial characteristics to the films, OEO can change flavor, aroma, and odor. Nevertheless, similarly as with other EOs, OEO is volatile and easily evaporates and/or decomposes during processing and preparation of the antimicrobial films. Therefore, its direct exposure to heat, pressure, light or oxygen is a technological challenge.

The objective of the present study was to originally explore the inherent capacity of the CFs to adsorb and hold polar components in order to develop, by conventional melt-processing methodologies, PHBV-based green composite sheets with antimicrobial properties of interest in active packaging applications. To this end, the first part of the study was focused on optimizing the processing conditions of the green composites. In particular, it was analyzed the effect of varying both the CF weight content and the screw speed during melt processing on the aspect ratio and dispersion of the fibers in the PHBV matrices. In the second part, for the optimal processing conditions, the thermal, mechanical, and barrier properties of the compression-molded PHBV sheets were evaluated as a function of the CF content. In the last part, the CFs were impregnated with OEO by an innovative spray coating methodology, incorporated again into PHBV, and the antimicrobial properties of the green composite sheets were evaluated.

2   Materisls and methods

2.1   Materials

Bacterial aliphatic copolyester PHBV was ENMAT™ Y1000 P, produced by Tianan Biologic Materials (Ningbo, China) and distributed by NaturePlast (Ifs, France). The product was delivered as off-white pellets packaged in plastics bags. The biopolymer resin presents a true density of 1.23 g/cm³ and a bulk density of 0.74 g/cm³, as determined by ISO 1183 and ISO 60, respectively. The melt flow index (MFI) is 5 – 10 g/10 min (190 °C, 2.16 kg), as determined by ISO 1133. The molar fraction of HV in the copolymer is 2 – 3 %, whereas the weight-average molecular weight (MW) is approximately 2.8×10^5 g/mol. According to the manufacturer, this resin is suitable for injection molding, thermoforming, and extrusion.

CFs were kindly supplied by Amorim Isolamentos, S.A. (Mozelos, Portugal) in the form of a liner roll. The fibrous layers were obtained from ripe coconuts, which were manually de-husked from the hard shell by driving the fruit down onto a spike to split it. 100% pure OEO was purchased from Gran Velada S.L. (Zaragoza, Spain) while food-grade paraffinic oil (grade 9578) was obtained from Quimidroga S.A. (Barcelona, Spain). 2,2,2-trifuoroethanol (TFE) with 99 % purity, d-limonene with 98 % purity, Nile Red (9-diethylamino-5H-benzo-α-phenoxazine-5-one), and dimethyl sulfoxide (DMSO) anhydrous with purity ≥99.9 % were all purchased from Sigma-Aldrich S.A. (Madrid, Spain). All chemical reagents were utilized as received.

2.2   Fibers functionalization

CFs were initially separated from the roll and chopped to a length of ca. 5 mm in a Granulator 20 – 18/JM from Grindo S.R.L. (Cologno Monzese, Italy). Chopped fibers were then sieved using a Test sieve model from Controls S.p.A. (Milano, Italy) with an aperture of 2 mm. The resultant bulk density of the CFs was 0.14 g/cm³, as determined by ISO 60. Figure 1 shows the different stages followed for the preparation of the CFs.

Figure 1. (**a**) As-received reel of coconut fibers (CFs); (**b**) Ground CFs; (**c**) Sieved CFs.

Part of the obtained CFs was impregnated with OEO in order to provide them with antibacterial functionality, the here so-called functionalization. For this purpose, a 2:1 (vol./vol.) paraffinic oil/OEO solution was prepared, as this was the highest OEO content without creating phase separation. This solution, with a density of 0.902 g/mL, was added at 15 wt.-% to the CFs by means of an air spray gun from Nutool (Doncaster, UK) connected to a 24 l 1.0HP PWB24S air compressor from PowerED® (Amiais de Baixo, Portugal) working at 2 bar. This way, the dried CFs were sprayed every 5 s while rotating at 58 rpm inside a drum attached to an ARTISAN 5KSM125EER household mixer from KitchenAid® (Michigan, USA).

2.3 Preparation of green composites

Prior to melt processing, the PHBV pellets and CFs were dried for 4 h at 80 °C in an oven to remove the residual humidity. Then, different PHBV formulations were melt compounded by twin-screw extrusion (TSE) varying the CF content, i.e. 0, 1, 3, 5, and 10 wt.-%, in a co-rotating intermeshing twin-screw extruder LSM 34 G l from Leistritz AG (Nuremberg, Germany). The screws have a diameter (D) of 34 mm and a length-to-diameter ratio (L/D) of 29. The modular barrel is equipped with 8 individual heating zones and is coupled to a strand die. The extruder layout with the detailed screw configuration is presented in Figure 2. Basically, the screw contains two mixing zones, each consisting of a series of kneading disks staggered at 90° (in order to induce dispersion), that are separated by conveying sections that work mostly partially filled. The components are fed separately upstream of each mixing zone. The PHBV pellets were fed into the main hopper with a volumetric DVM18-L feeder from Moretto S.p.A. (Massanzago, Italy) at a feeding rate of 2 kg/h. The CFs were first pre-mixed in a zipped bag with 1 part per hundred resin (phr) of paraffinic oil and then introduced in the extruder after melting the polymer, at L/D = 12, through the side feeder. As commonly faced with other low-density fibers, there were difficulties in guaranteeing a precise and constant feeding throughput. A venting port at L/D = 23 coupled to a vacuum pump enabled the removal of both residual moisture and volatiles. Three different screw speeds were tested, i.e., 75, 150, and 225 rpm, and the following decreasing temperature profile was fixed (from hopper to die): 195/190/185/180/175/170/165/160 °C. The extruded strand was cooled in a water bath, dried with an air-knife, and then pelletized by a rotary cutter. The minimum residence time was estimated by measuring the time that a blue masterbatch pellet would take from being introduced directly into the extruder until exiting from the die.
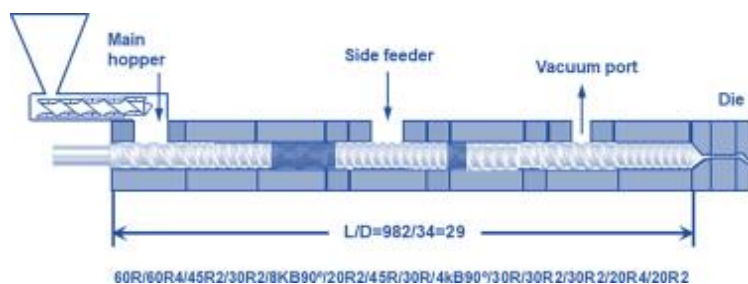
Figure 2. Detailed cylinder with screw configuration.

The compounded pellets were shaped into sheets with a thickness of ~500 μm by compression molding using a hydraulic press from Geo E. Moore & Son (Bham.) Ltd. (Birmingham, UK). About 10 g of material were placed in a hollow aluminum mold of 10×10 cm^2 and then introduced into the press. Materials were initially preheated at 190 °C for 1 min, without pressure, and subsequently hot-pressed for 3 min at 4 tons. Finally, the samples were cooled down to 25 °C by means of an internal water circulating system.

2.4   Characterization methods

2.4.1   *Sheet thickness and samples conditioning*

The thickness of the compression-molded sheets was measured with a digital micrometer series S00014 from Mitutoyo Corporation (Kawasaki, Japan), having $\pm$ 0.001 mm accuracy, at five random positions. Samples were aged for at least 15 days prior to any physical characterization in a desiccator at 25 °C and 0 % relative humidity (RH).

2.4.2   *Optical microscopy*

Dispersion quality of CFs in the green composites was assessed with a light transmission optical microscope Olympus BH-2 from Olympus Optical Co., Ltd (Tokyo, Japan), coupled to a digital camera system Leica DFC280 from Meyer Instruments, Inc. (Houston, Texas, USA). Fiber attrition was investigated by monitoring fiber length distribution on the PHBV composites processed with different CF contents and at different conditions. This method was performed by immersing a small sample of each specimen in TFE solvent at room temperature for

12 h. The resultant solution was centrifuged and filtered so that PHBV was removed and the recovered CFs were deposited onto microscopy glass slabs for observation. The OEO-containing CFs were analyzed by fluorescence microscopy using an Olympus BX51 from Olympus Optical Co., Ltd. The samples were previously dyed with Nile Red, a lipophilic dye, in a 0.25 mg/ml solution of DMSO at 1:10 dye/sample (vol./vol.), covered in aluminum foil to protect them from light exposure, and dried at 25 °C for at least 12 h prior to observation. The samples were analyzed at an emission wavelength between 470 and 490 nm.

2.4.3 Melt flow index

MFI of the neat PHBV and its green composites pellets were measured at 185 °C with a load of 1.2 kg using a MFI Daventest LPF-002 from Lloyd Instruments Ltd. (Bognor Regis, UK). Higher temperatures and weights triggered excessive mass outputs that impaired measurement accuracy. Data were reported as the mean value and standard error computed from 10 tests.

2.4.4 Thermal analysis

Thermal transitions were analyzed by differential scanning calorimetry (DSC) on a DSC-7 analyzer from PerkinElmer, Inc. (Waltham, MA, USA), equipped with a cooling accessory Intracooler 2 also from PerkinElmer, Inc. A heating step from -30 to 200 °C was followed by a cooling step to -30 °C under nitrogen atmosphere with a flow-rate of 20 mL/min. The scanning rate was 10 °C/min and an empty aluminum pan was used as reference. Calibration was performed using an indium sample. All tests were carried out at least in triplicate. The glass transition temperature (T_g), cold crystallization temperature (T_{cc}), enthalpy of cold crystallization (ΔH_{cc}), melting temperature (T_m), and enthalpy of melting (ΔH_m) were obtained from the first heating scan, while the crystallization temperature from the melt (T_c) and enthalpy of crystallization (ΔH_c) were determined from the cooling scan. The percentage of crystallinity (X_c) was determined using the following expression:

$$Xc = \left[\frac{\Delta H_m - \Delta H_{cc}}{\Delta H_m° \cdot (1-w)}\right] \cdot 100 \qquad (1)$$

where $\Delta H_m° = 146.6 \, J/g$ is the enthalpy corresponding to the melting of a 100% crystalline PHB sample [37] while the term 1-w represents the biopolymer weight fraction in the composite.

Thermogravimetric analysis (TGA) was performed in a TG-STDA model TGA/STDA851e/LF/1600 thermobalance from Mettler-Toledo, LLC (Columbus,

OH, USA). The samples, with a weight of ~15 mg, were heated from 50 to 900 °C at a heating rate of 10 °C/min under a nitrogen flow-rate of 50 mL/min.

2.4.5 *Tensile tests*

Dumbbell 500 μm-thick samples were die-cut from the compression-molded sheets and conditioned to ambient conditions, i.e., 25 °C and 50 % RH, for 24 h. Tensile tests were carried out at room temperature in a universal mechanical testing machine AGS-X 500 N from Shimadzu Corp. (Kyoto, Japan) in accordance with ASTM D638 (Type IV) standard. This was equipped with a 1-kN load cell and the cross-head speed was 10 mm/min. A minimum of six specimens were measured for each sample.

2.4.6 *Permeability tests*

The water vapor permeability (WVP) and limonene permeability (LP) were determined according to the ASTM 2011 gravimetric method. In the case of WVP, 5 ml of distilled water were poured into a Payne permeability cup ($\emptyset = 3.5$ cm) from Elcometer Sprl (Hermalle-sous-Argenteau, Belgium). The sheets were placed in the cups so that on one side they were exposed to 100% RH, avoiding direct contact with water. The cups containing the sheets were then secured with silicon rings and stored in a desiccator at 25 °C and 0% RH. Identical cups with aluminum foils were used as control samples to estimate water loss through the sealing. The cups were weighed periodically using an analytical balance with ±0.0001 g accuracy. Water vapor permeation rate (WVPR), also called water permeance when corrected for permeant partial pressure, was determined from the steady-state permeation slope obtained from the regression analysis of weight loss data per unit area versus time, in which the weight loss was calculated as the total cell loss minus the loss through the sealing. WVP was obtained, in triplicate, by correcting the permeance by the average sheet thicknesses.

For LP, similarly, 5 ml of d-limonene was placed inside the Payne permeability cups and the cups containing the sheets were stored under controlled conditions, i.e. 25 °C and 40 % RH. Limonene permeation rate (LPR) was obtained from the steady-state permeation slopes and the weight loss was calculated as the total cell loss minus the loss through the sealing plus the water sorption gained from the environment measured in samples with no permeant. LP was calculated taking into account the average sheet thickness in each case, measuring three replicates per sample.

Oxygen permeability (OP) was obtained from the oxygen transmission rate (OTR) measurements, recorded in duplicate, using an Oxygen Permeation Analyzer M8001 from Systech Illinois (Thame, UK) at 25 °C and 60 % RH. The samples were

previously purged with nitrogen in the humidity equilibrated samples and then exposed to an oxygen flow of 10 mL/min. The exposure area during the test was 5 cm^2. Sheet thickness and gas partial pressure were determined. Measurements were performed in duplicate.

2.4.7 *Antibacterial assays*

The antibacterial activity of the neat OEO, the OEO-containing CFs, and the green composite sheets with the OEO-containing CFs was evaluated against *Staphylococcus aureus* (*S. aureus*) ATCC 6538 P. This bacterial strain was obtained from the Spanish Type Culture Collection (CECT) (Valencia, Spain) and it was cultivated at optimal growth conditions in tryptone soy broth (TSB) from Oxoid Thermo Scientific (Basingstoke, UK), having a concentration of 6.3×10^8 colony forming units (CFU)/ml. Previous to each study, a 100-µl aliquot from the culture was transferred to TSB and grown at 37 °C to the mid-exponential phase of growth with an approximate count of 5×10^5 CFU/ml. To ensure sterilization, all materials were initially exposed to ultraviolet (UV) radiation for 30 min in a Biostar cabinet from Telstar S.A. (Madrid, Spain).

The effectiveness of the OEO and OEO-containing CFs against S. aureus was tested following the plate micro-dilution protocol, as described in the Methods for Dilution Antimicrobial. Susceptibility Tests for Bacteria That Grow Aerobically; Approved Standard—Tenth. Edition (M07-A10) by the Clinical and Laboratory Standards Institute (CLSI). For this, a 96-well plate with an alpha numeric coordination system (columns 1–12 and rows A-H) were used, where 10 µl of the tested samples were introduced in the wells with 90 µl of the bacteria medium. In the wells corresponding to A, B, C, E, F, and G columns different concentrations of OEO, i.e. 0.078, 0.156, 0.312, 0.625, 1.25, 2.5, 5, 10, 20, and 40 µl/ml, and of OEO-containing CFs, i.e. 0.315, 0.625, 1.25, 2.5, 5, 10, 25, 50, 100, and 250 µg/ml were tested, in triplicate, from rows 1 to 10. Columns D and H were used as the control of OEO and OEO-containing CFs, respectively, without bacteria. Row 11 was taken as the positive control, i.e. only TSB, and row 12 was used as the negative control, i.e. *S. aureus* in TSB. The plates were incubated at 37 °C for 24 h. Thereafter, 10 µl of resazurin solution, 100 µg/ml in TBS, a metabolic indicator obtained from MP Biomedicals, LLC (Illkirch, France), was added to each well and incubated again at 37 °C for 2 h. Upon obtaining the resazurin change, the wells were read through color difference. The minimum inhibitory concentration (MIC) was determined as the lowest concentration of OEO and OEO-containing CFs presenting growth inhibition.

A modification of the Japanese Industrial Standard (JIS) Z 2801:2010 was performed to evaluate the bacterial efficiency on the sheets surface. This technique is useful to

determine the antimicrobial activity of finished products, particularly including polymer composite pieces [38]. Briefly, a bacterial suspension of *S. aureus* of about 5×10^5 CFU/mL was spread uniformly on the surface of sheets with dimensions of 2×2 cm² and then covered by an inert 10-μm LDPE film of 1.5×1.5 cm². After 24 h of incubation at 95% RH, bacteria were recovered with phosphate-buffered saline (PBS), inoculated onto tryptic soy agar (TSA) plates, and incubated at 37 °C for 24 h to quantify the number of viable bacteria. PHBV sheets with different CF contents were analyzed, using both sheets without fibers and with fibers without OEO as the negative controls. The antimicrobial activity was evaluated as synthesized, i.e. 1 day after preparation, and 15 days later. Surface reduction (R) was calculated as follows:

$$R = \left[log \left(\frac{B}{A} \right) - log \left(\frac{C}{A} \right) \right] = log \left(\frac{B}{C} \right) \tag{2}$$

where A is the average of the number of viable bacteria on the control sample immediately after inoculation, B is the average of the number of viable bacteria on the control sample after 24 h, and C is the average of the number of viable bacteria on the test sample after 24 h. Three replicate experiments were performed for each sample and the antibacterial activity was evaluated with the following assessment: Nonsignificant (R < 0.5), slight (R ≥ 0.5 and <1), significant (R ≥ 1 and <3), and strong (R ≥ 3).

3 Results and discussions

3.1 Melt processability

Figure 3 shows the surface view of the green composite sheets varying the CF contents and processed at different processing conditions. In all cases, the green composite sheets exhibited a smooth, defect-free, and uniform surface, in which CFs appeared randomly dispersed. Distribution was relatively uniform, albeit some small areas seem to contain lower CF concentration. As expected, the CF content highly influenced on the color intensity of the PHBV sheets. Then, sheets produced with the highest CF contents, i.e. 5 and 10 wt.-%, presented a wood-like visual feature, which could be aesthetically suitable to imitate solid wood parts for boards, lids or containers of interest in, for instance, rigid packaging. In contrast, the processing conditions had a minor influence on both surface aspect and distribution of the CFs into the PHBV matrix. Only the sheets obtained from green composites compounded at 225 rpm presented a slight color increase, which was probably caused by thermal degradation arising from the viscous dissipation associated to flow under higher shear-rates.
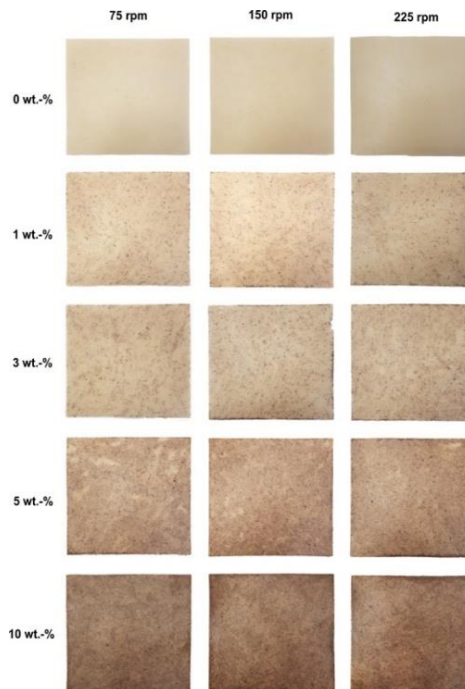
Figure 3. Surface appearance of the compression-molded sheets as a function of the poly(3-hydroxybutyrate-co-3-hydroxyvalerate) (PHBV) and coconut fibers (CFs) weight content and screw speed.

CFs in the green composite sheets were imaged by optical microscopy, after dissolving and filtrating PHBV. Representative pictures are displayed in Figure 4. Residence time and fiber dimensions were evaluated in order to select the optimal screw speed for which the set temperature and feed-rate were kept constant. Table 1 reports both characteristics for each composition and screw speed. As expected, at a given feed-rate, residence time was gradually reduced with increasing screw speed, as flow along the screw was more effective and the number of fully filled channels decreased. For instance, for the neat PHBV formulation, residence time decreased from 131 s, at 75 rpm, to 97 s and 64 s, at 150 rpm and 225 rpm, respectively. The incorporation of CFs slightly increased the residence time due to their lower bulk density in relation to the PHBV pellets, i.e. the total volume occupied by the material in the extruder increased though the output remained constant. For all processing conditions, CFs presented a similar diameter, varying in the range 100 – 400 μm and with a mean value of approximately 215 μm, whereas their length significantly decreased with increasing both the content and screw speed. Specifically, the average fiber length decreased from above 1900 μm, for the composite formulations with 1 wt.-% CFs, down to below 600 μm, for those containing 10 wt.-% CFs. This corresponds to a decrease of the fiber aspect ratio from approximately 9 to 2.5. Fiber lengths also decreased with increasing the screw speed, which is expected as stresses are larger for faster screw speeds. Interestingly, the green composite with 10 wt.-% CFs presented the highest fiber length at 150 rpm, i.e. approximately 1179 μm, and also the lowest at 75 rpm, i.e. approximately 542 μm.
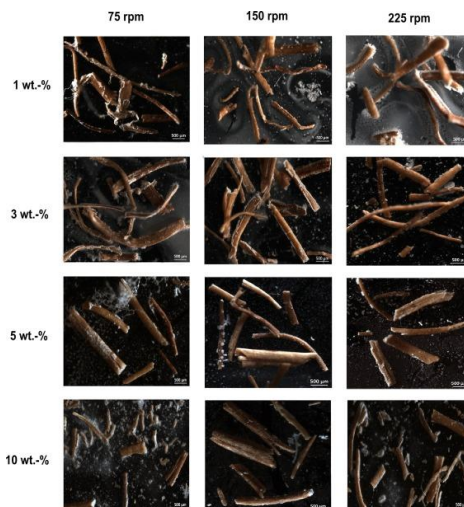
Figure 4. Optical microscopy images of the coconut fibers (CFs) extracted from the green composite sheets at different weight contents and screw speed. Scale markers of 500 μm.

Table 1. Residence time (tR) and mean fiber length during melt compounding as a function of the poly(3-hydroxybutyrate-co-3-hydroxyvalerate) (PHBV) and coconut fibers (CFs) content and screw speed

PHBV content (wt.-%)	CF content (wt.-%)	Screw speed (rpm)	t_R (s)	Fiber length (µm)
100	0	75	131 ± 3	–
100	0	150	97 ± 2	–
100	0	225	64 ± 1	–
99	1	75	132 ± 5	1914.5 ± 686.3
99	1	150	98 ± 3	1848.4 ± 634.6
99	1	225	65 ± 1	1486.2 ± 451.3
97	3	75	134 ± 4	1784.3 ± 718.9
97	3	150	100 ± 1	1711.6 ± 505.4
97	3	225	66 ± 2	1404.5 ± 683.4
95	5	75	136 ± 5	1760.4 ± 446.5
95	5	150	102 ± 2	1633.4 ± 491.6
95	5	225	68 ± 1	1309.6 ± 671.7
90	10	75	143 ± 5	542.3 ± 190.8
90	10	150	106 ± 3	1178.9 ± 333.9
90	10	225	70 ± 2	715.2 ± 302.2

In order to correlate fiber attrition to melt viscosity, MFI was evaluated on the PHBV samples processed at 150 rpm. As one can observe in Figure 5, the MFI values decreased with increasing the CFs content. This means that melt viscosity of the composite formulations was higher than the neat PHBV formulation and, thus, the intensity of the thermomechanical stresses raised. This was mainly related to the intensification of fiber-to-fiber collisions. While fiber dispersion requires stresses to be larger than the cohesive strength of the aggregates, larger stresses can also favor fibers rupture [39]. As a result, composites formulated with more CFs presented higher viscosity and lower lengths. However, the lowest MFI value was observed for the composite formulation with 3 wt.-% CFs and then it increased for the larger CF contents. This viscosity decrease at high CF contents suggests an increase of biopolymer degradation or melt-shear thinning due to the presence of more fibers, which is known to occur in PHBV materials [40]. Therefore, the complex interplay concerning reduced melt viscosity at higher CF contents, high residence times at low screw speeds, and thermal degradation of PHBV due to possible viscous heating, may explain the non-trivial evolution of fiber length.
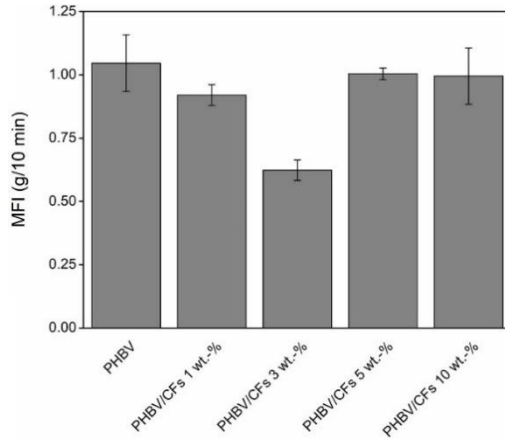
Figure 5. Melt flow index (MFI) of the green composite pellets as function of the weight content of coconut fibers (CFs). Test performed at 185 °C with a load of 1.2 kg.

From the above and within the experimental window tested herein, it was observed that the optimal screw speed to process the PHBV/CFs composites is 150 rpm. This processing condition delivered the most balanced fiber distribution, average fiber length, and intermediate residence times. In particular, the fiber aspect ratio remained in the 5.5 – 9.0 range, decreasing with increasing the CF content, and the residence time was of the order of 100 s. It can be thus considered that this processing condition could be beneficial to process both thermally sensitive PHBV and thermolabile additives.

3.2 Sheets characterization

The green composite formulations melt-compounded at 150 rpm were thereafter compression-molded into sheets and these were characterized in terms of their thermal, mechanical, and barrier properties.

Table 2 summarizes the thermal properties determined by DSC. Within the experimental precision, all PHBV sheets presented similar values of Tg, Tc, and Tm (about −3 °C, 121 °C, and 173 °C, respectively). Similar results have been reported in the literature for other PHBV materials, indicating that the HV content plays the major role in defining the thermal transitions [41]. In addition, cold crystallization was not observed and all the samples crystallized from the melt in a single peak. Interestingly, the presence of the CFs significantly affected the biopolymer degree of crystallization. While the neat PHBV sheet presented a X_c of approximately 54 %, the addition of 1 – 5 wt.-% CFs reduced it to values in the 45 – 50% range and X_c

increased to about 58 % for the 10 wt.-% CF content. This result suggests that crystal growth in the green composites was controlled by two competing factors, namely nucleation and confinement. As with other PHBV composites [13], the presence of low contents of long fibers inhibited the chain-folding process of PHBV molecules, hindering molecular organization at the crystal growth front. Conversely, the existence of a high content of shorter fibers seems to provide a nucleating effect. The latter can be related to the degradation process triggered by the high CF content, as explained above, by which PHBV molecules were shorter and, thus, easier to crystallize.

Table 2. Thermal properties of the compression-molded sheets made of poly(3-hydroxybutyrate-co-3-hydroxyvalerate) (PHBV) and coconut fibers (CFs). The glass transition temperature (T_g), melting temperature (T_m), and normalized enthalpy of melting (ΔH_m) were obtained from the differential scanning calorimetry (DSC) curves during the first heating scan while the crystallization temperature (T_c) and normalized crystallization (ΔH_c) from the cooling scan

Sample	DSC Parameters					
	T_g (ºC)	T_c (ºC)	T_m (ºC)	ΔH_c (J/g)	ΔH_m (J/g)	X_c (%)
PHBV	−3.3 ± 0.8	120.6 ± 0.1	172.8 ± 0.2	84.7 ± 2.4	79.4 ± 0.9	54.1 ± 0.6
PHBV/CFs 1 wt.-%	−2.4 ± 0.3	120.2 ± 0.9	173.8 ± 1.3	78.3 ± 4.2	64.9 ± 1.1	44.7 ± 0.8
PHBV/CFs 3 wt.-%	−2.3 ± 0.9	120.4 ± 1.1	173.9 ± 1.4	74.3 ± 4.4	66.6 ± 3.5	46.9 ± 0.5
PHBV/CFs 5 wt.-%	−2.2 ± 0.4	121.0 ± 0.6	172.9 ± 0.5	75.5 ± 2.6	69.8 ± 2.7	50.1 ± 0.9
HBV/CFs 10 wt.-%	−1.8 ± 0.6	119.8 ± 0.5	172.5 ± 1.0	76.8 ± 3.0	76.8 ± 3.2	58.2 ± 1.4

Concerning the TGA data, listed in Table 3, one can observe that thermal decomposition of the PHBV composites started in the range of 270 – 280 °C, presenting a degradation temperature (T_{deg}) close to 300 °C with a mass loss of approximately 70 %. The incorporation of CFs slightly reduced the thermal stability of PHBV, but it also delayed the amount of mass loss during degradation. It is also worthy to note that the amount of residual mass increased, approximately from 3 % to 6 %, which can be related to the presence of inorganic impurities in the fibers. In general, the addition of CFs up to 10 wt.-% did not significantly alter the thermal degradation profile of PHBV, thus, positively not impairing its processing window.

Table 3. Thermal properties of the compression-molded sheets made of poly(3-hydroxybutyrate-co-3-hydroxyvalerate) (PHBV) and coconut fibers (CFs). The onset degradation temperature, defined as the temperature at 5% weight loss ($T_{5\%}$), degradation temperature (T_{deg}), and residual mass at 900 °C were obtained from the thermogravimetric analysis (TGA) curves

Sample	TGA Parameters			
	$T_{5\%}$ (°C)	T_{deg} (°C)	Mass loss (%)	Residual mass (%)
PHBV	77 ± 0.3	298 ± 0.5	72.19 ± 0.6	3.2 ± 0.2
PHBV/CFs 1 wt.-%	276 ± 0.5	296 ± 0.5	70.99 ± 0.3	3.5 ± 0.2
PHBV/CFs 3 wt.-%	275 ± 0.4	295 ± 0.4	70.78 ± 0.4	3.5 ± 0.3
PHBV/CFs 5 wt.-%	274 ± 0.5	293 ± 0.3	64.85 ± 0.5	4.6 ± 0.3
HBV/CFs 10 wt.-%	273 ± 0.4	291 ± 0.4	63.79 ± 0.3	5.8 ± 0.2

Table 4 shows the tensile properties of PHBV and its green composite with CFs. The neat PHBV sheet presented a tensile modulus of ca. 3.7 GPa, a tensile strength of ca. 34 MPa, and an elongation at break of ca.1.2 %. These properties clearly indicate that the PHBV sheets were rigid and brittle. As expected, the incorporation of CFs further increased, though not significantly, the tensile modulus and also reduced both the tensile strength and elongation at break. The same response has been reported for other compression-molded green composite sheets based on PHAs [9,42], which have been mainly related to a poor fiber–matrix adhesion. The 5 wt.-% CF-containing sheet presented the highest tensile modulus, i.e. approximately 4.1 GPa, with tensile strength and elongation-at-break values of approximately 29 MPa and 0.9 %, respectively. It is also worthy to mention the low elastic modulus observed for the green composite sheet containing 10 wt.-% CFs, i.e. ~3.7 GPa, which can be related to the presence of fibers with lower mean fiber lengths, as previously shown in Table 1. The lowest values of tensile strength and elongation at break were also observed for the green composite sheet with 10 wt.-% CFs, i.e. approximately 25 MPa and 0.7 %, respectively. Therefore, the CFs acted as an effective reinforcement of PHBV matrices when their length exceeds a critical threshold, in this case approximately 1500 µm, which corresponds to an aspect ratio close to 7. However, the exact mechanism for the reinforcement might go beyond the effect of fiber size, as both PHBV matrix thermal degradation and composite enhanced crystallinity in the sheet with 10 wt.-% CFs may add complexity to the mechanical–structural relationships.

Table 4. Mechanical properties of the compression-molded sheets made of poly(3-hydroxybutyrate-co-3-hydroxyvalerate) (PHBV) and coconut fibers (CFs) in terms of tensile modulus (E), tensile strength at yield (σ_y), and elongation at break (ε_b)

Sample	E (MPa)	σ_y (MPa)	ε_b (%)
PHBV	3671 ± 180	33.8 ± 2.1	1.18 ± 0.15
PHBV/CFs 1 wt.-%	3815 ± 164	30.7 ± 3.4	1.06 ± 0.10
PHBV/CFs 3 wt.-%	3916 ± 288	29.3 ± 2.0	0.95 ± 0.04
PHBV/CFs 5 wt.-%	4093 ± 197	28.6 ± 2.0	0.88 ± 0.12
PHBV/CFs 10 wt.-%	3720 ± 125	24.7 ± 1.3	0.67 ± 0.09

Finally, the barrier properties to water vapor, limonene, and oxygen were determined and the permeability values are included in Table 5. The barrier performance is, in fact, one of the main parameters of application interest for food packaging. One can observe that the permeability to both water and limonene vapors slightly raised by increasing the CF content. Such increase was higher in the case of water vapor, reaching permeability values close to $4 \times 10^{-15}\,\mathrm{kg\,m\,m^{-2}\,Pa^{-1}\,s^{-1}}$. Since water vapor is mainly a diffusivity-driven property in PHAs due to their low water sorption nature [43], the increase in permeability to water vapor can be ascribed to the hydrophilic character of the filler and possibly also to increased free volume at the fiber–matrix interface. To put these values into a more packaging context, WVP values of the here-developed green composite sheets are in the same order of magnitude as their petroleum-based counterpart polyethylene terephthalate (PET) films, i.e. $2.30 \times 10^{-15}\,\mathrm{kg\,m\,m^{-2}\,Pa^{-1}\,s^{-1}}$ [44].

Table 5. Barrier properties of the compression-molded sheets made of poly(3-hydroxybutyrate-co-3-hydroxyvalerate) (PHBV) and coconut fibers (CFs) in terms of water vapor permeability (WVP), limonene permeability (LP), and oxygen permeability (OP)

Sample	WVP x 10^{15} (kg m m^{-2} Pa^{-1} s^{-1})	LP x 10^{14} (kg m m^{-2} Pa^{-1} s^{-1})	OP x 10^{18} (m^3 m m^{-2} Pa^{-1} s^{-1})
PHBV	1.83 ± 0.47	1.17 ± 0.19	0.80 ± 0.14
PHBV/CFs 1 wt.-%	1.93 ± 0.34	1.19 ± 0.31	0.77 ± 0.09
PHBV/CFs 3 wt.-%	3.60 ± 0.46	1.25 ± 0.22	0.73 ± 0.08
PHBV/CFs 5 wt.-%	3.93 ± 0.58	1.38 ± 0.27	0.17 ± 0.06
PHBV/CFs 10 wt.-%	3.96 ± 0.57	1.48 ± 0.24	0.74 ± 0.05

Limonene transport properties are also important in packaging applications because this vapor is usually used as a standard system to test aroma barrier. The effect of fiber content on LP was relatively small and the neat PHBV and green composite sheets with CFs showed values in the range of $1.1–1.5 \times 10^{-14}\,\mathrm{kg\,m\,m^{-2}\,Pa^{-1}\,s^{-1}}$. In this sense, limonene, as opposed to moisture, is a strong plasticizing component for PHAs and, then, solubility plays a more important role in permeability than diffusion. For example, Sanchez-Garcia, Gimenez, and Lagaron [45] reported a limonene

uptake of ca. 12.7 wt.-% for films made of PHBV with 12 mol.-% HV prepared by solvent casting, resulting in a LP value of 1.99×10^{-13} kg m m^{-2} Pa^{-1} s^{-1}. Interestingly, the here-prepared green composite sheets were 13 – 17 times more barrier to limonene, which can be ascribed to both the lower HV content of the here-used copolyester and also to the compression molding methodology. The observed increase in permeability when introducing CFs, though slight, may be related to a sorption phenomenon at the filler–matrix interface. In any case, the here-obtained PHBV-based sheets still presented LP values close to those previously reported for PHB films, i.e. 8.8×10^{-15} kg m m^{-2} Pa^{-1} s^{-1}, and approximately 8 – 10 times lower than PET films, i.e. 1.17×10^{-13} kg·m·m^{-2}·Pa^{-1}·s^{-1}, both obtained by compression molding [46].

In relation to oxygen, the presence of CFs induced a slight reduction in permeability though the trend was not monotonic. Since oxygen is a noncondensable small permeant, the presence of the cellulosic fibers can block oxygen diffusion while the heterogeneities within the composite can serve as preferential paths for the oxygen molecules. The highest barrier effect was observed for the PHBV/CFs 5 wt.-%, with a OP value of 1.73×10^{-19} m^3 m m^{-2} Pa^{-1} s^{-1}, which is close to that of PET films, i.e. 1.35×10^{-19} m^3 m m^{-2} Pa^{-1} s^{-1} [44]. This suggests that, at this intermediate fiber content, the contribution of the blocking effect over the heterogeneities was optimal. Overall, the here-obtained PHBV-based composite sheets presented OP values in the $0.7 - 0.8 \times 10^{-18}$ m^3 m m^{-2} Pa^{-1} s^{-1} range, being slightly lower than those recently observed for electrospun homopolyester PHB films [47] but higher than conventional 100-μm PHB films prepared by compression molding [46].

3.3   Antibacterial activity

In the last part of this study, the CFs were impregnated with different contents of an oil–OEO mixture by means of an in-house developed spraying methodology. Figure 6 shows the fluorescence images taken by optical microscopy on the resultant OEO-containing fibers. One can observe that the oil–OEO mixture, shown as yellow-to-orange areas in the images, was homogenously distributed along the fibers surface for contents up to 15 wt.-%. However, at the highest tested content, i.e. 45 wt.-%, the oily extract eventually saturated the fibers and accumulated around their outer surface. Based on this observation, the CFs containing 15 wt.-% oil–OEO mixture, which in turns provided a final content of 5 wt.-% OEO, were selected to further functionalize the green composites with antibacterial properties. As the CF content in the biopolymer was kept at 1 – 10 wt.-%, this resulted in a concentration range of 0.05 – 0.5 wt.-% OEO in the PHBV sheets.
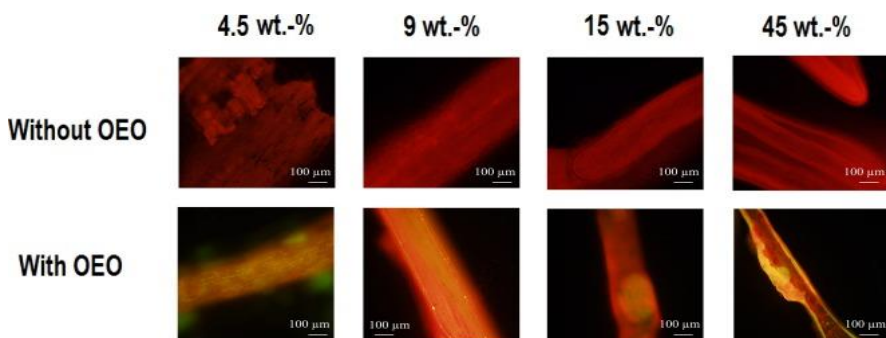
Figure 6. Fluorescence microscopy images of the coconut fibers (CFs) impregnated with different weight contents of oil–oregano essential oil (OEO) mixture. Images were taken with an emission wavelength between 470 and 490 nm. Scale markers of 100 μm.

The MIC values, defined as the lowest concentration of a biocide substance that is capable of inhibiting bacterial growth, of both the neat OEO and OEO-containing CFs were determined using the plate micro-dilution protocol. While the neat OEO presented a MIC value against *S. aureus* of 0.312 μl/ml, this value was significantly higher for the OEO-containing CFs, i.e. 25 μg/ml, which corresponds to a OEO concentration of 1.25 μg/ml. This reduction in antibacterial effectiveness, of about 4 times, can be related to partial losses during the spraying process, a heterogeneous distribution of the OEO, and/or to an in-depth entrapment of the antibacterial oil into fibers regions that were not accessible for interaction with bacteria (e.g. pores). It is also worthy to indicate that the here-reported MIC values for OEO were relatively low, being for instance one order of magnitude lower than those reported by dos Santos Rodrigues et al. [48] against different planktonic and sessile cells of *S. aureus* isolates.

In relation to the possible biological mechanism exerted by OEO on *S. aureus*, Dadalioğlu and Evrendilek [49] attributed this effect to two particular components: the phenolic compound carvacrol and the monoterpene p-cymene. According to Zivanovic et al. [36], the proposed action of phenolic compounds is based on their attack on the phospholipid cell membrane, which causes increased permeability and leakage of cytoplasm, or on their interaction with enzymes located at the cell wall. Indeed, most studies investigating the antibacterial activity of OEO agree that, generally, the extract is slightly more active against Gram-positive (G+) than Gram-negative (G−) bacteria [30,32,36]. Not only the type of bacteria but also the source and concentration of the active plant extract compounds and the film composition play a key role in the antimicrobial activity of OEO. For instance, whey protein isolated (WPI)-based films with 1 wt./vol.-% OEO prepared by Oussalah et al. [33]

were effective against different bacterial colonies on the surface of beef. However, Seydim and Sarikus [35] observed that a content of at least 2 wt.-% OEO in WPI films was needed to reach the minimum inhibitory level against the same bacteria.

Finally, Table 6 includes the antibacterial effect against *S. aureus* of the green composite sheets with varying functionalized CF contents. It can be observed that both the unfilled PHBV sheet and the different green composite sheets containing CFs without OEO showed no inhibition effect on the bacterial growth (R ≤ 0.5). In contrast, the incorporation of OEO-containing CFs into the PHVB sheets exhibited a significant antibacterial activity. At the initial day, i.e. for the tests carried out 1 day after production of the green composite sheets, bacterial reduction on the sheets surface gradually increased with the OEO-containing CFs content. At the lowest content, i.e. 1 wt.-% OEO-containing CFs, the green composite sheet presented a slight antibacterial activity (R = 0.97). For higher contents, i.e. 3 – 10 wt.-% OEO-containing CFs, the sheets generated a significant surface reduction (R ≥ 1 and <3). Although none of the sheets produced a strong reduction (R ≥ 3), contents as low as 3 wt.-% OEO-containing CFs successfully inhibited the bacterial growth. Indeed, materials with surface reduction values in the range 1 – 2 are usually considered as bacteriostatic [50]. Therefore, final OEO contents of only 0.15 wt.-% in the green composites, which corresponds to a OEO-containing CFs loading of 3 wt.-%, were able to provide a bacteriostatic effect against *S. aureus*. As also shown in the table, after 15 days, the green composite sheets successfully kept a significant antibacterial activity. In particular, the sheets with OEO-containing CFs loadings of 5 and 10 wt.-% still presented significant (R ≥ 1 and <3) values of reduction while these presented slight (R ≥ 0.5 and <1) and nonsignificant (R ≤ 0.5) values for loadings of 3 and 1 wt.-%, respectively. This suggests that, though part of OEO was released from the sheets over time, the CFs were still able to retain a significant amount of the active oil.

Table 6. Antibacterial activity against *Staphylococcus aureus* of the compression-molded sheets made of poly(3-hydroxybutyrate-co-3-hydroxyvalerate) (PHBV) and coconut fibers (CFs) loaded with oregano essential oil (OEO)

Sample	Initial		After 15 days	
	Bacterial counts [log (CFU/ml)]	R	Bacterial counts [log (CFU/ml)]	R
Inoculation	5.69 ± 0.10	---	5.69 ± 0.10	---
Control (t = 0 h)	5.70 ± 0.03	---	5.68 ± 0.44	---
Control (t = 24 h)	5.69 ± 0.03	---	5.68 ± 0.44	---
PHBV	5.32 ± 0.50	0.37 ± 0.49	5.30 ± 0.05	0.38 ± 0.41
PHBV/CFs 1 wt.-%	5.48 ± 0.18	0.21 ± 0.15	5.42 ± 0.51	0.26 ± 0.65
PHBV/CFs 1 wt.-% + OEO	4.72 ± 0.05	0.97 ± 0.18	5.56 ± 0.17	0.12 ± 0.29
PHBV/CFs 3 wt.-%	5.39 ± 1.11	0.30 ± 1.14	5.54 ± 0.56	0.14 ± 0.47
PHBV/CFs 3 wt.-% + OEO	4.21 ± 0.50	1.48 ± 0.64	4.78 ± 0.09	0.90 ± 0.65
PHBV/CFs 5 wt.-%	5.36 ± 0.50	0.33 ± 0.51	5.62 ± 0.05	0.06 ± 0.45
PHBV/CFs 5 wt.-% + OEO	4.15 ± 0.70	1.54 ± 0.53	4.58 ± 0.09	1.10 ± 0.12
PHBV/CFs 10 wt.-%	5.35 ± 0.09	0.34 ± 0.09	5.60 ± 0.16	0.08 ± 0.56
PHBV/CFs 10 wt.-% + OEO	3.96 ± 0.33	1.73 ± 0.40	4.32 ± 0.26	1.36 ± 0.41

Previous studies based on films loaded with OEO against food spoilage microorganisms have shown that a minimum concentration of approximately 1 wt.-% of active material was necessary to ensure antibacterial efficacy. For instance, Benavides et al. [31] incorporated OEO in alginate films prepared by solvent casting where active contents at a level of 1.0 wt./vol.-% provided antibacterial properties. In another study, Hosseini et al. [32] prepared OEO-containing fish gelatin/chitosan films also by the casting method, showing antimicrobial performance at 1.2 wt./vol.-%. Pelissari et al. [34] recently produced starch/chitosan films in which OEO was incorporated at 0.1–1 wt.-% by blow film extrusion. The antimicrobial activity against *S. aureus* was only evaluated qualitatively by the disk inhibition zone assay, producing halos between 13.26 and 30.81 mm. The here-attained results then suggest that antimicrobial efficiency of the green composites based on OEO-containing CFs is about 6 – 7 times higher than that observed in previous research works. However, all these studies are certainly difficult to compare in a straight way, even for the same bacteria, due to differences in the film nature, the selected methodology of film preparation, the performed antimicrobial test, etc.

4   Conclusions

The first part of the present study was focused on finding the right processing conditions to optimally prepare green composites made of PHBV and CFs. Incorporation of different weight contents of CFs into a PHBV matrix was successfully achieved by TSE, varying the screw speed, and afterward shaped into sheets by compression molding. Optimal incorporation of the CFs into the PHBV matrix was attained at 150 rpm since this provided the best balance between dispersion and fiber attrition. This processing condition led to easily processable green composite formulations with the most balanced fiber distribution, average fiber length, and intermediate residence times. In particular, the fibers aspect ratio varied from 5.5 to 9, which decreased with increasing the CF content, and the residence time was of the order of 100 s. It was considered that this processing condition is beneficial to process both PHBV, due to its intrinsic narrow processing window and poor melt strength, and OEO, which is thermolabile and easily evaporates and/or decomposes during processing. In the second part of the study, the green composite sheets prepared at 150 rpm were fully characterized in terms of their thermal, mechanical, and barrier properties. Results showed that the incorporation of CFs into PHBV generated green composite sheets with similar thermal stability, even at the highest content, thus positively not impairing its processing window. In general, the green composites presented a slightly higher rigidity but lower ductility. It was particularly observed that the CFs acted as an effective reinforcement in the PHBV matrix when their length exceeds a critical threshold of 1500 μm, which corresponds to an aspect ratio close to 7. In relation to the barrier properties, it was observed that both the WVP and LP values were slightly reduced due to the CFs presence, which was related to a sorption phenomenon at the filler–matrix interface. Interestingly, the oxygen barrier performance was improved for intermediate CFs contents due to the contribution of the blocking effect over the heterogeneities was optimal. Finally, in the third part of the study, the CFs were impregnated with different OEO contents by an in-house developed spraying methodology and thereafter incorporated again into the green composites to generate sheets with antibacterial activity. Through this approach, it was possible to successfully achieve bacteriostatic effect against *S. aureus* from OEO-containing CF contents of only 3 wt.-%. This was ascribed to the high capacity of CFs to entrap active substances, being able to resist typical processing conditions of thermoplastic materials produced in the packaging industry. Interestingly, OEO was released in a slow manner to the green composite sheet surface, remaining at effective concentrations for a period of at least 15 days.

The scientific merit of this work relays on the development of a fully bio-based formulation, where a natural antimicrobial is incorporated within the structure of an

agro-food waste filler, which then acts as a carrier. In addition, the filler also serves to improve the physical performance and potentially reduce the cost of the overall formulation giving the current high price of commercial PHBV. This technology adds to actual strategies to pursue Circular Economy's approaches for the design of packaging materials. The active antimicrobial performance is, indeed, an added value also for the formulation because it will potentially increase the food quality and safety of the packed foods.

5 References

1. Yang H-, Kim H-, Park H-, Lee B-, Hwang T-. Water absorption behavior and mechanical properties of lignocellulosic filler-polyolefin bio-composites. *Compos. Struct.* **2006**, 72(4), 429-37.
2. Zini E, Scandola M. Green composites: An overview. *Polym. Compos.* **2011**, *32*(12), 1905-15.
3. Bogoeva-Gaceva G, Avella M, Malinconico M, Buzarovska A, Grozdanov A, Gentile G, Errico ME. Natural fiber eco-composites. *Polym. Compos.* **2007**, *28*(1), 98-107.
4. Joshi SV, Drzal LT, Mohanty AK, Arora S. Are natural fiber composites environmentally superior to glass fiber reinforced composites? *Compos. Part A Appl. Sci. Manuf.* **2004**, *35*(3), 371-6.
5. Faruk O, Bledzki AK, Fink H-, Sain M. Progress report on natural fiber reinforced composites. *Macromol. Mater. Eng.* **2014**, *299*(1), 9-26.
6. Bugnicourt E, Cinelli P, Lazzeri A, Alvarez V. Polyhydroxyalkanoate (PHA): Review of synthesis, characteristics, processing and potential applications in packaging. *Express Polym. Lett.* **2014**, *8*(11), 791-808.
7. Torres-Giner S, Montanes N, Boronat T, Quiles-Carrillo L, Balart R. Melt grafting of sepiolite nanoclay onto poly(3-hydroxybutyrate-co-4-hydroxybutyrate) by reactive extrusion with multi-functional epoxy-based styrene-acrylic oligomer. *Eur. Polym. J.* **2016**, *84*, 693-707.
8. Kunioka M, Tamaki A, Doi Y. Crystalline and thermal properties of bacterial copolyesters: Poly(3-hydroxybutyrate-co-3-hydroxyvalerate) and poly(3-hydroxybutyrate-co-4-hydroxybutyrate). *Macromolecules* **1989**, *22*(2), 694-7.
9. Torres-Giner S, Montanes N, Fombuena V, Boronat T, Sanchez-Nacher L. Preparation and characterization of compression-molded green composite sheets made of poly(3-hydroxybutyrate) reinforced with long pita fibers. *Adv. Polym. Technol.* **2018**, *37*(5), 1305-15.
10. Avella M, La Rota G, Martuscelli E, Raimo M, Sadocco P, Elegir G, Riva R. Poly(3-hydroxybutyrate-co-3-hydroxyvalerate) and wheat straw fibre composites: Thermal, mechanical properties and biodegradation behaviour. *J. Mater Sci.* **2000**, *35*(4), 829-36.
11. Barkoula NM, Garkhail SK, Peijs T. Biodegradable composites based on flax/polyhydroxybutyrate and its copolymer with hydroxyvalerate. *Ind. Crops Prod.* **2010**, *31*(1), 34-42.
12. Teramoto N, Urata K, Ozawa K, Shibata M. Biodegradation of aliphatic polyester composites reinforced by abaca fiber. *Polym. Degradation Stab.* **2004**, *86*(3), 401-9.
13. Cunha M, Berthet M-, Pereira R, Covas JA, Vicente AA, Hilliou L. Development of polyhydroxyalkanoate/beer spent grain fibers composites for film blowing applications. *Polym. Compos.* **2015**, *36*(10), 1859-65.
14. Rosa MF, Chiou B-, Medeiros ES, Wood DF, Williams TG, Mattoso LHC, Orts WJ, Imam SH. Effect of fiber treatments on tensile and thermal properties of starch/ethylene vinyl alcohol copolymers/coir biocomposites. *Bioresour. Technol.* **2009**, *100*(21), 5196-202.
15. Gu H. Tensile behaviours of the coir fibre and related composites after NaOH treatment. *Mater. Des.* **2009**, *30*(9), 3931-4.
16. Tomczak F, Sydenstricker THD, Satyanarayana KG. Studies on lignocellulosic fibers of brazil. part II: Morphology and properties of brazilian coconut fibers. *Compos. Part A Appl. Sci. Manuf.* **2007**, *38*(7), 1710-21.
17. Hasan M, Hoque ME, Mir SS, Saba N, Sapuan SM. Manufacturing of coir fibre-reinforced polymer composites by hot compression technique. *Manufacturing of Natural Fibre Reinforced Polymer Composites* **2015**, 309-30.
18. Rosa MF, Medeiros ES, Malmonge JA, Gregorski KS, Wood DF, Mattoso LHC, Glenn G, Orts WJ, Imam SH. Cellulose nanowhiskers from coconut husk fibers: Effect of preparation conditions on their thermal and morphological behavior. *Carbohydr. Polym.* **2010**, *81*(1), 83-92.
19. Satyanarayana KG, Pillai CKS, Sukumaran K, Pillai SGK, Rohatgi PK, Vijayan K. Structure property studies of fibres from various parts of the coconut tree. *J. Mater. Sci.* **1982**, *17*(8), 2453-62.
20. Choudhury A, Kumar S, Adhikari B. Recycled milk pouch and virgin low-density polyethylene/linear low-density polyethylene based coir fiber composites. *J. Appl. Polym. Sci.* **2007**, *106*(2), 775-85.
21. Owolabi O, Czvikovszky T. Composite materials of radiation-treated coconut fiber and thermoplastics. *J. Appl. Polym. Sci.* **1988**, *35*(3), 573-82.
22. Mir SS, Nafsin N, Hasan M, Hasan N, Hassan A. Improvement of physico-mechanical properties of coir-polypropylene biocomposites by fiber chemical treatment. *Mater. Des.* **2013**, *52*, 251-7.
23. Wambua P, Ivens J, Verpoest I. Natural fibres: Can they replace glass in fibre reinforced plastics? *Compos. Sci. Technol.* **2003**, *63*(9), 1259-64.

24. Corradini E, De Morais LC, De Rosa MF, Mazzetto SE, Mattoso LHC, Agnelli JAM. A preliminary study for the use of natural fibers as reinforcement in starch-gluten-glycerol matrix. *Macromol. Sympos.* **2006**, *245-246*, 558-64.

25. Geethamma VG, Mathew KT, Lakshminarayanan R, Thomas S. Composite of short coir fibres and natural rubber: Effect of chemical modification, loading and orientation of fibre. *Polymer* **1998**, *39*(6-7), 1483-91.

26. Westerlind BS, Berg JC. Surface energy of untreated and surface-modified cellulose fibers. *J. Appl. Polym. Sci.* **1988**, *36*(3), 523-34.

27. Bhatnagar A, Vilar VJP, Botelho CMS, Boaventura RAR. Coconut-based biosorbents for water treatment-A review of the recent literature. *Adv. Colloid Interface Sci.* **2010**, *160*(1-2), 1-15.

28. López P, Sánchez C, Batlle R, Nerín C. Development of flexible antimicrobial films using essential oils as active agents. *J. Agric. Food Chem.* **2007**, *55*(21), 8814-24.

29. Hosseini SF, Zandi M, Rezaei M, Farahmandghavi F. Two-step method for encapsulation of oregano essential oil in chitosan nanoparticles: Preparation, characterization and in vitro release study. *Carbohydr. Polym.* **2013**, *95*(1), 50-6.

30. Burt S. Essential oils: Their antibacterial properties and potential applications in foods - A review. *Int. J. Food Microbiol.* **2004**, *94*(3), 223-53.

31. Benavides S, Villalobos-Carvajal R, Reyes JE. Physical, mechanical and antibacterial properties of alginate film: Effect of the crosslinking degree and oregano essential oil concentration. *J. Food Eng.* **2012**, *110*(2), 232-9.

32. Hosseini SF, Rezaei M, Zandi M, Farahmandghavi F. Bio-based composite edible films containing origanum vulgare L. essential oil. *Ind. Crops Prod.* **2015**, *67*, 403-13.

33. Oussalah M, Caillet S, Salmiéri S, Saucier L, Lacroix M. Antimicrobial and antioxidant effects of milk protein-based film containing essential oils for the preservation of whole beef muscle. *J. Agric. Food Chem.* **2004**, *52*(18), 5598-605.

34. Pelissari FM, Grossmann MVE, Yamashita F, Pined EAG. Antimicrobial, mechanical, and barrier properties of cassava starch-chitosan films incorporated with oregano essential oil. *J. Agric. Food Chem.* **2009**, *57*(16), 7499-504.

35. Seydim AC, Sarikus G. Antimicrobial activity of whey protein based edible films incorporated with oregano, rosemary and garlic essential oils. *Food Res. Int.* **2006**, *39*(5), 639-44.

36. Zivanovic S, Chi S, Draughon AF. Antimicrobial activity of chitosan films enriched with essential oils. *J. Food Sci.* **2005**, *70*(1), M45-51.

37. Barham PJ, Keller A, Otun EL, Holmes PA. Crystallization and morphology of a bacterial thermoplastic: Poly-3-hydroxybutyrate. *J. Mater. Sci.* **1984**, *19*(9), 2781-94.

38. Torres-Giner S, Torres A, Ferrándiz M, Fombuena V, Balart R. Antimicrobial activity of metal cation-exchanged zeolites and their evaluation on injection-molded pieces of bio-based high-density polyethylene. *J. Food Saf.* **2017**, *37*(4).

39. Torres-Giner S. Preparation of conductive carbon black-filled polymer nanocomposites via melt compounding. *Conductive Materials and Composites* **2016**, 117-64.

40. Hilliou L, Teixeira PF, Machado D, Covas JA, Oliveira CSS, Duque AF, Reis MAM. Effects of fermentation residues on the melt processability and thermomechanical degradation of PHBV produced from cheese whey using mixed microbial cultures. *Polym. Degradation Stab.* **2016**, *128*, 269-77.

41. Shang L, Fei Q, Zhang YH, Wang XZ, Fan D-, Chang HN. Thermal properties and biodegradability studies of poly(3-hydroxybutyrate-co-3-hydroxyvalerate). *J. Polym. Environ.* **2012**, *20*(1), 23-8.

42. Shibata M, Oyamada S, Kobayashi S-, Yaginuma D. Mechanical properties and biodegradability of green composites based on biodegradable polyesters and lyocell fabric. *J. Appl. Polym. Sci.* **2004**, *92*(6), 3857-63.

43. Razumovskii LP, Iordanskii AL, Zaikov GE, Zagreba ED, McNeill IC. Sorption and diffusion of water and organic solvents in poly(β-hydroxybutyrate) films. *Polym. Degradation Stab.* **1994**, *44*(2), 171-5.

44. Lagarón J-. Multifunctional and nanoreinforced polymers for food packaging. *Multifunctional and Nanoreinforced Polymers for Food Packaging* **2011**, 1-28.

45. Sanchez-Garcia MD, Gimenez E, Lagaron JM. Morphology and barrier properties of solvent cast composites of thermoplastic biopolymers and purified cellulose fibers. *Carbohydr. Polym.* **2008**, *71*(2), 235-44.

46. Sanchez-Garcia MD, Gimenez E, Lagaron JM. Novel PET nanocomposites of interest in food packaging applications and comparative barrier performance with biopolyester nanocomposites. *J. Plast. Film Sheeting* **2007**, *23*(2), 133-48.

47. Cherpinski A, Torres-Giner S, Cabedo L, Méndez JA, Lagaron JM. Multilayer structures based on annealed electrospun biopolymer coatings of interest in water and aroma barrier fiber-based food packaging applications. *J. Appl. Polym. Sci.* **2018**, *135*(24).

48. dos Santos Rodrigues JB, de Carvalho RJ, de Souza NT, de Sousa Oliveira K, Franco OL, Schaffner D, de Souza EL, Magnani M. Effects of oregano essential oil and carvacrol on biofilms of *staphylococcus aureus* from food-contact surfaces. *Food Control* **2017**, *73*, 1237-46.

49. Dadalioğlu I, Evrendilek GA. Chemical compositions and antibacterial effects of essential oils of turkish oregano (origanum minutiflorum), bay laurel (laurus nobilis), spanish lavender (lavandula stoechas L.), and fennel (foeniculum vulgare) on common foodborne pathogens. *J. Agric. Food Chem.* **2004**, *52*(26), 8255-60.

50. Castro-Mayorga JL, Fabra MJ, Pourrahimi AM, Olsson RT, Lagaron JM. The impact of zinc oxide particle morphology as an antimicrobial and when incorporated in poly(3-hydroxybutyrate-co-3-hydroxyvalerate) films for food packaging and food contact surfaces applications. *Food Bioprod. Process* **2017**, *101*, 32-44.

CHAPTER III

Electrospun Active Biopapers of Food Waste Derived Poly(3-hydroxybutyrate-co-3-hydroxyvalerate) with Short-Term and Long-Term Antimicrobial Performance

Kelly J. Figueroa-Lopez, Sergio Torres-Giner, Daniela Enescu, Luis Cabedo, Miguel A. Cerqueira, Lorenzo M. Pastrana and Jose M. Lagaron

Electrospun Active Biopapers of Food Waste Derived Poly(3-hydroxybutyrate-co-3-hydroxyvalerate) with Short-Term and Long-Term Antimicrobial Performance

Abstract

This research reports about the development by electrospinning of fiber-based films made of poly(3-hydroxybutyrate-co-3-hydroxyvalerate) (PHBV) derived from fermented fruit waste, so-called bio-papers, with enhanced antimicrobial performance. To this end, different combinations of oregano essential oil (OEO) and zinc oxide nanoparticles (ZnONPs) were added to PHBV solutions and electrospun into mats that were, thereafter, converted into homogeneous and continuous films of ~130 μm. The morphology, optical, thermal, mechanical properties, crystallinity, and migration into food simulants of the resultant PHBV-based bio-papers were evaluated and their antimicrobial properties were assessed against *Staphylococcus aureus* (*S. aureus*) and *Escherichia coli* (*E. coli*) in both open and closed systems. It was observed that the antimicrobial activity decreased after 15 days due to the release of the volatile compounds, whereas the bio-papers filled with ZnONPs showed high antimicrobial activity for up to 48 days. The electrospun PHBV biopapers containing 2.5 wt.% OEO + 2.25 wt.% ZnONPs successfully provided the most optimal activity for short and long periods against both bacteria.

Keywords: PHBV; essential oils; inorganic nanoparticles; biopapers; electrospinning; migration; active packaging

1   Introduction

The packaging industry has increased the demand of active materials obtained from renewable resources due to the environmental concerns related to the extensive use of conventional plastics and also to the consumer requests for safer, more nutritious, and high-quality food [1]. Polyhydroxyalkanoates (PHAs) are bio-based and biodegradable aliphatic polyesters of high potential to replace polyolefins in packaging applications [2]. PHAs are synthesized in the mitochondria of a wide range of Gram-negative (G−) and Gram-positive (G+) microorganisms [3]. They can be divided into short chain length (scl-PHAs) with monomers with three to five carbon atoms and medium chain length (mcl-PHAs) with monomers with more than six carbons [4]. Among them, scl-PHAs are the most studied, including the poly(3-hydroxybutyrate) (PHB or P3HB) homopolyester and its copolymer poly(3-hydroxybutyrate-co-3-hydroxyvalerate) (PHBV). The latter shows lower crystallinity and melting point as well as greater flexibility, which broadens its industrial applicability [4,5]. In order to confer active properties to PHAs, several substances can be incorporated into the biopolymers such as essential oils (EOs) and inorganic or metal nanoparticles (MNPs) [6,7].

EOs are the product of the secondary metabolism of plants, separated from the aqueous phase, which is formed by various volatile components such as terpenes, alcohols, acids, esters, epoxies, aldehydes, ketones, amines, and sulphides, among others [8]. This wide range of compounds are responsible for the strong biological activity and also the antioxidant, antimicrobial, antifungal, and antiviral properties of plants [9]. In addition, EOs are biologically safe and have a low risk of causing resistance in pathogens [10]. In addition, they are classified as Generally Recognized as Safe (GRAS) by the U.S. Food and Drug Administration (FDA) [11]. Among them, oregano essential oil (OEO) is one of the most important and it is widely used in the pharmaceutical, food, and cosmetics industries [12]. It comes from the genus Origanum that belongs to the Lamiaceae family [13], which is constituted by more than 38 monoterpenoids [14]. Their main active compounds are carvacrol, thymol, p-cymene, and γ-terpinene, which are responsible for its high antimicrobial and antioxidant activities [15,16]. These active compounds have been particularly related to the inhibition of G− bacteria such as *Escherichia coli* (*E. coli*), *Pseudomonas aeruginosa* (*P. aeruginosa*), and *Salmonella typhimurium* (*S. typhimurium*) and G+ bacteria including *Staphylococcus aureus* (*S. aureus*), *Listeria monocytogenes* (*L. monocytogenes*), *Bacillus subtilis* (*B. subtilis*), *Streptococcus pyogenes* (*S. pyogenes*), and *Alicyclobacillus acidoterrestris* (*A. acidoterrestris*) [12,15,17-19]. Some other studies have also demonstrated the high antioxidant activity of OEO, which ranges from 80% to 90% inhibition of free radicals of 2,2-diphenyl-1-

picrylhydrazyl (DPPH) and 2,2′-azino-bis-(-3-ethylbenzothiazoline-6-sulfonic acid) (ABTS) [12,20,21] due to the presence of hydroxyl groups (–OH) in its chemical structure [22].

Zinc oxide (ZnO) is an inorganic material, which can have up to three crystal structures including hexagonal wurtzite, cubic zinc-blende structure, and a rarely-observed cubic rock-salt (NaCl-type) [23]. The wurtzite form is the most thermodynamically stable structure in environmental conditions. The zinc-blende structure is metastable while the cubic rock-salt structure is stable under extreme pressure [24]. Particles of ZnO are the fourth most used metal particles in the world after those of iron, aluminum, and copper. It is commonly used in sunscreens and also in the food industry, which presents some advantages over other metallic substances due to its high mechanical stability, thermal stability at an ambient temperature, biocompatibility, and low cost and toxicity [25,26]. ZnO is also among the five zinc compounds categorized as GRAS by the U.S. FDA (21CFR182.8991) [27-29]. Zinc oxide nanoparticles (ZnONPs) can be synthesized by mechanochemical processing, sol-gel methods, and spray pyrolysis [30,31]. The antimicrobial effect of ZnONPs is exerted by different mechanisms of action such as reactive oxygen species (ROS), ion release (Zn^{2+}), membrane dysfunction, nanoparticle penetration, interruption, and blockage of transmembrane electron transport. ZnONPs cause irreversible damage as they disintegrate the membrane and increase its permeability [32,33,34]. Numerous investigations have reported a broad spectrum of ZnONPs bactericide in most G− and G+ bacteria such as *E. coli*, *Salmonella enteritidis* (*S. enteritidis*), *S. typhimurium*, *Proteus vulgaris* (*P. vulgaris*), *Klebsiella pneumonia* (*K. pneumoniae*), *S. pyogenes*, *Aeromonas hydrophila* (*A. hydrophila*), *B. subtilis*, *S. aureus*, *L. monocytogenes*, P. aeruginosa, *Enterococcus faecalis* (*E. faecalis*), Sarcina lutea (*S. lutea*), and more [35- 40].

The combined use of such organic-inorganic substances can offer several advantages in the development of novel active materials. For instance, a good dispersion of ZnONPs in an EO-containing PHA matrix can be effectively achieved and the properties of the resultant composite are improved [41]. From a chemical point of view, the integration of MNPs in polymers can be attained by a stable incrustation of the nanoparticles in the polymer matrix without having any chemical interaction or an anchorage of the nanoparticles on the surface by means of covalent, ionic, or hydrogen bonds [42]. Additionally, this combination can improve the mechanical properties, thermal stability, conductivity, and chemical resistance of polymers. Their composites can also show antimicrobial and antioxidant properties for different periods of time [43-45]. Therefore, they can contribute to the design of active packaging that extends the shelf life of the products by a mechanism that delays or

inhibits the microbial, enzymatic, and oxidative reactions, which are the main causes of food deterioration [46,47]. Then, the resultant packaging can serve to improve the distribution logistics and food preservation [48]. For instance, Al-Jumaili et al. [49] developed nanocomposite films combining renewable geranium essential oil (GEO) with ZnO. These sustainable nanocomposite films were proposed as active coatings of medical devices. In another study, Sani et al. [50] studied the effect of the combination of Melissa essential oil (MEO) and ZnO in chitosan composite films. The resultant composite showed a great deal of potential as antimicrobial and biodegradable films in food packaging applications. Ahmed et al. [51] also developed antimicrobial films incorporating ZnONPs in combination with clove essential oil (CEO) into polylactide/polyethylene glycol/poly(ε-caprolactone) (PLA/PEG/PCL) blends by solution casting. The films showed antibacterial efficacy for 21 days of storage at 4 °C against *S. aureus* and *E. coli* inoculated in scrambled egg. Heydari-Majd et al. [45] also developed active packaging films based on polylactide (PLA) containing ZnONPs and the Zataria multiflora Boiss essential oil aimed to extend the shelf life of meat products.

In this regard, the electrospinning technology offers the option to form high-performance active and bioactive systems based on polymer yarns of nanofibers with high surface-to-volume ratios by the application of high electrical fields to polymer solutions [52]. The resultant electrospun materials containing the active-releasing agents can then be incorporated into multilayer structures as coatings [53] or interlayers, [54] having a potential application in antimicrobial systems [55]. Furthermore, the application of annealing a thermal post-treatment below the biopolymer's melting temperature (T_m) allows us to obtain continuous and highly transparent films of more interest in the field of packaging [56]. Our previous research works have previously demonstrated that electrospun PHA films, that is, biopapers, containing either neat OEO [57,58] or ZnONPs [59], can exert a strong antimicrobial activity against different bacterial strains. The term "biopapers" refers to fiber-based materials made of natural polymers that are non-fiber based in origin such as PHAs. This is similar to conventional papers that refer to fiber-based materials made of cellulose or nanopapers to those made of nanocellulose. Moreover, the active packaging toward traditional packaging (total "inert" packaging) is designed to add valuable properties to foodstuff (e.g., extending the shelf life of foodstuff). Nevertheless, there are serious challenges faced by its commercialization due to the possible migration of the active additive from food packaging into foodstuff, and whose effects on consumer health are unknown [60].

In this context, the objective of this research was to assess the potential of the electrospinning technology to develop active biopapers of PHBV containing mixtures

of OEO and ZnONPS to achieve both short-term and long-term strong antimicrobial performance. Initially, both antimicrobial agents were characterized and the content of ZnONPs in PHBV was optimized. Then, the electrospun hybrid PHBV biopapers were characterized in terms of their morphology, optical, thermal, and mechanical properties, and crystallinity. Thereafter, the antimicrobial activity of the electrospun biopapers was evaluated against strains of *E. coli* and *S. aureus* in an open and closed system for 48 days and, compared to equivalent biopapers, based on neat OEO or ZnONPs. Lastly, the amount of ZnONPs that might migrate from the electrospun PHBV biopapers into different food simulants was analyzed.

2 Materials and Methods

2.1 Materials

PHBV with a molar fraction of 3-hydroxyvalerate (HV) of ~20 % was produced at the Universidade NOVA (UNOVA) de Lisboa (Lisbon, Portugal) at a pilot-plant scale. The copolyester was produced by means of mixed microbial cultures fed with fermented fruit that was supplied by SumolCompal S.A. (Lisbon, Portugal) as a waste from manufacturing fruit juice. Further details about the preparation of this PHA can be found elsewhere [61].

OEO, purity >99 % and a relative density of 0.925 – 0.955 g/mL, was provided by Gran Velada S.L. (Zaragoza, Spain). ZnONPs (CR-4FCC1), 99 % purity, specific surface of 4.5 m2/g, bulk density of 40 lb/ft3, and specific gravity of 5.6 were obtained from GH Chemicals LTD® (Saint Hyacinthe, QC, Canada).

Methanol, HPLC grade with 99.9 % purity and chloroform, reagent grade with 99.8 % purity, were both obtained from Panreac S.A. (Barcelona, Spain). 1-butanol, reagent grade with 99.5 % purity, and DPPH were both obtained from Sigma-Aldrich S.A. (Madrid, Spain). Ethanol absolute ($\geq$ 99.9 % vol.) was supplied by Honeywell® (Frankfurt, Germany). Acetic acid glacial (99 %) was supplied by Fisher Chemical® (Loughborough, UK). Zinc standard for calibration of ICP (TraceCERT®, 1000 mg/L zinc metal of high-purity quality prepared with 2 % nitric acid suitable for trace analysis and high-purity water, 18.2 MΩ.cm, 0.22 µm filtered) and nitric acid (70 vol%) were supplied by Sigma-Aldrich (Darmstadt, Germany).

2.2 Preparation of the Solutions for Electrospinning

The PHBV solution for electrospinning was prepared by dissolving 10% (wt/vol) of the biopolymer in a mixture of chloroform/1-butanol 75:25 (vol/vol) at room temperature. A solution containing OEO at 10 wt.% in PHBV was also produced in the same conditions based on our previous research work [57]. To select the optimal concentration of ZnONPs in PHBV, different solutions with contents of 1 wt.%, 3 wt.%, 6 wt.%, and 10 wt.% of ZnONPs in PHBV were prepared. The formulations based on the combination of OEO and ZnONPs were tested by preparing PHBV solutions with 7.5 wt.% OEO + 0.75 wt.% ZnONPs, 5 wt.% OEO + 1.5 wt.% ZnONPs, and 2.5 wt.% OEO + 2.25 wt.% ZnONPs.

2.3 Preparation of the Electrospun Biopapers

All the PHBV solutions containing OEO and ZnONPs were electrospun, in the same conditions, in a Fluidnatek® LE500. A high-throughput

electrospinning/electrospraying pilot line was manufactured and commercialized by Bioinicia S.L. (Valencia, Spain). Electrospining was performed by means of a 24 emitter multi-nozzle injector that was scanning vertically onto a metallic plate. The process conditions during electrospinning consisted of a flow-rate of 6 mL/h per single emitter, a voltage of 17 kV, and a tip-to-collector distance of 20 cm.

The resultant electrospun mats were subjected to annealing in a 4122-model press from Carver, Inc. (Wabash, IN, USA). The thermal post-treatment was performed at 125 °C, for 15 s, without pressure, based on previous conditions [57]. The resultant film samples, known as biopapers, had an average thickness of approximately 80 – 130 µm.

2.4   Characterization

2.4.1   Thickness

The thickness of all the biopapers was measured, prior to testing, using a digital micrometer S00014 from Mitutoyo, Corp. (Kawasaki, Japan) with an accuracy of ±0.001 mm. Five different points of the samples were measured including one in the middle and two in each end.

2.4.2   Morphology

Scanning electron microscopy (SEM), by means of a Hitachi S-4800 (Tokyo, Japan), and transmission electron microscopy (TEM), using a JEOL 1010 (Peabody, MA, USA), were used to determine the particle shape and size (diameter) distributions of ZnONPs and of the morphology of the electrospun PHBV fibers and their corresponding biopapers containing OEO and ZnONPs. For analyzing the dispersion of the ZnONPs in the electrospun PHBV fibers, the fibers were collected on a sandwich-type holder (Agar Scientific-G230, Agar Scientific Ltd., Essex, UK) with a mesh size of 3.05 mm. For the SEM cross-section observations, the biopapers were cryo-fractured by immersion in liquid nitrogen. The samples for SEM analysis were previously sputtered with a gold-palladium mixture for 3 min under vacuum. An accelerating voltage of 10 kV and a working distance of 8 – 10 mm was used during SEM analysis. For TEM, an acceleration voltage of 100 kV was employed. The size distribution of the particles and average fiber diameters was determined via ImageJ software using, at least, 20 microscopy images.

2.4.3   Transparency

The light transmission of the biopapers was determined using an UV–Vis spectrophotometer VIS3000 from Dinko, Instruments (Barcelona, Spain). To this

end, the absorption of light at wavelengths between 200 nm and 700 nm was measured in specimens sized 50 mm × 30 mm. Transparency (T) and opacity (O) were determined using Equations (1) and (2), respectively [62].

$$T = \frac{A_{600}}{L} \tag{1}$$

$$O = A_{500}\,L \tag{2}$$

where L is the biopaper thickness (mm), while A_{500} and A_{600} are the absorbance at 500 and 600 nm, respectively.

2.4.4 Color

Color of the biopapers was determined with a Chroma Meter CR-400 from Konica Minolta (Tokyo, Japan). The color difference (ΔE*) was calculated using Equation (3) [62].

$$\Delta E^* = [(\Delta L^*)^2 + (\Delta a^*)^2 + (\Delta b^*)^2]^{0.5} \tag{3}$$

where ΔL*, Δa*, and Δb* corresponded to the differences between the brightness and color parameters of the PHBV biopapers containing the active substances and the values of the neat PHBV biopaper. The color change was evaluated according to the following criteria [63]: the difference was unnoticeable if ΔE* < 1. Only an experienced observer can notice the difference for ΔE* ≥ 1 and < 2. An unexperienced observer notices the difference when ΔE* ≥ 2 and < 3.5. A clear noticeable difference is noted if ΔE* ≥ 3.5 and < 5, and the observer notices different colors when ΔE* ≥ 5. Tests were performed in triplicate.

2.4.5 X-Ray Diffraction Analysis

Wide angle X-ray diffraction (WAXD) was performed on the biopaper samples using a Bruker AXS D4 Endeavour diffractometer from Bruker Corporation (Billerica, MA, USA). The samples were scanned, at room temperature, in reflection mode using incident CuKα radiation (k = 1.5406 Å), while the generator was set up at 40 kV and the filament current was set at 40 mA. The data were collected over the range of scattering angles (2θ) comprised in the 5 – 40° range. Peak fitting was carried out using Igor Pro software package and Gaussian function was used to fit the experimental diffraction profiles obtained.

2.4.6 Thermal Analysis

The thermal properties were studied by thermogravimetric analysis (TGA) in a thermobalance TGA/STDA851e/LF/1600 from Mettler Toledo Inc (Schwarzenbach, Switzerland) under nitrogen atmosphere. After conditioning the samples in the sensor for 5 min at 30 °C, the samples were heated from 25 °C to 700 °C at a heating rate of 10 °C/min. The first derivative of thermogravimetry (DTG) curves, expressing the weight loss rate as the function of time, were also obtained using TA analysis software. All the tests were carried out in triplicate.

2.4.7 Mechanical Tests

Tensile tests were performed on an Instron Testing Machine Model 4469 from Instron Corp (Canton, MA, USA) according to ASTM Standard D 638. The biopapers were dumbbell-shaped to 115 mm × 16 mm. The cross-head speed was fixed at 10 mm/min. Four samples were tested for each biopaper and the average values of the mechanical parameters and standard deviations were reported.

2.4.8 Antimicrobial Activity

S. aureus CECT240 (ATCC 6538p) and *E. coli* CECT434 (ATCC 25922) strains were obtained from the Spanish Type Culture Collection (CECT, Valencia, Spain). The bacterial strains were stored in phosphate buffered saline (PBS) with 10 wt% tryptic soy broth (TSB) obtained from Conda Laboratories (Madrid, Spain) and 10 wt% glycerol at −80 °C. Previous to each study, a loopful of bacteria was transferred to 10 mL of TSB and incubated at 37 °C for 24 h. A 100-µL aliquot from the culture was again transferred to TSB and grown at 37 °C to the mid-exponential phase of growth. The optical density showing an absorbance value of 0.20 and measured at 600 nm in a UV–Vis spectrophotometer VIS3000 from Dinko, Instruments (Barcelona, Spain) determined that the initial bacterial concentration was approximately a 5×10^5 CFU/mL.

The values of minimum inhibitory concentration (MIC) and minimum bactericide concentration (MBC) of the OEO and ZnONPs were tested against the two selected food-borne bacteria following the plate micro-dilution protocol described in the "Methods for Dilution Antimicrobial. Susceptibility Tests for Bacteria That Grow Aerobically; Approved Standard Tenth. Edition (M07-A10)" by the Clinical and Laboratory Standards Institute (CLSI). During this test, a 96-well plate with an alpha numeric coordination system (columns 12 and rows A-H) were used, where 10 µL of the tested samples were introduced in the wells with 90 µL of the bacteria medium. In the wells corresponding to A, B, C, E, F, and G columns, different concentrations

of ZnONPs and OEO (0.078, 0.156, 0.312, 0.625, 1.25, 2.5, 5, 10, 20, and 40 μg/mL) were tested, in triplicate, from rows 1 to 10. Columns D and H were used as a control of ZnONPs and OEO in TSB without bacteria. Rows 11 and 12 were taken as the positive control, that is, only TSB, and a negative control, that is, *S. aureus* and *E. coli* in TSB, respectively. The plates were incubated at 37 °C for 24 h. Thereafter, 10 μL of resazurin, a metabolic indicator, was added to each well and incubated again at 37 °C for 2 h. Upon obtaining the resazurin change, the wells were read through a color difference. The MIC value was determined as the lowest concentration of OEO and ZnONPs presenting growth inhibition.

The antimicrobial performance of the electrospun PHBV biopapers was determined based on the guidelines of the Japanese Industrial Standard JIS Z2801 (ISO 22196:2007) for film samples [64]. The dimension of the biopapers was 1.5 cm × 1.5 cm. Onto the PHBV biopapers containing OEO and ZnONPs (test films) and PHBV biopaper without OEO and ZnONPs (negative control film), a microorganism suspension of S. aureus and E. coli was applied. Thereafter, the inoculated samples were placed in open bottles and incubated for 24 h at 24 °C and at a relative humidity (RH) of at least 95 %. Bacteria were recovered with PBS, 10-fold serially diluted, and incubated for 24 h at 37 °C to quantify the number of viable bacteria by a conventional plate count. The antimicrobial activity reduction (R) was evaluated from 1 (initial day), 8, 15, 22, 30, 40, and 48 days using Equation (4).

$$R = \left[log \left(\frac{B}{A} \right) - log \left(\frac{C}{A} \right) \right] = log \left(\frac{B}{C} \right) \tag{4}$$

where A is the average of the number of viable bacteria on the control sample immediately after inoculation, B is the average of the number of viable bacteria on the control sample after 24 h, and C is the average of the number of viable bacteria on the test sample after 24 h. The next assessment was followed to evaluate the antibacterial activity of the biopapers [65]: Nonsignificant reduction if $R < 0.5$, a slight reduction when $R \geq 0.5$ and < 1, a reduction that was significant when $R \geq 1$ and < 3, and a reduction was strong if $R \geq 3$. Experiments were performed in triplicate.

2.4.9   Migration test

The specific migration test conditions established by European Normative EC 13130-1:2004 were followed to determine the migration of ZnONPs from the electrospun PHBV-based biopapers. This process was performed by full immersion of the PHBV biopapers containing OEO and ZnONPs (size: 0.5 dm^2 and weighted accurately) in two food simulants that were sealed in clean wide-mouth jars. These simulant

systems consisted of an ethanol solution in water (83.33 mL at 10 vol% at 40 °C for 10 days) and acetic acid in water (83.33 mL at 3% wt/vol at 40 °C for 10 days). The blanks were food simulants without the biopaper samples filled into sealed jars and stored under the same conditions. After the incubation period, that is, 10 days, the biopapers containing OEO and ZnONPs were removed whereas the ethanol and acetic acid simulants were evaporated on an electric hot plate, digested with 1.2 mL of 70 % HNO_3, and resuspended in 12 mL of an ultrapure water vial with 1.2 mL of 70 % HNO3 vol/vol. The samples were then introduced for metal quantification by Inductively Coupled Plasma-Optical Emission Spectrometry (ICP-OES) using Spectrometer ICPE-9000 (Shimadzu®, Kioto, Japan) operating in the wavelength range from 167 nm to 800 nm, and equipped with torch axial or radial configuration, an ultrasonic nebulizer for higher sensitivity, and a charge coupled device (CCD) detector. The wavelength range was set from 167 nm to 800 nm. The instrumental parameters employed for ICP-OES analysis consisted of a nebulizer gas flow (0.70 L/min Ar), an auxiliary gas flow (0.60 L/min Ar), plasma (10 L/min Ar), Ar Gas P (478.66 kPa), and ICP radio frequency (RF) power (1.20 kW), whereas the direction was axial, the rotation speed was 20 rpm, the CCD temperature was −15 °C, and the vacuum level was 6.9 Pa. The linearity of the calibration curve was considered acceptable by achieving a correlation coefficient R2 > 0.999. All results were blank subtracted and the specific migration tests were performed in triplicate.

2.5   Statistical Analysis

The results were evaluated with a 95 % significance level ($p \leq 0.05$) by the analysis of variance (ANOVA). To identify significant differences among the samples, a multiple comparison test (Tukey) was followed using the software OriginPro8 (OriginLab Corporation, Northampton, MA, USA).

3 Results and Discussions

3.1 Characterization of the Antimicrobial Agents

TEM was conducted to evaluate the morphology of ZnONPs and their micrographs are presented in Figure 1. In Figure 1a, one can observe the TEM micrograph of the ZnONPs powder, which showed aggregates of cubic-like and rectangular particles with sizes below 100 nm. Figure 1b shows the surface of a single ZnONP, which have a surface of approximately 80×20 nm^2. As observed in the particle histogram shown in Figure 1c, most of the ZnONPs presented sizes between 85 nm and 105 nm, which have an average size of ~98 nm. This morphology is similar to that reported by Naphade and Jog [66] and Ogunyemi et al. [67] who described nanoparticles with elongated and cubic morphologies with lengths from 40 nm to 100 nm and diameters of ca. 50 nm.
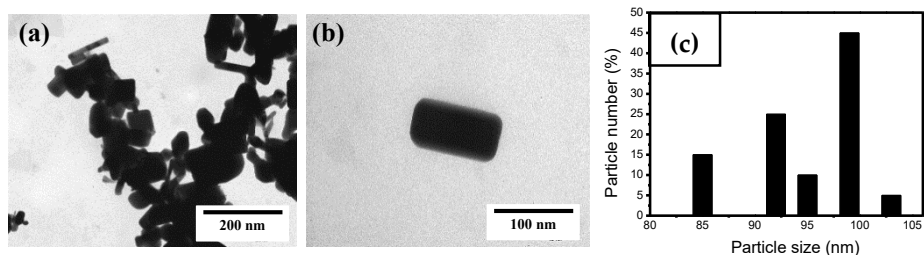
Figure 1. (**a,b**) Transmission electron microscopy (TEM) micrographs of zinc oxide nanoparticles (ZnONPs) showing scale markers of 200 nm and 100 nm, respectively. (**c**) Histogram of particle sizes.

Table 1 shows the MIC and MBC values of the neat OEO or ZnONPs against the strains of *S. aureus* and *E. coli*, selected as representative G+ and G− foodborne bacteria, respectively. OEO presents a good antibacterial effect against both bacterial strains, which achieve identical MIC and MBC values, that is, 0.625 μL/mL, against *E. coli*, and 0.312 μL/mL, against *S. aureus* [57]. The similar MIC and MBC values obtained by natural compounds have been described to inhibit the microbial growth and eliminate 99.9 % of the microorganisms [68]. In particular, the antimicrobial activity of OEO has been related to its high content in carvacrol and thymol [15]. Further details about the antimicrobial properties of OEO can be found in our previous research works [5,57]. Alternatively, it can be observed that ZnONPs presented the same values of MIC and MBC for both *E. coli* and *S. aureus* bacteria. In particular, the inhibition of the two strains was attained at 0.156 μg/mL. In this regard, Salah et al. [69] reported a MIC value for ZnONPs of 2 μg/mL against *E. coli* and *B. subtilis* bacteria and the *S. cerevisiae* yeast. The differences observed in the

antimicrobial activity of the nanoparticles can be related to their morphology and synthesis process. For instance, several authors have indicated that, at high concentrations, aggregates of nanoparticles may form precipitates that decrease the ZnONPs' antimicrobial activity [35,69]. It is also worthy to mention that the antimicrobial activity of ZnONPs is attributed to the release of ions Zn^{2+}, which penetrate the cellular wall of bacteria or adhere to the cell by an electrostatic interaction. This phenomenon leads to the generation of reactive oxygen species (ROS), such as O^{2-} and OH^- radicals, on the surface of particles that cause a dysfunction of the membrane and, therefore, the destruction of the bacterial cells [70,71]. Thus, it was confirmed that ZnONPs present a broad spectrum of inhibition for both G+ and G− bacteria [26].

Table 1. Minimum inhibitory concentration (MIC) and minimum bactericidal concentration (MBC) of the neat oregano essential oil (OEO) and zinc oxide nanoparticles (ZnONPs) against *Staphylococcus aureus* (*S. aureus*) and *Escherichia coli* (*E. coli*)

Active agent	Bacteria	MIC	MBC
OEO	*E. coli*	0.625 µL/mL	0.625 µL/mL
	S. aureus	0.312 µL/mL	0.312 µL/mL
ZnONPs	*E. coli*	0.156 µg/mL	0.156 µg/mL
	S. aureus	0.156 µg/mL	0.156 µg/mL

3.2   Optimization of the Electrospun PHBV/ZnONPs Biopapers

The morphology and the antimicrobial properties of the electrospun PHBV fibers and biopapers containing ZnONPs were also analyzed by SEM and TEM in order to select the optimal content of nanoparticles in the biopolymer. Figure 2 shows the SEM micrographs of the electrospun PHBV fibers. In particular, Figure 2a shows the SEM images of the neat PHBV fibers, whereas Figure 2b includes the PHBV fibers containing 10 wt.% OEO, which were also included in the study for comparison. In both cases, the PHBV fibers presented a mean diameter of approximately 0.8 µm, which is agreement with our previous works reporting the morphology of electrospun PHBV fibers [57,58]. Figure 2c–f corresponds to the PHBV fibers, without OEO, containing ZnONPs at 1 wt.%, 3 wt.%, 6 wt.%, and 10 wt.%. It can be seen that, in all cases, the mean diameters of the fibers were in the 0.88 – 0.97 µm range. The electrospun PHBV fibers presented a smooth surface morphology without beads. No further changes were observed in the fibers' morphology after the ZnONPs incorporation with the exception that some nanoparticles were also observed on the fibers surface, which indicates that part of ZnONPs were not incorporated into the PHBV matrix.
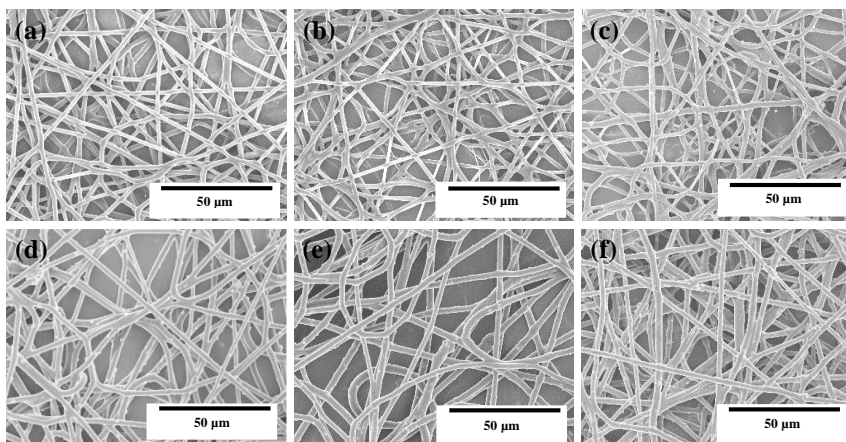
Figure 2. Scanning electron microscopy (SEM) micrographs of the electrospun fibers of poly(3-hydroxybutyrate-co-3-hydroxyvalerate) (PHBV): (**a**) Neat PHBV; (**b**) PHBV containing 10 wt% oregano essential oil (OEO); (**c**) PHBV containing 1 wt% zinc oxide nanoparticles (ZnONPs); (**d**) PHBV containing 3 wt% ZnONPs; (**e**) PHBV containing 6 wt% ZnONPs; (**f**) PHBV containing 10 wt% ZnONPs. Scale markers of 50 μm in all cases.

Figure 3 shows the TEM micrographs of the nanocomposite fibers to evaluate the dispersion of the nanoparticles within the fibers. In Figure 3a, which corresponds to the fibers containing 1 wt.% of ZnONPs, it can be seen that the nanoparticles were efficiently encapsulated in the PHBV fibers during the electrospinning process even though they were randomly distributed within the biopolymer matrix. A similar morphology was attained for the electrospun fibers with a ZnONPs content of 3 wt.%, shown in Figure 3b. In general, the nanoparticles showed a relatively good dispersion within the PHBV matrix. However, it can be observed that, as the nanofillers content increased, the ZnONPs tended to form agglomerates. Therefore, the samples containing 6 wt.% and 10 wt.% ZnONPs (Figure 3c,d, respectively) showed fiber regions with agglomerated ZnONPs. This effect was particularly noticeable for the electrospun PHBV fibers filled with the 10 wt.% ZnONPs. This morphological observation supports the previously described thickening observed by SEM for the PHBV fibers attained for the highest ZnONPs loadings.
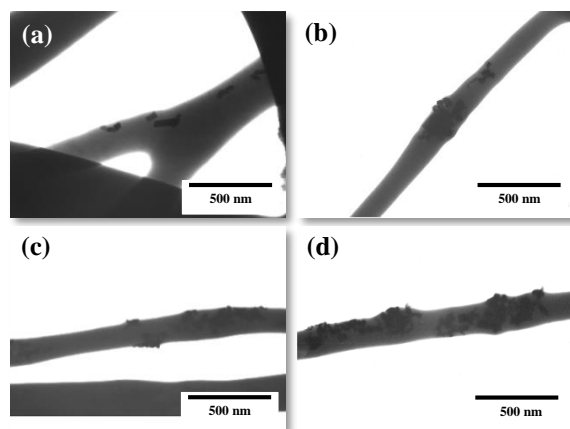
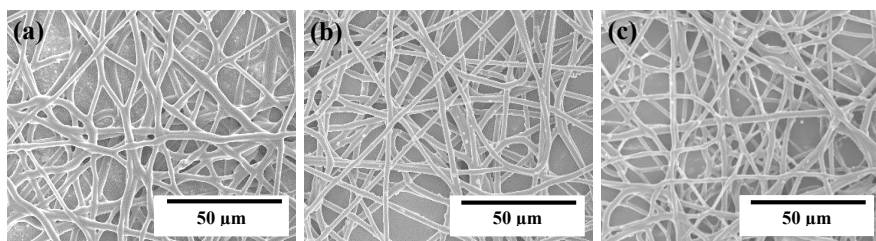**Figure 3.** Transmission electron microscopy (TEM) micrographs of the electrospun fibers of poly(3-hydroxybutyrate-co-3-hydroxyvalerate) (PHBV) containing zinc oxide nanoparticles (ZnONPs) at: (**a**) 1 wt%; (**b**) 3 wt%; (**c**) 6 wt%; (**d**) 10 wt%. Scale markers of 500 nm in all cases.

The resultant electrospun mats were annealed at 125 °C in order to produce continuous films composed of fibers, which are called biopapers. Figure 4 shows the SEM images of the electrospun materials after the thermal post-treatment at 125 °C in both their cross-section and top views. The biopapers of neat PHBV, presented in Figure 4a,b and of the PHBV containing 10 wt.% OEO, presented in Figure 4c,d, showed a similar thickness of ~80 μm. The neat PHBV biopaper exhibited a homogeneous and continuous structure, which is similar to the morphologies reported recently by Melendez-Rodriguez et al. [61], even though, in the previous study, the films showed a higher porosity due to the presence of high loadings of eugenol that plasticized the PHBV matrix, which was evaporated/migrated during the annealing process. Similarly, the OEO-containing PHVB biopapers presented some small pores in their cross section due to the evaporation of the volatiles during the thermal post-treatment. The top view and cross section of the PHBV biopapers containing 1 wt.% ZnONPs are gathered in Figure 4e,f, where it can be observed that the biopaper surface was also homogenous. Similar morphologies can be seen in Figure 4g,h for the PHBV biopapers filled with 3 wt.% ZnONPs. However, in the case of the biopapers containing 6 wt.%, shown in Figure 4i,j and 10 wt% ZnONPs, in Figure 4k,l, the presence of nanoparticles altered their surface, which affected the film homogeneity and generated cracks. The presence of ZnONPs also increased significantly the biopaper thicknesses to ~130 μm, in all the biopaper samples, which can be related to confinement restrictions of the fibers' reorganization by the nanoparticles' presence during annealing.
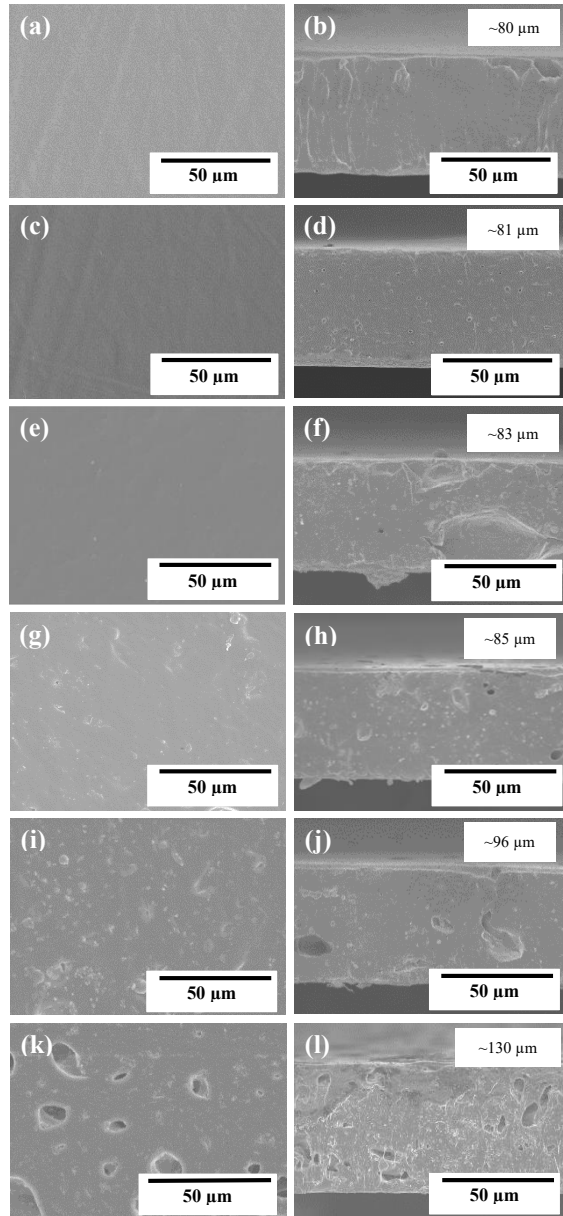
Figure 4. Scanning electron microscopy (SEM) micrographs in a top view (left) and a cross-section (right) of the electrospun biopapers of poly(3-hydroxybutyrate-co-3-hydroxyvalerate) (PHBV): (**a,b**) Neat PHBV; (**c,d**) PHBV containing 10 wt% oregano essential oil (OEO); (**e,f**) PHBV containing 1 wt% zinc oxide nanoparticles (ZnONPs); (g,h) PHBV containing 3 wt% ZnONPs; (**i,j**) PHBV containing 6 wt% ZnONPs; (**k,l**) PHBV containing 10 wt% ZnONPs. Scale markers of 50 μm in all cases.

Lastly, the antimicrobial properties in an open system of the electrospun PHBV biopapers filled with the different contents of ZnONPs against *S. aureus* and *E. coli* were studied and the results are gathered in Figure 5. Film samples with concentrations of 1 wt.% and 3 wt.% ZnONPs showed strong inhibition (R ≥ 3) against both strains after 24 h. Interestingly, when the concentration of ZnONPs increased, the antimicrobial activity decreased. This effect can be related to the previously mentioned phenomenon of agglomeration, once the viable active surface of ZnONPs was reduced when they formed agglomerates and, therefore, reduced the ion-releasing process and, thus, their effectiveness. As reported earlier, the size, morphology, and specific surface area of ZnONPs can greatly affect the antibacterial properties and, thus, the agglomeration of ZnONPs must be avoided [35]. These results are also in accordance with a previous work of Padmavathy and Vijayaraghavan [72] who determined that the antibacterial activity of ZnO against *E. coli* was stronger when the particle size decreased and the particle dispersion was improved.
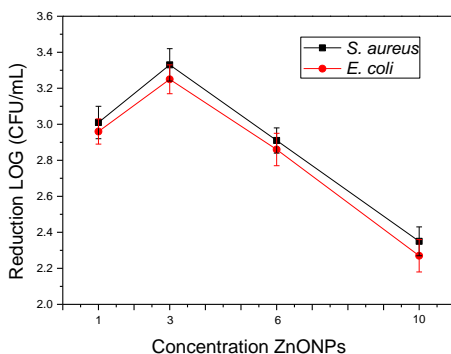
Figure 5. Antimicrobial properties of the electrospun biopapers of poly(3-hydroxybutyrate-co-3-hydroxyvalerate) (PHBV) containing zinc oxide nanoparticles (ZnONPs) against *Staphylococcus aureus* (*S. aureus*) and *Escherichia coli* (*E. coli*) in an open system for 24 h.

Based on the obtained results, 3 wt.% was selected as the optimal content of ZnONPs in PHBV. The resultant electrospun biopapers were not only more uniform and homogeneous, but they also offered the highest antibacterial properties at a relatively low content. The here-attained optimal content of ZnONPs in PHBV was two times lower than that previously obtained by Castro-Mayorga et al. [59] who reported a reduction of approximately 3 log CFU/mL for *L. monocytogenes* with PHBV films filled with 6 wt.% ZnONPs. The differences observed can be related to methods employed for the incorporation of the ZnONPs such as direct melt-mixing, melt-mixing of pre-incorporated ZnONPs into PHBV, and coating of annealed electrospun

fiber mats over compression-molded PHBV films as well as the morphology and crystal-type of the nanoparticles.

3.3   Development of the Electrospun Hybrid PHBV Biopapers

The PHBV fibers containing the mixtures of OEO and ZnONPs, known as the hybrid fibers, were developed and compared to the previously prepared electrospun materials based on either neat PHBV or PHBV with 10 wt.% OEO or 3 wt.% ZnONPs. Figure 6 shows the SEM micrographs of the electrospun hybrid PHBV fibers. In Figure 6a, one can observe the morphology of the PHBV fibers containing 7.5 wt.% OEO + 0.75 wt.% ZnONPs. The mean diameter was 0.90 ± 0.28 μm and the fibers were smooth and also free of beaded regions. Similar morphologies were attained for the PHBV fibers containing 5 wt.% OEO + 1.5 wt.% ZnONPs and 2.5 wt.% OEO + 2.25 wt.% ZnONPs, respectively shown in Figure 6b,c. The fibers' diameters, however, slightly increased ($p \geq 0.005$) with the increase of the ZnONPs content and some nanoparticles were also placed outside the fibers. In particular, the mean diameters were 0.92 ± 0.32 μm and 0.94 ± 0.41 μm, for the PHBV fibers containing 5 wt.% OEO + 1.5 wt.% ZnONPs and 2.5 wt.% OEO + 2.25 wt.% ZnONPs, respectively. A similar effect was observed by Mousavi et al. [73] where the addition of cerium dioxide (CeO_2)/dendrimer nanoparticles significantly increased the diameter of electrospun pullulan/poly(vinyl alcohol) (PVA)/poly(acrylic acid) (PAA) fibers and it also induced surface roughness. This effect was ascribed to the high filler concentration, which promoted porosity and fiber thickening. In general, all the PHBV-based fibers presented a uniform and smooth surface, showing no surface or structural defects, which indicates that the addition of mixtures of OEO and ZnONPs positively did not alter fiber formation during electrospinning.

Figure 6. Scanning electron microscopy (SEM) micrographs of the electrospun fibers of poly(3-hydroxybutyrate-co-3-hydroxyvalerate) (PHBV) containing different amounts of oregano essential oil (OEO) and zinc oxide nanoparticles (ZnONPs): (**a**) PHBV + 7.5 wt.% OEO + 0.75 wt.% ZnONPs; (**b**) PHBV + 5 wt.% OEO + 1.5 wt.% ZnONPs; (**c**) PHBV + 2.5 wt.% OEO + 2.25 wt.% ZnONPs. Scale markers of 50 μm in all cases.

The morphology of the electrospun hybrid PHBV fibers was also analyzed by TEM to observe the effect of OEO on the dispersion of ZnONPs in the biopolymer matrix. Figure 7 gathers the TEM micrographs of the electrospun fibers. One can observe in Figure 7a,b, corresponding to the PHBV fibers containing 7.5 wt.% OEO + 0.75 wt.% ZnONPs and 5 wt.% OEO + 1.5 wt.% ZnONPs, respectively, that the nanoparticles were well dispersed along the biopolymer even though they also tended to agglomerate in certain regions. Agglomeration was more intense in the case of the PHBV fibers containing 2.5 wt.% OEO + 2.5 wt.% ZnONPs, shown in Figure 7c, suggesting that larger aggregate structures were formed as the nanoparticles' concentration increased. This phenomenon is in agreement with the results reported by Cherpinski et al. [74] who incorporated palladium nanoparticles (PdNPs) into electrospun fibers of PHB. Nanoparticle agglomeration can be ascribed to the large surface area of the nanoparticles and the electrostatic forces among them [75]. The hybrid fibers showed lower agglomerates of the nanoparticles when compared with the ZnONPs-containing PHBV fibers without OEO, as seen in Figure 3, which suggests that the presence of the oil favored the dispersion of the nanoparticles. This effect can be ascribed to a potential plasticization of the PHBV matrix that could facilitate cluster breakup and separation of nanoparticles during electrospinning.
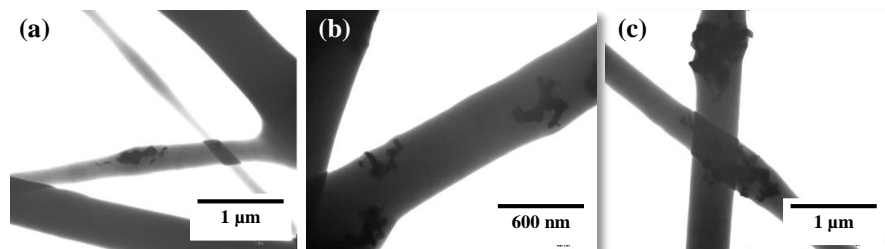
Figure 7. Transmission electron microscopy (TEM) micrographs of the electrospun fibers of poly(3-hydroxybutyrate-co-3-hydroxyvalerate) (PHBV) containing different amounts of oregano essential oil (OEO) and zinc oxide nanoparticles (ZnONPs): (**a**) PHBV + 7.5 wt.% OEO + 0.75 wt.% ZnONPs; (**b**) PHBV + 5 wt.% OEO + 1.5 wt.% ZnONPs; (**c**) PHBV + 2.5 wt.% OEO + 2.25 wt.% ZnONPs. Scale markers of 1 μm in all cases.

Figure 8 shows the SEM images of the electrospun materials after annealing at 125 °C in their cross-section and top views. On the top views of the samples included in Figure 8a,c,e, it can be observed that all the biopapers exhibited a homogeneous surface without cracks and/or pores, similar to those SEM images shown in Figure 4 for electrospun PHBV filled with ZnONPs. However, all the biopapers also showed several pores in the cross-section, which can be related to the partial evaporation of the oily particles derived from OEO enclosed in the PHBV matrix during the thermal

post-treatment as well as the presence of ZnONP agglomerates. Similar voids, though smaller, were recently observed in electrospun PHBV filled with silica microparticles containing eugenol prepared by Melendez-Rodriguez et al. [58]. The pores were significantly bigger for the PHBV biopaper containing 2.5 wt.% OEO + 2.25 wt.% ZnONPs, shown in Figure 8f, in comparison with the cross-sections of the biopaper samples of PHBV containing 7.5 wt.% OEO + 0.75 wt.% ZnONPs and 5 wt.% OEO + 1.5 wt.% ZnONPs, respectively, which are presented in Figure 8b,d. This observation confirms that the formation of large voids was mainly ascribed to the nanoparticle agglomerates, as previously observed in Figure 7c. On the other hand, Ejaz et al. [46] reported a significant increase in the thickness of gelatin type B films obtained by casting when ZnONPs were incorporated in combination with CEO. Likewise, Castro-Mayorga et al. [59] obtained thicker films after the incorporation of ZnONPs, which was also influenced by the amount and shape of nanoparticles.
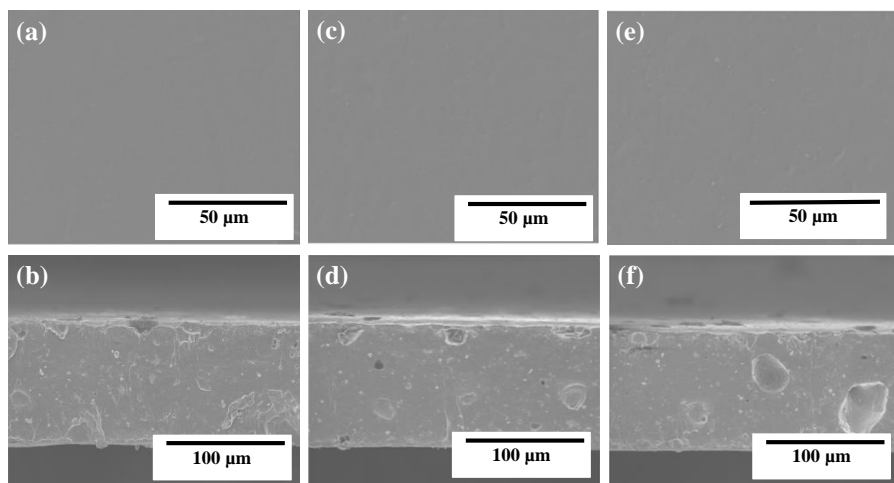
Figure 8. Scanning electron microscopy (SEM) micrographs in top view (top) and cross-section (bottom) of the electrospun biopapers of poly(3-hydroxybutyrate-co-3-hydroxyvalerate) (PHBV) containing different amounts of oregano essential oil (OEO) and zinc oxide nanoparticles (ZnONPs): (**a,b**) PHBV + 7.5 wt.% OEO + 0.75 wt.% ZnONPs; (**c,d**) PHBV + 5 wt.% OEO + 1.5 wt.% ZnONPs; (**e,f**) PHBV + 2.5 wt.% OEO + 2.25 wt.% ZnONPs. Scale markers of 50 μm and 100 μm, respectively.

3.4 Optical Properties of the Electrospun Hybrid PHBV Biopapers

Figure 9 shows the visual aspect of the electrospun PHBV biopapers for evaluating their contact transparency. The effect of the combined addition of OEO and ZnONPs on the color coordinates (L*, a*, b*) and the values of ΔE, T, and O of the electrospun PHBV biopapers are shown in Table 2. The optical properties of the neat PHBV

biopaper and the PHBV biopapers with either 10 wt.% OEO or 3 wt.% ZnONPs were also included for comparison purposes. It can be observed that all PHBV-based biopapers presented contact transparency but the presence of both OEO and ZnONPs reduced brightness and increased opacity, which was measured by the L* and O values, respectively. The biopapers develop a low-intense yellow color when OEO was incorporated, which was confirmed by the increase in the b* coordinate. Transparency was noticeably reduced with the ZnONPs content even though the effect of the nanoparticles on the color change was relatively low. On the opposite side, all the OEO-containing biopapers resulted in samples in which an observer can notice different colors ($\Delta E^* \geq 5$). For instance, the ΔE value of the PHBV biopapers only containing OEO was 8.36, whereas this value for the biopapers only containing ZnONPs was 1.83. Therefore, the biopapers containing OEO and ZnONPs mixtures presented intermediate ΔE values and the color was more affected by the OEO content. Therefore, among the hybrid PHBV biopapers, the highest color change was observed for the PHBV film containing 7.5 wt.% OEO + 0.75 wt.% ZnONPs, that is, 7.64.
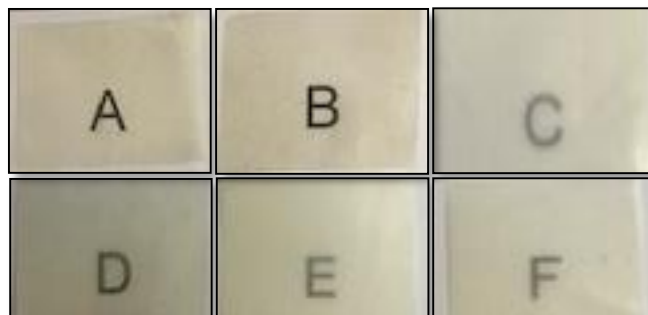
Figure 9. Visual aspect of the electrospun biopapers of poly(3-hydroxybutyrate-co-3-hydroxyvalerate) (PHBV): (**a**) Neat PHBV, (**b**) PHBV + 10 wt.% oregano essential oil (OEO), (**c**) PHBV + 3 wt.% zinc oxide nanoparticles (ZnONPs), (**d**) PHBV + 7.5 wt.% OEO + 0.75 wt.% ZnONPs, (**e**) PHBV + 5 wt.% OEO + 1.5 wt.% ZnO-NPs, and (**f**) PHBV + 2.5 wt.% OEO + 2.25 wt.% ZnONPs.

Table 2. Color parameters and transparency characteristics of the electrospun biopapers of poly(3-hydroxybutyrate-co-3-hydroxyvalerate) (PHBV) containing oregano essential oil (OEO) and zinc oxide nanoparticles (ZnONPs)

Sample	a^*	b^*	L^*	ΔE^*	T	O
PHBV	0.87 ± 0.07[a]	-0.38 ± 0.02[a]	89.82 ± 0.06[a]	---	3.13 ± 0.02[a]	0.016 ± 0.06[a]
PHBV + 10 wt% OEO	1.13 ± 0.05[b]	6.67 ± 0.03[b]	85.35 ± 0.07[b]	8.36 ± 0.08[a]	3.55 ± 0.03[a]	0.019 ± 0.08[a]
PHBV+ 3 wt% ZnONPs	0.56 ± 0.04[a]	-0.96 ± 0.05[c]	88.11 ± 0.06[a]	1.83 ± 0.05[b]	9.60 ± 0.06[b]	0.052 ± 0.05[b]
PHBV+2.5wt% OEO+2.25wt% ZnONPs	-0.92 ± 0.03[c]	4.32 ± 0.02[d]	86.80 ± 0.03[c]	5.87 ± 0.03[c]	8.08 ± 0.04[c]	0.041 ± 0.05[c]
PHBV + 5 wt% OEO + 1.5 wt% ZnONPs	-0.65 ± 0.06[d]	3.14 ± 0.09[e]	84.10 ± 0.07[d]	6.88 ± 0.09[d]	7.17 ± 0.05[d]	0.037 ± 0.05[c]
PHBV + 7.5 wt% OEO + 0.75 wt% ZnONPs	-0.55 ± 0.08[e]	5.35 ± 0.06[f]	84.96 ± 0.06[bd]	7.64 ± 0.08[e]	5.03 ± 0.06[e]	0.027 ± 0.05[d]

L*: Luminosity (+L luminous, −L dark), a*: red/green coordinates (+a red, −a green), b*: yellow/blue coordinates (+b yellow, −b blue), ΔE^*: color difference, T: transparency, and O: Opacity. a–f Different letters in the same column indicate a significant difference ($p < 0.05$).

Table 3. Thermal properties of the zinc oxide nanoparticles (ZnONPs), oregano essential oil (OEO), and electrospun biopapers of poly(3-hydroxybut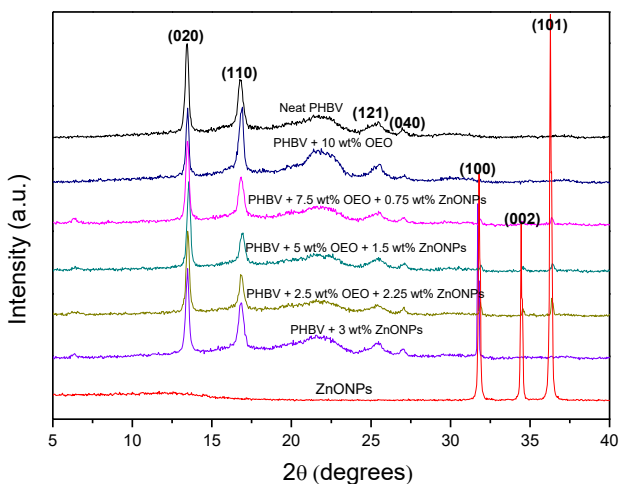yrate-co-3-hydroxyvalerate) (PHBV) containing OEO and ZnONPs in terms of temperature at 5% mass loss ($T_{5\%}$), degradation temperature (T_{deg}), mass loss at T_{deg}, and residual mass at 700 °C

Sample	$T_{5\%}$ (°C)	T_{deg} (°C)	Mass loss (%)	Residual mass (%)
OEO	101.5 ± 2.3	178.4 ± 0.89	74.16 ± 0.6	0.14 ± 0.5
ZnONPs	---	---	0.030 ± 0.5	99.97 ± 1.6
PHBV	251.5 ± 1.6	279.0 ± 1.1	55.23 ± 0.8	2.10 ± 0.7
PHBV + 10 wt% OEO	197.5 ± 2.7	283.6 ± 0.9	69.58 ± 1.0	2.16 ± 1.3
PHBV + 3 wt% ZnONPs	261.7 ± 2.3	275.6 ± 0.8	32.91 ± 1.4	4.35 ± 1.4
PHBV + 2.5 wt% OEO + 2.25 wt% ZnONPs	227.8 ± 2.1	261.4 ± 1.1	33.46 ± 0.7	3.77 ± 1.0
PHBV + 5 wt% OEO + 1.5 wt% ZnONPs	211.8 ± 1.3	263.3 ± 0.9	36.36 ± 1.9	3.44 ± 1.7
PHBV + 7.5 wt% OEO + 0.75 wt% ZnONPs	205.7 ± 1.9	268.9 ± 1.7	38.82 ± 1.5	3.15 ± 0.8

Therefore, the presence of ZnONPs decreased transparency, showing T values from 3.13, for the neat PHBV biopaper, to 9.60, for the PHBV biopaper filled with 3 wt.% ZnONPs. Similarly, it increased opacity, which presented O values from 0.016 to 0.052. Thus, the addition of ZnONPs did not strongly affect the visual color of the samples, but the measurements of these parameters showed statistically significant differences ($p < 0.05$). Moreover, it showed a significantly reduction in the transmission of visible and ultraviolet (UV) light of the electrospun PHBV biopapers by changing the scattering of light. This capacity to block UV light is intrinsically attributed to ZnO, which additionally shows photocatalytic activity [26,76] and can influence the optical properties of films. In this regard, Wang et al. [77] determined that the large ZnO contents in carboxymethyl/chitosan films increased the UV absorption due to the dispersion of light generated by the high crystallinity of this filler. In this regard, films with UV block properties can be of great interest in food packaging for application in photosensitive products.

3.5 Thermal Stability of the Electrospun Hybrid PHBV Biopapers

The weight loss curves of OEO, ZnONPs, and of the electrospun PHBV biopapers obtained by TGA are gathered in Figure 10. The values of the onset degradation temperature, that is, the temperature at 5 % weight loss ($T_{5\%}$), degradation temperature (T_{deg}), and residual mass at 700 °C are summarized in Table 3. One can observe that OEO presented a low thermal stability, which shows values of $T_{5\%}$ and T_{deg} of 101.5 °C and 178.4 °C, respectively, with a respective weight loss of 74.16 % at T_{deg}, corresponding to the volatilization and/or degradation of low-molecular weight (MW) volatile compounds present in the OEO (e.g., carvacrol, thymol, and pinene) [57]. On the opposite end, it can be observed that ZnONPs were thermally stable in the whole range of temperatures tested.

The neat PHBV biopaper was thermally stable up to 251.5 °C, which shows a T_{deg} value of 278.7 °C (47.74 wt %) and a residual mass of 2.10 wt%. These thermal values are relatively similar to those reported for PHBV materials in previous research works [78,79,80], where the thermal decomposition reaction of the biopolymer chain occurred sharply in one single and sharp step from approximately 270 °C to 280 °C. The presence of OEO considerably reduced the onset of degradation of PHBV, which shows a $T_{5\%}$ value of 197.5 °C. The ZnONPs-containing PHBV biopaper showed a higher $T_{5\%}$ value but lower value of Tdeg than the neat PHBV biopaper, which could be attributed to the thermal conductivity and catalytic properties of the ZnONPs. This effect on the thermal properties is similar to that reported by Castro-Mayorga et al. [59] for electrospun PHBV films containing 6 wt.% ZnONPs. All the PHBV biopapers containing the OEO and ZnONPs mixtures

showed a similar thermal decomposition process with a unique degradation stage that started around ~260 °C. Although the values of T_{deg} were reduced, the loss of mass at T_{deg} was smaller compared with those of neat PHBV and OEO-containing PHBV biopapers. This may indicate that ZnONPs delayed the thermal degradation process of PHBV. In this regard, the incorporation of ZnONPs can improve the thermal resistance of polymer materials due to the barrier effect of the nanoparticles that could hinder the transport of decomposition products from the bulk biopolymer matrix. Likewise, the high thermal conductivity of ZnO can also help heat dissipation within the composite, which results in enhanced thermal stability [81]. Furthermore, all the PHBV biopapers showed a residual mass in the range of 2 – 5 %, which increased slightly with the ZnONPs' content.
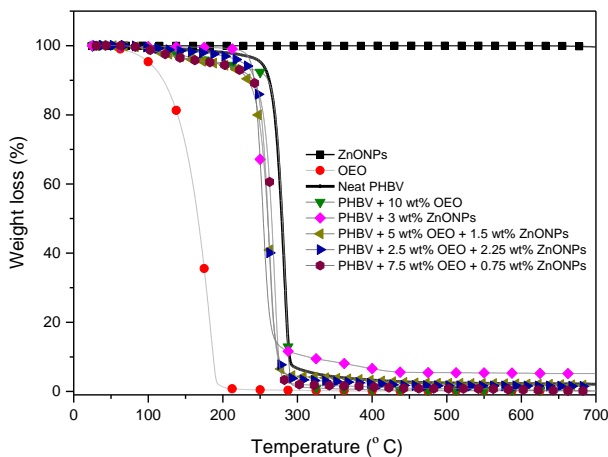
Figure 10. Evolution of weight (%) as a function of temperature of the zinc oxide nanoparticles (ZnONPs), oregano essential oil (OEO), and electrospun biopapers of poly(3-hydroxybutyrate-co-3-hydroxyvalerate) (PHBV) containing OEO and ZnONPs.

## 3.6 Mechanical Properties of the Electrospun Hybrid PHBV Biopapers

Tensile modulus (E), tensile strength at yield (σy), and elongation at break (ϵb) were calculated from the stress–strain curves, estimated from the force (F) vs. distance (d) data. The mechanical properties of the electrospun PHBV-based biopapers are shown in Table 4. The biopaper made of neat PHBV presented an E value of 1125 MPa, a σy value of 12.6 MPa, and a ϵb value of 1.71 %. These results are in the same range than those reported by Melendez-Rodriguez et al. [58] for electrospun films of neat PHBV, where E was 1252 MPa, σy was 18.1 MPa, and ϵb was 2.4 %. The

incorporation of OEO reduced the E value to 814 MPa, which can be ascribed to a plasticizing effect of the oil molecules on the biopolymer matrix, which reduced the intermolecular forces and increased the mobility of the PHBV chains [82]. Thus, it increased both the σy and εb to values of 18 MPa and 4.53 %, respectively, and also toughness from 0.124 mJ/mm3 to 0.560 mJ/mm3. A similar improvement in ductility was reported by Melendez-Rodriguez et al. [58] after the introduction of eugenol in electrospun PHBV films. In relation to ZnONPs, one can observe that the nanoparticles induced a reinforcement on PHBV so that the values of E and σy increased in these film samples to 1286 MPa and 17.1 MPa and, as expected, it resulted in a decrease in ductility showing a value of εb of 1.26 %. Similarly, Díez-Pascual et al. [81] reported a mechanical strength improvement with the addition of ZnONPs in the range of 1 – 5 wt% in PHB, which shows an increase in the E and σy values of up to 43% and 32%, respectively. The reinforcement attained can be influenced by different factors such as load dispersion, the degree of crystallinity of the polymer, and the interfacial adhesion of the nanoparticles to the biopolymer matrix. The electrospun PHBV biopapers containing the OEO and ZnONPs mixtures presented a similar mechanical resistance, which showed E values in the 700 – 900 MPa range. This is very similar to that of the OEO-containing PHBV biopaper, whereas the values of σy remained in the range of 14 – 15 MPa. As the content of OEO in the biopaper increased, the flexibility and toughness of the samples improved. Thus, the electrospun PHBV biopapers containing 7.5 wt.% OEO + 0.75 wt.% ZnONPs showed the lowest E value, that is, 778 MPa, but also the highest εb value, that is, approximately 5 %. In this regard, Ejaz et al. [46] reported a decrease in the σy values and an increase in the εb values for bovine skin gelatin films filled with 2 wt% ZnONPs in combination with cinnamon oil. Chun et al. [83] also found that the addition of silver nanoparticles (AgNPs) and ZnONPs decreased the rigidity and tensile strength of PLA films. This effect was ascribed to a reduction of the biopolymer's MW, which improved the mobility of the PLA chains by a chain-scission process during processing.

3.7   Crystallinity of the Electrospun Hybrid PHBV Biopapers

Wide Angle X-ray Diffraction (WAXD) experiments were conducted on the electrospun biopapers of PHBV to ascertain their crystallinity. The diffractograms are plotted in Figure 11. Most of the characteristic peaks at 2θ of PHBV were clearly detected for the neat PHBV diffractogram, that is, 13.4°, 16.9°, 25.5°, and 27.1°. According to the literature [84], these peaks correspond to the (020), (110), (121), and (040) lattice planes of the orthorhombic unit cells of PHB. The PHB crystal lattice is characteristic for the PHBV with HV contents below 37 % [85]. This is the case of the present PHBV. There were no changes in position of the PHBV diffraction peaks with the addition of OEO or ZnONPs, which suggests that the crystalline structure of PHBV was not altered. One can also observe that ZnONPs presented three main peaks in the studied range, corresponding to the (100), (002), and (101) reflections. The presence of these peaks in the diffractograms of the ZnONPs-containing PHBV sample confirmed the presence of the nanoparticles in the biopaper. The low relative intensity of these peaks in the samples can be attributed to a dilution effect.

Figure 11. Diffractograms of the zinc oxide nanoparticles (ZnONPs) and electrospun biopapers of poly(3-hydroxybutyrate-co-3-hydroxyvalerate) (PHBV) containing oregano essential oil (OEO) and ZnONPs.

3.8 Antimicrobial Activity of the Electrospun Hybrid PHBV Biopapers

Figure 12 gathers the results of antimicrobial activity in an open and closed system, respectively, for 48 days, of the electrospun PHBV biopapers containing different OEO and ZnONP mixtures against the *S. aureus* and *E. coli* strains. The antimicrobial properties of the PHBV biopapers containing OEO 10 wt.% and ZnONPs 3 wt.% are also included for comparison. It can be observed that the OEO-containing PHBV biopaper presented a strong reduction (R $\geq$ 3) for *S. aureus* and a significant reduction (R $\geq$ 1 and < 3) of *E. coli* for 15 days in both systems, which is slightly higher in the closed system. This slight difference between the two tested systems can be attributed to the release and accumulation of volatile OEO compounds into the closed headspace, which contributed to a greater inhibition of bacterial growth. From day 22, however, the inhibition of the PHBV biopaper for both strains decreased significantly due to the complete release of the active volatile compounds, which resulted in a decrease of the active properties of the biopapers. In the case of the PHBV biopapers containing ZnONPs 3 wt.%, the reduction achieved was slightly lower for both bacteria and systems in comparison with that achieved for the OEO-containing PHBV biopapers during the first 15 days. However, it was still strong (R $\geq$ 3) and, interestingly, it also improved during the 48 days of the assay. The strong activity of ZnONPs can be attributed to different mechanisms of action in the presence of moisture, such as the release of Zn^{2+} ions, reactive oxygen species (e.g., superoxide, hydroxyl, and hydrogen peroxide radicals) that are able to penetrate the bacterial wall and cause irreversible damage to the bacterial cellular structure [86]. Therefore, the antibacterial activity can be improved with time as the nanoparticles remained active by contact and due to the high humidity of both systems that favored their release and accumulation on the biopaper surface. It is also worthy to mention that, in all cases, the results obtained showed that the G+ bacteria are more sensitive than G− ones to both OEO and ZnONPs. As reported by other authors, the cell wall structure of *E. coli* is composed mainly of lipopolysaccharides and a thin layer of peptidoglycan that hinders the penetration of negatively charged reactive oxygen species formed by the presence of ZnONPs [87].

Table 4. Mechanical properties of the electrospun biopapers of poly(3-hydroxybutyrate-co-3-hydroxyvalerate) (PHBV) containing oregano essential oil (OEO) and zinc oxide nanoparticles (ZnONPs) in terms of tensile modulus (E), tensile strength at yield (σ_y), elongation at break (ε_b), and toughness

Sample	E (MPa)	σ_y(MPa)	ε_b(%)	Toughness (mJ/mm³)
PHBV	1125 ± 441^a	12.6 ± 2.7^a	1.71 ± 0.35^a	0.124 ± 0.005^a
PHBV + 10 wt% OEO	814 ± 82^b	18.5 ± 0.5^b	4.53 ± 0.41^b	0.560 ± 0.076^b
PHBV + 3 wt% ZnONPs	1286 ± 142^c	17.1 ± 0.9^c	1.26 ± 0.23^c	0.244 ± 0.048^c
PHBV + 2.5 wt% OEO + 2.25 wt% ZnONPs	855 ± 118^d	14.5 ± 2.4^d	3.28 ± 0.32^d	0.303 ± 0.061^d
PHBV + 5 wt% OEO + 1.5 wt% ZnONPs	801 ± 93^b	14.8 ± 4.5^d	4.35 ± 1.28^b	0.446 ± 0.273^e
PHBV + 7.5 wt% OEO + 0.75 wt% ZnONPs	778 ± 102^e	14.1 ± 3.8^d	5.01 ± 1.34^e	0.485 ± 0.249^e

[a–e] Different letters in the same column indicate a significant difference ($p < 0.05$).
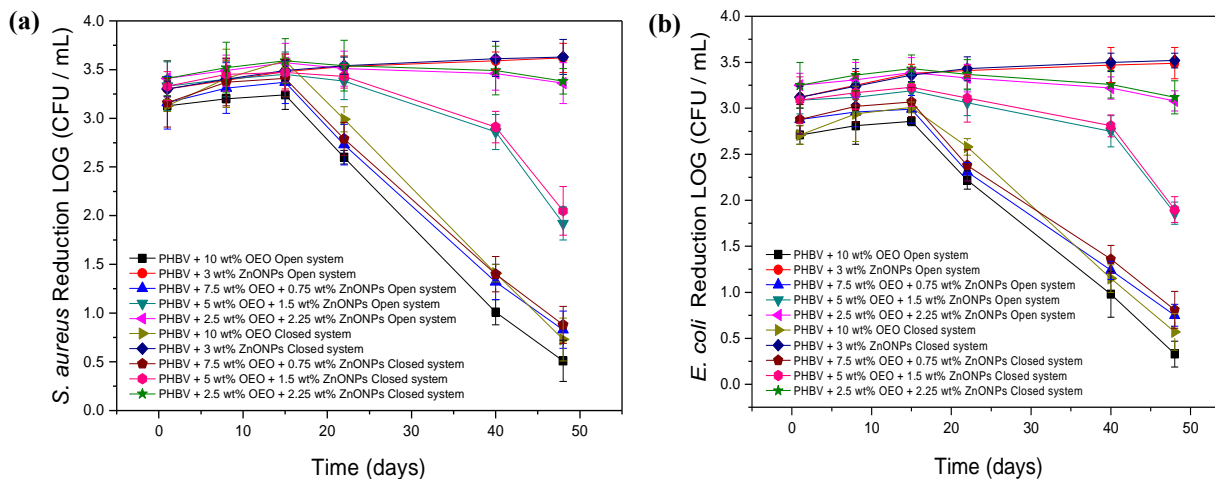
Figure 12. Antimicrobial activity of the electrospun biopapers of poly(3-hydroxybutyrate-co-3-hydroxyvalerate) (PHBV) containing oregano essential oil (OEO) and zinc oxide nanoparticles (ZnONPs) against (**a**) *S. aureus* and (**b**) *E. coli* in the open and closed systems for 48 days.

The electrospun hybrid PHBV biopapers, that is, the fiber-based film samples containing the different mixtures of OEO and ZnONPs, also showed a high antimicrobial activity against both bacterial strains in the two systems. During the first 15 days, that is, in the short term, the PHBV biopaper containing 2.5 wt.% OEO + 2.25 wt.% ZnONPs showed the highest reduction values among the materials tested. The fact that the antimicrobial activity of the hybrid biopaper at this particular composition was even slightly higher than both biopapers based on each antimicrobial agent reveals the synergism attained in the combination of OEO and ZnONPs. This observation suggests that the release of OEO from the PHBV matrix was improved due to the presence of the nanoparticles and/or the antimicrobial effectiveness of the inorganic nanoparticles was enhanced. In the latter case, previous studies have demonstrated that vegetal extract containing polyphenols, such as the tannins, glycosides, and flavonoids, could act as reducing and capping agents [88]. Therefore, the reaction between nanoparticles and the polyphenolic compounds carvacrol and thymol, which are the major constituents of OEO, can potentially improve the antimicrobial activity of ZnONPs. Furthermore, the PHBV biopapers containing 5 wt.% OEO + 1.5 wt.% ZnONPs and 7.5 wt.% OEO + 0.75 wt.% ZnONPs presented intermediate values of reduction but are still strong ($R \geq 3$). Then, both biopapers showed a performance reduction in the antimicrobial activity with time similar to that observed for the OEO-containing PHBV biopaper. On day 48, this reduction was significant ($R \geq 1 < 3$) for the PHBV biopapers containing 5 wt.% OEO + 1.5 wt.% ZnONPs and slight ($R \geq 0.5$ and < 1) in the case of the PHBV biopaper containing 7.5 wt.% OEO + 0.75 wt.% ZnONPs. The time evolution in the antimicrobial activity of the PHBV biopaper containing 2.5 wt.% OEO + 2.25 wt.% ZnONPs was relatively similar to that observed for the PHBV biopaper filled with 3 wt.% ZnONPs, even in the conditions of the open system. Therefore, the strong reduction ($R \geq 3$) observed in the long term of these electrospun hybrid biopapers can be mainly attributed to the ZnONPs presence, which successfully managed to maintain the antimicrobial activity against the two bacterial strains in both systems.

The long-term antimicrobial performance of different nanoparticles has been previously employed to develop different active films. For instance, Emamifar et al. [28] studied the antimicrobial effect of low-density polyethylene (LDPE) films containing TiO_2 95 wt% + AgNPs 5 wt% and ZnONPs. The results showed that the microbial growth rate of *Lactobacillus plantarum* (*L. plantarum*) was significantly reduced for loadings of 1.5–5 wt% and 0.25–1 wt% of TiO_2 + AgNPs and ZnONPs, respectively, during 112 days of study. This points out that the antimicrobial activity of ZnONPs significantly outperforms that of TiO_2 + AgNPs. Chu et al. [83] also achieved a significant reduction of $2 - 3$ Log_{10} CFU/mL in the growth of *E. coli* by

using PLA films containing AgNPs 0.5 wt% and ZnONPs 3 wt% after 12 h of study. Therefore, the relative low content of nanoparticles used in the here-developed hybrid film, that is, 2.25 wt%, represents a technological achievement to develop antimicrobial performance with short-term and long-term performance. In this regard, Ejaz et al. [46] also determined a strong antimicrobial activity of bovine skin gelatin films containing ZnONPs 2 wt% + CEO 50 wt% against *L. monocytogenes* and *S. typhimurium* tested in vitro for 20 days at a refrigerated storage. This result confirms the potential synergism between EOs and nanoparticles, which were able to penetrate through the bacterial cell membrane to alter the cell structure.

3.9 Migration Assessment of the Electrospun Hybrid PHBV Biopapers

The amount of ZnONPs that migrate from the PHBV biopapers were tested in different food simulants. Results showed that a greater amount of zinc was released in the acidic solution than in the alcoholic solution. The amount of zinc migrated from the PHBV-based biopapers increased for the samples with higher concentrations of ZnONPs, which shows values of 1.28 ± 0.58 mg/L (PHBV + 7.5 wt.% OEO + 0.75 wt.% ZnONPs), 3.91 ± 1.64 mg/L (PHBV + 5 wt.% OEO + 1.5 wt.% ZnONPs), 6.05 ± 0.81 mg/L (PHBV + 2.5 wt.% OEO + 2.25 wt.% ZnONPs), and 12.87 ± 2.04 mg/L (PHBV + 3 wt.% ZnONPs). This behavior could be caused by the high solubility of ZnONPs in acetic acid that, on the one hand, triggered a higher release of it in the food simulant and, on the other hand, it can promote partially acidolysis of the polymer. The latter phenomenon could be observed with the naked eye in the PHBV + 3 wt% ZnONPs sample in 3% (wt./vol.) acetic acid. Similar results were reported by the European Food Safety Authority (EFSA) [89] where the migration of zinc uncoated and coated with [3-(methacryloxy)propyl] trimethoxysilane (MEMO) into 3 % acetic acid reached 17.3 mg/kg, whereas, in 10 % ethanol, it reached values up to 80 µg/kg. The amount of zinc released in the alcoholic solution showed values below the limit allowed. In particular, the values obtained were 0.45 ± 0.04 mg/L (PHBV + 7.5 wt.% OEO + 0.75 wt.% ZnONPs), 0.61 ± 0.1 mg/L (PHBV + 2.5 wt.% OEO + 2.25 wt.% ZnONPs), and 0.62 ± 0.2 mg/L (PHBV + 3 wt.% ZnONPs). In light of the above findings, and, according to the current specific migration limit (SML), 5 mg/kg food or food simulant for soluble ionic zinc was set out by the European Plastics Regulation (EU 2016/1416) [90]. The PHBV biopapers containing 3 wt.% ZnONPs and 2.5 wt.% OEO + 2.25. wt.% ZnONPs exceed the current SML value in acid aqueous solutions, whereas the PHBV biopapers containing 5 wt.% OEO + 1.5 wt.% ZnONPs and 7.5 wt.% OEO + 0.75 wt.% ZnONPs comply with the current regulation. In the ethanol aqueous food

simulants, all the tested PHBV biopapers were under the current SML values. This result suggests that the present PHBV-based biopapers can be used as food packaging for alcoholic foods but, for acidic food, biopapers with a concentration above 2.25 % ZnONPs are restricted.

4 Conclusions

The non-renewable origin of most currently used polymers and their lack of biodegradability is behind their excessive carbon and water footprints and also waste management concerns, which results in an increased research interest in the development of more environmentally compatible and economically sustainable packaging materials. Current strategies to solve these problems within Circular Bioeconomy scenarios include the development of biopolymers obtained from agricultural wastes and food processing by-products, the second generation of feedstock, and the application of nanotechnology and active packaging technologies to tailor their properties. In the case of PHAs, their production by mixed cultures derived from biowaste can also represent an opportunity to reduce the costs of the fermentation and downstream processes by the use of a cost-effective raw material. In this research, hybrid submicron fibers of biowaste derived PHBV containing varying amounts of OEO and ZnONPs were successfully developed by electrospinning. The electrospun mats were turned into actual films of ~130 μm by applying a thermal post-treatment at 125 °C. The resultant PHBV-based biopapers exhibited a homogeneous surface even though they also showed some cracks and/or pores due to the partial volatilization of OEO and the presence of ZnONPs agglomerates. The biopapers showed contact transparency, but they also developed a slightly yellow appearance when the OEO was incorporated and a higher opacity with the increase of ZnONPs content. The dual incorporation of OEO and ZnONPs decreased the tensile modulus but positively increased the ductility and toughness of the biopapers, whereas the crystallinity of PHBV was unaffected. The OEO-containing PHBV biopapers showed a strong inhibition for the first 15 days of storage (short-term inhibition). However, it decreased from day 22 due to the complete release of the volatile compounds. Alternatively, the electrospun PHBV biopapers containing ZnONPs showed a high and slightly increasing antimicrobial activity with time for 48 days (long-term inhibition). The electrospun hybrid PHBV biopapers containing 2.5 wt% OEO + 2.25 wt% ZnONPs attained the highest antimicrobial properties in the short term and also high performance in the long term. Lastly, the migration tests performed on the biopaper samples containing ZnONPs revealed that the nanoparticles tend to easily release in acidic solutions due to the partial solubility of PHBV to this medium, whereas they comply with the current SML values for food simulants based on aqueous ethanol (10%). Although the main antimicrobial activity was related to the presence of ZnONPs, their combination with OEO yielded biopapers with high reduction values using lower contents of the inorganic nanoparticles. Furthermore, the presence of the essential oil can also add additional active functionalities such as the previously reported antioxidant activity to extend

shelf-life even further. Therefore, novel antimicrobial biopapers with high potential applications in the food packaging field can be successfully prepared by electrospinning and subsequent annealing of biopolymers incorporating low OEO contents and moderate-to-low ZnONP content. Potential applications of the developed biopapers are foreseen in active food packaging for the protection and preservation of perishable foods.

5   References

1. Mihindukulasuriya, S.D.F.; Lim, L.T. Nanotechnology development in food packaging: A review. *Trends Food Sci. Technol.* **2014**, *40*, 149–167.
2. Singh, A.K.; Srivastava, J.K.; Chandel, A.K.; Sharma, L.; Mallick, N.; Singh, S.P. Biomedical applications of microbially engineered polyhydroxyalkanoates: An insight into recent advances, bottlenecks, and solutions. *Appl. Microbiol. Biotechnol.* **2019**, *103*, 2007–2032.
3. Bugnicourt, E.; Cinelli, P.; Lazzeri, A.; Alvarez, V. Polyhydroxyalkanoate (pha): Review of synthesis, characteristics, processing and potential applications in packaging. *Express Polym. Lett.* **2014**, *8*, 791–808.
4. Lemechko, P.; Le Fellic, M.; Bruzaud, S. Production of poly(3-hydroxybutyrate-co-3-hydroxyvalerate) using agro-industrial effluents with tunable proportion of 3-hydroxyvalerate monomer units. *Int. J. Biol. Macromol.* **2019**, *128*, 429–434.
5. Torres-Giner, S.; Hilliou, L.; Melendez-Rodriguez, B.; Figueroa-Lopez, K.J.; Madalena, D.; Cabedo, L.; Covas, J.A.; Vicente, A.A.; Lagaron, J.M. Melt processability, characterization, and antibacterial activity of compression-molded green composite sheets made of poly(3-hydroxybutyrate-co-3-hydroxyvalerate) reinforced with coconut fibers impregnated with oregano essential oil. *Food Packag. Shelf Life* **2018**, *17*, 39–49.
6. Garcia, C.V.; Shin, G.H.; Kim, J.T. Metal oxide-based nanocomposites in food packaging: Applications, migration, and regulations. *Trends Food Sci. Technol.* **2018**, *82*, 21–31.
7. Domínguez, R.; Barba, F.J.; Gómez, B.; Putnik, P.; Bursać Kovačević, D.; Pateiro, M.; Santos, E.M.; Lorenzo, J.M. Active packaging films with natural antioxidants to be used in meat industry: A review. *Food Res. Int.* **2018**, *113*, 93–101.
8. Figueroa-Lopez, K.J.; Andrade-Mahecha, M.M.; Torres-Vargas, O.L. Spice oleoresins containing antimicrobial agents improve the potential use of bio-composite films based on gelatin. *Food Packag. Shelf Life* **2018**, *17*, 50–56.
9. Robledo, S.N.; Pierini, G.D.; Nieto, C.H.D.; Fernández, H.; Zon, M.A. Development of an electrochemical method to determine phenolic monoterpenes in essential oils. *Talanta* **2019**, *196*, 362–369.
10. Hu, Y.; Zhang, J.; Kong, W.; Zhao, G.; Yang, M. Mechanisms of antifungal and anti-aflatoxigenic properties of essential oil derived from turmeric (*Curcuma longa* L.) on aspergillus flavus. *Food Chem.* **2017**, *220*, 1–8.
11. da Rocha Neto, A.C.; Beaudry, R.; Maraschin, M.; Di Piero, R.M.; Almenar, E. Double-bottom antimicrobial packaging for apple shelf-life extension. *Food Chem.* **2019**, *279*, 379–388.
12. Dutra, T.V.; Castro, J.C.; Menezes, J.L.; Ramos, T.R.; do Prado, I.N.; Machinski, M.; Mikcha, J.M.G.; Filho, B.A.d.A. Bioactivity of oregano (*Origanum vulgare*) essential oil against *Alicyclobacillus* spp. *Ind. Crops Prod.* **2019**, *129*, 345–349.
13. Mechergui, K.; Jaouadi, W.; Coelho, J.P.; Khouja, M.L. Effect of harvest year on production, chemical composition and antioxidant activities of essential oil of oregano (*Origanum vulgare* subsp glandulosum (desf.) ietswaart) growing in north africa. *Ind. Crops Prod.* **2016**, *90*, 32–37.
14. Sari, M.; Biondi, D.M.; Kaâbeche, M.; Mandalari, G.; D'Arrigo, M.; Bisignano, G.; Saija, A.; Daquino, C.; Ruberto, G. Chemical composition, antimicrobial and antioxidant activities of the essential oil of several populations of algerian origanum glandulosum desf. *Flavour Fragr. J.* **2006**, *21*, 890–898.
15. Reyes-Jurado, F.; Cervantes-Rincón, T.; Bach, H.; López-Malo, A.; Palou, E. Antimicrobial activity of mexican oregano (*Lippia berlandieri*), thyme (*Thymus vulgaris*), and mustard (*Brassica nigra*) essential oils in gaseous phase. *Ind. Crops Prod.* **2019**, *131*, 90–95.
16. Leyva-López, N.; Gutiérrez-Grijalva, E.P.; Vazquez-Olivo, G.; Heredia, J.B. Essential oils of oregano: Biological activity beyond their antimicrobial properties. *Molecules* **2017**, *22*, 989.
17. Burt, S. Essential oils: Their antibacterial properties and potential applications in foods—A review. *Int. J. Food Microbiol.* **2004**, *94*, 223–253.
18. Deans, S.G.; Ritchie, G. Antibacterial properties of plant essential oils. *Int. J. Food Microbiol.* **1987**, *5*, 165–180.
19. Santurio, J.M.; Santurio, D.F.; Pozzatti, P.; Moraes, C.; Franchin, P.R.; Alves, S.H. Atividade antimicrobiana dos óleos essenciais de orégano, tomilho e canela frente a sorovares de salmonella enterica de origem avícola. *Ciência Rural* **2007**, *37*, 803–808.
20. Rodríguez-Meizoso, I.; Marin, F.R.; Herrero, M.; Señorans, F.J.; Reglero, G.; Cifuentes, A.; Ibáñez, E. Subcritical water extraction of nutraceuticals with antioxidant activity from oregano. Chemical and functional characterization. *J. Pharm. Biomed. Anal.* **2006**, *41*, 1560–1565.

21. Mechergui, K.; Coelho, J.A.; Serra, M.C.; Lamine, S.B.; Boukhchina, S.; Khouja, M.L. Essential oils of *Origanum vulgare* L. Subsp. Glandulosum (desf.) ietswaart from tunisia: Chemical composition and antioxidant activity. *J. Sci. Food Agric.* **2010**, *90*, 1745–1749.

22. Kulisic, T.; Radonic, A.; Katalinic, V.; Milos, M. Use of different methods for testing antioxidative activity of oregano essential oil. *Food Chem.* **2004**, *85*, 633–640.

23. Kulkarni, S.B.; Patil, U.M.; Salunkhe, R.R.; Joshi, S.S.; Lokhande, C.D. Temperature impact on morphological evolution of ZnO and its consequent effect on physico-chemical properties. *J. Alloys Compd.* **2011**, *509*, 3486–3492.

24. Özgür, U.; Alivov, Y.I.; Liu, C.; Teke, A.; Reshchikov, M.A.; Doğan, S.; Avrutin, V.; Ch, S.J.; Morkoç, H. A comprehensive review of ZnO materials and devices. *J. Appl. Phys.* **2005**, *98*, 11.

25. Moezzi, A.; McDonagh, A.M.; Cortie, M.B. Zinc oxide particles: Synthesis, properties and applications. *Chem. Eng. J.* **2012**, *185–186*, 1–22.

26. Jones, N.; Ray, B.; Ranjit, K.T.; Manna, A.C. Antibacterial activity of ZnO nanoparticle suspensions on a broad spectrum of microorganisms. *FEMS Microbiol. Lett.* **2008**, *279*, 71–76.

27. Bradley, E.L.; Castle, L.; Chaudhry, Q. Applications of nanomaterials in food packaging with a consideration of opportunities for developing countries. *Trends Food Sci. Technol.* **2011**, *22*, 604–610.

28. Emamifar, A.; Kadivar, M.; Shahedi, M.; Soleimanian-Zad, S. Effect of nanocomposite packaging containing ag and ZnO on inactivation of lactobacillus plantarum in orange juice. *Food Control* **2011**, *22*, 408–413.

29. Espitia, P.J.P.; Soares, N.d.F.F.; Coimbra, J.S.d.R.; de Andrade, N.J.; Cruz, R.S.; Medeiros, E.A.A. Zinc oxide nanoparticles: Synthesis, antimicrobial activity and food packaging applications. *Food Bioprocess Technol.* **2012**, *5*, 1447–1464.

30. Turner, S.; Tavernier, S.M.F.; Huyberechts, G.; Biermans, E.; Bals, S.; Batenburg, K.J.; Van Tendeloo, G. Assisted spray pyrolysis production and characterisation of ZnO nanoparticles with narrow size distribution. *J. Nanopart. Res.* **2010**, *12*, 615–622.

31. Johar Abdullah, M.; Putrus, G.A.; Chong, J.; Karim Mohamad, A. Nanostructure of ZnO fabricated via french process and its correlation to electrical properties of semiconducting varistor. *Synth. React. Inorg. Metal Org. Nano Metal Chem.* **2006**, *36*, 155–159.

32. Eskandari, M.; Haghighi, N.; Ahmadi, V.; Haghighi, F.; Mohammadi, S.R. Growth and investigation of antifungal properties of ZnO nanorod arrays on the glass. *Phys. B Condens. Matter* **2011**, *406*, 112–114.

33. Sawai, J.; Yoshikawa, T. Quantitative evaluation of antifungal activity of metallic oxide powders (MgO, CaO and ZnO) by an indirect conductimetric assay. *J. Appl. Microbiol.* **2004**, *96*, 803–809.

34. Zhang, L.; Jiang, Y.; Ding, Y.; Daskalakis, N.; Jeuken, L.; Povey, M.; O'Neill, A.J.; York, D.W. Mechanistic investigation into antibacterial behaviour of suspensions of ZnO nanoparticles against *E. coli*. *J. Nanopart. Res.* **2010**, *12*, 1625–1636.

35. Kumar, R.; Umar, A.; Kumar, G.; Nalwa, H.S. Antimicrobial properties of ZnO nanomaterials: A review. *Ceram. Int.* **2017**, *43*, 3940–3961.

36. Ramani, M.; Ponnusamy, S.; Muthamizhchelvan, C.; Cullen, J.; Krishnamurthy, S.; Marsili, E. Morphology-directed synthesis of ZnO nanostructures and their antibacterial activity. *Coll. Surf. B Biointerfaces* **2013**, *105*, 24–30.

37. Jain, A.; Bhargava, R.; Poddar, P. Probing interaction of gram-positive and gram-negative bacterial cells with ZnO nanorods. *Mater. Sci. Eng. C* **2013**, *33*, 1247–1253.

38. Shinde, V.V.; Dalavi, D.S.; Mali, S.S.; Hong, C.K.; Kim, J.H.; Patil, P.S. Surfactant free microwave assisted synthesis of ZnO microspheres: Study of their antibacterial activity. *Appl. Surf. Sci.* **2014**, *307*, 495–502.

39. Stanković, A.; Dimitrijević, S.; Uskoković, D. Influence of size scale and morphology on antibacterial properties of ZnO powders hydrothemally synthesized using different surface stabilizing agents. *Coll. Surf. B Biointerfaces* **2013**, *102*, 21–28.

40. Ng, Y.H.; Leung, Y.H.; Liu, F.Z.; Ng, A.M.C.; Gao, M.H.; Chan, C.M.N.; Djurišić, A.B.; Leung, F.C.C.; Chan, W.K. Antibacterial activity of ZnO nanoparticles under ambient illumination—The effect of nanoparticle properties. *Thin Solid Films* **2013**, *542*, 368–372.

41. Malini, M.; Thirumavalavan, M.; Yang, W.-Y.; Lee, J.-F.; Annadurai, G. A versatile chitosan/ZnO nanocomposite with enhanced antimicrobial properties. *Int. J. Biol. Macromol.* **2015**, *80*, 121–129.

42. Kickelbick, G. Concepts for the incorporation of inorganic building blocks into organic polymers on a nanoscale. *Prog. Polym. Sci.* **2003**, *28*, 83–114.

43. Bumbudsanpharoke, N.; Choi, J.; Park, H.J.; Ko, S. Zinc migration and its effect on the functionality of a low density polyethylene-ZnO nanocomposite film. *Food Packag. Shelf Life* **2019**, *20*, 100301.

44. Mo, Z.; Lin, J.; Zhang, X.; Fan, Y.; Xu, X.; Xue, Y.; Liu, D.; Li, J.; Hu, L.; Tang, C. Morphology controlled synthesis zinc oxide and reinforcement in polyhydroxyalkanoates composites. *Polym. Compos.* **2014**, *35*, 1701–1706.

45. Heydari-Majd, M.; Ghanbarzadeh, B.; Shahidi-Noghabi, M.; Najafi, M.A.; Hosseini, M. A new active nanocomposite film based on PLA/ZnO nanoparticle/essential oils for the preservation of refrigerated otolithes ruber fillets. *Food Packag. Shelf Life* **2019**, *19*, 94–103.

46. Ejaz, M.; Arfat, Y.A.; Mulla, M.; Ahmed, J. Zinc oxide nanorods/clove essential oil incorporated type b gelatin composite films and its applicability for shrimp packaging. *Food Packag. Shelf Life* **2018**, *15*, 113–121.

47. Wu, H.; Lei, Y.; Zhu, R.; Zhao, M.; Lu, J.; Xiao, D.; Jiao, C.; Zhang, Z.; Shen, G.; Li, S. Preparation and characterization of bioactive edible packaging films based on pomelo peel flours incorporating tea polyphenol. *Food Hydrocoll.* **2019**, *90*, 41–49.

48. Chen, H.; Li, L.; Ma, Y.; McDonald, T.P.; Wang, Y. Development of active packaging film containing bioactive components encapsulated in β-cyclodextrin and its application. *Food Hydrocoll.* **2019**, *90*, 360–366.

49. Al-Jumaili, A.; Mulvey, P.; Kumar, A.; Prasad, K.; Bazaka, K.; Warner, J.; Jacob, M.V. Eco-friendly nanocomposites derived from geranium oil and zinc oxide in one step approach. *Sci. Rep.* **2019**, *9*, 5973.

50. Sani, I.K.; Pirsa, S.; Tağı, Ş. Preparation of chitosan/zinc oxide/melissa officinalis essential oil nano-composite film and evaluation of physical, mechanical and antimicrobial properties by response surface method. *Polym. Test.* **2019**, *79*, 106004.

51. Ahmed, J.; Mulla, M.; Jacob, H.; Luciano, G.; T.B., B.; Almusallam, A. Polylactide/poly(ε-caprolactone)/zinc oxide/clove essential oil composite antimicrobial films for scrambled egg packaging. *Food Packag. Shelf Life* **2019**, *21*, 100355.

52. Torres-Giner, S.; Pérez-Masiá, R.; Lagaron, J.M. A review on electrospun polymer nanostructures as advanced bioactive platforms. *Polym. Eng. Sci.* **2016**, *56*, 500–527.

53. Torres-Giner, S.; Martinez-Abad, A.; Lagaron, J.M. Zein-based ultrathin fibers containing ceramic nanofillers obtained by electrospinning. II. Mechanical properties, gas barrier, and sustained release capacity of biocide thymol in multilayer polylactide films. *J. Appl. Polym. Sci.* **2014**, *131*, 9270–9276.

54. Quiles-Carrillo, L.; Montanes, N.; Lagaron, J.M.; Balart, R.; Torres-Giner, S. Bioactive multilayer polylactide films with controlled release capacity of gallic acid accomplished by incorporating electrospun nanostructured coatings and interlayers. *Appl. Sci.* **2019**, *9*, 533.

55. Torres-Giner, S. Novel antimicrobials obtained by electrospinning methods. In *Antimicrobial Polymers*; John Wiley & Sons, Inc.: Hoboken, NJ, USA, 2011; pp. 261–285.

56. Cherpinski, A.; Torres-Giner, S.; Cabedo, L.; Lagaron, J.M. Post-processing optimization of electrospun submicron poly(3-hydroxybutyrate) fibers to obtain continuous films of interest in food packaging applications. *Food Addit. Contam. Part A Chem. Anal. Control Expo. Risk Assess.* **2017**, *34*, 1817–1830.

57. Figueroa-Lopez, K.J.; Vicente, A.A.; Reis, M.A.M.; Torres-Giner, S.; Lagaron, J.M. Antimicrobial and antioxidant performance of various essential oils and natural extracts and their incorporation into biowaste derived poly(3-hydroxybutyrate-co-3-hydroxyvalerate) layers made from electrospun ultrathin fibers. *Nanomaterials* **2019**, *9*, 144.

58. Melendez-Rodriguez, B.; Figueroa-Lopez, K.J.; Bernardos, A.; Martínez-Máñez, R.; Cabedo, L.; Torres-Giner, S.; Lagaron, J.M. Electrospun antimicrobial films of poly(3-hydroxybutyrate-co-3-hydroxyvalerate) containing eugenol essential oil encapsulated in mesoporous silica nanoparticles. *Nanomaterials* **2019**, *9*, 227.

59. Castro-Mayorga, J.L.; Fabra, M.J.; Pourrahimi, A.M.; Olsson, R.T.; Lagaron, J.M. The impact of zinc oxide particle morphology as an antimicrobial and when incorporated in poly(3-hydroxybutyrate-*co*-3-hydroxyvalerate) films for food packaging and food contact surfaces applications. *Food Bioprod. Process.* **2017**, *101*, 32–44.

60. Enescu, D.; Cerqueira, M.A.; Fucinos, P.; Pastrana, L.M. Recent advances and challenges on applications of nanotechnology in food packaging. A literature review. *Food Chem. Toxicol.* **2019**, *134*, 110814.

61. Melendez-Rodriguez, B.; Castro-Mayorga, J.L.; Reis, M.A.M.; Sammon, C.; Cabedo, L.; Torres-Giner, S.; Lagaron, J.M. Preparation and characterization of electrospun food biopackaging films of poly(3-hydroxybutyrate-*co*-3-hydroxyvalerate) derived from fruit pulp biowaste. *Front. Sustain. Food Syst.* **2018**, *2*, 38.

62. Figueroa-Lopez, K.J.; Andrade-Mahecha, M.M.; Torres-Varga, O.L. Development of antimicrobial biocomposite films to preserve the quality of bread. *Molecules* **2018**, *23*, 212.

63. Agüero, A.; Morcillo, M.d.C.; Quiles-Carrillo, L.; Balart, R.; Boronat, T.; Lascano, D.; Torres-Giner, S.; Fenollar, O. Study of the influence of the reprocessing cycles on the final properties of polylactide pieces obtained by injection molding. *Polymers* **2019**, *11*, 1908.

64. Figueroa-Lopez, K.J.; Castro-Mayorga, J.L.; Andrade-Mahecha, M.M.; Cabedo, L.; Lagaron, J.M. Antibacterial and barrier properties of gelatin coated by electrospun polycaprolactone ultrathin fibers containing black pepper oleoresin of interest in active food biopackaging applications. *Nanomaterials* **2018**, *8*, 199.

65. Torres-Giner, S.; Torres, A.; Ferrándiz, M.; Fombuena, V.; Balart, R. Antimicrobial activity of metal cation-exchanged zeolites and their evaluation on injection-molded pieces of bio-based high-density polyethylene. *J. Food Saf.* **2017**, *37*, e12348.

66. Naphade, R.; Jog, J. Electrospinning of phbv/ZnO membranes: Structure and properties. *Fibers Polym.* **2012**, *13*, 692–697.

67. Ogunyemi, S.O.; Abdallah, Y.; Zhang, M.; Fouad, H.; Hong, X.; Ibrahim, E.; Masum, M.M.I.; Hossain, A.; Mo, J.; Li, B. Green synthesis of zinc oxide nanoparticles using different plant extracts and their antibacterial activity against *Xanthomonas oryzae* pv. oryzae. *Artif. Cells Nanomed. Biotechnol.* **2019**, *47*, 341–352.

68. Castilho, P.C.; Savluchinske-Feio, S.; Weinhold, T.S.; Gouveia, S.C. Evaluation of the antimicrobial and antioxidant activities of essential oils, extracts and their main components from oregano from Madeira island, Portugal. *Food Control* **2012**, *23*, 552–558.

69. Salah, N.; Al-Shawafi, W.M.; Alshahrie, A.; Baghdadi, N.; Soliman, Y.M.; Memic, A. Size controlled, antimicrobial ZnO nanostructures produced by the microwave assisted route. *Mater.Sci. Eng. C* **2019**, *99*, 1164–1173.

70. Kaushik, M.; Niranjan, R.; Thangam, R.; Madhan, B.; Pandiyarasan, V.; Ramachandran, C.; Oh, D.-H.; Venkatasubbu, G.D. Investigations on the antimicrobial activity and wound healing potential of ZnO nanoparticles. *Appl. Surf. Sci.* **2019**, *479*, 1169–1177.

71. Yang, T.; Oliver, S.; Chen, Y.; Boyer, C.; Chandrawati, R. Tuning crystallization and morphology of zinc oxide with polyvinylpyrrolidone: Formation mechanisms and antimicrobial activity. *J. Coll. Interface Sci.* **2019**, *546*, 43–52.

72. Padmavathy, N.; Vijayaraghavan, R. Enhanced bioactivity of ZnO nanoparticles—An antimicrobial study. *Sci. Technol. Adv. Mater.* **2008**, *9*, 035004.

73. Mousavi, S.; Shahraki, F.; Aliabadi, M.; Haji, A.; Deuber, F.; Adlhart, C. Nanofiber immobilized ceo2/dendrimer nanoparticles: An efficient photocatalyst in the visible and the uv. *Appl. Surf. Sci.* **2019**, *479*, 608–618.

74. Cherpinski, A.; Gozutok, M.; Sasmazel, H.T.; Torres-Giner, S.; Lagaron, J.M. Electrospun oxygen scavenging films of poly(3-hydroxybutyrate) containing palladium nanoparticles for active packaging applications. *Nanomaterials* **2018**, *8*, 469.

75. Ding, X.; Li, Y.; Si, Y.; Yin, X.; Yu, J.; Ding, B. Electrospun polyvinylidene fluoride/sio2 nanofibrous membranes with enhanced electret property for efficient air filtration. *Compos. Commun.* **2019**, *13*, 57–62.

76. Serrà, A.; Zhang, Y.; Sepúlveda, B.; Gómez, E.; Nogués, J.; Michler, J.; Philippe, L. Highly active ZnO-based biomimetic fern-like microleaves for photocatalytic water decontamination using sunlight. *Appl. Catal. B Environ.* **2019**, *248*, 129–146.

77. Wang, H.; Gong, X.; Miao, Y.; Guo, X.; Liu, C.; Fan, Y.Y.; Zhang, J.; Niu, B.; Li, W. Preparation and characterization of multilayer films composed of chitosan, sodium alginate and carboxymethyl chitosan-ZnO nanoparticles. *Food Chem.* **2019**, *283*, 397–403.

78. Ten, E.; Turtle, J.; Bahr, D.; Jiang, L.; Wolcott, M. Thermal and mechanical properties of poly(3-hydroxybutyrate-co-3-hydroxyvalerate)/cellulose nanowhiskers composites. *Polymer* **2010**, *51*, 2652–2660.

79. Fabra, M.J.; Lopez-Rubio, A.; Lagaron, J.M. Nanostructured interlayers of zein to improve the barrier properties of high barrier polyhydroxyalkanoates and other polyesters. *J. Food Eng.* **2014**, *127*, 1–9.

80. Ke, Y.; Qu, Z.; Wu, G.; Wang, Y. Thermal and in vitro degradation properties of the nh2-containing phbv films. *Polym. Degrad. Stab.* **2014**, *105*, 59–67.

81. Díez-Pascual, A.M.; Díez-Vicente, A.L. Poly(3-hydroxybutyrate)/ZnO bionanocomposites with improved mechanical, barrier and antibacterial properties. *Int. J. Mol. Sci.* **2014**, *15*, 10950–10973.

82. Tongnuanchan, P.; Benjakul, S.; Prodpran, T. Physico-chemical properties, morphology and antioxidant activity of film from fish skin gelatin incorporated with root essential oils. *J. Food Eng.* **2013**, *117*, 350–360.

83. Chu, Z.; Zhao, T.; Li, L.; Fan, J.; Qin, Y. Characterization of antimicrobial poly (lactic acid)/nano-composite films with silver and zinc oxide nanoparticles. *Materials* **2017**, *10*, 659.

84. Marschessault, R.H.; Monasterios, C.J.; Morin, F.G.; Sundararajan, P.R. Chiral poly(β-hydroxyalkanoates): An adaptable helix influenced by the alkane side-chain. *Int. J. Biol. Macromol.* **1990**, *12*, 158–165.

85. Skrbić, Z.; Divjaković, V. Temperature influence on changes of parameters of the unit cell of biopolymer phb. *Polymer* **1996**, *37*, 505–507.

86. Rodríguez-Tobías, H.; Morales, G.; Grande, D. Comprehensive review on electrospinning techniques as versatile approaches toward antimicrobial biopolymeric composite fibers. *Mater. Sci. Eng. C* **2019**, *101*, 306–322.

87. Amna, T.; Hassan, M.S.; Barakat, N.A.M.; Pandeya, D.R.; Hong, S.T.; Khil, M.-S.; Kim, H.Y. Antibacterial activity and interaction mechanism of electrospun zinc-doped titania nanofibers. *Appl. Microbiol. Biotechnol.* **2012**, *93*, 743–751.

88. Saha, R.; Subramani, K.; Petchi Muthu Raju, S.A.K.; Rangaraj, S.; Venkatachalam, R. Psidium guajava leaf extract-mediated synthesis of ZnO nanoparticles under different processing parameters for hydrophobic and antibacterial finishing over cotton fabrics. *Prog. Org. Coat.* **2018**, *124*, 80–91.

89. EFSA Panel on Food Contact Materials, Enzymes, Flavourings and Processing Aids (CEF). Scientific opinion on the safety evaluation of the substance zinc oxide, nanoparticles, uncoated and coated with [3-(methacryloxy)propyl] trimethoxysilane, for use in food contact materials. *EFSA J.* **2015**, *13*, 4063.

90. European Commission (EC). *Commission Regulation (EU): Plastic Materials and Articles Intended to Come Into Contact with Food 2016/1416*; European Commission: Brussels, Belgium, **2016**; Volume 2019.
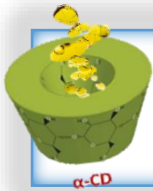
CHAPTER IV

Development of electrospun active films of poly(3-hydroxybutyrate-co-3-hydroxyvalerate) by the incorporation of cyclodextrin inclusion complexes containing oregano essential oil

K. J. Figueroa-Lopez, D. Enescu, S. Torres-Giner, L. Cabedo, M. A. Cerqueira, L. Pastrana, P. Fuciños, J.M. Lagaron

Development of electrospun active films of poly(3-hydroxybutyrate-co-3-hydroxyvalerate) by the incorporation of cyclodextrin inclusion complexes containing oregano essential oil

Abstract

This paper reports the development of biodegradable active packaging films of poly(3-hydroxybutyrate-co-3-hydroxyvalerate) (PHBV) by the incorporation of alpha- and gamma-cyclodextrins (α-CD and γ-CDs) containing oregano essential oil (OEO). Herein, both the kneading method (KM) and freeze-drying method (FDM) were first explored for the preparation of α-CD:OEO and γ-CD:OEO inclusion complexes at host:guest ratios of 80:20 wt/wt and 85:15 wt/wt, respectively. The results showed that KM was the most efficient method for the encapsulation of OEO in the CDs cavity in terms of simplicity and rapidity, while it was also yielded the inclusion complexes with the highest antimicrobial and antioxidant performance. The α-CD:OEO and γ-CD:OEO inclusion complexes obtained by KM were thereafter incorporated at 10, 15, 20, 25, and 30 wt% into PHBV fibres by electrospinning and annealed at 160 ºC to produce contact transparent films. It was observed that the optimal concentration of α-CD:OEO and γ-CD:OEO inclusion complexes for homogeneous and continuous film formation was attainad at contents of 15 and 25 wt%, respectively. Higher antimicrobial and antioxidant activities were obtained for the γ-CD:OEO inclusion complexes due to the greater encapsulation efficiency of OEO in γ-CD, resulting in PHBV films with good performance for up to 15 days. This aspect, together with their improved thermal stability and mechanical strength, give interesting applications to these biopolymer films in the design of active-releasing packaging materials to maintain the physical, chemical, and microbiological characteristics of food products.

1   Introduction

Essential oils (EOs) are mixtures of volatile organic compounds obtained from aromatic plants that are well known for their fragrant properties. They are also used in food preservation and as antimicrobial, analgesic, sedative, anti-inflammatory, spasmolytic, and locally anaesthetic remedies [1,2]. Their mechanisms of active action, particularly at the antimicrobial level, have been well reported [3,4]. The global market of EOs was 226.9 kton/year in 2018 [5] while approximately 160 ones are considered as Generally Recognized as Safe (GRAS) by the U.S. Food and Drug Administration (FDA). Therefore, their application is currently growing in the food and beverage, personal care & cosmetics, aromatherapy, and pharmaceutical industries [6-9].

Among EOs, oregano essential oil (OEO) is one of the most interesting since it is FDA approved and it is also included by the Council of Europe in the list of chemical flavourings that may be added to foodstuffs [10]. In particular, OEO contains a mixture of bioactive related components such as carvacrol and thymol that can be used as antioxidant and antimicrobial agents for active packaging purposes [11]. However, the incorporation of OEO into a food packaging material is a challenging task due to several factors such as potent flavour changes, variations of the sensory perception as a consequence of oxidation, high volatility, chemical instability, low solubility in aqueous systems, etc. [12]. In particular, OEO can evaporate easily and decompose and oxidize during formulation, processing, and storage due to exposure to heat, pressure, light or oxygen [13,14]. These inconveniences can be effectively minimized by encapsulation processes in different systems such as films, capsules, liposomes or inclusion complexes [15,16,17]. Encapsulation allows creating a physical barrier between the core and the wall materials to protect OEO from the external medium (moisture, heat, light, etc.) and, thus, it enhances stability and maintains bioactivity [18].

Cyclodextrins (CDs) are cyclic oligosaccharide consisting of six, that is, alpha-cyclodextrin (α-CD), seven, that is, beta-cyclodextrin (β-CD) or eight, that is, gamma-cyclodextrin (γ-CD) glucopyranose units modified starch molecules shaped like a hollow truncated cone [19]. CDs are fairly water soluble, however β-CD shows remarkably lower solubility than α-CD and γ-CD. During crystallization in an aqueous medium, some molecules of water are entrapped into the CD cavity whereas other molecules of water are present as integral parts of the crystal structure, the so-called crystal water. CDs inclusion complexes are formed by the substitution of the water molecules of the CD cavity by the appropriate guest molecule [20,21]. These inclusion complexes can be used to encapsulate different compounds since CDs cannot only stabilize the compound encapsulated against the degradation

mechanisms triggered by environmental conditions, but they also can reduce the sensory changes by masking strong flavours [16,21]. Furthermore, the CDs can also offer a controlled and sustained release of aromatic substances [16,22]. In addition, the CDs are inert and do not interfere with the biological properties of EOs [19,23]. They are additionally relatively cost-effective, biodegradable, do not pose a significant safety concern, and encapsulation can be performed both in solution and solid-state [15]. Several procedures have been developed to prepare CDs-based inclusion complexes, for instance the kneading method (KM), the co-precipitation, the heating in a sealed container, the freeze-drying method (FDM), the spray drying, and the supercritical fluid technology [24]. The EOs are thermolabile substances sensitive to the effects of light, oxygen, humidity and high temperatures and can be lost activity. It is for this reason that the electrospinning encapsulation technology has been used for the protection, stabilization, solubilization and delivery of the active substances [25]. In this regard, the electrospinning process is a novel technology that produces ultrathin fibrous mats made of a wide range of polymers and biopolymers with fibre diameters ranging from several nanometres to a few microns [26]. This technique is highly suitable for the nanoencapsulation of active and bioactive substances, which is the case of EOs, due to both the high surface-to-volume ratios of the electrospun materials and the high porosity of their mats [27,28]. Furthermore, it allows processing volatile substances such as EOs because the process is performed at room temperature [29]. The resultant electrospun fibres can be potentially applied in sustainable food packaging applications [30] either in the form of coatings or interlayers with bioplastic films [31,32]. Moreover, the electrospun mats can be subjected to a thermal post-treatment, also called annealing, by which they form mechanically strong and transparent films with little porosity due to the fibres coalescence [33]. According to the advantages described above, electrospinning has been recently employed to produce multi-functional fibres from different biopolymers [25], such as polyhydroxyalkanoates (PHAs), that are biodegradable microbial polyesters [34]. Indeed, PHAs are excellent candidates for food packaging applications due to their resistance to water, low oxygen permeability, thermoplastic processability, and good physical and mechanical properties [35].

In this context, the aim of this research work was first to encapsulate OEO into α- and γ-CDs and the resultant inclusion complexes were incorporated into poly(3-hydroxybutyrate-*co*-3-hydroxyvalerate) (PHBV) fibres by electrospinning. The PHBV electrospun mats containing the α-CD:OEO and γ-CD:OEO inclusion complexes were subjected to annealing develop transparent films with improved antioxidant and antimicrobial activity that can be of interest in the design of biodegradable active packaging to extend the shelf life of food products.

2 Materials and Methods

2.1 Materials

OEO with a purity >99 % and a density of 0.925 – 0.955 g/mL was obtained from Gran Velada S.L. (Zaragoza, Spain) and it was processed as received. Wacker Chemie AG (Munich, Germany) supplied the two food-grade cyclodextrin (CDs): α-CD, known as the trademark - CAVAMAX® W6 FOOD with molecular (M_W) of 972.84 g/mol and γ-CD, known as the trademark - CAVAMAX® W8 FOOD with M_W of 1297 g/mol. Their respective empirical formulas are $C_{36}H_{60}O_{30}$ and $C_{48}H_{80}O_{40}$ while further details are gathered in Table 1. Commercial PHBV was ENMAT™ Y1000P, produced by Tianan Biologic Materials (Ningbo, China) and delivered in the form of pellets by Nature Plast (Ifs, France). According to the manufacturer, this biopolymer resin presents a density of 1.23 g/cm³ and a melt flow index (MFI) of 5 – 10 g/10 min (190 ºC, 2.16 Kg). The 3HV fraction in the copolyester is 2 – 3 mol.-%. 2,2,2-trifluoroethanol (TFE), ≥99% purity and 2,2-diphenyl-1-picrylhydrazyl radical (DPPH) were purchased from Sigma Aldrich S.A. (Madrid, Spain). Ethanol, analytical grade with a purity of 99.8%, was supplied by Sigma-Aldrich. Water Milli-Q® was obtained using a Millipore purification system (resistivity > 18.2 MΩ·cm at 25 ºC).

Table 1. Molecular dimensions and physical properties of α- and γ-cyclodextrins (CDs) [21]

Type of cyclodextrin	Nº of Glucose units	Molecular weight (g/mol)	Molecular Dimensions (Å)			Solubility at 25 ºC (g/100 mL H_2O)
			Inside diameter	Outside diameter	Height	
α	6	973	5.7	13.7	7.0	14.50
β	7	1135	7.8	15.3	7.0	1.85
γ	8	1297	9.5	16.9	7.0	23.20

2.2 Preparation of Inclusion complexes

2.2.1 Freeze Drying Method (FDM)

The preparation of the inclusion complexes by FDM was carried out according to Santos et al. [36]. The selected weight ratios between host: guest (α-CD:OEO or γ-CD:OEO) were 80:20 wt/wt and 85:15 wt/wt based on the maximum encapsulation efficiency reported by Petrovi et al. [37] and Haloci et al. [38]. To this end, α-CD or γ-CD was dissolved in 2.5 mL of distilled water, then was added OEO and the resultant mixture was magnetically stirred at 250 rpm in a sealed container for 48 h at room temperature (25 ºC) to allow complex formation. Paraffin film and aluminium foil was used to prevent loss of volatiles and to protect the samples from

the light. The suspensions were then frozen first at -20 ºC for 24 h and then at -80 ºC for 24 h and finally lyophilized at -50 ºC and 0.1 mbar in a Freeze Dryer (LyoQuest -55 Plus Eco Telstar® Life Science solutions, Hampton, VA, USA) until the water was sublimated (approximately 48 h). The freeze-dried IC was weighed, sealed, and stored at -20 ºC.

2.2.2 Kneading Method (KM)

The preparation of the inclusion complexes by the KM was carried out according to Santos et al. [36] and Hedges [39]. For this, α-CD or γ-CD was dissolved in 0.25 mL of distilled water, after which it was added OEO and kneaded thoroughly in a mortar and pestle for 18 min until a homogenous blend was obtained. The weight ratios OEO:α-CD or α-CD and γ-CD γ-CD were the same as that used at FDM (that is, 20:80 w/w and 15:85 w/w, respectively). The kneaded inclusion complexes (pasty mass) obtained was dried in a desiccator under vacuum for 48 h at room temperature (25 ºC) and then weighed, sealed, and stored at -20 ºC.

2.3 Characterization of the Inclusion Complexes

2.3.1 Encapsulation Efficiency and Loading Capacity

First of all, 10 mg of each type of inclusion complexes (α-CD:OEO and γ-CD:OEO at 80:20 and 15:85 weight ratios), were dispersed in 10 mL of absolute ethanol and stirred for 30 min in an Eppendorf mixer device (ThermoMixer™ C, Fisher Scientific®, Hampton, VA, USA) at 1000 rpm to allow the entrapped OEO in the CD cavity to be released to the solution for analysis. Then, the solution obtained was sonicated in an ultrasonic bath for 30 min at 37 kHz and 90 W at room temperature and, thereafter, centrifuged for 30 min at 2500 rpm to remove any CD from the solution. This resulted in a solution with a supernatant containing the OEO, which was used for analysis. The OEO content was determined spectrophotometrically (Ultraviolet-Visible spectrophotometer, UV-VIS 2250, Shimadzu) monitoring the absorbance at wavelength 275 nm. This wavelength absorption belongs to the maximum absorbance wavelength of carvacrol, which is the most representative compound and the major component of OEO [36]. From this wavelength absorption, the mass of the encapsulated OEO in the absolute ethanol solutions was calculated. A calibration curve of the absorbance versus the concentration of the OEO was previously performed by using OEO solutions of known concentrations dissolved in ethanol.

The encapsulation efficiency (EE, %) and loading capacity (LC, %), for each sample, were calculated according to Equations (1) and (2), respectively [36]. Encapsulation efficiency (EE, %) is the encapsulated amount of essential oil expressed as a

percentage of the quantity initially used to prepare the solid inclusion complex. The UV-VIS analysis was carried out in triplicate.

$$\text{Encapsulation Efficiency (\%)} = \frac{\text{Total amount of encapsualted essential oil (mg)}}{\text{Initial amount of OEO to be encapsulated (mg)}} \times 100 \text{ (\%)} \quad (1)$$

$$\text{Loading Capacity (\%)} = \frac{\text{Total amount of encapsualted essential oil (mg)}}{\text{Total amount of inclusion complexes (mg)}} \times 100 \text{ (\%)} \quad (2)$$

2.3.2 *Morphological Characterization of the Inclusion Complexes*

The morphology of the empty CDs and CD:OEO inclusion complexes were examined using a scanning electron microscope (SEM, FEI Quanta 650 FEG, *Thermo Fisher Scientific®,* Germany). The samples were fixed on aluminium stubs with a double-stick conductive carbon substrate and sputter-coated with gold for 63 s at a working pressure of 1.4 E^{-3} mbar before the SEM measurements to prevent the build-up of a negative electric charge in the specimen, which would induce "imaging artefacts" and to enhance resolution. Observations were carried out with voltage acceleration of 10 kV and15 kV at spot 3. Transmission Electron Microscopy (TEM) was also used. Droplets of 0.1 % (w/v) and 1 % (w/v) aqueous suspensions (empty "*as-received*" α-CD and γ-CD; α-CD:OEO and γ-CD:OEO inclusion complexes) were placed on a copper grid and air-dried overnight. For negative staining, one drop of UranyLess 22409 was used. Observations were carried out with voltage acceleration of 200 kV at α_3, spot 1 and magnification: 30KX-100KX (JEOL JEM 2100, Izasa Scientific®, Carnaxide, Portugal).

The X-ray diffractograms of empty α-CD and γ-CD; α-CD:OEO and γ-CD:OEO inclusion complexes were obtained by wide-angle X- ray diffraction (WAXD) using an X-ray diffractometer (PANalitycal X'pert MPD-PRO (PANalytical, Model: X PERT PRO MRD) Bragg-Brentano θ-θ geometry using CuKα radiation at 45kV and 40 mA. The 2θ scan range was 5° - 80° with a step size of 0.01° and a time/step of 0.5 s.

2.4 Preparation of Electrospun Films

2.4.1 *Preparation of Solutions*

A PHBV solution for electrospinning was prepared by dissolving 10 % of biopolymer in TFE (wt/vol) at room temperature. The γ-CD:OEO and α-CD:OEO inclusion complexes were incorporated into the PHBV solution at 10, 15, 20, 25, and 30 wt% in relation to the biopolymer. PHBV solutions with γ-CD and α-CD (25 and 15 wt%, respectively), without OEO, were also prepared as control samples.

2.4.2　Electrospinning

The PHBV solutions containing γ-CD:OEO and α-CD:OEO were electrospun using a high-throughput electrospinning/electrospraying pilot line Fluidnatek® LE 500 manufactured and commercialized by Bioinicia S.L. (Valencia, Spain). The solutions were processed under a constant flow using a 24 emitter multi-nozzle injector, scanning vertically onto a flat slightly negatively charged collector. A voltage difference of 18 kV, a flow-rate of 6 mL/h per single emitter, and a tip-to-collector distance of 20 cm were used as these were the most optimal conditions [40].

2.4.3　Annealing

A thermal pots-treatment below the biopolymer's melting temperature (T_m) was thereafter applied to the electrospun mats in a 4122-model press from Carver, Inc. (Wabash, IN, USA). The mat samples were placed in the hot plates of the press at 160 ºC and closed, for 10 seconds, without pressure. These conditions were selected based on our previous study [40]. The resultant samples had an average thickness of approximately 80 μm.

2.4.4　Characterization of the Electrospun Films

2.4.4.1　Film Thickness

Before testing, the thickness of all films was measured using a digital micrometer (S00014, Mitutoyo, Corp., Kawasaki, Japan) with ± 0.001 mm accuracy. Measurements were performed and averaged in five different points, two in each end and one in the middle.

2.4.4.2　Morphology

The particle shape and size (diameter) distributions of γ-CD and α-CD, the PHBV electrospun fibres and their films containing the γ-CD:OEO and α-CD:OEO inclusion complexes were examined by SEM in a Hitachi S-4800 (Tokyo, Japan) and TEM in Hitachi HT7700 (Tokyo, Japan). For cross-section observations by SEM, the films were previously cryo-fractured by immersion of the sample in liquid nitrogen. The SEM micrographs were taken at an accelerating voltage of 10 kV and a working distance of 8 – 10 mm, the samples were previously sputtered with a gold-palladium mixture for 3 min under vacuum. The size distribution of the particles and average fibres diameter was determined via ImageJ software using at least 20 SEM images.

2.4.4.3 Transparency

The light transmission of the films was determined in specimens of 50 mm x 30 mm by quantifying the absorption of light at wavelengths between 200 and 700 nm, using a UV–Vis spectrophotometer VIS3000 from Dinko, Instruments (Barcelona, Spain). The transparency value (T) was calculated using Equation (3) [41]:

$$T = \frac{A_{600}}{L} \qquad (3)$$

Where A_{600} is the absorbance at 600 nm and L is the film thickness (mm).

2.4.4.4 Thermal Analysis

Thermogravimetric analysis (TGA) of the γ-CD, α-CD, films containing γ-CD:OEO and α-CD:OEO was performed under nitrogen atmosphere in a Thermobalance TG-STDA Mettler Toledo model TGA/STDA851e/LF/1600 analyser. TGA curves were obtained after conditioning the samples in the sensor for 5 min at 30 °C. The samples were then heated from 25 °C to 700 °C at a heating rate of 10 °C/min. The first derivatives of the thermogravimetry (DTG) curves, expressing the weight loss rate as the function of time, were obtained using TA analysis software. All tests were carried out in triplicate.

2.4.4.5 Mechanical Tests

Tensile tests were performed according to the ASTM Standard D 638 on an Instron Testing Machine (Model 4469; Instron Corp; Canton, MA, USA). The film samples were dumbbell-shaped. The cross-head speed was fixed at 10 mm/min. At least six samples were tested for each material, and the average values of the mechanical parameters and standard deviations were reported. Tensile modulus (E), tensile strength at break (σ_b), and elongation at break (ε_b) were calculated from the stress–strain curves, estimated from the force–distance data.

2.5 Antimicrobial Activity

Staphylococcus aureus CECT240 (ATCC 6538p) and *Escherichia coli* CECT434 (ATCC 25922) strains were obtained from the Spanish Type Culture Collection (CECT: Valencia, Spain) and stored in phosphate-buffered saline (PBS) with 10 wt% tryptic soy broth (TSB, Conda Laboratories, Madrid, Spain) and 10 wt.% glycerol at −80 ºC. Previous to each study, a loopful of bacteria was transferred to 10 mL of TSB and incubated at 37 ºC for 24 h. A 100 µL aliquot from the culture was again

transferred to TSB and grown at 37 ºC to the mid-exponential phase of growth. The approximate count of 5 x 10^5 CFU/mL of culture having absorbance value of 0.20 as determined by optical density at 600 nm (UV–Vis spectrophotometer VIS3000 from Dinko, Instruments, Barcelona, Spain).

The minimum inhibitory concentration (MIC) and bactericide (MIB) values of the γ-CD:OEO and α-CD:OEO inclusion complexes against food-borne bacteria was tested following the plate micro-dilution protocol based on our previous work [11]. For this, 96-well plates with an alpha numeric coordination system (columns 12 and rows A-H) were used, where 10 µL of the tested samples were introduced in the wells with 90 µL of the bacteria medium. In the wells corresponding to A, B, C, E, F, and G columns different concentrations of CD/OEO (0.039, 0.078, 0.156, 0.312, 0.625, 1.25, 2.5, 5, 10, 20 µg/mL), were tested, in triplicate, from rows 1 to 10. Columns D and H were used as control of CD:OEO in TSB without bacteria. Row 11 was taken as a positive control, that is, only TSB, and row 12 was used as a negative control, that is, *S. aureus* and *E. coli* in TSB. The plates were incubated at 37 °C for 24 h. Thereafter, 10 µL of resazurin, a metabolic indicator, was added to each well and incubated again at 37 °C for 2 h. Upon obtaining the resazurin change, the wells were read through the colour difference. The MIC value was determined as the lowest concentration of γ-CD:OEO and α-CD:OEO presenting growth inhibition.

The antimicrobial performance of the electrospun PHBV films containing γ-CD:OEO and α-CD:OEO was evaluated by using a modification of the Japanese Industrial Standard (JIS) Z2801 (ISO 22196:2007) [42]. A microorganism suspension of *Staphylococcus aureus* (*S. aureus*) and *Escherichia coli* (*E. coli*) was applied onto the test films containing the γ-CD:OEO and α-CD:OEO inclusion complexes and the films without CD:OEO (negative control) sizing 1.5 cm x 1.5 cm that were placed in either open bottles. After incubation at 24 °C and at a relative humidity (RH) of at least 95 % for 24 h, bacteria were recovered with PBS, 10-fold serially diluted and incubated at 37 °C for 24 h in order to quantify the number of viable bacteria by conventional plate count. The antimicrobial activity was evaluated from 1 (initial day), 8, and 15 days. The value of the antimicrobial activity (*R*) was calculated using Equation (4):

$$R = \left[Log \left(\frac{B}{A} \right) - Log \left(\frac{C}{A} \right) \right] = Log \left(\frac{B}{C} \right) \tag{4}$$

Where *A* is the average of the number of viable bacteria on the control sample immediately after inoculation, *B* is the average of the number of viable bacteria on the control sample after 24 h, and *C* is the average of the number of viable bacteria on the test sample after 24 h. Three replicate experiments were performed for each

sample and the antibacterial activity was evaluated with the following assessment: Nonsignificant (R<0.5), slight (R≥0.5 and<1), significant (R≥1 and<3), and strong (R≥3) [43].

2.6 Antioxidant Activity

The 2,2,1-diphenyl-1-picrylhydrazyl (DPPH) inhibition assay was used to evaluate the free radical scavenging activity of the neat OEO, γ-CD:OEO, α-CD:OEO, and the electrospun PHBV films containing γ-CD:OEO and α-CD:OEO. Samples were weighed in triplicate in cap vials, and then an aliquot of the DPPH solution (0.05 g/L in methanol) was added to each one. Vials without samples were also prepared as controls. All the samples were prepared and immediately stored at room temperature for 2 h in darkness. After this, the absorbance of the solution was measured at 517 nm in the UV 4000 spectrophotometer from Dinko Instruments. Results were expressed as the percentage of inhibition to DPPH following Equation (5) [44] and µg equivalent of Trolox per gram of sample, employing a previously prepared calibration curve of Trolox.

$$Inhibition\ DPPH\ (\%) = \frac{A_{Control} - (A_{sample} - A_{blank})}{A_{control}} * 100 \qquad (5)$$

Where $A_{control}$, A_{blank}, and A_{sample} are the absorbance values of the DPPH solution, methanol with the test sample, and the test sample, respectively.

2.7 Statistical Analysis

The results of the encapsulation efficiency and loading capacity of the CD:OEO inclusion complexes, mechanical tests, and antioxidant activity assays were evaluated by analysis of variance (ANOVA) and a multiple comparison test (Tukey) with 95 % significance level (p <0.05). For this purpose, we used the software OriginPro8 (OriginLab Corporation, USA).

3 Results and Discussions

3.1 Encapsulation Efficiency of the CD:OEO Inclusion Complexes

The EE and LC of the α-CD:OEO and γ-CD:OEO inclusion complexes prepared by FDM and KM are presented in Table 2. Although the results showed that both α-CD and γ-CD are efficient wall materials for encapsulation of OEO, the preparation method and the weight ratio (CDs:OEO) are also key factors to obtain an optimal EE. Indeed, FDM yielded lower encapsulation efficiency (from 36.03 % to 96.7 %) than KM (from 71.2 % to 98.5 %). This is in accordance with the results described by Ozdemir et al. (2018), who studied the encapsulation of black paper oleoresin in β-CD with encapsulation efficiencies from 90.2 % to 79.3 % for KM and FDM, respectively. The higher encapsulation efficiency obtained by KM compared to FDM can be related to the high shear rate applied [45] and the use of a low amount of water during the IC formation. In an aqueous solution, the CD cavity is slightly polar and occupied by water molecules, and can therefore be readily replaced by appropriate guest molecules, that are less polar than water [46]. It is also worthy of mentioning that some differences in the EE values could be associated with evaporation of volatile components during the preparation process studies [36,45]. In conclusion, the preparation parameters of the α-CD:OEO and γ-CD:OEO inclusion complexes, that is, weight ratio host-guest, nature of cyclodextrin, use of co-solvent and its quantity, mixing time, and shear rate applied could affect the properties of the obtained complexes such as the encapsulation yield. Thus, based on the results obtained in terms of EE, KM revealed to be the most efficient method for the encapsulation of OEO in the CD cavity, which also added value in terms of simplicity, rapidity, and the desired characteristics of the final product.

Table 2. Encapsulation efficiency (EE,%) and loading capacity (LC,%) values of the α- and γ-cyclodextrin: oregano essential oil inclusion complexes (α-CD:OEO and γ-CD:OEO) by kneading method (KM) and freeze-drying method (FDM)

Method	Inclusion Complex	EE (%)*	LC (%)*
KM	γ-CD:OEO 80: 20 w/w	98.50 ± 0.7^a	19.60 ± 0.1^a
	α-CD:OEO 80: 20 w/w	92.60 ± 3.6^a	18.60 ± 0.7^a
	γ-CD:OEO 85: 15 w/w	71.20 ± 6.5^a	10.80 ± 1.0^a
	α-CD:OEO 85: 15 w/w	96.20 ± 1.4^a	14.40 ± 0.2^a
FDM	γ-CD:OEO 80: 20 w/w	93.60 ± 2.5^b	18.70 ± 0.5^b
	α-CD:OEO 80: 20 w/w	36.03 ± 1.2^b	7.20 ± 0.2^b
	γ-CD:OEO 85: 15 w/w	96.70 ± 0.6^b	14.50 ± 0.1^b
	α-CD:OEO 85: 15 w/w	50.02 ± 2.6^b	7.50 ± 0.4^b

*Values given are averages of triplicate samples ± standard deviations. Average values with different superscript letters differ statistically ($p < 0.05$); (a and b: indicate statistically difference among formulations KM vs FDM, values followed by the same letter are not statistically different according to Tukey's Multiple Range Test.

3.2   Morphology of the CD:OEO Inclusion Complexes

Figure 1 gathers the SEM micrographs of the α-CD:OEO and γ-CD:OEO inclusion complexes. It can observe that the size and shape of the α-CD:OEO and γ-CD:OEO inclusion complexes (Figure 1b, 1d, 1e, 1f, 1g, 1h) are completely different from the empty α- and γ- CDs (Figure 1a, 1c, 1i, 1j). The shape of empty "*as-received*" α- and γ- CDs appear uneven and the size ranged from 24 up to 254 μm. Large particle sizes were observed suggesting that CDs piled up forming large aggregates. The relatively larger size of empty "*as-received*" α- and γ- CD can be attributed to the agglomeration of empty "*as-received*" α- and γ- CD particles via hydrogen bonding. In the absence of a guest molecule, empty "as-received" α- and γ- CD tended to cluster due to lack of significant net charge on the particles, that is, no repulsive forces were produced to prevent agglomeration [47]. This is also consistent with the observation of smaller particles attraction and adherence to the larger particles (see in detail in Figure 1a, $1a_1$, $1a_2$ and 1c, $1c_1$, $1c_2$). Similar observations were reported by Santos et al. [36]. Contrarily, this behavior was not observed in the formed α-CD:OEO and γ-CD:OEO inclusion complexes. In particular, the reduction of the particle size in the α-CD:OEO and γ-CD:OEO inclusion complexes indicated a conformational change of empty α-CD and γ-CD that obstructed their agglomeration [48,49]. Indeed, compared with

empty "*as-received*" α- and γ- CD (particle size from 24 up to 254 µm; similar to that found by Gauret et al. [50], their inclusion complexes showed a remarkable decrease in particle size, range from ~5 µm up to the nanometric level (~100 nm) and with well-defined lamella shaped (tetragonal crystals). In both types of inclusion complexes were observed lamella-like sheets and microrods (Figure 1b and 1d).
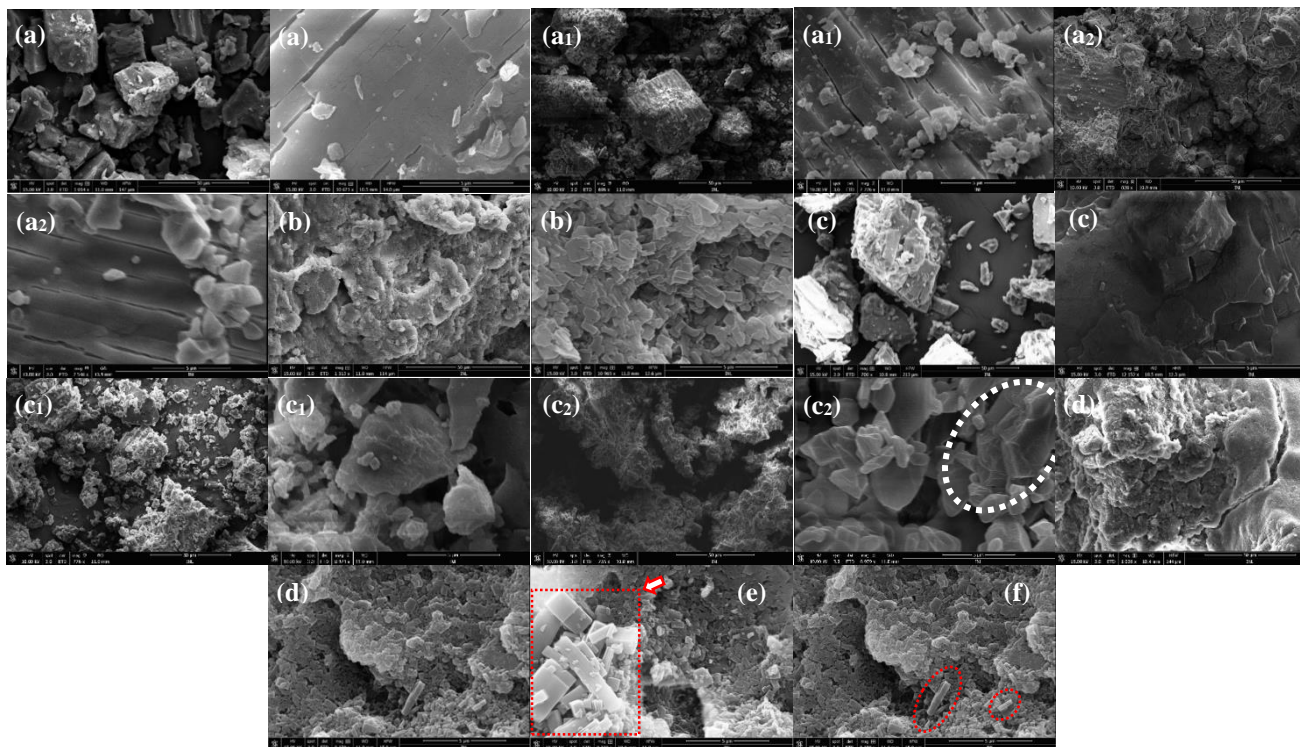
Figure 1. Scanning electron microscopy images of (**a**) empty "*as-received*" α-CD (10671x and 1014x); (**a₁**) empty "*kneaded for18 min at R.T.*" α-CD (7226x and 696x); (**a₂**) empty "*kneaded for18 min with 0.25 mL distilled water at R.T.*" α-CD (7546x and 828x); (**b**) α-CD:OEO inclusion complex (80:20 w/w, KM) (10965x and 1313x); (**c**) empty "*as-received*" γ-CD (12152x and 700x); (**c₁**) empty "*kneaded for 18 min at R.T.*" γ-CD) (8924x and 776x); (**c₂**) empty "*kneaded for 18 min with 0.25 mL distilled water at R.T.*" γ-CD (6979x and 755x); (**d**) γ-CD:OEO inclusion complex (80:20 w/w, KM) (9379x and 1036x); (**e**) α-CD:OEO inclusion complex, and (**f**) γ-CD:OEO inclusion complex.

In addition, the microrods from inclusion complexes had a very high aspect ratio (see Figure 1e and 1f). Observation over a large number of SEM images suggests that these long microrods stack together to produce the lamella-like sheets. The morphological similarity of both α-CD:OEO and γ-CD:OEO inclusion complexes can be explained by considering the solubility of the used CDs (see previous Table 1). In this regard, Saokham et al. [51], and the referenced cited within examined the solubility of α and γ differences compared with β-CD. Briefly, γ-CD, which is the largest of the three, is the most soluble (23.20 mg/100 ml H2O) while β-CD, which is in the intermediate, is the least soluble in water (1.8 g/100 ml H2O). These differences in the solubility of the CDs are related to the way the CD glucose units are geometrically aligned with each other. It has been proposed that in the β-CD molecule, all the 7 glucose units lie in the same plane. Hence, in this arrangement, all the glucose primary hydroxyl groups at the CD narrower end can form hydrogen bonds with each other. At the same time, all the secondary hydroxyl groups at the wider CD opening form hydrogen bonds with each other. The hydrogen bonding below and above the ring leads to secondary belts which increases the rigidity of the β-CD and therefore causes low solubility. As opposite, α- and γ-CD which do not have secondary belts therefore their structures are flexible, are hence very soluble due to the availability of free hydroxyl (–OH) groups. During trituration of cyclodextrins in an aqueous medium, a few water molecules could entrap into the cyclodextrin cavity, whereas other molecules of water are present as integral parts of the crystal structure (crystal water). According to Rusa et al. [52], Szeijtli [21], and Das et al. [53] the CD inclusion complexes are formed by the substitution of included water from cyclodextrin cavity by the appropriate guest molecule.

Using the above reasoning, the threading of OEO can occur faster in α-CD and γ-CD molecules than in β-CD. Hence, the morphological similarity of both types of inclusion complexes (α-CD:OEO and γ-CD:OEO) studied in this work could be explained using the above reasoning. Moreover, the particle size distribution appears quite homogenous and have rather smooth and parallel surfaces (Figure 1b, 1d, 1e, 1f, 1g, 1h). They all have sharp edges, as expected from crystalline structures. The growth of the crystals is definitely preferential in 2D (lamella-shape). Figure 1g and 1h show other details: the two arrows point out the thickness, around a few hundreds of nm, of a platelet with a size of 100 nm - ~ 5µm. Smaller platelets (under 500 nm) appear to have the same thickness. These results show that the morphological characteristic of inclusion complexes are indeed different from empty "*as-received*" α-CD and γ- CD; empty "*kneaded for 18 minutes at R.T.*" α-CD and γ- CD, and empty "*kneaded for 18 minutes with 0.25 mL distilled water at R.T.*" α-CD and γ- CD. This morphological difference between the empty CDs and the inclusion complexes

obtained is in agreement with the observations reported by Guimaraes et al. [48] and the references cited within.
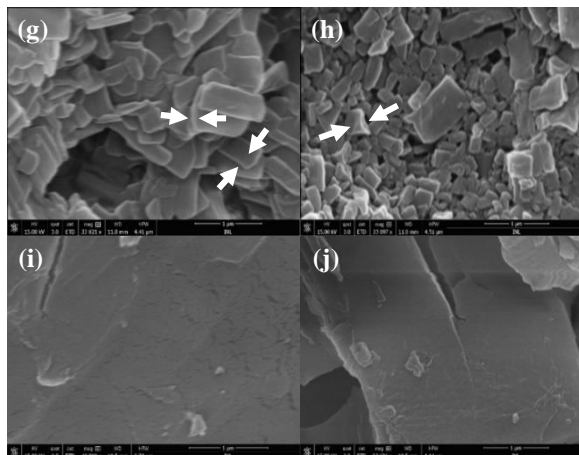
To elucidate if the morphology, in terms of particle size and well-defined shape, of empty "*as-received*" α- and γ-CD was changed due to the encapsulation of EO (i.e., low particle size and well-definite lamella shape), was performed SEM also on empty "*kneaded for18 minutes at R.T.*" α- and γ- CD, and empty "*kneaded for 18 minutes at R.T. with 0.25 ml distilled water (the same quantity used at the preparation of inclusion complex)*" α- and γ- CD. The results showed that compared with empty "*as-received*" α- and γ- CD there is not significant morphological modification after their kneaded for 18 minutes at R.T. (Figure 1a$_1$ and 1c$_1$) as well as after their kneaded for 18 minutes at R.T. with 0.25 ml distilled water (Figure 1a$_2$ and 1c$_3$). The presence of aggregates of size from ~2 up to 242 μm with undefined shape was revealed, except for empty "kneaded 18 minutes at R.T. with 0.25 ml distilled water" γ-CD which showed a defined shape, that is, prisms shape structure (Figure 1c$_2$). Similar observations on "the agglomeration of the free cyclodextrin "were revealed by Rakmai et al. [54]. It indicates the hydrogen bonding of the cyclodextrin molecules (empty) interact with each other in water producing the cluster of CD. In addition, Shan et al. [55] have demonstrated that CDs particle agglomeration might be induced also by the moisture content.

The α-CD:OEO and γ-CD:OEO inclusion complexes morphology in the aqueous suspension was also observed using TEM, and Figure 2 shows clear lamella shapes with diameters from 0.1 to ~1 μm.

In detail, at 0.1 % (w/v) were detected single lamellas with diameters of 350 nm over a large number of grid holes (Figure 2a), whereas in Figure 2b$_{1-3}$ were displayed several representative TEM micrographs for 1 % (w/v), lamellas with diameters 170 - 519 nm. In addition, some of these lamellas fused together as indicated by the white arrow, indicating that the lamellas do not simply interact through their surfaces but are able to merge completely in aggregate. Thus, TEM measurements corroborated the results that were obtained from SEM, that is, a well-defined lamella-shape structures of the inclusion complexes. In contrast, empty γ-CD (1 % w/v, aqueous suspension vortex 10 minutes at 2500 rpm, R.T) presented aggregates made up of a larger number of small spherical particles with diameters between 5 nm and 325 nm (Figure 2c$_{1,2}$). These spherical particles seem to interact and form rod-like shape structure with diameters between 406 nm and 1786 nm (inset of Figure 2c$_{3,4}$ diameter: 790.86 nm). Empty α-CD and α-CD:OEO inclusion complexes revealed similar morphologies (data not shown). These results support the hypothesis that the spherical particles are not indefinitely stable, thus tend to form a larger structure. These observations are in agreement with those revealed by several research groups such as Harada et al. [56-58], and Ceccato et al. [59] who reported the formation of the so-called "molecular tube" a rod-like rigid molecule with an empty hydrophobic cavity that can behave as a host for ions or small organic molecules. Furthermore, Bonini et al. [60] reported evidence of β-cyclodextrin self-aggregation in water. It was showed also that the concentration plays a critical key on their morphology so that polydisperse spherical objects with diameters of about 100 nm were present at low concentration, whereas micrometre planar aggregates are predominated at higher concentrations.
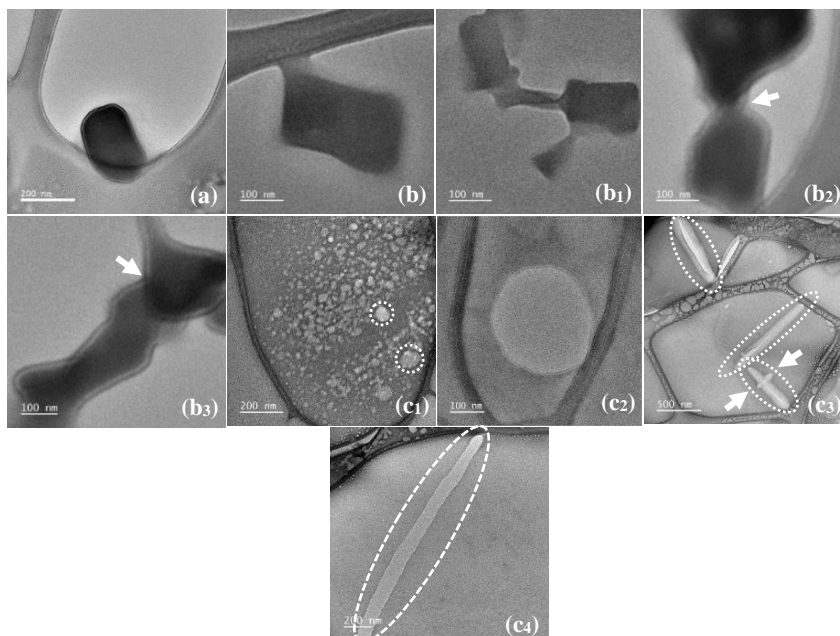
Figure 2. TEM micrographs of (**a**) 0.1% (w/v) γ-CD:OEO inclusion complex (80:20 w/w, KM) aqueous suspension vortex 10 min at 2500 rpm, R.T.; (**b₁₋₃**) 1% (w/v) γ-CD:OEO inclusion complex (80:20 w/w, KM) aqueous suspension vortex 10 min at 2500 rpm, R.T; (**c₁₋₄**) empty "*as-received*" γ- CD aqueous solution vortex 10 min at 2500 rpm, R.T.

Finally, WAXD studies were conducted to confirm the formation of CD:OEO inclusion complexes. According to Marques [16] and references cited herein, X-ray powder diffraction is the most useful method for the detection of inclusion complexes formation, especially in the case of the guest in the form of liquid molecules (e.g., oils and volatiles), because the liquid guest molecules produce no diffraction patterns and any changes in the diffractogram reflects the formation of a new crystal lattice. Figure 3 shows the WAXD patterns of empty "*as-received*" α-CD and γ-CD compared with their inclusion complexes. Empty "*as-received*" α-CD and γ-CD differed from each other in their diffraction patterns. The WAXD pattern of empty "as-received" α-CD and γ-CD revealed several diffraction peaks which are indicative of their crystalline nature, but, according to Rusa et al. [52] for α-CD there are three salient peaks associated with its crystal structure occurring at $2\theta = 12.1°$, $14.5°$, and $21.8°$ (Figure 3a). In the diffractograms of both CD:OEO inclusion complexes, some of these characteristic diffraction peaks disappear.

For the α-CD:OEO inclusion complex, a new intense diffraction peak appeared at $2\theta = 19.6°$, which was not observed in empty "*as-received*" α-CD. According to Rusa

et al. [52], the peak at 2θ ~20º in the WAXD of α-CD inclusion complexes is characteristic for the channel structure of α-CD when including long guest molecules and polymers in particular. In the γ-CD:OEO inclusion complex, a new sharp diffraction peak at 2θ= 7.6º (Figure 3b) was revealed. This peak was not observed in empty "as-received" γ-CD. According to Harada et al. [20], and Rusa et al. [52] this peak has been suggested as an indicator for γ-CD inclusion complex channel structures. Hence, this behavior can be attributed to an interaction between CD and OEO showing the presence of a new solid phase.
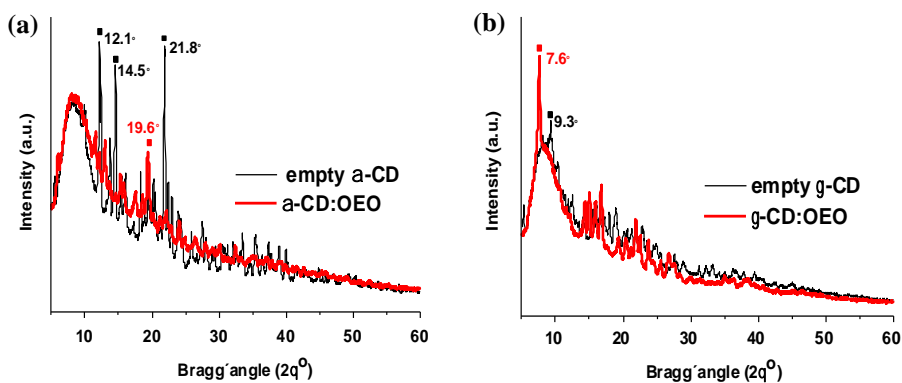
Figure 3. X-Ray patterns of (**a**) empty "*as-received*" α-CD and α-CD:OEO inclusion complexes (80:20 w/w, KM) (**b**) empty "*as-received*" γ-CD and γ-CD:OEO inclusion complexes (80:20 w/w, KM).

3.3 Morphology of the Electrospun CD:OEO Inclusion Complexes-Containing PHBV Films

The SEM micrographs of the electrospun fibres of the neat PHBV and the fibres containing the γ-CD:OEO and α-CD:OEO inclusion complexes are shown in Figure 4. The mean fibre diameters obtained from the SEM images are gathered in Table 3. The diameters of the electrospun fibres of neat PHBV were 0.89 ± 0.30 μm, being very similar to those reported in our previous research work [40]. As shown in Figure 4a-e, the electrospun PHBV fibres containing different concentrations of γ-CD:OEO inclusion complexes, that is, 10, 15, 20, 25, and 30 wt%, presented mean diameters ranging between 0.87 - 0.91 μm. Up to contents of 25 wt% γ-CD:OEO inclusion complexes, the electrospinning process yielded regular and continuous fibres of PHBV. In the case of the PHBV fibres mat containing 30 wt% γ-CD:OEO IC, the fibrilar morphology was affected, losing the homogeneity and continuity due to the high concentration of CD. Figure 4f-j show the SEM micrographs of the electrospun fibers of PHBV containing different concentrations of α-CD:OEO inclusion

complexes, that is, 10, 15, 20, 25, and 30 wt%. The electrospun fibres containing 10 and 15 wt% α-CD:OEO showed mean diameters of approximately 0.89 and 0.90 μm, respectively, being homogeneous and with smooth surfaces. The diameter of the fibers containing 20 wt.% α-CD:OEO inclusion complexes increased, presenting a mean value of 1.03 ± 0.25 μm, and beaded regions due to potential CD agglomerations. It can be observed that the electrospun PHBV fibers with 25 and 30 wt.% α-CD:OEO inclusion complexes, respectively shown in Figure 4i and 4j, presented mean diameters of 1.17 and 1.22 μm. This slight increase in the fiber diameters can be related to the relatively high amount of CDs incorporated that aggregated during electrospinning and resulted in destabilization of the electrified jet. These results are in agreement with the previous reports of [61], concluding that at low hydroxypropyl-β-CD/laponite concentrations, the fibers do not present any significant change in diameter and shape while, at high concentrations, the diameter of the nanocomposite nanofibers decreases and aggregates are also formed. Furthermore, changes in the solution properties such as viscosity or conductivity may cause variations in the electrospun morphologies. For instance, Aytac et al. [62] determined that the diameters of nanofibers containing methylated-β-CD/linalool were lower than those of hydroxypropyl-β-CD/linalool due to the lower viscosity and higher conductivity of the aqueous solution. Therefore, the most optimal fibrillary morphologies were attained for PHBV containing 25 wt.% γ-CD:OEO and 15 wt.% α-CD:OEO inclusion complexes.
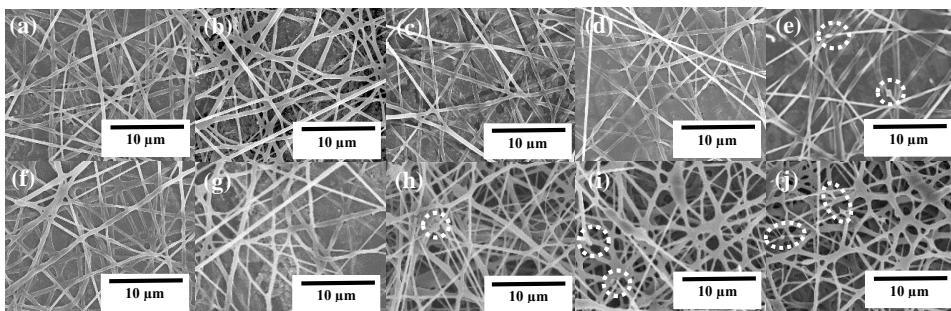
Figure 4. Scanning electron microscopy micrographs of electrospun fibres of poly(3-hydroxybutyrate-*co*-3-hydroxyvalerate) (PHBV) containing α- and γ-cyclodextrin: oregano essential oil inclusion complexes (γ-CD:OEO and α-CD:OEO): (**a**) 10 wt% γ-CD:OEO; (**b**) 15 wt% γ-CD:OEO; (**c**) 20 wt% γ-CD:OEO; (**d**) 25 wt% γ-CD:OEO; (**e**) 30 wt% γ-CD:OEO; (**f**) 10 wt*%* α-CD:OEO; (**g**) 15 wt% α-CD:OEO; (**h**) 20 wt% α-CD:OEO; (**i**) 25 wt% α-CD:OEO, and (**j**) 30 wt% α-CD:OEO. Scale markers of 10 μm in all cases.

Table 3. Mean diameters and thickness of the electrospun fibers and film thicknesses of poly(3-hydroxybutyrate-co-3-hydroxyvalerate) (PHBV) containing oregano essential oil γ- and α-cyclodextrin inclusion complexes (γ-CD:OEO and α-CD:OEO)

Sample	Fiber diameter (μm)	Film thickness (μm)
PHBV	0.89 ± 0.30	64 ± 0.75
PHBV + 10 wt% γ-CD:OEO	0.87 ± 0.15	61 ± 1.10
PHBV + 15 wt% γ-CD:OEO	0.88 ± 0.22	63 ± 0.98
PHBV + 20 wt% γ-CD:OEO	0.86 ± 0.18	70 ± 0.94
PHBV + 25 wt% γ-CD:OEO	0.85 ± 0.27	72 ± 0.72
PHBV + 30 wt% γ-CD:OEO	0.91 ± 0.32	77 ± 0.68
PHBV + 10 wt% α-CD:OEO	0.89 ± 0.20	73 ± 0.99
PHBV + 15 wt% α-CD:OEO	0.90 ± 0.17	75 ± 0.77
PHBV + 20 wt% α-CD:OEO	1.03 ± 0.25	81 ± 0.91
PHBV + 25 wt% α-CD:OEO	1.17 ± 0.19	83 ± 0.86
PHBV + 30 wt% α-CD:OEO	1.22 ± 0.12	85 ± 0.69

The electrospun fibres mats were thereafter subjected to annealing in order to obtain a continuous film [11,40]. The surface and cross-section areas of the PHBV films containing γ-CD:OEO and α-CD:OEO inclusion complexes were observed by SEM images. As shown in Figure 5, the surface of the electrospun PHBV films containing 10, 15, 20, and 25 wt% γ-CD:OEO inclusion complexes were homogeneous and continuous, showing mean thicknesses of 61 ± 1.1, 63 ± 0.98, 70 ± 0.94, and 72 ± 0.72 μm, respectively (see Table 3). This is in agreement with the electrospun fibre morphologies described above (see Figure 4) that showed proper fibre formation until 25 wt%. Moreover, the film containing 30 wt% showed a surface with some cracks due to the high concentration of γ-CD:OEO inclusion complexes that difficulted the formation of a continuous film with a higher thickness (~ 77 ± 0.68 μm). The film thicknesses also increased with the concentration of γ-CD:OEO inclusion complexes. Based on these results, the best concentration to attain uniform and homogenous films of PHBV was 25 wt% γ-CD:OEO inclusion complex.
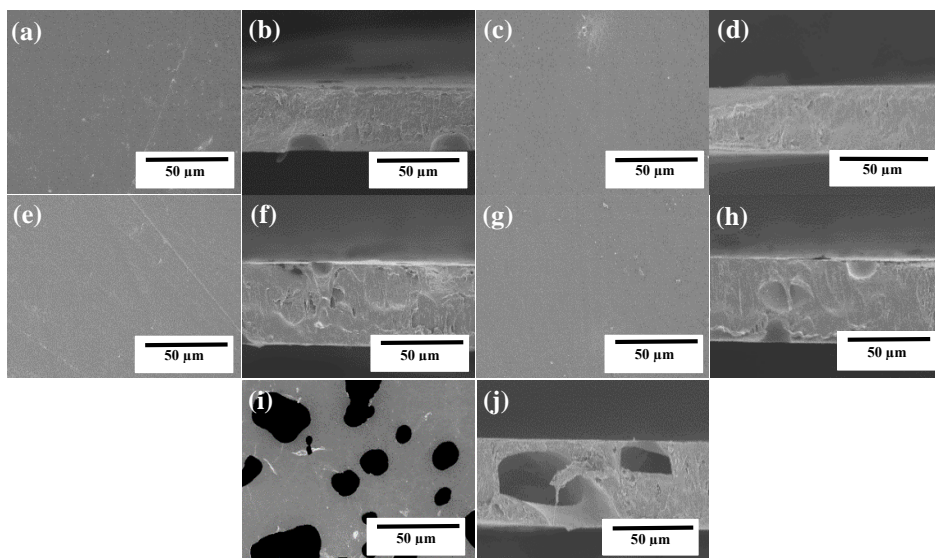
Figure 5. Scanning electron microscopy micrographs of electrospun films of poly(3-hydroxybutyrate-*co*-3-hydroxyvalerate) (PHBV) containing -cyclodextrin:oregano essential oil inclusion complexes (γ-CD:OEO): (**a, b**) 10 wt% γ-CD:OEO; (**c, d**) 15 wt% γ-CD:OEO; (**e, f**) 20 wt% γ-CD:OEO; (**g, h**) 25 wt% γ-CD:OEO, and (**i, j**) 30 wt% γ-CD:OEO. Scale markers of 50 μm in all cases.

Figure 6 showed the surface and cross-section of the films containing α-CD:OEO inclusion complexes. The thicknesses of the films containing 10 and 15 wt.% of α-CD:OEO inclusion complexes were 73 ± 0.99 and 75 ± 0.77 μm, respectively. These films also showed a homogeneous surface. The film thicknesses increased with the amount added of α-CD:OEO inclusion complexes, reaching values of 81 ± 0.91, 83 ± 0.86, and 85 ± 0.69 μm for 20, 25, and 30 wt% of α-CD:OEO, respectively (see Table 3). Increasing the concentration from 20 wt.% also affected the surface and generated cracks with different sizes. This phenomenon has been ascribed to the weak interfacial bond between the CDs and the biopolyester matrix [63]. In this context, Melendez-Rodriguez et al. [40] also found that at high concentrations of silica nanoparticles with eugenol, that is, 15 and 20 wt%, the electrospun films showed greater porosity and also some plastic deformation, which was attributed to a plasticization generated by the released oil and a possible migration during the annealing process. In this case, the best concentration to get uniform and homogenous films was 15 wt% of α-CD:OEO inclusion complexes.

Figure 6. Scanning electron microscopy (SEM) micrographs of electrospun films of poly(3-hydroxybutyrate-*co*-3-hydroxyvalerate) (PHBV) containing α-cyclodextrin:oregano essential oil inclusion complexes (α-CD:OEO): (**a, b**) 10 wt% α-CD:OEO; (**c, d**) 15 wt% α-CD:OEO; (**e, f**) 20 wt% α-CD:OEO; (**g, h**) 25 wt% α-CD:OEO, and (**i, j**) 30 wt% α-CD:OEO. Scale markers of 10 μm in all cases. Scale markers of 50 μm in all cases.

3.4 Visual Aspect of the Electrospun CD:OEO Inclusion Complexes-Containing PHBV Films

The visual aspect of the electrospun PHBV films containing different concentrations of γ-CD:OEO and α-CD:OEO inclusion complexes was observed to ascertain their contact transparency. In Figure 7 it can be observed that the contact transparency was high but some differences among the samples were also seen. The neat PHBV film had a transparency value of 4.78 ± 0.08 and opacity of 0.037 ± 0.001. When 10 wt.% of γ-CD:OEO inclusion complex was incorporated, slight changes were observed with respect to the neat PHBV´s transparency whereas opacity values without significant differences were obtained. The transparency value and opacity of the films containing 15, 20, and 25 wt% γ-CD:OEO inclusion complexes increased significantly respect to neat PHBV and 10 wt.%. When 30 wt.% of γ-CD:OEO inclusion complex was incorporated, the transparency and opacity values were higher respect to the others samples (9.23 ± 0.59 and 0.065 ± 0.004, respectively). Also, the films containing α-CD:OEO inclusion complexes presented high changes in the transparency and opacity respect to the γ-CD:OEO inclusion complexes. In particular, for the film sample containing 10 wt% α-CD:OEO inclusion complex, a

transparency value of 6.36 ± 0.63 and opacity of 0.047 ± 0.005 was obtained. For the films containing 15 and 20 wt% of α-CD:OEO inclusion complexes, the values were similar while those based on 25 and 30 wt% of α-CD:OEO inclusion complexes presented the highest values. For both inclusion complexes, the increment of the concentration caused a light scattering that produced lower transparency and higher opacity. This phenomenon can be important in the design of food packaging materials due to some food products are sensible to the ultraviolet-visible (UV-Vis) light, which can trigger different enzymatic and oxidative reactions [41].

$T = 5.73 \pm 0.34$	$T = 6.11 \pm 0.14$	$T = 6.45 \pm 0.11$	$T = 6.54 \pm 0.35$	$T = 9.23 \pm 0.59$
γ-CD:OEO 10%	γ-CD:OEO 15%	γ-CD:OEO 20%	γ-CD:OEO 25%	γ-CD:OEO 30%
$O = 0.039 \pm 0.002$	$O = 0.042 \pm 0.001$	$O = 0.047 \pm 0.001$	$O = 0.048 \pm 0.002$	
$T = 6.36 \pm 0.63$	$T = 7.00 \pm 1.56$	$T = 7.50 \pm 0.97$	$T = 8.81 \pm 0.71$	$T = 12.72 \pm 0.33$
α-CD:OEO 10%	α-CD:OEO 15%	α-CD:OEO 20%	α-CD:OEO 25%	α-CD:OEO 30%
$O = 0.047 \pm 0.005$	$O = 0.052 \pm 0.009$	$O = 0.055 \pm 0.006$	$O = 0.067 \pm 0.005$	$O = 0.078 \pm 0.002$

Figure 7. Visual aspect of electrospun films of poly(3-hydroxybutyrate-*co*-3-hydroxyvalerate) (PHBV) containing γ- and α-cyclodextrin:oregano essential oil inclusion complexes (γ-CD:OEO and α-CD:OEO). Films are 2×2 cm^2.

3.5 Thermal Stability of the Electrospun CD:OEO Inclusion Complexes-Containing PHBV Films

The TGA curves for the neat PHBV, γ-CD, α-CD, inclusion complexes of γ-CD:OEO and α-CD:OEO, and the PHBV films containing the inclusion complexes are shown in Figure 8. The values of mass loss at 5% ($T_{5\%}$), mass at 160 °C (%), which corresponds to the annealing temperature applied to the electrospun mats to produce the films (see section 2.4.4.4), degradation temperature (T_{deg}), weight loss at T_{deg} (%), and residual mass (%) at 700 °C are gathered in Table 4. In our previous study, the TGA curve for the neat OEO showed a low thermal stability. In particular, it presented a mass loss at 160 °C around of 40.3 %, having its T_{deg} value at 178.4 °C and the mass loss at T_{deg} was 74.16%, corresponding to the volatilization and/or degradation of principal volatile compounds such as carvacrol, thymol, and pinene [11]. This value is also similar to the Tdeg of 168 °C reported by Guimarães et al. [48]. The mass losses at 160 °C for the empty CDs were 8.86 % (γ-CD) and 9.42 % (α-CD), while the T_{deg} values were 323.12 °C with a mass loss of 83.01 % for γ-CD and 326.43 °C with a mass loss of 86.29 % for α-CD. As other authors have indicated

[64], the thermal degradation of powdered molecules can be affected by different factors such as chemical structure, crystallinity, crystal size, and morphology. Thus, the thermal stability of CDs depends on the size of the crystal, showing greater thermal stability the larger crystals [65,66]. When OEO was encapsulated into CDs, the inclusion complexes enhanced the thermal stability due to the interactions between the guest molecule and the cavity of the cyclodextrins achieving a protection of the volatiles compounds [29]. The mass loss for γ-CD:OEO inclusion complexes at 160 ºC was nearly 16.9%, having a T_{deg} of 326.28 ºC with a mass loss of 86.11 % at T_{deg}. In the case of α-CD:OEO inclusion complexes, the mass loss at 160 ºC was 9.69% and T_{deg} was 330.50 ºC with a mass loss at T_{deg} of approximately 85.70%. The inclusion complexes showed two mass losses, one below 100 °C corresponding to the loss of water from the cavity and another above 280 °C, which is attributed to the main thermal degradation of CDs [62]. In this regard, Shin et al. [67] reported similar results for triacetyl (TA) encapsulated in β-CD, obtaining a Tdeg of 293.99 °C for β-CD and for the inclusion complex of TA-β-CD its T_{deg} was 340.62 ºC. The thermal degradation of the PHBV films containing inclusion complexes increased slightly the value of Tdeg respect to the neat PHBV. The mass loss values at 160 ºC for all films containing CDs and the inclusion complexes were similar, showing values between 1.21 and 1.71 %. The slight differences can be ascribed to the size and load capacity of the two tested CDs. The value of Tdeg for the PHBV with 25 wt.% γ-CD:OEO was 322.52 ºC with a mass loss of 96.12 %, while Tdeg for the PHBV with 25 wt.% γ-CD without OEO was slightly lower (320.11 ºC). Furthermore, the PHBV film containing 15 wt% α-CD:OEO showed a T_{deg} around 313.70 ºC with a mass loss of 96.98 % and the films with 15 wt% α-CD without OEO presented a T_{deg} of 309.27 ºC and mass loss around 96.28 %. Then, one can conclude that the thermal stability of OEO was improved in the electrospun PHBV films. In this regard, Yildiz et al. [68] reported an improvement of the thermal stability of CD:menthol inclusion complex in aqueous solutions nanofibers. Other studies have also suggested that the incorporation of substances such as powder, nanoparticles or EOs into electrospun biopolymer films increased their maximum decomposition temperature [40,69,70].
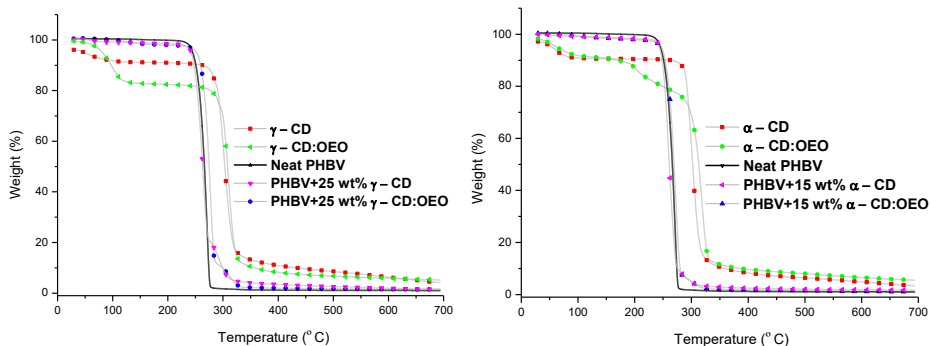
Figure 8. Thermogravimetric analysis (TGA) curves for the γ- and α-cyclodextrin: oregano essential oil inclusion complexes (γ-CD:OEO and α-CD:OEO), and the electrospun films of poly(3-hydroxybutyrate-*co*-3-hydroxyvalerate) (PHBV) containing γ-CD:OEO and α-CD:OEO inclusion complexes.

Table 4. Thermal properties defined as mass loss at 5% ($T_{5\%}$), mass at 160 °C, degradation temperature (T_{deg}), weight loss at T_{deg}, and residual mass at 700 °C for oregano essential oil (OEO), γ- and α-cyclodextrins (γ-CD and α-CD), their inclusion complexes (γ-CD:OEO and α-CD:OEO), and the electrospun films of poly(3-hydroxybutyrate-*co*-3-hydroxyvalerate) (PHBV) and PHBV containing γ-CD and α-CD and γ-CD:OEO and α-CD:OEO inclusion complexes

Sample	$T_{5\%}$ (ºC)	Mass at 160 ºC (%)	T_{deg} (ºC)	Mass loss (%)	Residual mass (%)
PHBV	245.03	0.15	278.70	97.73	2.10
OEO	46.26	40.3	178.40	74.16	0.14
γ-CD	49.23	8.86	323.12	83.01	4.15
α-CD	55.21	9.42	326.43	86.39	3.38
γ-CD:OEO	81.60	16.9	326.28	86.11	5.23
α-CD:OEO	62.97	9.63	330.50	85.70	5.51
PHBV + 25 wt% γ-CD	240.95	1.21	320.11	95.13	1.56
PHBV + 25 wt% γ-CD:OEO	252.02	1.71	322.52	96.12	1.48
PHBV + 15 wt% α-CD	241.55	1.31	309.27	96.28	1.71
PHBV + 15 wt% α-CD:OEO	247.23	1.63	313.70	96.98	1.11

3.6 Mechanical Properties of the Electrospun CD:OEO Inclusion Complexes-Containing PHBV Films

The mechanical properties of the electrospun PHBV films containing the inclusion complexes are shown in Table 5. The neat PHBV film presented an E value of 1252 MPa, a σb value of 18.1 MPa, and a εb value of 2.4 %, being very similar to the values reported in our previous work [40]. The elastic modulus increased when CDs were included in the PHBV matrix. The E value for the PHBV film with 25 wt% γ-CD was 1692 MPa and, for the PHBV film with 15 wt% α-CD, the E value was 1594 MPa. Likewise, the E values were higher in the PHBV films containing CDs with

OEO compared with the films with CDs without OEO, showing an E value of 1472 MPa for the PHBV with 25 wt% γ-CD:OEO and an E value of 1698 MPa for the PHBV with 15 wt% α-CD:OEO. These significant increases of elasticity of PHBV films were induced by the presence of powder particles, that is, CDs, which potentially generated low interfacial interactions between the hydrophilic compounds of γ-CD and α-CD and the hydrophobic PHBV matrix and OEO, producing a reduction in ductility and consequently an increment in mechanical resistance [70]. Indeed, the values of σb decreased in the PHBV containing CDs, with values between 9.04 MPa and 9.83 MPa, while the εb values of PHBV films also decreased from 2.4 % to 0.78 % due to presence of CDs and OEO. As reported earlier by Shin et al. [67], the addition of β-CD containing allyl isothiocyanate (AITC) reduced the tensile strength and elongation by 84 % and 96 %, respectively, of LDPE films obtained by extrusion. In another work, Melendez-Rodriguez et al. [40] reported an improvement of the elastic modulus and tensile strength of electrospun PHBV films when mesoporous silica nanoparticles containing eugenol were incorporated. The PHBV films here-prepared with the inclusion complexes are slightly less deformable and therefore have greater elasticity than films produced using other commercial biopolymers, which facilitates the development of materials for the design of packaging to protect food [69].

Table 5. Mechanical properties in terms of elastic modulus (E), tensile strength at break (σ_b), elongation at break (ε_b) for the electrospun films of poly(3-hydroxybutyrate-*co*-3-hydroxyvalerate) (PHBV) and PHBV containing α- and γ-cyclodextrins (γ-CD and α-CD) and the oregano essential oil (OEO) inclusion complexes (γ-CD:OEO and α-CD:OEO)

Sample	E (MPa)	σ_b(MPa)	ε_b(%)
Neat PHBV	1252 ± 79[a]	18.1 ± 2.1[a]	2.4 ± 0.3[a]
PHBV + 25 wt% γ-CD	1692 ± 434[b]	9.04 ± 4.2[b]	0.78 ± 0.3[b]
PHBV + 25 wt% γ-CD:OEO	1472 ± 136[c]	9.83 ± 0.8[b]	1.25 ± 0.2[c]
PHBV + 15 wt% α-CD	1594 ± 260[d]	9.10 ± 2.5[b]	0.95 ± 0.3[d]
PHBV + 15 wt% α-CD:OEO	1698 ± 764[b]	9.77 ± 4.6[b]	0.85 ± 2.6[e]

a–e Different letters in the same column indicate a significant difference (p < 0.05).

3.7 Antimicrobial activity of the Electrospun CD:OEO Inclusion Complexes-Containing PHBV Films

Table 6 showed the MIC and MBC values of γ-CD:OEO, and α-CD:OEO against *S. aureus* and *E. coli*. In our previous studies [11], it was reported that the MIC and MBC values for pure OEO against *S. aureus* was 0.312 µL/mL and for *E. coli* was 0.625 µL/mL. Results showed that the encapsulation of OEO in CDs increased the antibacterial activity. The MIC and MBC values of γ-CD:OEO against *S. aureus* was 0.039 µg/mL and against *E. coli* was 0.078 µg/mL. In the case of α-CD:OEO, the

MIC ad MBC values were 0.078 µg/mL, against *S. aureus*, and 0.156 µg/mL, against *E. coli*, so that these values agree with those reported by Liang et al. [71] for α-CD:carvacrol (MIC = 0.125 µg/mL). The higher antibacterial activity of the γ-CD:OEO inclusion complex can be attributed to its larger cavity size (see previous Table 1, γ-CD inner diameter is 9.5 Å while α-CD inner diameter is 5.7 Å) and improved encapsulation efficiency and loading capacity (see Table 2) compared with the α-CD:OEO inclusion complex. For both inclusion complexes, *S. aureus* was more sensitive than *E. coli*. In this regard, inclusion complexes have been reported to elevate the aqueous solubility of encapsulated hosts resulting in improved antimicrobial efficiency of EOs and their components at lower concentration [53]. Zhang et al. [72] evaluated the antimicrobial activity of γ-CD:alamethicin complex against *L. monocytogenes*, showing that the use of CD increased the solubility of alamethicin in aqueous medium thereby allowing more alamethicin to interact with the cell membranes resulting in a higher antimicrobial activity.

Table 6. Minimum inhibitory concentration (MIC) and minimum bactericidal concentration (MBC) of the oregano essential oil α- and γ-cyclodextrin inclusion complexes (γ-CD:OEO and α-CD:OEO) against *S. aureus* and *E. coli*

Sample	Bacteria	MIC	MBC
γ-CD:OEO	*E. coli*	0.078 µg/mL	0.078 µg/mL
	S. aureus	0.039 µg/mL	0.039 µg/mL
α-CD:OEO	*E. coli*	0.156 µg/mL	0.156 µg/mL
	S. aureus	0.078 µg/mL	0.078 µg/mL

Figure 9 shows the antibacterial activity results of the PHBV films containing 25 wt% of γ-CD:OEO and 15 wt% of α-CD:OE inclusion complexes in both open and closed systems for up to 15 days. The films used as control, that is, samples without the inclusion complexes, presented an *E. coli* and *S. aureus* growth in the range between 4.16 x 10^6 and 6.05 x 10^6 CFU/mL. As shown in Figure 9a, the reduction versus *S. aureus* and *E. coli* for the films containing 25 wt% of γ-CD:OEO inclusion complex was strong (R ≥ 3), reaching a reduction for up to 3.63 and 3.28 Log_{10} (CFU/mL), respectively, after 15 days of evaluation. The PHBV films containing 15 wt% of α-CD:OEO at day 1 presented a significant inhibition (R ≥ 1 and <3) and at days 3, 8, and 15 the inhibition was strong, showing a reduction of up to 3.15 Log_{10} (CFU/mL) against *S. aureus*. The inhibition achieved for *E. coli* was significant, obtaining a reduction of 2.64 Log_{10} (CFU/mL) at day 15. These results correlate well with the antimicrobial properties included in Table 6 and Figure 9 that show that the antibacterial activity of the γ-CD:OEO inclusion complexes was higher than the α-CD:OEO inclusion complexes.

The reduction of the *S. aureus* and *E. coli* using PHBV films containing 25 wt% γ-CD:OEO inclusion complexes and 15 wt% α-CD:OEO inclusion complexes in a closed system for up to 15 days of analysis are showed in Figure 9b. All values in the closed system showed slightly higher values of reduction compared with the open system due to the release of the volatile compounds that were accumulated in the headspace. The film containing 25 wt% γ-CD:OEO inclusion complexes presented a strong activity against both bacteria during the 15 days of the study (R ≥ 3). The antimicrobial activity for γ-CD:OEO inclusion complexes was higher than α-CD:OEO inclusion complexes, which is in accordance to the characteristics of the γ-type of CD due to its higher solubility and bigger pore size [21]. Moreover, this is produced by the CD inclusion complexes mechanism that increases the solubility and, therefore, provides an efficient release of the hydrophobic agent in bacterial medium [71]. Likewise, Celebioglu et al. [73] observed that films containing HPβ-CD:triclosan and HPγ-CD:triclosan inclusion complexes showed better antibacterial activity against both bacteria compared to the film with uncomplexed pure triclosan. Furthermore, the inhibition of *S. aureus* was slightly higher compared to *E. coli* due to the cellular wall differences between Gram-negative (G-) and Gram-positive (G+) bacteria [54].
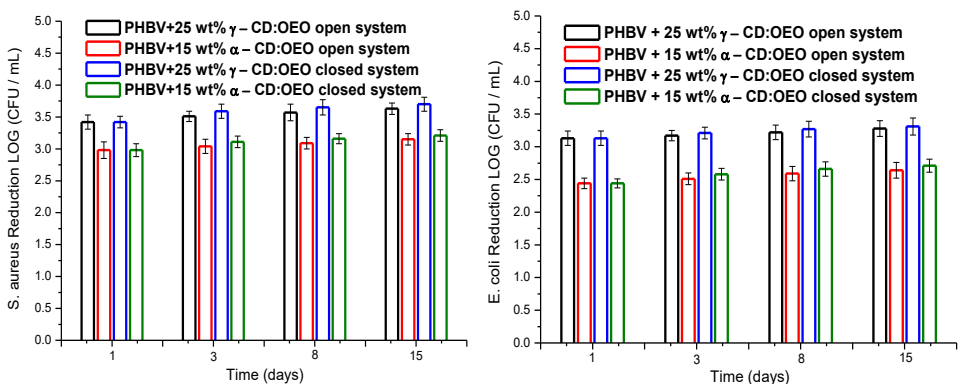
Figure 9. Antimicrobial activity of the electrospun films of poly(3-hydroxybutyrate-*co*-3-hydroxyvalerate) (PHBV) containing 25 wt% γ-cyclodextrin: oregano essential oil inclusion complex (γ-CD:OEO) and 15 wt% α-cyclodextrin: oregano essential oil inclusion complex (α-CD:OEO) in an open and closed system for 15 days against *S. aureus* and *E. coli*.

3.8 Antioxidant Activity of the Electrospun CD:OEO Inclusion Complexes-Containing PHBV Films

The inhibition percentage (%) of DPPH and concentration (eq. trolox/g sample) of DPPH for the pure OEO, γ-CD:OEO inclusion complexes, α-CD:OEO inclusion

complexes, and the electrospun PHBV films containing γ-CD:OEO and α-CD:OEO inclusion complexes are shown in Figure 10 and Table 7. These systems were also evaluated in an open and closed system for 15 days. Neat OEO presented a high percentage of inhibition (91.96 %) attributed to its main active compounds (carvacrol, thymol, p-cymene, and γ-terpinene) [11]. The DPPH inhibition for γ-CD:OEO inclusion complexes was 82.51 % and for α-CD:OEO inclusion complexes it was 76.32 %. Therefore, OEO decreased the percentage of inhibition when it was encapsulated in CDs, which can be related to the encapsulation efficiency and loading capacity of the inclusion complexes reported above in Table 2. The higher antioxidant activity attained with γ-CD:OEO inclusion complexes can be related to its greater encapsulation efficiency when compared with α-CD:OEO inclusion complexes. As indicated by Lu et al. [74], the antioxidant activity of resveratrol in free form showed little difference with that of resveratrol in complex form at the same concentration. The antioxidant activity of biodegradable films is generally proportional to the amount of bioactive compounds added whereas the thermal process to obtain the films can also highly affect bioactivity since most bioactive compounds are sensitive to temperatures above 80 °C [75]. The electrospun films containing OEO, that is, PHBV with 10 wt% OEO, showed a low inhibition of DPPH (24.54 %) with respect to the films containing the inclusion complexes, which were 53.16 % for PHBV with 25 wt% of γ-CD:OEO inclusion complexes and 45.34 % for PHBV with 15 wt% of α-CD:OEO inclusion complexes, at day 1 of evaluation. From day 3, all the PHBV films started to show lower antioxidant activity. In the closed system, the films presented a slightly higher DPPH inhibition than the films of the open system due to the release of OEO volatile compounds to the simulated packaging headspace. For the last day of evaluation, that is, day 15, the PHBV with 10 wt% of OEO films showed an inhibition of DPPH in the open and closed system of 14.90 – 15.24 % (15.75 – 16.47 µg eq trolox/g sample), respectively. The PHBV film containing 15 wt% of α-CD:OEO inclusion complexes presented an inhibition of 36.11 – 37.24 % (38.42 – 39.26 µg eq trolox/g sample) while the PHBV film with 25 wt% of γ-CD:OEO inclusion complexes presented the highest antioxidant activity with a DPPH inhibition of 45.26 – 47.02 % (48.17 – 49.95 µg eq trolox/g sample). These results demonstrate that the here-prepared inclusion complexes can successfully protect the volatile compounds responsible for the active properties of OEO, a thermolabile substance, in a similar way that observed in the antimicrobial test. These results also agree with the research work of Aytac et al. [62] where the antioxidant activity of electrospun fibres of PLA containing β-CD:gallic acid was slightly superior to the fibres of PLA containing neat gallic acid, being this effect attributed to the solubility of gallic acid in alcohols and the position of gallic acid in the cavity

of β-CD. Likewise, Kaolaor et al. [76] determined a high antioxidant activity of β-CD:curcumin in poly(vinyl alcohol) (PVOH) blend films, which was attributed to the complexity of curcumin in the cavity of β-CD. In conclusion, the electrospun films of PHBV incoporating 25 wt% of γ-CD:OEO inclusion complex managed to maintain a high antioxidant activity for a longer period, which indicates that this film can be used in the design of active packaging to maintain the physical, chemical, and microbiological characteristics of the food products [77].
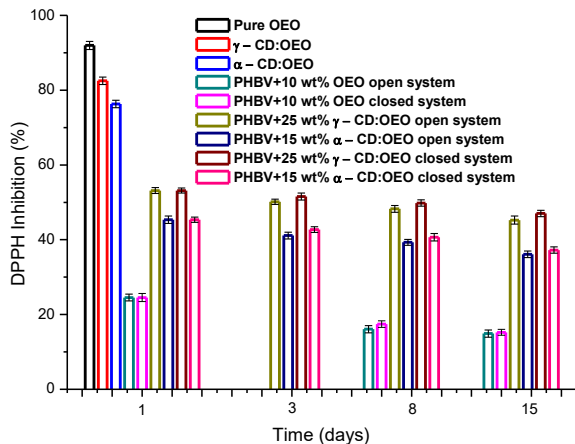
Figure 10. Inhibition percentage (%) of 2,2-diphenyl-1-picrylhydrazyl radical (DPPH) for pure oregano essential oil (OEO), γ- and α-cyclodextrin:oregano essential oil inclusion complex (γ-CD:OEO and α-CD:OEO), and the electrospun poly(3-hydroxybutyrate-co-3-hydroxyvalerate) (PHBV) films containing 25 wt% γ-CD:OEO, and 15 wt% α-CD:OEO inclusion complexes in an open a closed system for 15 days.

Table 7. Concentration (eq. trolox/g sample) of 2,2-diphenyl-1-picrylhydrazyl radical (DPPH) for the electrospun poly(3-hydroxybutyrate-*co*-3-hydroxyvalerate) (PHBV) films containing 25 wt% oregano essential oil γ-cyclodextrin inclusion complex (γ-CD:OEO) and 15 wt% OEO α-cyclodextrin inclusion complex (α-CD:OEO) in an open a closed system for 15 days

Sample	Day	Open system	Closed system
		Eq. trolox/g sample) of DPPH	Eq. trolox/g sample) of DPPH
Pure OEO	1	91.96 ± 0.03^a	---
γ-CD:OEO	1	82.51 ± 0.06^b	---
α-CD:OEO	1	76.32 ± 0.22^c	---
PHBV + 10 wt% OEO	1	26.48 ± 0.04^d	26.48 ± 0.04^d
	8	16.82 ± 0.09^e	17.57 ± 0.04^e
	15	15.75 ± 0.06^e	16.47 ± 0.01^e
PHBV + 25 wt% γ-CD:OEO	1	57.40 ± 0.07^f	57.40 ± 0.07^f
	3	53.24 ± 0.17^g	56.03 ± 0.09^f
	8	51.42 ± 0.17^g	52.95 ± 0.09^g
	15	48.17 ± 0.09^h	49.95 ± 0.51^h
PHBV + 15 wt% α-CD:OEO	1	47.48 ± 0.07^h	$47.48 \pm 0.07^{h,i}$
	3	41.86 ± 0.09^i	45.89 ± 0.58^i
	8	40.13 ± 0.08^i	$42.91 \pm 0.17^{i,j}$
	15	38.42 ± 0.09^i	39.26 ± 0.17^j

Means ± S.D.

a-j Different letters indicate a significant difference among the samples ($p < 0.05$).

4 Conclusions

Herein, KM and FDM were explored for the encapsulation of OEO in two cyclodextrins types (α-CD and γ-CD). The results of this study showed that the encapsulation efficiency was influenced by the encapsulation method and the cyclodextrin type. Although both methods showed high encapsulation efficiencies, KM revealed to be the most efficient method for encapsulating OEO in the CD cavities, and it also offers some other advantages in terms of rapidity (KM: 18 minutes versus FDM > 48 h for the formation of inclusion complex), and the desired characteristics of the final product since the γ-CD:OEO (80:20 wt/wt) showed EE and LC values of 98.5 % and 19.6 %, respectively. The α-CD:OEO and γ-CD:OEO inclusion complexes presented high antimicrobial and antioxidant activities, which allowed their incorporation into PHBV fibres by electrospinning and subsequent annealing for film formation. The best concentration of α-CD:OEO and γ-CD:OEO inclusion complexes for homogeneous and continuous film formation were observed at 15 wt% α-CD:OEO and 25 wt% γ-CD:OEO inclusion complexes. The films showed high contact transparency whereas the mechanical properties were improved by the addition of the α-CD:OEO and γ-CD:OEO inclusion complexes in the PHBV matrix. The antimicrobial and antioxidant activities for the γ-CD:OEO inclusion complexes were higher than for the α-CD:OEO inclusion complexes, which is in accordance to the higher solubility of OEO in the γ-type of CD and its bigger pore size. The antimicrobial and antioxidant activity of the bioactive films were successfully maintained for up to 15 days due to the high protection offerered by the encapsulation system. In the light of the aforementioned findings, the here-developed electrospun CD:OEO inclusion complexes-containing PHBV films show a great deal of potential to be used in biodegradable active packaging applications to extend the shelf life of foodstuff.

5 References

1. Bakkali F, Averbeck S, Averbeck D, Idaomar M. Biological effects of essential oils - A review. *Food Chem. Toxicol.* **2008**, 46(2), 446-75.
2. Ribeiro-Santos R, Andrade M, Melo NRD, Sanches-Silva A. Use of essential oils in active food packaging: Recent advances and future trends. *Trends Food Sci. Technol.* **2017**, *61*, 132-40.
3. Owen L, Laird K. Synchronous application of antibiotics and essential oils: Dual mechanisms of action as a potential solution to antibiotic resistance. *Crit. Rev. Microbiol.* **2018**, *44*(4), 414-35.
4. Sharifi-Rad J, Sureda A, Tenore GC, Daglia M, Sharifi-Rad M, Valussi M, Tundis R, Sharifi-Rad M, Loizzo MR, Oluwaseun Ademiluyi A, Sharifi-Rad R, Ayatollahi SA, Iriti M. Biological activities of essential oils: From plant chemoecology to traditional healing systems. *Molecules* **2017**, *22*(1).
5. Research GV. Essential oils market size, share & trends analysis report by application (cleaning & home, medical, food & beverages, spa & relaxation), by product, by sales channel, and segment forecasts (research). (978-1-68038-549-6). **2018**.
6. Bakhtiary F, Sayevand HR, Khaneghah AM, Haslberger AG, Hosseini H. Antibacterial efficacy of essential oils and sodium nitrite in vacuum processed beef fillet. *Appl. food biotechnol.* **2018**, *5*(1), 1-10.
7. Prakash B, Kedia A, Mishra PK, Dubey NK. Plant essential oils as food preservatives to control moulds, mycotoxin contamination and oxidative deterioration of agri-food commodities - potentials and challenges. *Food Control* **2015**, *47*, 381-91.
8. Prakash B, Singh P, Kedia A, Dubey NK. Assessment of some essential oils as food preservatives based on antifungal, antiaflatoxin, antioxidant activities and in vivo efficacy in food system. *Food Res. Int.* **2012**, *49*(1), 201-8.
9. Raut JS, Karuppayil SM. A status review on the medicinal properties of essential oils. *Ind. Crops Prod.* **2014**, *62*, 250-64
10. De Vincenzi M, Stammati A, De Vincenzi A, Silano M. Constituents of aromatic plants: Carvacrol. *Fitoterapia* **2004**, *75*(7-8), 801-4.
11. Figueroa-Lopez KJ, Vicente AA, Reis MAM, Torres-Giner S, Lagaron JM. Antimicrobial and antioxidant performance of various essential oils and natural extracts and their incorporation into biowaste derived poly(3-hydroxybutyrate-co-3-hydroxyvalerate) layers made from electrospun ultrathin fibers. *Nanomaterials* **2019**, *9*(2)
12. Ju J, Chen X, Xie Y, Yu H, Guo Y, Cheng Y, Qian H, Yao W. Application of essential oil as a sustained release preparation in food packaging. *Trends Food Sci. Technol.* **2019**, *92*, 22-32.
13. Beirão-da-Costa S, Duarte C, Bourbon AI, Pinheiro AC, Januário MIN, Vicente AA, Beirão-da-Costa ML, Delgadillo I. Inulin potential for encapsulation and controlled delivery of oregano essential oil. *Food Hydrocolloids* **2013**, *33*(2), 199-206.
14. Hosseini SF, Zandi M, Rezaei M, Farahmandghavi F. Two-step method for encapsulation of oregano essential oil in chitosan nanoparticles: Preparation, characterization and in vitro release study. *Carbohydr. Polym.* **2013**, *95*(1), 50-6.
15. Crini G. Review: A history of cyclodextrins. *Chem. Rev.* **2014**, 114(21), 10940-75.
16. Marques HMC. A review on cyclodextrin encapsulation of essential oils and volatiles. *Flavour Fragrance J.* **2010**, *25*(5), 313-26.
17. Sherry M, Charcosset C, Fessi H, Greige-Gerges H. Essential oils encapsulated in liposomes: A review. *J. Liposome Res.* **2013**, *23*(4), 268-75.
18. Sagiri SS, Anis A, Pal K. Review on encapsulation of vegetable oils: Strategies, preparation methods, and applications. *Polym. Plast. Technol. Eng.* **2016**, *55*(3), 291-311.
19. Del Valle EMM. Cyclodextrins and their uses: A review. *Process Biochem.* **2004**, *39*(9), 1033-46.
20. Harada A, Suzuki S, Okada M, Kamachi M. Preparation and characterization of inclusion complexes of polyisobutylene with cyclodextrins. *Macromolecules* **1996**, *29*(17), 5611-4.
21. Szejtli J. Introduction and general overview of cyclodextrin chemistry. *Chem. Rev.* **1998**, *98*(5), 1743-53.
22. Wang CX, Chen SL. Fragrance-release property of ß-cyclodextrin inclusion compounds and their application in aromatherapy. *J. Ind. Text* **2005**, *34*(3), 157-66.
23. Bilia AR, Guccione C, Isacchi B, Righeschi C, Firenzuoli F, Bergonzi MC. Essential oils loaded in nanosystems: A developing strategy for a successful therapeutic approach. *Evid. Based Complement Altern. Med.* **2014**.
24. Loftsson T, Brewster ME. Pharmaceutical applications of cyclodextrins. 1. drug solubilization and stabilization. *J. Pharm. Sci.* **1996**, *85*(10), 1017-25.

25. Gao N, Yang J, Wu Y, Yue J, Cao G, Zhang A, Ye L, Feng Z. β-Cyclodextrin functionalized coaxially electrospun poly(vinylidene fluoride)@ polystyrene membranes with higher mechanical performance for efficient removal of phenolphthalein. *React Funct. Polym.* **2019**, *141*, 100-11.
26. Li D, Xia Y. Electrospinning of nanofibers: Reinventing the wheel? *Adv. Mater*. **2004**, 16(14), 1151-70.
27. Torres-Giner S, Pérez-Masiá R, Lagaron JM. A review on electrospun polymer nanostructures as advanced bioactive platforms. *Polym. Eng. Sci.* **2016**, *56*(5), 500-27.
28. Torres-Giner S, Wilkanowicz S, Melendez-Rodriguez B, Lagaron JM. Nanoencapsulation of aloe vera in synthetic and naturally occurring polymers by electrohydrodynamic processing of interest in food technology and bioactive packaging. *J. Agric. Food Chem*. **2017**, *65*(22), 4439-48.
29. Kayaci F, Uyar T. Encapsulation of vanillin/cyclodextrin inclusion complex in electrospun polyvinyl alcohol (PVA) nanowebs: Prolonged shelf-life and high temperature stability of vanillin. *Food Chem.* **2012**, *133*(3), 641-9.
30. Torres-Giner S, Busolo M, Cherpinski A, Lagaron JM. CHAPTER 10 electrospinning in the packaging industry electrospinning: From basic research to commercialization. **2018**.
31. Quiles-Carrillo L, Montanes N, Lagaron JM, Balart R, Torres-Giner S. Bioactive multilayer polylactide films with controlled release capacity of gallic acid accomplished by incorporating electrospun nanostructured coatings and interlayers. *Appl. Sci.* **2019**, *9*(3)
32. Torres-Giner S, Martinez-Abad A, Lagaron JM. Zein-based ultrathin fibers containing ceramic nanofillers obtained by electrospinning. II. mechanical properties, gas barrier, and sustained release capacity of biocide thymol in multilayer polylactide films. *J. Appl. Polym. Sci*. **2014**, *131*(18), 9270-6.
33. Cherpinski A, Torres-Giner S, Cabedo L, Lagaron JM. Post-processing optimization of electrospun submicron poly(3-hydroxybutyrate) fibers to obtain continuous films of interest in food packaging applications. *Food Addit. Contam. Part A Chem. Anal Control Exposure Risk Assess* **2017**, *34*(10), 1817-30.
34. Zhang J, Shishatskaya EI, Volova TG, da Silva LF, Chen G-. Polyhydroxyalkanoates (PHA) for therapeutic applications. *Mater Sci. Eng. C* **2018**, *86*, 144-50.
35. Dietrich K, Dumont M-, Del Rio LF, Orsat V. Sustainable PHA production in integrated lignocellulose biorefineries. *New Biotechnol.* **2019**, *49*, 161-8.
36. Santos EH, Kamimura JA, Hill LE, Gomes CL. Characterization of carvacrol beta-cyclodextrin inclusion complexes as delivery systems for antibacterial and antioxidant applications. *LWT - Food Sci. Technol*. **2015**, *60*(1), 583-92.
37. Petrovic GM, Stojanovic GS, Radulovic NS. Encapsulation of cinnamon oil in β-cyclodextrin. *J. Med. Plants Res.* **2010**, *4*(14), 1382-90.
38. Haloci E, Toska V, Shkreli R, Goci E, Vertuani S, Manfredini S. Encapsulation of satureja montana essential oil in β-cyclodextrin. *J. Incl. Phenom. Macrocyclic Chem*. **2015**, *80*(1-2), 147-53.
39. Hedges AR. Industrial applications of cyclodextrins. *Chem. Rev.* **1998**, *98*(5), 2035-44.
40. Melendez-Rodriguez B, Figueroa-Lopez KJ, Bernardos A, Martínez-Máñez R, Cabedo L, Torres-Giner S, Lagaron JM. Electrospun antimicrobial films of poly(3-hydroxybutyrate-co-3-hydroxyvalerate) containing eugenol essential oil encapsulated in mesoporous silica nanoparticles. *Nanomaterials* **2019**, *9*(2).
41. Figueroa-Lopez KJ, Andrade-Mahecha MM, Torres-Vargas OL. Development of antimicrobial biocomposite films to preserve the quality of bread. *Molecules* **2018**, *23*(1).
42. Figueroa-Lopez KJ, Castro-Mayorga JL, Andrade-Mahecha MM, Cabedo L, Lagaron JM. Antibacterial and barrier properties of gelatin coated by electrospun polycaprolactone ultrathin fibers containing black pepper oleoresin of interest in active food biopackaging applications. *Nanomaterials* **2018**, *8*(4).
43. Torres-Giner S, Torres A, Ferrándiz M, Fombuena V, Balart R. Antimicrobial activity of metal cation-exchanged zeolites and their evaluation on injection-molded pieces of bio-based high-density polyethylene. *J. Food Saf.* **2017**, *37*(4).
44. Busolo MA, Lagaron JM. Antioxidant polyethylene films based on a resveratrol containing clay of interest in food packaging applications. *Food Packaging Shelf Life* **2015**, *6*, 30-41.
45. Ozdemir N, Pola CC, Teixeira BN, Hill LE, Bayrak A, Gomes CL. Preparation of black pepper oleoresin inclusion complexes based on beta-cyclodextrin for antioxidant and antimicrobial delivery applications using kneading and freeze drying methods: A comparative study. *LWT - Food Sci. Technol*. **2018**, *91*, 439-45.
46. Ponce Cevallos PA, Buera MP, Elizalde BE. Encapsulation of cinnamon and thyme essential oils components (cinnamaldehyde and thymol) in β-cyclodextrin: Effect of interactions with water on complex stability. J. Food Eng. **2010**, *99*(1), 70-5.

47. Hill LE, Gomes C, Taylor TM. Characterization of beta-cyclodextrin inclusion complexes containing essential oils (trans-cinnamaldehyde, eugenol, cinnamon bark, and clove bud extracts) for antimicrobial delivery applications. *LWT - Food Sci. Technol*. **2013**, *51*(1), 86-93.

48. Guimarães AG, Oliveira MA, Alves RDS, Menezes PDP, Serafini MR, De Souza Araújo AA, Bezerra DP, Quintans LJ. Encapsulation of carvacrol, a monoterpene presents in the essential oil of oregano, with β-cyclodextrin, improves the pharmacological response on cancer pain experimental protocols. *Chem. Biol. Interact*. **2015**, *227*, 69-76.

49. Seo E-, Min S-, Choi M-. Release characteristics of freeze-dried eugenol encapsulated with β-cyclodextrin by molecular inclusion method. *J. Microencapsulation* **2010**, *27*(6), 496-505.

50. Gaur S, Lopez EC, Ojha A, Andrade JE. Functionalization of lipid-based nutrient supplement with β-cyclodextrin inclusions of oregano essential oil. *J. Food Sci.* **2018**, *83*(6), 1748-56.

51. Saokham P, Muankaew C, Jansook P, Loftsson T. Solubility of cyclodextrins and drug/cyclodextrin complexes. *Molecules* **2018**, *23*(5).

52. Rusa CC, Bullions TA, Fox J, Porbeni FE, Wang X, Tonelli AE. Inclusion compound formation with a new columnar cyclodextrin host. *Langmuir* **2002**, *18*(25), 10016-23.

53. Das S, Subuddhi U. Studies on the complexation of diclofenac sodium with β-cyclodextrin: Influence of method of preparation. *J. Mol. Struct.* **2015**, *1099*, 482-9.

54. Rakmai J, Cheirsilp B, Mejuto JC, Torrado-Agrasar A, Simal-Gándara J. Physico-chemical characterization and evaluation of bio-efficacies of black pepper essential oil encapsulated in hydroxypropyl-beta-cyclodextrin. *Food Hydrocolloids* **2017**, *65*, 157-64.

55. Shan L, Tao E-, Meng Q-, Hou W-, Liu K, Shang H-, Tang J-, Zhang W-. Formulation, optimization, and pharmacodynamic evaluation of chitosan/phospholipid/β-cyclodextrin microspheres. *Drug Des. Dev. Ther.* **2016**, *10*, 417-29.

56. Harada A, Kamachi M. Complex formation between poly (ethylene glycol) and α-cyclodextrin. *Macromolecules* **1990**, *23*(10), 2821-3.

57. Harada A, Li J, Kamachi M. The molecular necklace: A rotaxane containing many threaded α-cyclodextrins. *Nature* **1992**, *356*(6367), 325-7.

58. Harada A, Li J, Kamachi M. Synthesis of a tubular polymer from threaded cyclodextrins. *Nature* **1993**, *364*(6437), 516-8.

59. Ceccato M, Lo Nostro P, Rossi C, Bonechi C, Donati A, Baglioni P. Molecular dynamics of novel α-cyclodextrin adducts studied by 13C-NMR relaxation. J. Phys. Chem. B. 1997, *101*(26), 5094-9.

60. Bonini, M.; Rossi, S.; Karlsson, G.; Almgren, M.; Lo Nostro, P.; Baglioni, P. Self-Assembly of β-Cyclodextrin in Water. Part 1: Cryo-TEM and Dynamic and Static Light Scattering. *Langmuir* **2006**, *22*, 1478-1484.

61. Topuz F, Uyar T. Electrospinning of nanocomposite nanofibers from cyclodextrin and laponite. *Compos. Commun.* **2019**, *12*, 33-8.

62. Aytac Z, Ipek S, Durgun E, Tekinay T, Uyar T. Antibacterial electrospun zein nanofibrous web encapsulating thymol/cyclodextrin-inclusion complex for food packaging. *Food Chem*. **2017**, *233*, 117-24.

63. Ashori A, Jonoobi M, Ayrilmis N, Shahreki A, Fashapoyeh MA. Preparation and characterization of polyhydroxybutyrate-co-valerate (PHBV) as green composites using nano reinforcements. Int. *J. Biol. Macromol.* **2019**, *136*, 1119-24.

64. Campos EVR, Proença PLF, Oliveira JL, Melville CC, Vechia JFD, De Andrade DJ, Fraceto LF. Chitosan nanoparticles functionalized with β-cyclodextrin: A promising carrier for botanical pesticides. *Sci. Rep.* **2018**, *8*(1).

65. Giordano F, Novak C, Moyano JR. Thermal analysis of cyclodextrins and their inclusion compounds. *Thermochim. Acta* **2001**, *380*(2), 123-51.

66. Nakanishi K, Masukawa T, Nadai T, Yoshii K, Okada S, Miyajima K. Sustained release of flufenamic acid from a drug-triacetyl-β- cyclodextrin complex. *Biol. Pharm. Bull.* **1997**, *20*(1), 66-70.

67. Shin J, Kathuria A, Lee YS. Effect of hydrophilic and hydrophobic cyclodextrins on the release of encapsulated allyl isothiocyanate (AITC) and their potential application for plastic film extrusion. *J. Appl. Polym. Sci*. **2019**, *136*(42).

68. Yildiz ZI, Celebioglu A, Kilic ME, Durgun E, Uyar T. Menthol/cyclodextrin inclusion complex nanofibers: Enhanced water-solubility and high-temperature stability of menthol. *J. Food Eng*. **2018**, *224*, 27-36.

69. Quiles-Carrillo L, Montanes N, Lagaron JM, Balart R, Torres-Giner S. In situ compatibilization of biopolymer ternary blends by reactive extrusion with low-functionality epoxy-based Styrene–Acrylic oligomer. *J. Polym. Environ*. **2019**, *27*(1), 84-96.

70. Zainuddin S, Kamrul Hasan SM, Loeven D, Hosur M. Mechanical, fire retardant, water absorption and soil biodegradation properties of poly(3-hydroxy-butyrate-co-3-valerate) nanofilms. *J Polym. Environ.* **2019**, *27*(10), 2292-304.

71. Liang H, Yuan Q, Vriesekoop F, Lv F. Effects of cyclodextrins on the antimicrobial activity of plant-derived essential oil compounds. *Food Chem.* **2012**, *135*(3), 1020-7.

72. Zhang M, Wang J, Lyu Y, Fitriyanti M, Hou H, Jin Z, Zhu X, Narsimhan G. Understanding the antimicrobial activity of water soluble γ-cyclodextrin/alamethicin complex. *Colloids Surf. B Biointerfaces* **2018**, *172*, 451-8.

73. Celebioglu A, Umu OCO, Tekinay T, Uyar T. Antibacterial electrospun nanofibers from triclosan/cyclodextrin inclusion complexes. *Colloids Surf. B. Biointerfaces* **2014**, *116*, 612-9.

74. Lu Z, Cheng B, Hu Y, Zhang Y, Zou G. Complexation of resveratrol with cyclodextrins: Solubility and antioxidant activity. *Food Chem.* **2009**, *113*(1), 17-20.

75. Jouki M, Yazdi FT, Mortazavi SA, Koocheki A. Quince seed mucilage films incorporated with oregano essential oil: Physical, thermal, barrier, antioxidant and antibacterial properties. *Food Hydrocolloids* **2014**, *36*, 9-19.

76. Kaolaor A, Phunpee S, Ruktanonchai UR, Suwantong O. Effects of β-cyclodextrin complexation of curcumin and quaternization of chitosan on the properties of the blend films for use as wound dressings. *J. Polym. Res.* **2019**, *26*(2).

77. Robertson GL. Food Packaging: Principles and Practice. **1993**.

CHAPTER V

Development of electrospun poly(3-hydroxybutyrate-*co*-3-hydroxyvalerate) monolayers containing eugenol and their application in multilayer antimicrobial food packaging

K.J. Figueroa-Lopez, L. Cabedo, J.M. Lagaron, and S. Torres-Giner

Development of electrospun poly(3-hydroxybutyrate-*co*-3-hydroxyvalerate) monolayers containing eugenol and their application in multilayer antimicrobial food packaging

Abstract

In this research, different contents of eugenol in the 2.5-25 wt.% range were first incorporated into ultrathin fibers of poly(3-hydroxybutyrate-co-3-hydroxyvalerate) (PHBV) by electrospinning and then subjected to annealing to obtain antimicrobial monolayers. The most optimal concentration of eugenol in PHBV monolayer was 15 wt.% since it showed high electrospinnability and thermal stability and also yielded the highest bacterial reduction against *Staphylococcus aureus* (*S. aureus*) and *Escherichia coli* (*E. coli*). This eugenol-containing monolayer was then selected to be applied as an interlayer between a structural layer made of a cast-extruded poly(3-hydroxybutyrate) (PHB) sheet and a commercial PHBV film as the food contact layer. The whole system was, thereafter, annealed at 160 °C to develop multilayer active packaging material. The resultant multilayers showed high hydrophobicity, strong adhesion and mechanical resistance, and improved barrier properties against water vapor and limonene vapors. The antimicrobial activity of the multilayer structure was also evaluated in both open and closed systems for up to 15 days, showing significant reductions (R ≥ 1 and < 3) for the two strains of food-borne bacteria. Higher inhibition values were particularly attained against *S. aureus* due to the higher activity of eugenol in the cell membrane of Gram positive (G+) bacteria. The multilayer also provided the highest antimicrobial activity for the closed system, which better resembles the actual packaging and it was related to the headspace accumulation of the volatile compounds. Hence, the here-developed multilayers fully based on polyhydroxyalkanoates (PHAs) show a great deal of potential for antimicrobial packaging applications using biodegradable materials to increase both quality and safety of food products.

Keywords: PHA, essential oils, multilayer, antimicrobial activity, electrospinning.

1   Introduction

Active antimicrobial packaging is one of the most relevant emerging technologies in the food industry. It aims to control enzymatic, chemical, physical, and microbiological reactions that deteriorate food through the inclusion of active substances and their controlled release to the surface in contact with food [1,2]. Biodegradable polymers have recently emerged as an alternative to gradually replace the use of petrochemical polymers in packaging applications, which are known to generate irreversible environmental damage [3,4]. Furthermore, polymers used in packaging can also be obtained from the valorization of food-processing by-products and agricultural or industrial wastes, being more sustainable and cost-effective [5]. Polyhydroxyalkanoates (PHAs) are among the most commonly used thermoplastic biopolyesters in food packaging applications because they have similar properties to some conventional non-degradable plastics [6,7]. PHAs can be obtained from over 155 monomer subunits through fermentation by some bacteria from different renewable carbon sources that are accumulated as intracellular storage granules [8]. For instance, Bhatia et al. [9] obtained high biomass (Yx/s, 0.31 g/g) and PHA (Yp/s, 0.14 g/g) yields using Ralstonia eutropha 5119 bacteria and Miscanthus biomass hydrolysate (MBH) as carbon source. In another research work, Bhatia et al. [10] obtained a high PHB production (1.24 g/L) with 2 % (w/v) starch as carbon source, using an *Escherichia coli* strain produced using different plasmids containing the amylase gene of Panibacillus sp. and PHB synthesis genes from Ralstonia eutropha. Park et al. [11] studied different PHA-producing strains, concluding that Halomonas sp. YLGW01 produced the highest amount of PHB [94.6 ± 1.8 % (w/w)] using fructose as carbon source. Hong et al. [12] determined the optimal growth and production conditions, environments with different salinity, carbon sources, and nitrogen sources of the Vibrio proteolyticus strain in the PHA production. It was concluded that the use of a medium containing 2 % (w/v) fructose, 0.3 % (w/v) yeast extract, and 5 % (w/v) sodium chloride (NaCl) in M9 minimal medium resulted in high PHA (54.7 %) and biomass (4.94 g/L) contents. The structure and physical properties of PHAs vary depending on the bacteria specie, substrate (carbon source), and cultivation conditions [13]. PHAs are a typically linear aliphatic polyesters consisting of repetitive hydroxy acids (HAs) connected together by an ester bond [14]. According to the number of carbon atoms in the monomers, PHAs are classified in groups of short chain length (scl-PHAs), which consists of 3-5 carbon atoms (C3-C5), and medium chain length (mcl-PHAs) with 6-14 carbon atoms (C6-C14) [15,16]. Microbial synthesis of PHAs have the capacity to produce copolymers from mixed substrates by different methods, such as metabolic engineering, co-culture of microbes, and feeding of the various precursors during fermentation [17-19]. Typical

examples of scl-PHAs are poly(3-hydroxybutyrate) (PHB), poly(3-hydroxybutyrate-co-3-hydroxyvalerate (PHBV), and poly(3-hydroxybutyrate-co-4-hydroxybutyrate) [P(3HB-co-4HB)]. The most representative mcl-PHAs are poly(3-hydroxybutyrate-co-3-hydroxyhexanoate) [P(3HB-co-3HHx)] and poly(3-hydroxyhexanoate-co-3-hydroxyoctanoate) [P(3HHx-co-3HO)] [20,21]. PHB is the most abundant type of PHA but it is brittle and shows low thermal stability, which limits their industrial applications. For this reason, PHB is currently being replaced by PHBV due to the better processability and physical properties of the copolyester, such as higher flexibility improved toughness, and lower melting point and level of crystallinity [22,23]. PHAs can be processed by different melt-processing techniques such as injection molding [24], extrusion [25], and compression molding [26]. Electrospinning is one of latest technologies to process PHAs in the form of monolayer and multilayer films by the application of high electric voltages and annealing treatments, having the main advantage to operate at room temperatures [27,28]. The latter process, therefore, opens up the incorporation thermolabile substances into electrospun biopolymer films including natural extracts [29].

Essential oils are natural substances obtained by secondary metabolite of plants such as flowers, stems, leaves, seeds, etc. [30]. Different studies have reported multiple active and bioactive properties for essential oils, including antibacterial, antimitotic, antisepticise, and antiviral properties, due to the presence of aldehydes and phenols, for instance carvacrol, eugenol or thymol [31]. Among them, eugenol ($C_{10}H_{12}O_2$) is the main active phenolic compound present in the clove essential oil [32], which shows strong antibacterial activity against a wide range of Gram negative (G-) bacteria, including *Escherichia coli* (*E. coli*), *Salmonella typhimurium*, *Pseudomonas aeruginosa*, and also Gram positive (G+) bacteria, including *Staphylococcus aureus* (*S. aureus*), *Listeria monocytogenes* (*L. monocytogenes*) [33,34]. The action of essential oils against bacteria is based on interfering chemically with the synthesis or function of principal components of bacteria as well as blocking their antimicrobial resistance mechanisms. In this way, these natural antimicrobial substances are known to affect the bacterial protein biosynthesis, deoxyribonucleic acid (DNA) replication and repair, destroy cell membrane and wall or inhibit metabolism and structural integrity [35-38]. However, due to its high volatility, water insolubility, poor oxidation, and high thermal sensitivity, essential oils habitually need to be protected to preserve their activity [39]. In this way, the electrospinning technology offers multiples advantages for the nanoencapsulation of essential oils such as the use of mild temperatures [40] and materials with high surface-to-volume ratios and controlled porosity [41,42].

Multilayer films are combinations of different layers typically based on materials with dissimilar properties glued together to fulfill functions that monomaterials do not offer [43,44]. Multilayers are often composed of "structural" and "barrier" layers, usually on the outside and the inside, respectively. An "active" layer can additionally be added either on the outside or inside, depending on the application needs. Layers of adhesive polymers, also named "tie layers", are used as glue between the different layers where necessary. The purpose of using multilayer systems is to improve the properties of the food packaging due to the majority of polymers, particularly biopolymers, and paper present poor water resistance, low oxygen barrier, and reduced mechanical performance [45-47]. As a result, the multilayer present higher advantages than monolayer systems in terms of industrial process and applications in food packaging [48,49]. In this context, the electrospinning technology can result very effective to prepare active and bioactive multilayer structures with sustained released capacity by means of coatings or interlayers containing entrapped substances with functionality [50]. For instance, electrospun zein fibers in the form of coatings [51] or interlayers [52] have significantly improved the gas barrier properties and provided active performance to polylactide (PLA) films. Similarly, Fabra et al. [53,54] followed the same strategy to develop multilayer structures based on PHAs biopolyesters and electrospun zein nanofibers. Cherpinski et al. improved the water resistance of paper [55] and nanopaper [56] by coatings of electrospun films of PHB and other biopolymers. Quiles-Carrillo et al. [57] produced bioactive films with sustained antioxidant release capacity by means of multilayer structures of PLA containing electrospun fibers with gallic acid (GA). More recently, Akinalan Balik et al. [58] developed high-barrier multilayer films using an electrospun pectin-based film applied as an interlayer between two external layers of PHBV.

The main objective of this study was to develop a novel multilayer system based on PHBV with antimicrobial properties by electrospinning. To achieve this end, electrospun mats of PHBV fibers containing different amounts of eugenol were characterized and the most efficient was selected to coat PHB sheets. Thereafter, a food contact layer of PHB was put on the eugenol-containing electrospun layer and the whole structure was subjected to annealing at mild temperature to form a multilayer without the need to use a tie layer. The morphological, thermal, mechanical adhesion, and barrier properties to water and limonene vapors were determined. Finally, the antimicrobial activity of the multilayers against *S. aureus* and *E. coli* in both an open and closed system was tested for 15 days in order to ascertain their potential in active food packaging.

2 Materials and Methods

2.1 Materials

Bacterial aliphatic copolyester PHBV was ENMAT™ Y1000P, produced by Tianan Biologic Materials (Ningbo, China) and supplied by Ocenic Resins SL (Valencia, Spain). The biopolymer resin was delivered in pellets with a true density of 1.23 g/cm³. The molar fraction of HV in the copolymer is 2 – 3 %, while the molecular weight (MW) is approximately 2.8×10^5 g/mol. Bacterial aliphatic homopolyester PHB was provided in pellets by Biomer (Krailling, Germany) as P226F. It has a density of 1.25 g/cm³, a melt flow rate (MFR) of 10 g/10 min at 180 °C and 5 kg, a MW of 500 kDa, and a polydispersity index (PI) of 2. A 25-µm film of PHBV with a molar fraction of HV of 8 mol.% was purchased at GoodFellow Cambridge Limited (Huntindgon, UK) with the commercial reference BV301025. All the PHA grades are certified by the manufacturers both as compostable and food contact. 2,2,2-trifluorethanol (TFE), with 99 % purity, and eugenol, ReagentPlus®, with 99 % purity, were both purchased from Sigma-Aldrich S.A. (Madrid, Spain). Glycerol, phosphate buffered saline (PBS), and tryptic soy broth (TSB) were provided by Conda Laboratories (Madrid, Spain).

2.2 Preparation of the structural layer by cast extrusion

The PHB pellets were cast-extruded into sheets using a cast-roll machine MINI CAST 25 from EUR.EX.MA (Venegono, Italy). The extrusion speed was set at 25 rpm and the temperature profile, from the feeding zone to die head, was adjusted to 180–175–170–170–165–165–160 °C. PHBV sheets with an average thickness of ~500 µm were obtained by adjusting the speed of the calendar and the drag.

2.3 Preparation of the multilayers by electrospinning and annealing

2.3.1 *Solutions for electrospinning*

Different solutions for electrospinning were prepared by dissolving 10 % in weight (wt.%) of PHBV in TFE at room temperature. Eugenol was incorporated into the solutions at 2.5 wt.%, 5 wt.%, 10 wt.%, 15 wt.%, 20 wt.%, and 25 wt.% in relation to the PHBV content.

2.3.2　Electrospinning

The PHBV solutions containing eugenol were processed in a Fluidnatek® LE10 electrospinning benchtop equipment from Bioinicia S.L. (Valencia, Spain) with a variable high-voltage $0 - 30$ kV power supply and a motorized scanning injector. The PHBV solutions were transferred to a 30-mL plastic syringe and coupled by a Teflon tube to a stainless-steel needle ($\emptyset = 0.9$ mm) that was connected to the power supply. Thus, each PHBV solution was electrospun at room temperature, that is, 25 °C, for 2 h under a steady flow-rate of 6 mL/h, scanning horizontally toward a cast-extruded PHB sheet attached to the metallic collector. The applied voltage was 15 kV while the distance between the injector and collector was optimal at 15 cm. An electrospun mat of PHBV without eugenol was also deposited on the PHB sheets in the same conditions to produce the control multilayer. The same process was also carried out to collect individual interlayers on the collector without using the PHB sheets. In all cases, the resultant electrospun materials were stored in a desiccator at 25 °C and 0 % relative humidity (RH) for, at least, 48 h.

2.3.3　Annealing

The multilayer systems were produced according to the process schemed in Figure 1. Briefly, once the electrospun PHBV mats containing eugenol were coated on the cast-extruded PHB sheets, the food contact film of PHBV was deposited on the electrospun layer and the whole system was subjected to annealing. This thermal post-treatment was performed at 160 °C, below the biopolymer's melting point, for 10 ± 1 s, without pressure, using a hydraulic press 4122-model from Carver, Inc. (Wabash, IN, USA). The resultant multilayers were finally air cooled at room temperature. These conditions were selected based on our previous studies for thermally post-processing PHAs [59]. The same process was applied to single electrospun monolayers of PHBV for comparison purposes.
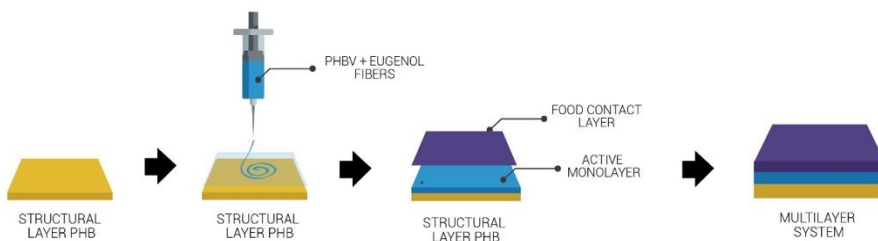
Figure 1. Process to obtain the poly(3-hydroxybutyrate) (PHB) sheet/electrospun poly(3-hydroxybutyrate-co-3-hydroxyvalerate) (PHBV) interlayer containing eugenol/PHBV film.

2.4 Characterization of the electrospun monolayers and multilayers

2.4.1 Thickness

Before testing, the thickness of all the monolayer and multilayer structures was measured using a digital micrometer (S00014, Mitutoyo, Corp., Kawasaki, Japan) with ± 0.001 mm accuracy. Measurements were performed and averaged in five different points with two in each end and one in the middle.

2.4.2 Morphology

The morphology of the electrospun fibers and the cross-sections of the films were examined by scanning electron microscopy (SEM). Cryofracture of the films was carried by immersing the samples in liquid nitrogen. The SEM micrographs were obtained using a Hitachi S-4800 electron microscope (Tokyo, Japan) at an accelerating voltage of 10 kV and a working distance of 8 – 10 mm. Prior to examination, all the samples were fixed to beveled holders using a conductive double-sided adhesive tape and sputtered for 3 min with a mixture of gold–palladium mixture under vacuum. Fiber sizes and film thickness were determined by means of the ImageJ 1.50i software using the SEM micrographs in their original magnification. At least 25 micrographs of each sample were used for the measurements.

2.4.3 Thermal analysis

Thermogravimetric analysis (TGA) of the neat eugenol oil and PHBV films was performed under nitrogen atmosphere in a Thermobalance TG-STDA Mettler Toledo model TGA/STDA851e/LF/1600 analyzer (Greifensee, Switzerland). TGA curves were obtained after conditioning the samples in the sensor for 5 min at 30 °C. The samples were then heated from 25 °C to 700 °C at a heating rate of 10 °C/min. All the thermal tests were carried out in triplicate.

2.4.4 Water contact angle

The wettability of the interlayers and multilayers surface was evaluated by the measurement of the dynamic water contact angle (WCA) in an Optical Tensiometer (Theta Lite, Staffordshire, UK). Five droplets were seeded at 5 µL/s on the surfaces of each studied sample sizing 2×5 cm^2 and the WCA values were averaged. Measurements were performed at 25 °C.

2.4.5   Mechanical adhesion

The adhesion capacity of the electrospun PHBV layer was assessed in a T-peel test according to ISO 11339:2010. To this end, the multilayer structure was assembled by sandwiching an electrospun PHBV interlayer in between two cast-extruded PHB films (200 mm x 150 mm) according to the sample geometry shown in Figure 2. Prior to the annealing step, a 150 mm x 50 mm Teflon film was inserted along the edge of the PHB sheets in order to prevent adhesion in the grip zone of the specimens (zone 1 in Figure 2). Adhesion tests consisted on measuring the force required to peel the two PHB sheets tieded by the electrospun PHBV interlayer by means of a uniaxial tensile test in a universal testing machine (Shimadzu AGS-X 500 N, Shimadzu Corporation, Kyoto, Japan) at room temperature with a cross-head speed of 10 mm/min.
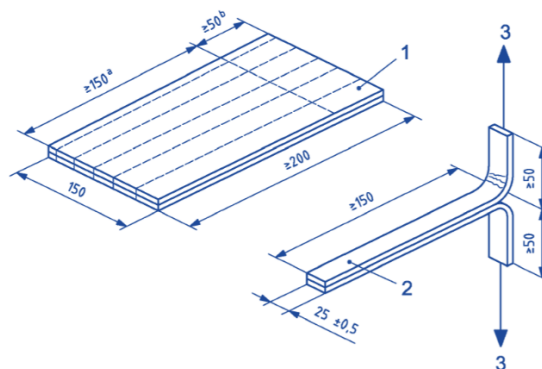
Figure 2. Sample geometry for the T-peel adhesion test.

2.4.6   Water vapor permeance

The water vapor permeability (WVP) of the different multilayers was determined according to the ASTM 2011 gravimetric method using Payne permeability cups (Elcometer SPRL, Hermelle/s, Liege, Belgium) of 3.5 cm diameter. One side of the films was exposed to 100 % RH by avoiding direct contact with liquid water. Then, the cups containing the films were secured with silicon rings and stored in a desiccator at 25 °C and 0 % RH. The cups were weighed periodically after the steady state was reached. Water vapor permeation rate corresponded to the slope value of the steady state line of time versus weight loss per unit area and the weight loss was calculated as the total loss minus the loss through the sealing. Water vapor permeance was obtained by correcting the water vapor permeation rate for the permeant partial pressure. Measurements were done in triplicate for each type of samples.

2.4.7 Limonene vapor permeance

Limonene permeability (LP) was measured as described above for WVP. For this, 5 mL of D-limonene was placed inside the Payne permeability cups and the cups containing the films were placed at controlled room conditions of 25 °C and 40 % RH. The limonene vapor permeation rates were estimated from the steady-state permeation slopes and the weight loss was calculated as the total cell loss minus the loss through the sealing. Limonene permeance was obtained by correcting the limonene vapor permeation rate for the permeant partial pressure. Tests were conducted in triplicate.

2.4.8 Antimicrobial tests

The antimicrobial performance of the monolayer and multilayer films was evaluated according to the Japanese Industrial Standard (JIS) Z 2801:2010. *S. aureus* CECT240 (ATCC 6538P) and *E. coli* CECT434 (ATCC 25922) strains were obtained from the Spanish Type Culture Collection (CECT) (Valencia, Spain) and stored in phosphate buffered saline (PBS) with 10 wt.% tryptic soy broth (TSB) and 10 wt.% glycerol at −80 ºC. Previous to each study, a loopful of bacteria was transferred to 10 ml of TSB and incubated at 37 ºC for 24 h. A 100-µL aliquot from the culture was again transferred to TSB and grown at 37 ºC to the mid-exponential phase of growth. An approximate count of 5×10^5 colony forming units (CFU)/mL of a culture having an absorbance value of 0.20 as determined by optical density at 600 nm using an UV–Vis spectrophotometer VIS3000 (Dinko, Instruments, Barcelona, Spain). A microorganism suspension of *S. aureus* and *E. coli* was applied onto the test monolayer and multilayer films sizing 1.5 cm x 1.5 cm containing eugenol that were placed in hermetically closed and open bottles, the here so-called closed and open systems, respectively. The electrospun PHBV monolayer without eugenol was used as the control film since it shows no antimicrobial activity [60,61]. After incubation at 24 °C and, at least, 95 % RH, for 24 h, bacteria were recovered with PBS, 10-fold serially diluted, and incubated at 37 °C for 24 h in order to quantify the number of viable bacteria by conventional plate count. The antimicrobial activity was evaluated at 1 (right after the film production), 8, and 15 days in both the closed and open systems. The value of the antimicrobial reduction (R) was calculated using the expression:

$$R = \left[log\left(\frac{B}{A}\right) - log\left(\frac{C}{A}\right) \right] = \log\left(\frac{B}{C}\right) \tag{1}$$

Where A is the mean of bacterial counts of the control sample immediately after inoculation, B is the mean of bacterial counts of the control sample after 24 h, and C is the mean of bacterial counts of the test sample after 24 h. Antimicrobial activity was evaluated with the following assessment: Nonsignificant ($R < 0.5$), slight ($R \geq 0.5$ and < 1), significant ($R \geq 1$ and < 3), and strong ($R \geq 3$) [62].

2.5   Statistical analysis

The results of the contact angle measurements, mechanical adhesion, water and limonene vapor permeance were evaluated by analysis of variance (ANOVA) and a multiple comparison test (Tukey) with 95 % significance level ($p \leq 0.05$). For this purpose, the software OriginPro8 (OriginLab Corporation, Northampton, MA, USA) was used.

3 Results and Discussions

3.1 Characterization and selection of the electrospun PHBV monolayer

3.1.1 *Morphology*

Figure 3 shows the morphology and the fiber diameters histogram of the electrospun PHBV fiber mats containing eugenol prior to annealing. In Figure 3a one can observe that the neat PHBV fibers presented a mean diameter of ~0.95 μm. Figure 3b corresponds to electrospun PHBV fibers with 2.5 wt.% of eugenol, which had a mean diameter of ~0.90 μm. In Figure 3c it can be seen that the fibers containing 5 wt.% of eugenol showed a mean diameter of ~0.7 μm, whereas the diameters in the fibers containing 10 wt.% of eugenol was ~0.6 μm (Figure 3d) and in the fibers with 15 wt.% eugenol was ~0.5 μm (Figure 3e). As it can be seen in the histograms, the fiber size decreased as the eugenol concentration increased. This effect can be ascribed to the plasticizing effect and reduction in the solution viscosity due to the presence of the oily substance [63,64]. Indeed, solution viscosity plays a major role in the fiber diameter during electrospinning and solutions with lower viscosities tend to result in fibers with lower diameters [65,66]. One can also observe in the SEM micrographs that higher concentrations of eugenol impaired the formation of PHBV fibers during electrospinning due to the potential agglomeration of the essential oil. In particular, Figure 3f shows that 20 wt.% of eugenol resulted in a partial breakage of the PHBV fibers, while 25 wt.% yielded fibers with beaded regions. Similar results were obtained during the electrospinning of PHBV with various essential oils, in which high contents of oil molecules prevented the formation of homogeneous fibers since the surface tension in the charged jet changed into droplets [59,67]. Therefore, eugenol contents of up to 15 wt.% led to electrospun PHBV fibers with smooth surfaces and free of defects or beaded regions so that higher contents of the essential oil were ruled out of the study.
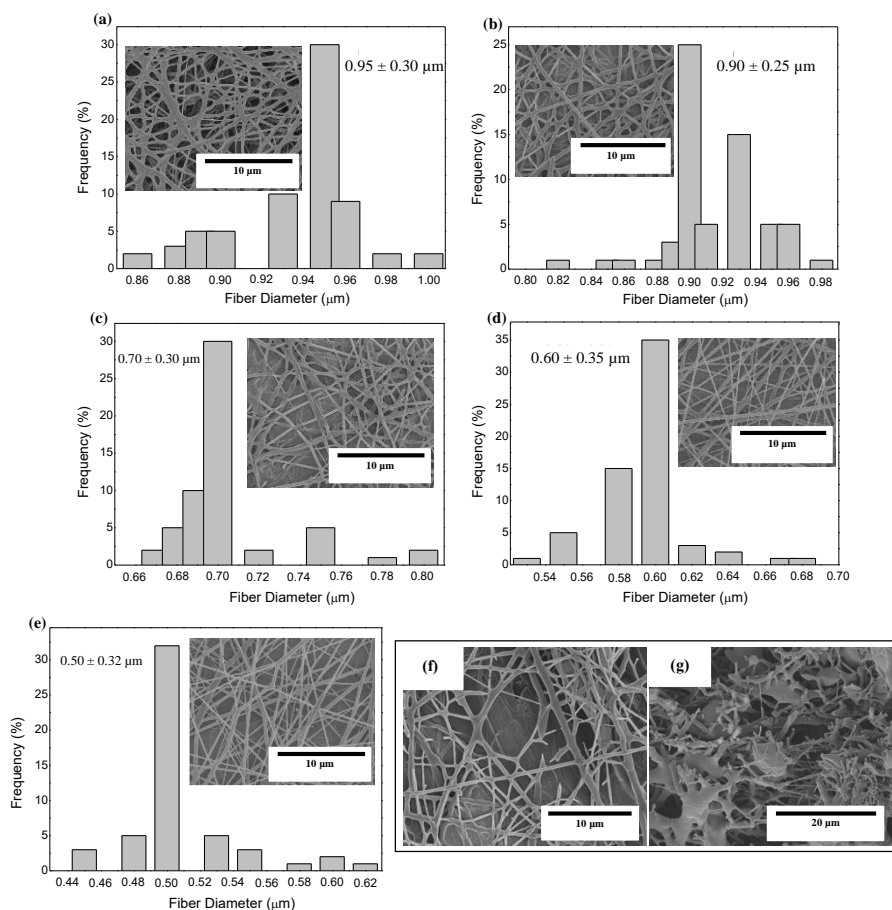
Figure 3. Scanning electron microscopy (SEM) micrographs of electrospun fiber mats of poly(3-hydroxybutyrate-co-3-hydroxyvalerate) (PHBV) containing eugenol and their histograms: (**a**) Neat PHBV; (**b**) 2.5 wt.%; (**c**) 5 wt.%; (**d**) 10 wt.%; (**e**) 15 wt.%; (**f**) 20 wt.%; (**g**) 25 wt.%.

The electrospun fibers mats were turned into actual films by the application of annealing at 160 °C for 10 s. The morphologies of the top views and cross-sections of the PHBV films containing eugenol were analyzed by SEM and they are gathered in Figure 4. It can be observed that the films of neat PHBV (Figures 4a, b) and PHBV containing 2.5 wt.% (Figures 4c, d), 5 wt.% (Figures 4e, f), 10 wt.% (Figures 4g, h), and 15 wt.% (Figures 4i, j) of eugenol were very similar. In all cases, the individual electrospun PHBV fibers successfully coalesced and merged without melting. All the films presented uniform and homogeneous surfaces, which is an indication of the good cohesion of the materials. The cross-sections of the films presented nearly the same thicknesses (~70 μm), demonstrating that the addition of eugenol did not affect

the morphology of the films. Similar observations were reported by Shen and Kamdem [68] who developed active biodegradable films of chitosan containing 10 – 30 % wt./wt. of citronella essential oil and cedarwood oil by casting and solvent-evaporation methods, showing a uniform film thicknesses. On the other hand, however, Haghighi et al. [69] observed a changed in the microstructure of films based on chitosan and gelatin after the incorporation of the essential oils eugenol and ginger. The authors observed the presence of pores in the films that indicated the occurrence of collapsed oil droplets due to the separation of aqueous phase during the drying step as result of their hydrophobic nature. In this way, the annealed electrospun mats present the advantage to develop more homogenous and continuous films containing essential oils over the casting method due to the drying steps are not necessary.
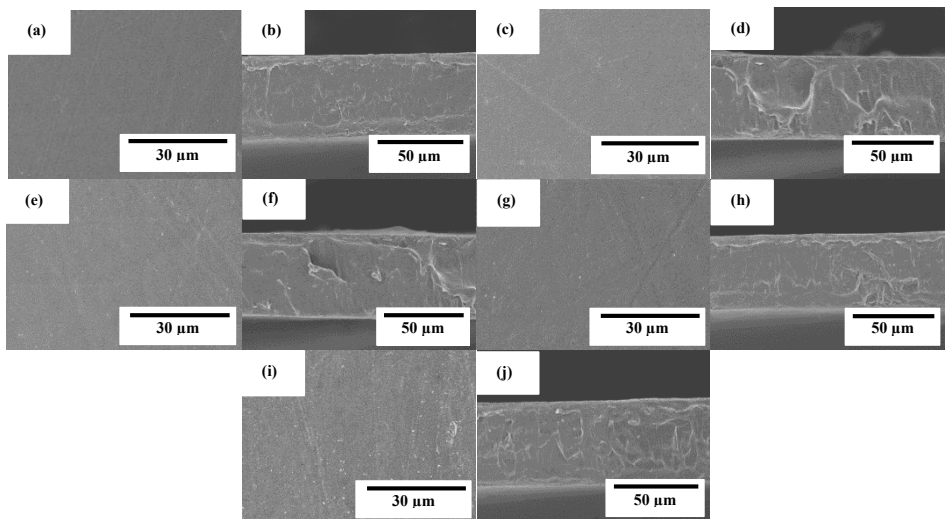
Figure 4. Scanning electron microscopy (SEM) micrographs of the electrospun monolayers of poly(3-hydroxybutyrate-co-3-hydroxyvalerate) (PHBV) containing eugenol: (**a, b**) neat PHBV; (**c, d**) 2.5 wt.%, eugenol; (**e, f**) 5 wt.%; (g, h) 10 wt.%; (**i, j**) 15 wt.% eugenol. Scale markers of 30 μm for all the top views and of 50 μm for all the cross-sections.

3.1.2   *Thermal stability*

Figure 5 shows the TGA curves obtained for the neat eugenol and the electrospun PHBV films containing eugenol. Table 1 gathers the most relevant thermal stability parameters obtained from the TGA curves, that is, the onset degradation temperature, measured at 5 % of weight loss ($T_{5\%}$), the degradation temperature (T_{deg}), and the mass loss at T_{deg} (%). One can observe that neat eugenol initiated thermal decomposition at approximately at 110 °C, showing a $T_{5\%}$ of 121.3 °C and presenting a maximum degradation peak, that is, Tdeg, at 203.5 °C with a mass loss at Tdeg of

86.68 %. This result confirms that this essential oil is thermally unstable and it cannot be processed at high temperatures. In this regard, Shao et al. [70] reported a thermal value for the maximum degradation of eugenol at 195 ºC, which is characteristic of its low-MW substances. It has been reported that eugenol decomposition is based on a first low-intense mass loss around 44 ºC associated to the release of volatiles molecules and the second mass loss occurs at 200 ºC where it takes places the complete degradation of the organic compounds [71]. As opposite, one can observe that the electrospun PHBV films were relatively stable, showing values of $T_{5\%}$ of 276.6 °C and T_{deg} of 304.7 °C with a mass loss at T_{deg} of 61.01 %. The films containing 2.5 wt.% and 5 wt.% of eugenol showed very similar thermal decomposition profiles, presenting their onset of degradation at 264.2 ºC and 265 ºC, respectively, and exhibiting T_{deg} values of 291.4 ºC and 293.3 ºC with respective mass losses of 71.18 % and 72.14 %. The electrospun PHBV film containing 10 wt.% of eugenol started thermal decomposition from 245.8 ºC, presenting a T_{deg} value of 293.1 ºC with a mass loss of 74.60 %. Finally, in the case of the electrospun PHBV film containing 15 wt.% of eugenol, it showed a significantly lower value of $T_{5\%}$, that is, 160.8 ºC, while T_{deg} was similar to the other films, that is, 293.3 ºC (76.36 %). The reduction observed in the onset of thermal degradation can be attributed to the low thermal stability of eugenol.

In order to better ascertain the thermal protection offered by the electrospun PHBV fibers, the mass loss of the samples was determined at 230 ºC since, at this temperature, eugenol was completely degraded (mass loss > 98%). This is in agreement with the findings reported by Cao et al. [32], who indicated that neat eugenol completely degrades at 225 °C with a weight loss of 96 %. Alternatively, it can be observed that PHBV remained highly stable at 230 ºC (mass loss < 5 %) since this temperature is below its T_{onset}. One can observe that the mass loss at 230 ºC increased from 2.15 %, for the electrospun PHBV film containing 2.5 wt.% of eugenol, up to 7.02 %, for the film with 15 wt.% of eugenol. However, one can also notice that the thermal stability of eugenol was relatively similar in all the PHBV films since the mass loss at 230 ºC decreased proportionally to the eugenol content. Therefore, the eugenol encapsulated in the PHBV films showed a significantly higher thermal stability than the free essential oil, though certain amount of eugenol was thermally degraded at temperatures above 200 ºC. Similar results were obtained by Da Silva et al. [73], who observed that eugenol entrapped in cellulose nanostructures and then incorporated in the poly(butylene adipate-co-terephthalate) (PBAT) prepared by solvent casting improved the thermal stability of pure eugenol. Likewise, the previous reports of our research group agreed with the thermal properties attain in the present study, showing that the thermal stability of essential oils incorporated

into PHAs by electrospinning was improved [59,67,74]. Therefore, the development of thermally stable systems expands the potential use of electrospinning for the design of active food packaging as an alternative to melt processing technologies such as extrusion or compression molding.

Table 1. Thermal properties of eugenol and electrospun monolayers of poly(3-hydroxybutyrate-co-3-hydroxyvalerate) (PHBV) containing eugenol in terms of: temperature at 5 % weight loss ($T_{5\%}$), degradation temperature (T_{deg}), mass loss at T_{deg}, and mass loss at 230 ℃, and thermal stability of eugenol at 230 ℃

Sample	$T_{5\%}$ (℃)	T_{deg} (℃)	Mass loss at T_{deg} (%)	Mass loss at 230 ℃ (%)
Eugenol	121.3 ± 1.5	203.5 ± 1.1	86.68 ± 0.7	98.12 ± 1.0
PHBV	276.6 ± 0.9	304.7 ± 1.6	61.01 ± 1.2	2.13 ± 0.7
PHBV + 2.5 wt.% Eugenol	264.2 ± 2.1	291.4 ± 0.7	71.18 ± 0.9	2.15 ± 1.1
PHBV + 5 wt.% Eugenol	265.0 ± 2.3	293.3 ± 2.5	72.14 ± 2.0	2.88 ± 2.0
PHBV + 10 wt.% Eugenol	245.8 ± 0.7	293.1 ± 1.3	74.60 ± 1.6	4.78 ± 1.6
PHBV + 15 wt.% Eugenol	160.8 ± 3.3	293.3 ± 1.9	76.36 ± 2.1	7.02 ± 2.1
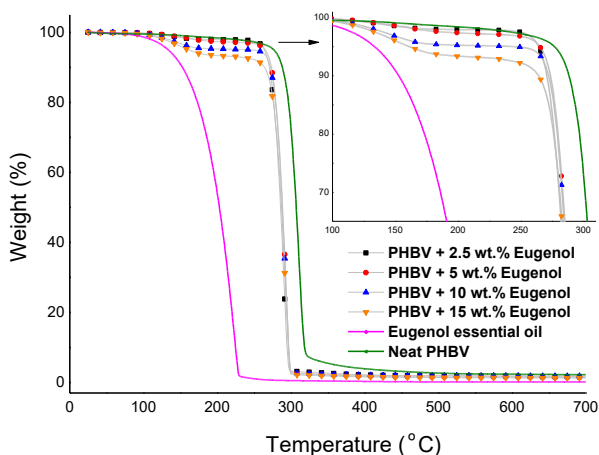
Figure 5. Thermogravimetric analysis (TGA) curves of eugenol and electrospun monolayers of poly(3-hydroxybutyrate-*co*-3-hydroxyvalerate) (PHBV) containing eugenol.

3.1.3 Antimicrobial activity

Table 2 shows the antimicrobial results of the electrospun PHBV monolayers containing different concentrations of eugenol evaluated after 24 h in the open system. This assessment was performed to determine the optimal concentration of eugenol in the PHBV monolayers to, thereafter, develop the multilayer active system. The antimicrobial results of the electrospun PHBV monolayers containing 2.5 wt.%

and 5 wt.% eugenol showed both significant reduction values (R ≥ 1 and < 3), whereas eugenol concentrations of 10 wt.% and 15 wt.% showed both a strong reduction (R ≥ 3) against *S. aureus*. Similar results were obtained for *E. coli*, in which the reduction was slight (R ≥ 0.5 and < 1) for 2.5 wt.% eugenol and significant (R ≥ 1 and < 3) for 5, 10, and 15 wt.% eugenol. A high inhibition was obtained for contents of 15 wt.% of eugenol, reaching a reduction of 3.35 and 2.90 against *S. aureus* and *E. coli*, respectively. Differences observed for both bacteria in the antimicrobial performance of eugenol have been ascribed to variances in the action mechanism of essential oils in the bacterial cell membrane and cytoplasm [38,74]. In particular, G-bacteria have higher resistance than G+ ones due to the cell membrane structure is based on complex lipopolysaccharides that restrict the diffusion rate of hydrophobic compounds of essential oils across the cell membranes. Besides, the solubility rate and the concentration of antimicrobial agents in the lipid moiety of the cell membranes, along with the hydrophobicity of the membrane surfaces, can all influence in the resistance of G- bacteria against these active compounds [75-77].

Table 2. Antibacterial reduction (R) for *Staphylococcus aureus* (*S. aureus*) and *Escherichia coli* (*E. coli*) of the electrospun monolayers of poly(3-hydroxybutyrate-co-3-hydroxyvalerate) (PHBV) containing different amounts of eugenol in the open system for 24 h

Bacteria	Eugenol (wt.%)	PHBV monolayer Log (CFU/mL) t = 0 h	PHBV monolayer Log (CFU/mL) t = 24 h	Active monolayer Log (CFU/mL)	R
S. aureus	2.5			5.16 ± 0.12	1.64 ± 0.50
	5			4.21 ± 0.21	2.59 ± 0.32
	10	6.82 ± 0.33	6.80 ± 0.56	3.79 ± 0.70	3.01 ± 0.66
	15			3.45 ± 0.32	3.35 ± 0.99
E. coli	2.5			5.79 ± 0.21	0.99 ± 0.78
	5			5.03 ± 0.18	1.75 ± 0.25
	10	6.76 ± 0.51	6.78 ± 0.63	4.31 ± 0.43	2.47 ± 0.36
	15			3.88 ± 0.37	2.90 ± 0.81

Based on the antimicrobial reduction attained for both strains and also taken into account the morphological and thermal stability results described above, one can consider that the best concentration of eugenol in the electrospun monolayers of PHBV is 15 wt.%. Hence, the PHBV monolayer films containing 15 wt.% were evaluated against *S. aureus* and *E. coli* strains in an open a closed system for a longer period, that is, up to 15 days. These conditions resemble better those found in actual packaging systems in terms of design and time so that the antimicrobial performance of the active materials can be more accurately determined. As one can observe in Table 3, the electrospun PHBV monolayers presented a strong inhibition (R ≥ 3) against *S. aureus* and a significant inhibition (R ≥ 1 and < 3) against *E. coli* during

the 15 days of evaluation. The different results obtained for the two tested systems, that is, the open system and the close one (actual packaging) are related with the expected accumulation of the volatile compounds in the headspace of the closed chamber, which can contribute to inhibiting the bacteria growth on the film surfaces. In this regard, Navikaite-Snipaitienea et al. [78] demonstrated that the release of eugenol to the headspace of sealed containers was very rapidly within 1 day and saturation in the packaging headspace was reached after 3 days. The coatings containing the highest amount of eugenol also showed the highest saturation concentration of active substance in the headspace. Similar results were reported in our previous study using oregano essential oil (OEO) and rosemary and green tea natural extracts, in which a slightly higher inhibition was achieved in the closed system in comparison with the open one after 15 days of storage against *S. aureus* and *E. coli* [59]. Therefore, the here-attained release and accumulation of volatiles compounds from the developed packaging system can be regarded as an advantage to better preserve food products during their shelf life period.

Table 3. Antibacterial reduction (R) for *Staphylococcus aureus* (*S. aureus*) and *Escherichia coli* (*E. coli*) of the electrospun monolayers of poly(3-hydroxybutyrate-co-3-hydroxyvalerate) (PHBV) containing 15 wt.% of eugenol in the open and closed systems for 1, 8, and 15 days

Bacteria	Day	Open system				Closed system		
		PHBV monolayer Log (CFU/mL) t = 0 h	PHBV monolayer Log (CFU/mL) t = 24 h	Active monolayer Log (CFU/mL)	R	PHBV monolayer Log (CFU/mL) t = 24 h	Active monolayer Log (CFU/mL)	R
S. aureus	1	6.75 ± 0.04	6.72 ± 0.002	3.49 ± 0.081	3.23 ± 0.05	6.72 ± 0.02	3.49 ± 0.08	3.23 ± 0.12
	8	6.64 ± 0.05	6.62 ± 0.007	3.31 ± 0.033	3.31 ± 0.07	6.70 ± 0.05	3.15 ± 0.07	3.55 ± 0.06
	15	6.77 ± 0.02	6.74 ± 0.010	3.33 ± 0.092	3.41 ± 0.11	6.74 ± 0.06	3.08 ± 0.06	3.66 ± 0.07
E. coli	1	6.80 ± 0.09	6.78 ± 0.011	4.08 ± 0.027	2.70 ± 0.07	6.78 ± 0.07	4.08 ± 0.07	2.70 ± 0.05
	8	6.71 ± 0.07	6.69 ± 0.041	3.87 ± 0.084	2.82 ± 0.12	6.75 ± 0.06	3.83 ± 0.09	2.92 ± 0.06
	15	6.77 ± 0.08	6.76 ± 0.030	3.81 ± 0.030	2.95 ± 0.10	6.76 ± 0.08	3.40 ± 0.08	3.36 ± 0.09

3.2 Characterization of the active multilayer

3.2.1 Morphology

Figure 6 shows the SEM micrographs in the top view and cross-section of the multilayer structures prepared with the electrospun interlayer of PHBV containing 15 wt.% of eugenol. The selected electrospun monolayer was incorporated in a sandwich-type structure between the cast-extruded PHB sheet (structural layer) and the 25-µm PHBV film (food contact layer). One can observe that both the PHB sheet (Figure 6a) and PHBV film (Figure 6b), which constitute the external layers of the multilayer structure, exhibited a smooth and homogenous surface. Figure 6c shows the cross-section of the multilayer system, where the electrospun PHBV monolayer can be seen as an interlayer effectively adhered to both external layers. The high adhesion achieved can be ascribed to the high surface-to-volume ratio of the electrospun fibers, in the submicron range, which efficiently adhered to the contact layer during the thermal post-treatment (annealing). Other recent studies have reported the potential of the electrospinning technology to develop multilayer structures based on the particular morphology of the fibers, even though different materials were employed to produce the layers. For instance, Cherpinski et al. [55] developed multilayer packaging structures based on paper/poly(vinyl alcohol)/PHB. It was observed that the multilayer structures self-adhered to the paper substrate during annealing and the applied electrospun biopolymer coatings yielded a significant improvement of the paper barrier properties to water and limonene vapors. In another study, Fabra et al. [79] studied the effect of different electrospun biopolyester coatings of poly(ε-caprolactone) (PCL), PLA, and PHB on the properties of thermoplastic corn starch (TPCS) films. The multilayers developed showed that the addition of electrospun biopolyester coatings led to an exponential oxygen gas and water vapor permeability reduction as the thickness of the electrospun coating increased. Fabra et al. [53] also obtained multilayer structures based on PHBV prepared by compression-molding and casting, which contained a high barrier interlayer made of electrospun zein nanofibers, concluding that the addition of a zein interlayer significantly improved oxygen barrier properties of the multilayer films prepared by both processing technologies. Similar results were formerly obtained by the use of multilayers of PLA film/electrospun zein fibers/PLA film, in which the introduction of the electrospun zein mat enhanced the barrier properties due to the large aspect ratio of the electrospun fibers by establishing a tortuous pathway for the diffusion of the oxygen gas molecules [51,52]. In another study, Wan et al. [80] developed bacterial cellulose multilayer films by incorporating interlayers of

electrospun zein fibers, which enhanced water resistance properties of the multilayer films.
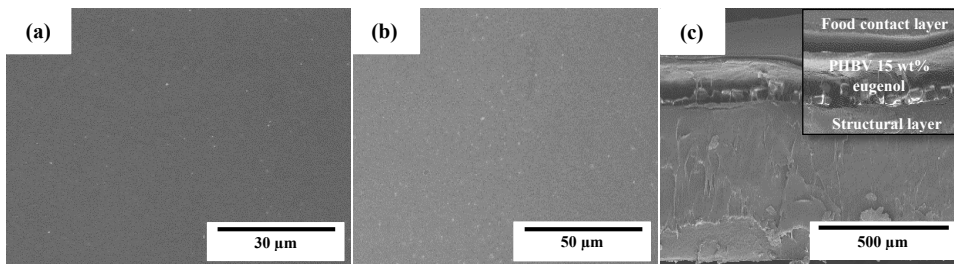
Figure 6. Scanning electron microscopy (SEM) micrographs of the multilayer structure of poly(3-hydroxybutyrate) (PHB) sheet/electrospun poly(3-hydroxybutyrate-co-3-hydroxyvalerate) (PHBV) interlayer containing eugenol/PHBV film: (**a**) top view of the structural layer of PHB: (**b**) top view of the food contact layer of PHBV; (**c**) multilayer cross-section.

3.2.2 Water contact angle

The WCA values of the electrospun PHBV monolayers with different eugenol contents and the multilayer containing 15 wt.% eugenol are presented in Figure 7. Figure 7a shows the contact angle for the electrospun PHBV monolayer without eugenol, showing a value of 86.77º. A similar WCA value, that is, 86º, was reported by Yoon et al. [81] for PHBV surfaces prepared by the electrospinning technique. As one can observe in Figures 7b-e, the values of WCA of the monolayers containing 2.5 wt.% (85.39º), 5 wt.% (85.21º), 10 wt.% (85.12º), and 15 wt.% of eugenol (85.08º) were very similar and slightly lower than that of PHBV without eugenol. The lower values can be ascribed to the reduction of the surface tension of the water drops on the film surface by the oily molecules of eugenol. It can also be observed that the food contact layer showed an WCA value of 70.91º (Figure 7f), whereas the structural layer of PHB presented a value of 72.68º (Figure 7g). The difference observed in hydrophobicity between the homopolyester and copolyester films are slight, being both hydrophobic polyesters, since the molar content of 3HV in the commercial copolyester is relatively low [82-84]. In an application context, Chang et al. [85] studied the WCA of plasma-treated and untreated PHB and PHBV films fabricated by solvent casting. It was observed that the untreated PHB and PHBV films led to WCA values of 76.0° and 72.5°, respectively and the value decreased in the CH_4/O_2 plasma-treated PHB (23.0°) and PHBV (18.5°) films. Finally, the active multilayer containing 15 wt.% eugenol in the electrospun interlayer of PHBV presented a WCA value of 75.53° (Figure 7h). This intermediate value between the external layers of the commercial PHAs and the other electrospun monolayers can be explained in terms of the high eugenol content present in the interlayer, in which

some essential oil could diffuse to the external food contact layer of PHBV and decreased its surface tension. In any case, all the samples yielded angles characteristic of hydrophobic materials according to the classification reported by Medina-Jaramillo et al. [86], where 'hydrophobic' and "hydrophilic" are defined for angles > 65° and < 65°, respectively.
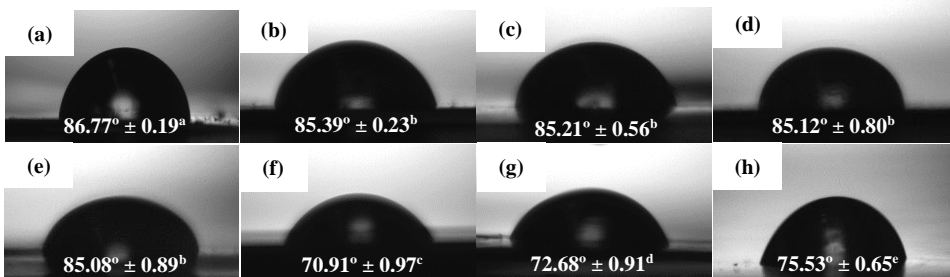
Figure 7. Water contact angle (WCA) of electrospun monolayer films of poly(3-hydroxybutyrate-co-3-hydroxyvalerate) (PHBV) containing eugenol: (**a**) without eugenol; (**b**) 2.5 wt.%; (**c**) 5 wt.%; (**d**) 10 wt.%; (**e**) 15 wt.%; (**f**) Food contact layer of PHBV, (**g**) Structural layer of poly(3-hydroxybutyrate) (PHB); (**h**) Multilayer containing 15 wt.% eugenol measured on the food contact layer side. a-e: Different superscripts indicate significant differences among samples (p < 0.05).

3.2.3 Mechanical adhesion

Table 4 shows the mechanical parameters in terms of tensile modulus (E), tensile strength at yield (σ_y), and elongation at break (ε_b) of the electrospun PHBV monolayer films containing eugenol. The table also includes the tensile properties of the cast-extruded sheet of PHBV, which constitutes the structural layer and, at the end, determines the whole mechanical properties of the multilayers. The tensile parameters of the structural layer are similar to those reported earlier for PHB films prepared by extrusion and thermo-compression, that is, approximately 2900 MPa, 37 MPa, and 4 % [25]. Alternatively, the neat PHBV monolayer obtained by electrospinning and subsequent annealing presented E, σ_y, and ε_b values of 1252 MPa, 18.1 MPa, and 2 %, which are in the range of the values reported by Corre et al. [87] for melt-extruded films. The incorporation of low contents of eugenol into the electrospun monolayers slightly improved all the mechanical properties, more notably the film elasticity. In particular, the electrospun PHBV monolayer film containing 2.5 wt.% of eugenol presented the highest E value, that is, 2884 MPa. Lower values were attained, however, at the highest content of eugenol, that is, 15 wt.%, which correlates well with the thermal properties reported above and suggests that the oil particles agglomerated in the biopolymer matrix and induced a plasticizing effect. Furthermore, the differences attained among the electrospun monolayers can

also be ascribed to interactions between the coalesced fibers in the electrospun film sample such as slip of fibers over one another, point bonding, alignment, etc. [88]. In comparison to PHA films containing essential oils prepared by solvent casting and melting routes, the here-attained electrospun PHBV films were more ductile but less mechanical resistant. For instance, melt-mixed PHB films prepared by Arrieta et al. [89] showed an E value of 1390 MPa, also showing a significant reduction after the incorporation of 15 wt.% of limonene since it is a strong plasticizer that contributes to reducing the intramolecular bonds of the biopolymer. In the work performed by Narayanan et al. [90], solvent-casted PHB films with different amounts of eugenol showed a σy reduction from 40 MPa, for neat PHB, to 23.5 MPa after the incorporation of the essential oil. In another study, compression-molded bilayer structures based on PHBV containing different essential oils at 15 wt.% were produced by Requena et al. [91], showing that the E and σy values ranged between 1141− 773 MPa and 27.6 − 17 MPa, respectively. These results confirm that the electrospun film show lower mechanical strength due to they consist of coalesced fibers and also show higher porosity [92]. In any case, all the developed monolayers showed sufficient strength to be successfully applied as interlayers in packaging applications.

Table 4. Mechanical properties of the electrospun monolayer films of poly(3-hydroxybutyrate-co-3-hydroxyvalerate) (PHBV) containing eugenol in terms of tensile modulus (E), tensile strength at yield (σ_y), and elongation at break (ε_b)

Sample	E (MPa)	σ_y(MPa)	ε_b(%)
Structural PHB sheet	3014 ± 86[a]	29.1 ± 3.3[a]	1.4 ± 0.3[a]
PHBV monolayer	1252 ± 79[a]	18.1 ± 2.1[a]	2.0 ± 0.2[a]
PHBV + 2.5 wt.% eugenol monolayer	2884 ± 70[b]	20.6 ± 4.8[b]	2.1 ± 0.2[a]
PHBV + 5 wt.% eugenol monolayer	2632 ± 73[c]	21.3 ± 0.8[c]	2.2 ± 0.1[a,b]
PHBV + 10 wt.% eugenol monolayer	2261 ± 29[d]	28.3 ± 1.4[d]	2.4 ± 0.7[b,c]
PHBV + 15 wt.% eugenol monolayer	1897 ± 51[e]	26.5 ± 1.8[e]	2.5 ± 0.4[c]

a-e: Different superscripts within the same column indicate significant differences among samples ($p < 0.05$).

Furthemore, the adhesion capacity of the electrospun PHBV layer to the structural and food contact layers was assessed by T-peel adhesion tests. For all the samples studied, the PHB film broke before the detachment of the adhesive union, thus revealing an excellent performance of the PHBV electrospun as tie-layer. A maximum stress of ~10 N/cm was reached at break of the PHB film, thus proving an adhesion force above that value.

3.2.4 Barrier performance

The WVP and LP values of the electrospun PHBV monolayers containing eugenol, food contact PHBV film, and structural PHB sheet are shown in Table 5. In the case of the food contact film, the permeability values were 6.27×10^{-14} Kg·m·m^{-2}·s^{-1}·Pa^{-1} and 5.17×10^{-14} Kg·m·m^{-2}·s^{-1}·Pa^{-1} for water and limonene vapors, respectively. These values were higher than those observed for both the electrospun PHBV monolayer without eugenol, that is, 4.05×10^{-14} Kg·m·m^{-2}·s^{-1}·Pa^{-1} and 3.75×10^{-14} Kg·m·m^{-2}·s^{-1}·Pa^{-1}, respectively, and also for the structural layer of PHB, that is, 1.75×10-15 Kg·m·m-2·s^{-1}·Pa^{-1} and 1.95×10^{-15} Kg·m·m^{-2}·s^{-1}·Pa^{-1}. This observation is related to the higher 3HV molar content of the biopolyester in the food contact layer, that is, 8 mol.%. In a context of packaging applications for food preservation, the present PHAs showed values of permeability relatively close to petroleum derived thermoplastics such as polyethylene terephthalate (PET), with WVP value around 5.2×10^{-15} Kg·m·m^{-2}·s^{-1}·Pa^{-1} [54,87]. The differences attained can be ascribed to the remaining porosity and, thus, lower continuity of the annealed fiber-based material [92]. One can also observe that the incorporation of eugenol into the PHBV monolayers decreased the permeability of both vapors whereas there were also significant differences for the electrospun monolayers containing eugenol. The monolayer PHBV films containing 2.5 and 5 wt.% of eugenol presented WPV values of 3.59×10^{-14} Kg·m·m^{-2}·s^{-1}·Pa^{-1} and 2.79×10^{-14} Kg·m·m^{-2}·s^{-1}·Pa^{-1} and LP values of 2.86×10^{-14} Kg·m·m^{-2}·s^{-1}·Pa^{-1} and 2.13×10^{-14} Kg·m·m^{-2}·s^{-1}·Pa^{-1}. For the monolayer PHBV films containing 10 wt.% and 15 wt.% of eugenol, the WVP values decreased to 1.98×10^{-14} Kg·m·m^{-2}·s^{-1}·Pa^{-1} and 0.95×10^{-14} Kg·m·m^{-2}·s^{-1}·Pa^{-1}, respectively. In the case of LP, values were respectively 1.83×10^{-14} Kg·m·m^{-2}·s^{-1}·Pa^{-1} and 0.81×10^{-14} Kg·m·m^{-2}·s^{-1}·Pa^{-1}. Since water vapor is mainly a diffusivity-driven property in PHAs due to their low water sorption nature [93], the decrease in permeability to water vapor can be ascribed to the hydrophobic character of eugenol, where the presence of the oily molecules dispersed in PHA matrix impaired the mobility of water molecules [61,67,94]. For limonene, as opposed to moisture, the aroma molecules are known to plasticize PHAs and, then, solubility plays a more important role in permeability than diffusion. Therefore, the lower permeability values attained indicate that eugenol also reduced the sorption of limonene in the PHBV matrix. Similar barrier improvements were reported by Melendez-Rodriguez et al. [67] when incorporated eugenol encapsulated in mesoporous silica nanoparticles in PHBV monolayers, though the barrier effect was mainly ascribed to the mineral nanofillers. Likewise, Hasheminya et al. [95] showed that Kefiran/carboxymethyl cellulose composite films incorporating Satureja Khuzestanica essential oil by solvent casting decreased significantly the WVP values due to interactions between the hydrophobic

compounds and the biopolymer. This phenomenon was explained by a reduction of the number of hydrophilic groups available that could diffuse into the continuous biopolymer phase.

The permeance of all the monolayers and multilayer was also determined by diving the permeability values into each sample thickness. Permeance is the time it takes the vapor to transmit through a unit area of film that has a vapor pressure difference between the two exposed surfaces of the film, therefore, the lower the permeance the higher the barrier of the film or sheet. One can observe that the water vapor and limonene permeances of the active multilayer were 0.03×10^{-10} Kg·m^{-2}·s^{-1}·Pa^{-1} and 0.02×10^{-10} Kg·m^{-2}·s^{-1}·Pa^{-1}, respectively. These values were slightly lower than those attained for the structural PHB sheet due to the presence of electrospun interlayers of PHBV containing eugenol and the higher thickness of the sample. The present multilayers can be compared with the multilayers prepared by Akinalan Balik et al. [58], who evaluated the water permeance of multilayer films that consisted of an electrospun pectin interlayer sandwiched between two electrospun PHBV films. The previous study reported higher permeance values for the neat PHBV/PHBV film (5×10^{-10} Kg·m^{-2}·s^{-1}·Pa^{-1}) mainly due to the lower total thickness of the multilayer (72 μm). In the case of PHBV/electrospun pectin/PHBV multilayer, the permeance value was also lower (1.75×10^{-10} kg·m^{-2}·Pa^{-1}·s^{-1}) even though the electrospun pectin highly improved the barrier performance of PHBV. Therefore, the here-prepared multilayers can be applied to medium barrier applications or even medium-to-high barrier applications at the current thickness.

Table 5. Permeance of water and limonene vapors and limonene of the structural poly(3-hydroxybutyrate) (PHB) sheet, food-contact poly(3-hydroxybutyrate-co-3-hydroxyvalerate) (PHBV) film, electrospun PHBV interlayers with different contents of eugenol, and multilayer with 15 wt.% eugenol

Sample	Thickness (mm)	Permeability		Permeance	
		Water vapor x 10^{14} (Kg·m·m^{-2}·s^{-1}·Pa^{-1})	Limonene vapor x 10^{14} (Kg·m·m^{-2}·s^{-1}·Pa^{-1})	Water vapor x 10^{10} (Kg·m^{-2}·s^{-1}·Pa^{-1})	Limonene vapor x 10^{10} (Kg·m^{-2}·s^{-1}·Pa^{-1})
Food contact PHBV film	0.025 ± 0.03[a]	6.27 ± 0.15[a]	5.17 ± 0.65[a]	25.08 ± 0.59[a]	20.68 ± 0.26[a]
Structural PHB sheet*	0.500 ± 0.07[b]	0.18 ± 0.50[b]	0.20 ± 0.10[b]	0.04 ± 0.01[b]	0.04 ± 0.01[b]
PHBV monolayer	0.070 ± 0.10[c]	4.05 ± 0.13[c]	3.75 ± 0.93[c]	5.87 ± 0.19[c]	5.44 ± 0.13[c]
PHBV + 2.5 wt.% eugenol monolayer	0.071 ± 0.11[c]	3.59 ± 0.54[d]	2.86 ± 0.42[d]	5.06 ± 0.77[c]	4.03 ± 0.59[d]
PHBV + 5 wt.% eugenol monolayer	0.073 ± 0.15[c]	2.79 ± 0.46[e]	2.13 ± 0.14[e]	3.83 ± 0.63[d]	2.92 ± 0.19[e]
PHBV + 10 wt.% eugenol monolayer	0.072 ± 0.13[c]	1.98 ± 0.37[f]	1.83 ± 0.11[e]	2.74 ± 0.51[e]	2.54 ± 0.15[e]
PHBV + 15 wt.% eugenol monolayer	0.071 ± 0.11[c]	0.95 ± 0.13[g]	0.81 ± 0.48[f]	1.33 ± 0.18[f]	1.14 ± 0.13[f]
Multilayer	0.580 ± 0.12[b]	---	---	0.03 ± 0.01[g]	0.02 ± 0.10[g]

a-g: Different superscripts within the same column indicate significant differences among samples ($p < 0.05$).
*Literature values [27].

3.2.5 *Antimicrobial activity*

Table 6 shows the antimicrobial properties of the multilayer system against *S. aureus* and *E. coli* strains in an open a closed system for up to 15 days. It can be observed that the multilayer presented a significant inhibition reduction (R ≥ 1 and < 3) against both bacterial strains in the all days of evaluation, reaching at day 15 R values of 1.84 for *S. aureus* and 1.47 for *E. coli*. Compared with the monolayer materials, lower values were obtained since the release rate was slower due to the presence of the food contact layer, which potentially hindered the diffusion of eugenol [96]. In any case, the R values obtained for these multilayers systems, ranging between 1.24 and 2.19, were still significant (R ≥ 1 and < 3) against both bacteria and in both tested systems. Similarly, Cerqueira et al. [61] developed active multilayers based on bilayers of PHBV/zein and PHBV containing cinnamaldehyde by electrospinning, achieving a good antimicrobial activity against *L. monocytogenes* with a logarithmic reduction around of 2.18 Log_{10} CFU/mL after 30 days of storage. Figueroa-Lopez et al. [42] also achieved a high reduction of *S. aureus* [3.9 Log_{10} (CFU/mL)] using active multilayer films based on gelatin, PCL, and black pepper oleoresin prepared by electrospinning. It is also worthy to note that the inhibition had a slight increase in the closed system at days 8 and 15 of evaluation, which is related to the accumulation of eugenol released from the multilayer in the headspace. Therefore, development of active packaging is foreseen to preserve food products for up to 15 days, maintaining their physical and microbiological quality [97]. Thus, the design of multilayer active systems can successfully allow the controlled release of the bioactive compounds.

In a food packaging content, it is also worthy to mention that a slow or sustained release supposes an advantage because, in some cases, the excess of volatiles substances can be affect the organoleptic food properties and result in consumer rejection. As reported by Ribes et al. [98], the presence of active compounds such as eugenol, carvacrol, and vanillin altered the sensory acceptance of fruit juices. It was observed that active compounds immobilized in silica supports induced a change on the aroma of juice samples, particularly for the samples containing eugenol. Thus, the use of multilayers can also successfully contribute to reducing the organoleptic impact of essential oils on the original aroma of food products.

Table 6. Antibacterial activity for *S. aureus* and *E. coli* of the poly(3-hydroxybutyrate) (PHB)/electrospun poly(3-hydroxybutyrate-co-3-hydroxyvalerate) (PHBV) containing eugenol/PHBV film multilayers in the open and closed systems for 15 days

Bacteria	Day	Open system				Closed system		
		Control PHBV Log (CFU/mL) t = 0 h	Control PHBV Log (CFU/mL) t = 24 h	Active Multilayer Log (CFU/mL)	R	Control PHBV Log (CFU/mL) t = 24 h	Active Multilayer Log (CFU/mL)	R
S. aureus	1	6.75 ± 0.04	6.72 ± 0.002	5.21 ± 0.05	1.51 ± 0.08	6.72 ± 0.02	5.21 ± 0.05	1.51 ± 0.08
	8	6.64 ± 0.05	6.62 ± 0.007	5.01 ± 0.05	1.61 ± 0.13	6.70 ± 0.05	4.76± 0.07	1.94 ± 0.10
	15	6.77 ± 0.02	6.74 ± 0.010	4.90 ± 0.02	1.84 ± 0.07	6.74 ± 0.06	4.55 ± 0.02	2.19 ± 0.13
E. coli	1	6.80 ± 0.09	6.78 ± 0.011	5.54 ± 0.06	1.24 ± 0.06	6.78 ± 0.07	5.54 ± 0.06	1.24 ± 0.09
	8	6.71 ± 0.07	6.69 ± 0.041	5.41 ± 0.07	1.28 ± 0.13	6.75 ± 0.06	5.26 ± 0.08	1.49 ± 0.11
	15	6.77 ± 0.08	6.76 ± 0.030	5.29 ± 0.09	1.47 ± 0.17	6.76 ± 0.08	5.05 ± 0.04	1.71 ± 0.07

4   Conclusions

A novel multilayer structure fully based on PHA with antibacterial properties was successfully produced by the electrospinning of PHBV fibers containing eugenol on a cast-extruded PHB sheet (structural layer) followed by the deposition of a PHBV film (food contact layer) and thereafter the application of annealing to the whole assembly at mild temperature. The amount of eugenol in the electrospun monolayer was optimal at 15 wt.% since it yielded high electrospinnability and provided the highest antibacterial properties against bacteria strains of *S. aureus* and *E. coli* as well as sufficient thermal stability. The resultant multilayer showed high hydrophobicity to be used in high humidity packaging environments, sufficient interlayer adhesion, a mechanical performance similar to the structural layer, and improved barrier properties against water and aroma vapors. The antimicrobial tests finally showed that the multilayer is very effective to reduce and control the growth of food-borne bacteria in both open and closed systems for up to 15 days. Moreover, through the multilayer design, the release of eugenol was sustained and it can be prolonged so that the organoleptic properties would be less affected. Further studies will be focused on analyzing the migration of eugenol from the multilayer active system into food simulants and the practical application of the multilayer in the form of packaging articles such as trays or lids to study the shelf life of food products and also their impact on the organoleptic properties.

5 References

1. Fu, Y.; Sarkar, P.; Bhunia, A.K.; Yao, Y. Delivery systems of antimicrobial compounds to food. *Trends in Food Science & Technology* **2016**, *57*, 165-177.
2. Petersen, K.; Væggemose Nielsen, P.; Bertelsen, G.; Lawther, M.; Olsen, M.B.; Nilsson, N.H.; Mortensen, G. Potential of biobased materials for food packaging. *Trends in Food Science & Technology* **1999**, *10*, 52-68.
3. Arena, U.; Di Gregorio, F. A waste management planning based on substance flow analysis. *Resources, Conservation and Recycling* **2014**, *85*, 54-66.
4. Kumar, G.; Ponnusamy, V.K.; Bhosale, R.R.; Shobana, S.; Yoon, J.-J.; Bhatia, S.K.; Rajesh Banu, J.; Kim, S.-H. A review on the conversion of volatile fatty acids to polyhydroxyalkanoates using dark fermentative effluents from hydrogen production. *Bioresource Technology* **2019**, *287*, 121427.
5. Shen, M.; Huang, W.; Chen, M.; Song, B.; Zeng, G.; Zhang, Y. (Micro)plastic crisis: Un-ignorable contribution to global greenhouse gas emissions and climate change. *Journal of Cleaner Production* **2020**, *254*, 120138.
6. Mannina, G.; Presti, D.; Montiel-Jarillo, G.; Carrera, J.; Suárez-Ojeda, M.E. Recovery of polyhydroxyalkanoates (PHAs) from wastewater: A review. *Bioresource Technology* **2020**, *297*, 122478.
7. Costa, S.S.; Miranda, A.L.; de Morais, M.G.; Costa, J.A.V.; Druzian, J.I. Microalgae as source of polyhydroxyalkanoates (PHAs) — A review. *International Journal of Biological Macromolecules* **2019**, *131*, 536-547.
8. Nielsen, C.; Rahman, A.; Rehman, A.U.; Walsh, M.K.; Miller, C.D. Food waste conversion to microbial polyhydroxyalkanoates. *Microb Biotechnol* **2017**, *10*, 1338-1352, doi:10.1111/1751-7915.12776.
9. Bhatia, S.K.; Gurav, R.; Choi, T.-R.; Jung, H.-R.; Yang, S.-Y.; Moon, Y.-M.; Song, H.-S.; Jeon, J.-M.; Choi, K.-Y.; Yang, Y.-H. Bioconversion of plant biomass hydrolysate into bioplastic (polyhydroxyalkanoates) using Ralstonia eutropha 5119. *Bioresource Technology* **2019**, *271*, 306-315.
10. Bhatia, S.K.; Shim, Y.-H.; Jeon, J.-M.; Brigham, C.J.; Kim, Y.-H.; Kim, H.-J.; Seo, H.-M.; Lee, J.-H.; Kim, J.-H.; Yi, D.-H., et al. Starch based polyhydroxybutyrate production in engineered Escherichia coli. *Bioprocess and Biosystems Engineering* **2015**, *38*, 1479-1484.
11. Park, Y.-L.; Bhatia, S.K.; Gurav, R.; Choi, T.-R.; Kim, H.J.; Song, H.-S.; Park, J.-Y.; Han, Y.-H.; Lee, S.M.; Park, S.L., et al. Fructose based hyper production of poly-3-hydroxybutyrate from Halomonas sp. YLGW01 and impact of carbon sources on bacteria morphologies. *International Journal of Biological Macromolecules* **2020**, *154*, 929-936.
12. Hong, J.-W.; Song, H.-S.; Moon, Y.-M.; Hong, Y.-G.; Bhatia, S.K.; Jung, H.-R.; Choi, T.-R.; Yang, S.-y.; Park, H.-Y.; Choi, Y.-K., et al. Polyhydroxybutyrate production in halophilic marine bacteria Vibrio proteolyticus isolated from the Korean peninsula. *Bioprocess and Biosystems Engineering* **2019**, *42*, 603-610.
13. Vu, D.H.; Åkesson, D.; Taherzadeh, M.J.; Ferreira, J.A. Recycling strategies for polyhydroxyalkanoate-based waste materials: An overview. *Bioresource Technology* **2020**, *298*, 122393.
14. Możejko-Ciesielska, J.; Kiewisz, R. Bacterial polyhydroxyalkanoates: Still fabulous? *Microbiological Research* **2016**, *192*, 271-282.
15. Torres-Giner, S.; Hilliou, L.; Melendez-Rodriguez, B.; Figueroa-Lopez, K.J.; Madalena, D.; Cabedo, L.; Covas, J.A.; Vicente, A.A.; Lagaron, J.M. Melt processability, characterization, and antibacterial activity of compression-molded green composite sheets made of poly(3-hydroxybutyrate-co-3-hydroxyvalerate) reinforced with coconut fibers impregnated with oregano essential oil. *Food Packaging and Shelf Life* **2018**, *17*, 39-49.
16. Vahabi, H.; Rohani Rad, E.; Parpaite, T.; Langlois, V.; Saeb, M.R. Biodegradable polyester thin films and coatings in the line of fire: the time of polyhydroxyalkanoate (PHA)? *Progress in Organic Coatings* **2019**, *133*, 85-89.
17. Jung, H.-R.; Jeon, J.-M.; Yi, D.-H.; Song, H.-S.; Yang, S.-Y.; Choi, T.-R.; Bhatia, S.K.; Yoon, J.-J.; Kim, Y.-G.; Brigham, C.J., et al. Poly(3-hydroxybutyrate-co-3-hydroxyvalerate-co-3-hydroxyhexanoate) terpolymer production from volatile fatty acids using engineered Ralstonia eutropha. *International Journal of Biological Macromolecules* **2019**, *138*, 370-378.
18. Rehm, B.H.A.; Steinbüchel, A. Biochemical and genetic analysis of PHA synthases and other proteins required for PHA synthesis. *International Journal of Biological Macromolecules* **1999**, *25*, 3-19.
19. Braunegg, G.; Lefebvre, G.; Genser, K.F. Polyhydroxyalkanoates, biopolyesters from renewable resources: Physiological and engineering aspects. *Journal of Biotechnology* **1998**, *65*, 127-161-
20. Bhatia, S.K.; Gurav, R.; Choi, T.-R.; Jung, H.-R.; Yang, S.-Y.; Song, H.-S.; Jeon, J.-M.; Kim, J.-S.; Lee, Y.-K.; Yang, Y.-H. Poly(3-hydroxybutyrate-co-3-hydroxyhexanoate) production from engineered

Ralstonia eutropha using synthetic and anaerobically digested food waste derived volatile fatty acids. *International Journal of Biological Macromolecules* **2019**, *133*, 1-10.

21. Tarawat, S.; Incharoensakdi, A.; Monshupanee, T. Cyanobacterial production of poly(3-hydroxybutyrate-co-3-hydroxyvalerate) from carbon dioxide or a single organic substrate: improved polymer elongation with an extremely high 3-hydroxyvalerate mole proportion. *Journal of Applied Phycology* **2020**, *32*, 1095-1102.

22. Bhatia, S.K.; Yoon, J.-J.; Kim, H.-J.; Hong, J.W.; Gi Hong, Y.; Song, H.-S.; Moon, Y.-M.; Jeon, J.-M.; Kim, Y.-G.; Yang, Y.-H. Engineering of artificial microbial consortia of Ralstonia eutropha and Bacillus subtilis for poly(3-hydroxybutyrate-co-3-hydroxyvalerate) copolymer production from sugarcane sugar without precursor feeding. *Bioresource Technology* **2018**, *257*, 92-101.

23. Quillaguamán, J.; Guzmán, H.; Van-Thuoc, D.; Hatti-Kaul, R. Synthesis and production of polyhydroxyalkanoates by halophiles: current potential and future prospects. *Applied microbiology and biotechnology* **2010**, *85*, 1687-1696.

24. Cinelli, P.; Seggiani, M.; Mallegni, N.; Gigante, V.; Lazzeri, A. Processability and degradability of PHA-based composites in terrestrial environments. *International Journal of Molecular Sciences* **2019**, *20*.

25. Melendez-Rodriguez, B.; Torres-Giner, S.; Aldureid, A.; Cabedo, L.; Lagaron, J.M. Reactive melt mixing of poly(3-hydroxybutyrate)/rice husk flour composites with purified biosustainably produced poly(3-hydroxybutyrate-co-3-hydroxyvalerate). *Materials* **2019**, *12*.

26. Torres-Giner, S.; Montanes, N.; Fombuena, V.; Boronat, T.; Sanchez-Nacher, L. Preparation and characterization of compression-molded green composite sheets made of poly(3-hydroxybutyrate) reinforced with long pita fibers. *Advances in Polymer Technology* **2018**, *37*, 1305-1315.

27. Cherpinski, A.; Torres-Giner, S.; Cabedo, L.; Lagaron, J.M. Post-processing optimization of electrospun submicron poly(3-hydroxybutyrate) fibers to obtain continuous films of interest in food packaging applications. *Food Additives and Contaminants - Part A Chemistry, Analysis, Control, Exposure and Risk Assessment* **2017**, *34*, 1817-1830.

28. Melendez-Rodriguez, B.; Torres-Giner, S.; Figueroa-Lopez, K.J.; Castro-Mayorga, J.L.; Lagaron, J.M.; Cabedo, L. On the use of high-throughput electrospinning to produce optimized packaging films from polyhydroxyalkanoates. In Proceedings of Annual Technical Conference - ANTEC, Conference Proceedings.

29. Radusin, T.; Torres-Giner, S.; Stupar, A.; Ristic, I.; Miletic, A.; Novakovic, A.; Lagaron, J.M. Preparation, characterization and antimicrobial properties of electrospun polylactide films containing Allium ursinum L. extract. *Food Packaging and Shelf Life* **2019**, *21*.

30. Tariq, S.; Wani, S.; Rasool, W.; Shafi, K.; Bhat, M.A.; Prabhakar, A.; Shalla, A.H.; Rather, M.A. A comprehensive review of the antibacterial, antifungal and antiviral potential of essential oils and their chemical constituents against drug-resistant microbial pathogens. *Microbial Pathogenesis* **2019**, *134*, 103580.

31. Dorman, H.J.D.; Deans, S.G. Antimicrobial agents from plants: antibacterial activity of plant volatile oils. *Journal of Applied Microbiology* **2000**, *88*, 308-316.

32. Cao, D.; Jia, C.; Ji, S.; Zhang, X.; Muhoza, B. Tannic acid-assisted cross-linked nanoparticles as a delivery system of eugenol: The characterization, thermal degradation and antioxidant properties. *Food Hydrocolloids* **2020**, *104*, 105717.

33. Kim, J.; Marshall, M.R.; Wei, C.-i. Antibacterial activity of some essential oil components against five foodborne pathogens. *Journal of Agricultural and Food Chemistry* **1995**, *43*, 2839-2845.

34. Walsh, S.E.; Maillard, J.-Y.; Russell, A.D.; Catrenich, C.E.; Charbonneau, D.L.; Bartolo, R.G. Activity and mechanisms of action of selected biocidal agents on Gram-positive and -negative bacteria. *Journal of Applied Microbiology* **2003**, *94*, 240-247.

35. ELGAYYAR, M.; DRAUGHON, F.A.; GOLDEN, D.A.; MOUNT, J.R. Antimicrobial Activity of Essential Oils from Plants against Selected Pathogenic and Saprophytic Microorganisms. *Journal of Food Protection* **2001**, *64*, 1019-1024.

36. Devi, K.P.; Nisha, S.A.; Sakthivel, R.; Pandian, S.K. Eugenol (an essential oil of clove) acts as an antibacterial agent against Salmonella typhi by disrupting the cellular membrane. *Journal of Ethnopharmacology* **2010**, *130*, 107-115.

37. Kohanski, M.A.; Dwyer, D.J.; Collins, J.J. How antibiotics kill bacteria: from targets to networks. *Nat Rev Microbiol* **2010**, *8*, 423-435.

38. Khameneh, B.; Iranshahy, M.; Soheili, V.; Fazly Bazzaz, B.S. Review on plant antimicrobials: a mechanistic viewpoint. *Antimicrob Resist Infect Control* **2019**, *8*, 118-118.

39. Li, Y.; Dong, Q.; Chen, J.; Li, L. Effects of coaxial electrospun eugenol loaded core-sheath PVP/shellac fibrous films on postharvest quality and shelf life of strawberries. *Postharvest Biology and Technology* **2020**, *159*, 111028.

40. Celebioglu, A.; Yildiz, Z.I.; Uyar, T. Fabrication of Electrospun Eugenol/Cyclodextrin Inclusion Complex Nanofibrous Webs for Enhanced Antioxidant Property, Water Solubility, and High Temperature Stability. *Journal of Agricultural and Food Chemistry* **2018**, *66*, 457-466.

41. Soares, R.M.D.; Siqueira, N.M.; Prabhakaram, M.P.; Ramakrishna, S. Electrospinning and electrospray of bio-based and natural polymers for biomaterials development. *Materials Science and Engineering: C* **2018**, *92*, 969-982.

42. Figueroa-Lopez, K.J.; Castro-Mayorga , J.L.; Andrade-Mahecha, M.M.; Cabedo, L.; Lagaron, J.M. Antibacterial and Barrier Properties of Gelatin Coated by Electrospun Polycaprolactone Ultrathin Fibers Containing Black Pepper Oleoresin of Interest in Active Food Biopackaging Applications. *Nanomaterials* **2018**, *8*, 1-13.

43. Marangoni Júnior, L.; Oliveira, L.M.d.; Bócoli, P.F.J.; Cristianini, M.; Padula, M.; Anjos, C.A.R. Morphological, thermal and mechanical properties of polyamide and ethylene vinyl alcohol multilayer flexible packaging after high-pressure processing. *Journal of Food Engineering* **2020**, *276*, 109913.

44. Gómez Ramos, M.J.; Lozano, A.; Fernández-Alba, A.R. High-resolution mass spectrometry with data independent acquisition for the comprehensive non-targeted analysis of migrating chemicals coming from multilayer plastic packaging materials used for fruit purée and juice. *Talanta* **2019**, *191*, 180-192.

45. Wang, L.; Chen, C.; Wang, J.; Gardner, D.J.; Tajvidi, M. Cellulose nanofibrils versus cellulose nanocrystals: Comparison of performance in flexible multilayer films for packaging applications. *Food Packaging and Shelf Life* **2020**, *23*, 100464.

46. Garrido-López, Á.; Tena, M.T. Study of multilayer packaging delamination mechanisms using different surface analysis techniques. *Applied Surface Science* **2010**, *256*, 3799-3805.

47. Úbeda, S.; Aznar, M.; Vera, P.; Nerín, C.; Henríquez, L.; Taborda, L.; Restrepo, C. Overall and specific migration from multilayer high barrier food contact materials – kinetic study of cyclic polyester oligomers migration. *Food Additives & Contaminants: Part A* **2017**, *34*, 1784-1794.

48. Anukiruthika, T.; Sethupathy, P.; Wilson, A.; Kashampur, K.; Moses, J.A.; Anandharamakrishnan, C. Multilayer packaging: Advances in preparation techniques and emerging food applications. *Comprehensive Reviews in Food Science and Food Safety* **2020**, *19*, 1156-1186.

49. Mount, E. Chapter 6 - Coextrusion equipment for multilayer flat films and sheets. In *Multilayer Flexible Packaging*, Wagner, J.R., Ed. William Andrew Publishing: Boston, **2010**, 75-95.

50. Torres-Giner, S.; Pérez-Masiá, R.; Lagaron, J.M. A review on electrospun polymer nanostructures as advanced bioactive platforms. *Polymer Engineering and Science* **2016**, *56*, 500-527.

51. Busolo, M.A.; Torres-Giner, S.; Laaron, J.M. Enhancing the gas barrier properties of polylactic acid by means of electrospun ultrathin zein fibers. In Proceedings of Annual Technical Conference - ANTEC, Conference Proceedings; pp. 2763-2767.

52. Torres-Giner, S.; Martinez-Abad, A.; Lagaron, J.M. Zein-based ultrathin fibers containing ceramic nanofillers obtained by electrospinning. II. Mechanical properties, gas barrier, and sustained release capacity of biocide thymol in multilayer polylactide films. *Journal of Applied Polymer Science* **2014**, *131*, 9270-9276.

53. Fabra, M.J.; Lopez-Rubio, A.; Lagaron, J.M. High barrier polyhydroxyalcanoate food packaging film by means of nanostructured electrospun interlayers of zein. *Food Hydrocolloids* **2013**, *32*, 106-114.

54. Fabra, M.J.; Lopez-Rubio, A.; Lagaron, J.M. Nanostructured interlayers of zein to improve the barrier properties of high barrier polyhydroxyalkanoates and other polyesters. *Journal of Food Engineering* **2014**, *127*, 1-9.

55. Cherpinski, A.; Torres-Giner, S.; Cabedo, L.; Méndez, J.A.; Lagaron, J.M. Multilayer structures based on annealed electrospun biopolymer coatings of interest in water and aroma barrier fiber-based food packaging applications. *Journal Applied Polymer Science* **2017**, 1-11.

56. Cherpinski, A.; Torres-Giner, S.; Vartiainen, J.; Peresin, M.S.; Lahtinen, P.; Lagaron, J.M. Improving the water resistance of nanocellulose-based films with polyhydroxyalkanoates processed by the electrospinning coating technique. *Cellulose* **2018**, *25*, 1291-1307.

57. Quiles-Carrillo, L.; Montanes, N.; Lagaron, J.M.; Balart, R.; Torres-Giner, S. Bioactive multilayer polylactide films with controlled release capacity of gallic acid accomplished by incorporating electrospun nanostructured coatings and interlayers. *Applied Sciences (Switzerland)* **2019**, *9*.

58. Akinalan Balik, B.; Argin, S.; Lagaron, J.M.; Torres-Giner, S. Preparation and Characterization of Electrospun Pectin-Based Films and Their Application in Sustainable Aroma Barrier Multilayer Packaging. *Applied Sciences* **2019**, *9*, 5136.

59. Figueroa-Lopez, K.J.; Vicente, A.A.; Reis, M.A.M.; Torres-Giner, S.; Lagaron, J.M. Antimicrobial and Antioxidant Performance of Various Essential Oils and Natural Extracts and Their Incorporation into Biowaste Derived Poly(3-hydroxybutyrate-co-3-hydroxyvalerate) Layers Made from Electrospun Ultrathin Fibers. *Nanomaterials (Basel, Switzerland)* **2019**, *9*.

60. Castro-Mayorga, J.L.; Fabra, M.J.; Pourrahimi, A.M.; Olsson, R.T.; Lagaron, J.M. The impact of zinc oxide particle morphology as an antimicrobial and when incorporated in poly(3-hydroxybutyrate-co-3-hydroxyvalerate) films for food packaging and food contact surfaces applications. *Food and Bioproducts Processing* **2017**, *101*, 32-44.

61. Cerqueira, M.A.; Fabra, M.J.; Castro-Mayorga, J.L.; Bourbon, A.I.; Pastrana, L.M.; Vicente, A.A.; Lagaron, J.M. Use of Electrospinning to Develop Antimicrobial Biodegradable Multilayer Systems: Encapsulation of Cinnamaldehyde and Their Physicochemical Characterization. *Food and Bioprocess Technology* **2016**, *9*, 1874-1884.

62. Torres-Giner, S.; Torres, A.; Ferrandiz, M.; Fombuena, V.; Balart, R. Antimicrobial activity of metal cation-exchanged zeolites and their evaluation on injection-molded pieces of bio-based high-density polyethylene. *Journal of Food Safety* **2017**, *37*, 1-12.

63. Jouki, M.; Yazdi, F.T.; Mortazavi, S.A.; Koocheki, A. Quince seed mucilage films incorporated with oregano essential oil: Physical, thermal, barrier, antioxidant and antibacterial properties. *Food Hydrocolloids* **2014**, *36*, 9-19.

64. Vieira, M.G.A.; da Silva, M.A.; dos Santos, L.O.; Beppu, M.M. Natural-based plasticizers and biopolymer films: A review. *European Polymer Journal* **2011**, *47*, 254-263.

65. Torres-Giner, S.; Gimenez, E.; Lagaron, J.M. Characterization of the morphology and thermal properties of Zein Prolamine nanostructures obtained by electrospinning. *Food Hydrocolloids* **2008**, *22*, 601-614.

66. Torres-Giner, S.; Ocio, M.J.; Lagaron, J.M. Development of active antimicrobial fiber based chitosan polysaccharide nanostructures using electrospinning. *Engineering in Life Sciences* **2008**, *8*, 303-314.

67. Melendez-Rodriguez, B.; Figueroa-Lopez, K.J.; Bernardos, A.; Martínez-Máñez, R.; Cabedo, L.; Torres-Giner, S.; M. Lagaron, J. Electrospun Antimicrobial Films of Poly(3-hydroxybutyrate-co-3-hydroxyvalerate) Containing Eugenol Essential Oil Encapsulated in Mesoporous Silica Nanoparticles. *Nanomaterials* **2019**, *9*, 227.

68. Shen, Z.; Kamdem, D.P. Development and characterization of biodegradable chitosan films containing two essential oils. *International Journal of Biological Macromolecules* **2015**, *74*, 289-296.

69. Haghighi, H.; Biard, S.; Bigi, F.; De Leo, R.; Bedin, E.; Pfeifer, F.; Siesler, H.W.; Licciardello, F.; Pulvirenti, A. Comprehensive characterization of active chitosan-gelatin blend films enriched with different essential oils. *Food Hydrocolloids* **2019**, *95*, 33-42.

70. Shao, Y.; Wu, C.; Wu, T.; Li, Y.; Chen, S.; Yuan, C.; Hu, Y. Eugenol-chitosan nanoemulsions by ultrasound-mediated emulsification: Formulation, characterization and antimicrobial activity. *Carbohydrate Polymers* **2018**, *193*, 144-152.

71. Piletti, R.; Bugiereck, A.M.; Pereira, A.T.; Gussati, E.; Dal Magro, J.; Mello, J.M.M.; Dalcanton, F.; Ternus, R.Z.; Soares, C.; Riella, H.G., et al. Microencapsulation of eugenol molecules by β-cyclodextrine as a thermal protection method of antibacterial action. *Materials Science and Engineering: C* **2017**, *75*, 259-271.

72. da Silva, C.G.; Kano, F.S.; dos Santos Rosa, D. Thermal stability of the PBAT biofilms with cellulose nanostructures/essential oils for active packaging. *Journal of Thermal Analysis and Calorimetry* **2019**, *138*, 2375-2386.

73. Figueroa-Lopez, K.J.; Enescu, D.; Torres-Giner, S.; Cabedo, L.; Cerqueira, M.A.; Pastrana, L.; Fuciños, P.; Lagaron, J.M. Development of electrospun active films of poly(3-hydroxybutyrate-co-3-hydroxyvalerate) by the incorporation of cyclodextrin inclusion complexes containing oregano essential oil. *Food Hydrocolloids* **2020**, *108*, 106013.

74. de Souza Moura, W.; de Souza, S.R.; Campos, F.S.; Sander Rodrigues Cangussu, A.; Macedo Sobrinho Santos, E.; Silva Andrade, B.; Borges Gomes, C.H.; Fernandes Viana, K.; Haddi, K.; Oliveira, E.E., et al. Antibacterial activity of Siparuna guianensis essential oil mediated by impairment of membrane permeability and replication of pathogenic bacteria. *Industrial Crops and Products* **2020**, *146*, 112142.

75. Alizadeh Behbahani, B.; Noshad, M.; Falah, F. Cumin essential oil: Phytochemical analysis, antimicrobial activity and investigation of its mechanism of action through scanning electron microscopy. *Microbial Pathogenesis* **2019**, *136*, 103716.

76. Nazzaro, F.; Fratianni, F.; De Martino, L.; Coppola, R.; De Feo, V. Effect of Essential Oils on Pathogenic Bacteria. *Pharmaceuticals* **2013**, *6*, 1451-1474.

77. Figueroa-Lopez, K.J.; Torres-Giner, S.; Enescu, D.; Cabedo, L.; Cerqueira, M.A.; Pastrana, L.M.; Lagaron, J.M. Electrospun Active Biopapers of Food Waste Derived Poly(3-hydroxybutyrate-co-3-

hydroxyvalerate) with Short-Term and Long-Term Antimicrobial Performance. *Nanomaterials* **2020**, *10*, 506.

78. Navikaite-Snipaitiene, V.; Ivanauskas, L.; Jakstas, V.; Rüegg, N.; Rutkaite, R.; Wolfram, E.; Yildirim, S. Development of antioxidant food packaging materials containing eugenol for extending display life of fresh beef. *Meat Science* **2018**, *145*, 9-15.

79. Fabra, M.J.; López-Rubio, A.; Cabedo, L.; Lagaron, J.M. Tailoring barrier properties of thermoplastic corn starch-based films (TPCS) by means of a multilayer design. *Journal of Colloid and Interface Science* **2016**, *483*, 84-92.

80. Wan, Z.; Wang, L.; Yang, X.; Guo, J.; Yin, S. Enhanced water resistance properties of bacterial cellulose multilayer films by incorporating interlayers of electrospun zein fibers. *Food Hydrocolloids* **2016**, *61*, 269-276.

81. Yoon, Y.I.; Moon, H.S.; Lyoo, W.S.; Lee, T.S.; Park, W.H. Superhydrophobicity of PHBV fibrous surface with bead-on-string structure. *Journal of Colloid and Interface Science* **2008**, *320*, 91-95.

82. Sombatmankhong, K.; Suwantong, O.; Waleetorncheepsawat, S.; Supaphol, P. Electrospun fiber mats of poly(3-hydroxybutyrate), poly(3-hydroxybutyrate-co-3-hydroxyvalerate), and their blends. *Journal of Polymer Science Part B: Polymer Physics* **2006**, *44*, 2923-2933.

83. Li, X.; Liu, K.L.; Wang, M.; Wong, S.Y.; Tjiu, W.C.; He, C.B.; Goh, S.H.; Li, J. Improving hydrophilicity, mechanical properties and biocompatibility of poly[(R)-3-hydroxybutyrate-co-(R)-3-hydroxyvalerate] through blending with poly[(R)-3-hydroxybutyrate]-alt-poly(ethylene oxide). *Acta Biomaterialia* **2009**, *5*, 2002-2012.

84. Han, J.; Wu, L.P.; Hou, J.; Zhao, D.; Xiang, H. Biosynthesis, characterization, and hemostasis potential of tailor-made poly(3-hydroxybutyrate-co-3-hydroxyvalerate) produced by Haloferax mediterranei. *Biomacromolecules* **2015**, *16*, 578-588.

85. Chang, C.-K.; Wang, H.-M.D.; Lan, J.C.-W. Investigation and Characterization of Plasma-Treated Poly(3-hydroxybutyrate) and Poly(3-hydroxybutyrate-co-3-hydroxyvalerate) Biopolymers for an In Vitro Cellular Study of Mouse Adipose-Derived Stem Cells. *Polymers* **2018**, *10*, 355.

86. Medina-Jaramillo, C.; Ochoa-Yepes, O.; Bernal, C.; Famá, L. Active and smart biodegradable packaging based on starch and natural extracts. *Carbohydrate Polymers* **2017**, *176*, 187-194.

87. Corre YM, Bruzaud S, Audic JL, Grohens Y. Morphology and functional properties of commercial polyhydroxyalkanoates: a comprehensive and comparative study. *Polymer Testing* **2012**, 1773, 31:226–35.

88. Kim, G.H.; Han, H.; Park, J.H.; Kim, W.D. An applicable electrospinning process for fabricating a mechanically improved nanofiber mat. *Polymer Engineering & Science* **2007**, *47*, 707-712, doi:10.1002/pen.20744.

89. Arrieta M.P.; López, A.; Hernández and Rayón, A. Ternary PLA–PHB–Limonene blends intended for biodegradable food packaging applications. *European Polymer Journal* **2014**, *50*, 255-270.

90. Narayanan A, Neera, Mallesha and K. V. Ramana: Synergized Antimicrobial Activity of Eugenol Incorporated Polyhydroxybutyrate Films Against Food Spoilage Microorganisms in Conjunction with Pediocin. *Applied Biochemistry and Biotechnology* **2013**, *170*(6), 1379-1388.

91. Requena, R.; Jiménez, A.; Vargas, M. and Chiralt A. Poly[(3-hydroxybutyrate)-co-(3-hydroxyvalerate)] active bilayer films obtained by compression moulding and applying essential oils at the interface. *Polymer International* **2016**, *65*(8), 883-891.

92. Alp-Erbay, E.; Figueroa-Lopez, K.J.; Lagaron, J.M.; Çağlak, E.; Torres-Giner, S. The impact of electrospun films of poly(ε-caprolactone) filled with nanostructured zeolite and silica microparticles on in vitro histamine formation by Staphylococcus aureus and Salmonella Paratyphi A. *Food Packaging and Shelf Life* **2019**, *22*, 100414.

93. Razumovskii, L.P.; Iordanskii, A.L.; Zaikov, G.E.; Zagreba, E.D.; McNeill, I.C. Sorption and diffusion of water and organic solvents in poly(β-hydroxybutyrate) films. *Polymer Degradation and Stability* **1994**, *44*, 171-175.

94. Figueroa-Lopez, K.J.; Andrade-Mahecha, M.M.; Torres-Vargas, O.L. Development of antimicrobial biocomposite films to preserve the quality of bread. *Molecules* **2018**, *23*, doi:10.3390/molecules23010212.

95. Hasheminya, S.-M.; Mokarram, R.R.; Ghanbarzadeh, B.; Hamishekar, H.; Kafil, H.S.; Dehghannya, J. Development and characterization of biocomposite films made from kefiran, carboxymethyl cellulose and Satureja Khuzestanica essential oil. *Food Chemistry* **2019**, *289*, 443-452.

96. Requena, R.; Vargas, M.; Chiralt, A. Obtaining antimicrobial bilayer starch and polyester-blend films with carvacrol. *Food Hydrocolloids* **2018**, *83*, 118-133.

97. Al-Tayyar, N.A.; Youssef, A.M.; Al-hindi, R. Antimicrobial food packaging based on sustainable Bio-based materials for reducing foodborne Pathogens: A review. *Food chemistry* **2020**, *310*, 125915.

98. Ribes, S.; Ruiz-Rico, M.; Pérez-Esteve, É.; Fuentes, A.; Barat, J.M. Enhancing the antimicrobial activity of eugenol, carvacrol and vanillin immobilised on silica supports against Escherichia coli or Zygosaccharomyces rouxii in fruit juices by their binary combinations. *LWT* **2019**, *113*, 108326.

CHAPTER VI

Development of Active Barrier Multilayer Films Based on Electrospun Antimicrobial Hot-Tack Food Waste Derived Poly(3-hydroxybutyrate-co-3-hydroxyvalerate) and Cellulose Nanocrystal Interlayers

K.J. Figueroa-Lopez, Sergio Torres-Giner, Inmaculada Angulo, Maria Pardo-Figuerez, Jose Manuel Escuin, Ana Isabel Bourbon, Luis Cabedo, Yuval Nevo, Miguel A. Cerqueira, and Jose M. Lagaron

Development of Active Barrier Multilayer Films Based on Electrospun Antimicrobial Hot-Tack Food Waste Derived Poly(3-hydroxybutyrate-co-3-hydroxyvalerate) and Cellulose Nanocrystals Interlayers

Abstract

Active multilayer films based on polyhydroxyalkanoates (PHAs) with and without high barrier coatings of cellulose nanocrystals (CNCs) were herein successfully developed. To this end, an electrospun antimicrobial hot-tack layer made of poly(3-hydroxybutyrate-co-3-hydroxyvalerate) (PHBV) derived from cheese whey, a by-product from the dairy industry, was deposited on a previously manufactured blown film of commercial food contact PHA-based resin. A hybrid combination of oregano essential oil (OEO) and zinc oxide nanoparticles (ZnONPs) were incorporated during the electrospinning process into the PHBV nanofibers at 2.5 and 2.25 wt%, respectively, in order to provide antimicrobial properties. A barrier CNC coating was also applied by casting from an aqueous solution of nanocellulose at 2 wt% using a rod at 1m/min. The whole multilayer structure was thereafter assembled in a pilot roll-to-roll laminating system, where the blown PHA-based film was located as the outer layers while the electrospun antimicrobial hot-tack PHBV layer and the barrier CNC coating were placed as interlayers. The resultant multilayer films, having a final thickness in the 130–150 µm range, were characterized to ascertain their potential in biodegradable food packaging. The multilayers showed contact transparency, interlayer adhesion, improved barrier to water and limonene vapors, and intermediate mechanical performance. Moreover, the films presented high antimicrobial and antioxidant activities in both open and closed systems for up to 15 days. Finally, the food safety of the multilayers was assessed by migration and cytotoxicity tests, demonstrating that the films are safe to use in both alcoholic and acid food simulants and they are also not cytotoxic for Caco-2 cells.

Keywords: PHBV; nanocellulose; multilayers; oregano essential oil; zinc nanoparticles; barrier films; active packaging; migration; cytotoxicity.

1   Introduction

Dependence of polymers to fossil fuels and environmental issues related to plastic wastes have motivated the research and development of biodegradable polymer materials based on renewable natural resources. Polyhydroxyalkanoates (PHAs) are one of the most commonly studied biodegradable biopolyesters that can be obtained by direct biosynthesis using microorganisms and enzymes. In particular, over 300 bacterial species have been reported to accumulate PHAs in their cytoplasm as carbon and energy storage granules [1]. PHAs are homo-, co-, and terpolymers in which their structure is principally constituted by (R)-hydroxy-fatty acids and basically consist of 3-, 4-, 5-, and 6-hydroxycarboxylic acids [2,3]. PHAs can be classified according to the number of carbons in their repeating units. This classification includes short-chain-length PHAs (scl-PHAs) with 3 to 5 carbon atoms, which main examples are poly(3-hydroxybutyrate) (PHB) and poly(3-hydroxybutyrate-co-3-hydroxyvalerate) (PHBV), showing properties similar to polypropylene (PP), medium-chain-length PHAs (mcl-PHAs) with 6 to 14 carbon atoms, such as poly(3-hydroxyhexanoate) (PHHx) and poly(3-hydroxyoctanoate) (PHO), which display elastic properties similar to rubbers and elastomers, and long-chain-length PHAs (lcl-PHAs) with more than 14 carbon atoms [3]. The PHB homopolymer and its copolymers with varying ratios of 3-hydroxyvalerate (3-HV), that is, PHBV are the most studied PHAs. The inclusion of the 3-HV comonomer reduces the degree of crystallization and crystallization rate of PHB and thus increases its flexibility and reduces its melting temperature (Tm) [4]. Both the biocompatibility and biodegradability characteristics of PHBV also make this biopolymer an outstanding material with broad applications in different sectors [5]. In this regard, the PHBV films present medium oxygen and water vapor barrier properties, which are relevant characteristics for the design of food packaging articles [6].

Multilayers consist of a sandwich-like structure made up of 12 or more layers typically based on plastics or other materials (e.g., paper) with dissimilar properties glued together where each layer contributes to improve the final properties of the article [7]. Multilayers are typically composed of "structural" and "barrier" layers usually on the outside and inside, respectively. An "active" layer can also be added, either on the outside or inside, depending on the final application. They are obtained by different methods, typically extrusion or solvent casting followed by lamination treatment as well as cast or film extrusion using multiple die designs, where each layer is usually glued by adhesives or "tie" layer resins [8]. In this regard, there are many reports about barrier multilayer systems, which combined hydrophobic biopolymers such as PHBV, polylactide (PLA) or poly(e-caprolactone) (PCL) with hydrophilic ones, such as zein, starch or gelatin, containing nanofillers to improve

the mechanical, water vapor, and oxygen barrier properties [8-12]. Likewise, active substances, such as essential oils and metallic nanoparticles, can be incorporated in one of the layers to confer antimicrobial and antioxidant properties to the final multilayer [13].

Cellulose nanocrystal (CNC) has become a new kind of nanofiller for the development of polymer nanocomposites due to its high aspect ratio and specific surface area, high elastic modulus and strength, as well as its non-toxicity, renewability, sustainability, and biocompatibility [14]. Also, it has been reported that CNC acts as a nucleating agent, increasing the polymer crystallization rate and providing increased mechanical properties [15]. CNC can be synthesized from a cellulosic source through isolation mechanisms that are usually attained through top-down methods, such as enzymatic, physical or chemical methodologies for extraction and isolation from crops, plants, and agricultural wastes. Acid hydrolysis of pre-treated (alkaline and bleaching) cellulose is the most commonly used method to isolate amorphous region from crystalline region to obtain CNC [16]. It has a relatively lower aspect ratio with a length of 50 – 500 nm and a width of 5 – 70 nm. The nanoparticles derived are pure cellulose and highly crystalline (~88%) with dimensions of ~100 – 200 nm (length) and cross-sections of ~5 – 10 nm [17]. CNC exhibits amphiphilic properties due to the high density of hydroxyl groups on their surface and the hydrophobic interactions generated by the crystalline organization along with extensive hydrogen bonding of polymer chains [18].

Among the potential active substances, the most studied ones are oregano essential oil (OEO) and zinc oxide nanoparticles (ZnONPs). Both substances are currently classified as Generally Recognized as Safe (GRAS) by the U.S. Food and Drug Administration (FDA) [19,20]. OEO is obtained by the secondary metabolism of plants and their antimicrobial, antifungal, and antioxidant activities are attributed to its principal volatile compounds, that is, carvacrol, thymol, p-cymene, and γ-terpinene [21,22]. ZnONPs are inorganic materials synthesized by mechanochemical processing, sol-gel methods, and spray pyrolysis. Zinc is one of the most used metal in the pharmacy and food industry due to their mechanical and thermal stabilities at ambient temperature, biocompatibility, antimicrobial activity, low cost, and toxicity [23,24]. Hence, the combination of inorganic and organic substances allows can confer improved active characteristics to the food packaging materials [24-27].

Electrospinning is an emergent technology with a great deal of potential in food packaging. It can create nano- and micro-scale structures, such as fibers and beads, with variable sizes and porosity of a wide range of polymers [28]. Fibers morphology can be controlled by the properties of the polymer solution, such as polymer type, viscosity, concentration, conductivity, surface tension, and solvent polarity, and also

by the processing conditions, for example flow rate, voltage, and distance to the collector [29]. Furthermore, since the process works at room temperature, it allows the processing of thermolabile substances, which is the case of most essential oils [30]. By the application of mild thermal post-treatments, the electrospinning has shown to be a promising method to obtain monolayer and multilayer systems for food packaging development with functional and active properties [12,22,27,31].

From the above, the aim of this study was to develop active and barrier multilayer films based on PHBV interlayers containing a previously optimized hybrid combination of OEO with ZnONPs and CNC coatings. For this purpose, a PHBV solution containing the active substances was deposited by electrospinning onto a blown film made of a commercial food contact PHA-based resin. The resultant bilayer was then covered on the electrospun layer side by another blown film. A similar structure was also developed including an inner solvent cast coating of CNC. Both multilayer structures were thereafter laminated by heat in a pilot roll-to-roll laminating system simulating an industrial process and the resultant multilayer films were characterized in terms of their morphological, optical, and barrier properties. Furthermore, the antimicrobial activity of the active multilayer film was evaluated against strains of *Staphylococcus aureus* (*S. aureus*) and *Escherichia coli* (*E. coli*) foodborne bacteria. Likewise, the antioxidant properties were evaluated in open and closed systems for up to 15 days. Finally, the amount of ZnONPs that might migrate from the active multilayer films into different food simulants and their cytotoxicity for Caco-2 cells were analyzed.

2 Materials and Methods

2.1 Materials

PHBV copolyester was obtained using mixed microbial cultures (MMCs) fed with fermented cheese whey (CW), an industrial residue of the dairy industry, and it was produced by Avecom (Wondelgem, Belgium) following a protocoled developed earlier [32]. The content of 3HV in PHBV was 20 % mol determined by gas chromatography (GC) using the method described by Lanham et al. [33] by means of a Bruker 430-GC gas chromatograph equipped with a FID detector and a BR-SWax column (60 m, 0.53 mm internal diameter, 1 mm film thickness, Bruker Optics Inc, Billerica, MA, USA). This PHBV was used to obtain an innovative active hot-tack by electrospinning.

A CNC aqueous solution at 2 wt% and a wetting agent at 0,1 wt% were supplied by Melodea Ltd. (Rehovot, Israel). Loctite Liofol PR1550 (primer) was obtained from Henkel Ibérica S.A. (Bilbao, Spain). YPACK210 film for flow-pack application was provided by Tecnopackaging (Zaragoza, Spain). OEO, with a purity >99 % and a relative density of 0.925 – 0.955 g/mL, was obtained from Gran Velada S.L. (Zaragoza, Spain). ZnONPs (CR-4FCC1), 99% purity, specific surface of 4.5 m^2/g, bulk density of 40 lb/ft3, and specific gravity of 5.6 were obtained from GH Chemicals LTD® (Quebec city, Quebec, Canada). Chloroform, reagent grade with 99.8 % purity, and methanol, high performance liquid chromatography (HPLC) grade with 99.9 % purity, were purchased from Panreac S.A. (Barcelona, Spain). Additionally, 1-butanol, reagent grade with 99.5 % purity, and 2,2-diphenyl-1-picrylhydrazyl radical (DPPH), and (±)-6-hydroxy-2,5,7,8-tetramethylchromane-2-carboxylic acid (Trolox), 97% purity, were purchased from Sigma Aldrich S.A. (Madrid, Spain). Ethanol absolute (≥ 99.9 % vol) was supplied by Honeywell® (Frankfurt, Germany). Acetic acid (AA) glacial (99 %) was supplied by Fisher Chemical® (Loughborough, UK). 100 % extra virgin olive oil (OO) was provided by Gallo® (Abrantes, Portugal). Zinc standard for inductively coupled plasma (ICP) calibration (TraceCERT®); 1000 mg/L zinc metal (high-purity quality) in 2 % nitric acid (HNO$_3$) (prepared with HNO$_3$ suitable for trace analysis and high-purity water, 18.2 MΩ.cm, 0.22 µm filtered) and HNO3 (70 % vol) were all supplied by Sigma-Aldrich (Darmstadt, Germany). Minimum essential media (MEM) was purchased from Milipore (Berlin, Germany). Trypsin - ethylenediaminetetraacetic acid (EDTA) (0.25 % trypsin-0.1 % EDTA), penicillin/streptomycin 100x, and fetal bovine serum (FBS) were all bought from Merck Millipore (Burlington, MA, USA). Sodium pyruvate solution 100 mM, resazurin sodium salt, and cell counting kit-8 (CCK-8) were obtained from Sigma-Aldrich (St. Louis, MO, USA).

2.2 Food Contact Blown Film

The commercial biodegradable food contact permitted compound YPACK210 was used to make the film. This was supplied by Ocenic Resins S.L. (Valencia, Spain). The compound is based on a commercial PHA, in which the content of PHA is 50 wt%. The film was obtained by film blowing in Tecnopackaging with a film blowing LABTECH LF400 equipment from Techlab Systems S.L. (Lezo, Spain). This machine has the following features: max. bubble diameter 350 mm, variable blowing speed, double screw extruder LE25-30/C, large 2.4-meter-high film tower, pneumatically operated film nip rolls, screw speed infinite variable from 0 to 300 RPM, and motorized adjustment of film tower height. The set parameters of the film blowing experiments were: a screw speed of 65 rpm, a screw pressure of 196 bar, a screw temperature profile of 170 °C / 170 °C / 168 °C / 168 °C, a superior roll speed of 1.8 m/min, a collection roll speed of 2.7 m/min, and a tower height of 1500 mm. The resulting blown film had a thickness of around 60 microns and a film width of 250 mm.

2.3 CNC Coating

A food contact primer (Loctite LIOFOL PR1550) was applied on corona discharged (100 watt.cm^2/min) YPACK210 film. The wetting agent was added into the primer to facilitate the coating of the food contact film surface. The coating trials were conducted, firstly at lab-scale by automatic film applicator and then at larger scale by ROKO (PrintCoat Instruments, Royston, UK). At a lab-scale, the food contact primer with wetting agent was put on the surface treated film by automatic film applicator with a profile rod coater of 6 µm - wet thickness. The primer was dried in oven at 90 °C for 1 min. On top of the primer, the CNC solution was coated using an automatic film applicator: Profile rod coater (100 µm- wet thickness), dry thickness of 2 µm, drying method at 90 °C for 15 min in oven. At large scale, the primer and wetting agent were mixed in an IKA Eurostar 6000 mixer (IKA®-Werke GmbH & Co. KG, Staufen, Germany) at low speed (200 rpm) to avoid bubbles. The food contact primer with wetting agent was put onto YPACK210 film by a meter bar head with a profile rod of 6 µm in Rotary Koater (ROKO) equipment. Drying was performed at 50 °C. Later, the CNC solution was applied on top of primer with a profile rod of 50 µm. Drying was performed at 90 °C at 1m/min to ensure complete drying of the CNC solution.

2.4   Electrospinning

A neat PHBV solution was prepared by dissolving 8 % (wt/vol) in a chloroform/1-butanol 75:25 (vol./vol.) mixture at room temperature. A solution containing 2.5 wt% OEO + 2.25 wt% ZnONPs in PHBV was also produced in the same conditions reported previously [21]. The PHBV solutions were electrospun for 2 h onto the YPACK210 films, with and without CNC, using a high-throughput electrospinning/electrospraying equipment Fluidnatek® LE 500 from Bioinicia S.L. (Valencia, Spain). Both solutions were processed under a constant flow using a 24 emitter multi-nozzle injector, scanning vertically onto the metallic plate. A voltage of 18.5 kV, a flow-rate of 6 mL/h per single emitter, and a tip-to-collector distance of 25 cm were used.

2.5   Multilayer Assembly

Once the active PHBV electrospun hot-tack was deposited onto the YPACK210 films with and without the CNC layer, another YPACK210 film was placed as the outer layer according to the scheme displayed in Figure 1. The resulting multilayer structure was assembled using a Reliant lamination equipment with rolls at a speed of 5 m/min at 140 °C during 20 s. The resultant multilayer samples had an average thickness in the 130 – 150 μm range.
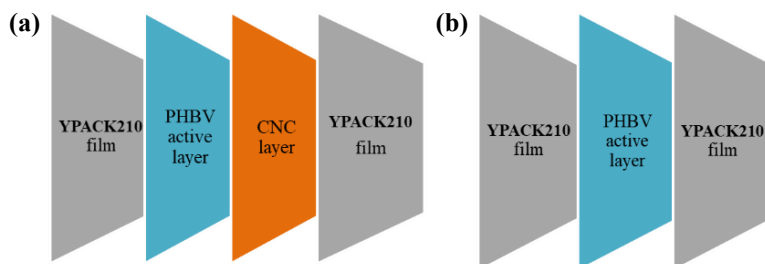
Figure 1. Scheme of the active multilayer films: (**a**) with cellulose nanocrystal (CNC) coating and (**b**) without CNC coating.

2.6   Characterization of the Multilayers

2.6.1   Film thickness

Before testing, the thickness of all films was measured using a digital micrometer (S00014, Mitutoyo, Corp., Kawasaki, Japan) with ± 0.001 mm accuracy. Measurements were performed and averaged in five different points, two in each end and one in the middle.

2.6.2   Morphology

The morphology of multilayer films was examined by scanning electron microscopy (SEM). The micrographs were taken using a Hitachi S-4800 electron microscope (Tokyo, Japan) at an accelerating voltage of 10 kV and a working distance of 8 – 10 mm. The samples were previously sputtered with a gold-palladium mixture for 3 min under vacuum. The average fiber diameter was determined via the ImageJ software v 1.41 using at least 20 SEM images.

2.6.3   Transparency

The light transmission of YPACK210 film and active multilayer films was determined in specimens of 50 mm x 30 mm by quantifying the absorption of light at wavelengths between 200 nm and 700 nm, using an UV–Vis spectrophotometer VIS3000 from Dinko, Instruments (Barcelona, Spain). The transparency value (T) was calculated using the following Formula (1):

$$T = \frac{A_{600}}{L} \tag{1}$$

Where and A_{600} is the absorbance at 600 nm, and L is the film thickness (mm).

2.6.4   Color

The color of the YPACK210 film and multilayer films was measured by using a Chroma Meter CR-400 (Konica Minolta, Tokyo, Japan) with illuminant D65. The color difference (ΔE*) was calculated by using the following Formula (2):

$$\Delta E = [(\Delta L^*)^2 + (\Delta a^*)^2 + (\Delta b^*)^2]^{0.5} \tag{2}$$

where ΔE*, Δa* and Δb* corresponded to the differences between the color parameters of multilayer films containing OEO and ZnONPs and the values of the reference film (neat blend) (a* = 0.74, b* = -0.41, L* = 90.44).

2.6.5   Water Vapor Permeance (WVP)

The water vapor permeance (WVP) of the multilayer films was determined according to the ASTM gravimetric method using Payne permeability cups (Elcometer SPRL, Hermelle/s, Lieja, Belgium) of 3.5 cm diameter. One side of the films was exposed to 100 % relative humidity (RH) by avoiding direct contact with liquid water. Then the cups containing the films were secured with silicon rings and stored in a desiccator at 25 °C and 0 % RH. The control samples were cups with aluminum films to estimate the solvent loss through the sealing and samples placed in cups but

without permeant. The cups were weighed periodically after the steady state was reached. Measurements were done in triplicate for each type of samples. WVP was calculated from the steady-state permeation slopes obtained from the regression analysis of weight loss data over time.

2.6.6 *Limonene Vapor Permeance (LP)*

Limonene vapor permeance was measured as described above for WVP. For this, 5 mL of D-limonene was placed inside the Payne permeability cups. The test was performed at 25 °C and 40 % RH. The control samples were cups with aluminum films to estimate the solvent loss through the sealing and samples placed in cups but without permeant to account for weight changes due to moisture sorption.

2.6.7 *Mechanical Test*

Tensile tests were conducted in a universal testing machine Shimatzu AGS-X 500N (Shimatzu, Kyoto, Japan) at room temperature with a cross-head speed of 10 mm/min. Dumbbell film samples according to ASTM D638 (Type IV) standard were die-cut from the multilayer assembly both in machine direction (MD) and in the transversal direction (TD). All the samples were stored in a vacuum desiccator at room temperature until tested. At least six samples were tested for each multilayer, and the average values of the mechanical parameters and standard deviations were reported.

2.6.8 *Antimicrobial Tests*

S. aureus CECT240 (ATCC 6538p) and *E. coli* CECT434 (ATCC 25922) strains were obtained from the Spanish Type Culture Collection (CECT, Valencia, Spain) and stored in phosphate buffered saline (PBS) with 10 wt% tryptic soy broth (TSB, Conda Laboratories, Madrid, Spain) and 10 wt % glycerol at −80 °C. Previous to each study, a loopful of bacteria was transferred to 10 mL of TSB and incubated at 37 °C for 24 h. A 100-μL aliquot from the culture was again transferred to TSB and grown at 37 °C to the mid-exponential phase of growth. The approximate count of 5 x 10^5 CFU / mL of culture having absorbance value of 0.20 as determined by optical density at 600 nm (Agilent 8453 UV–visible spectrum system, Agilent Technologies Deutschland GmbH, Waldbronn, Germany).

The antimicrobial performance of the active multilayer films was evaluated by using a modification of the Japanese Industrial Standard JIS Z2801 (ISO 22196:2007) [12]. A microorganism suspension of *S. aureus* and *E. coli* was applied onto the active multilayer films containing OEO/ZnONPs with CNC (measured by both sides) and

without CNC, and in the multilayers without OEO and ZnONPs (as negative control). The samples, sizing 1.5 cm x 1.5 cm, were placed in either hermetically closed or open bottles, the here so-called closed and open systems. After incubation at 24 °C at least 95 %RH for 24 h, bacteria were recovered with PBS, 10-fold serially diluted, and incubated at 37 °C for 24 h in order to quantify the number of viable bacteria by conventional plate count. The antimicrobial activity was evaluated from 1 (initial day), 3, 8, and 15 days. The value of the antimicrobial activity (R) was calculated as follows:

$$R = \left[Log\left(\frac{B}{A}\right) - Log\left(\frac{C}{A}\right) \right] = Log\left(\frac{B}{C}\right) \tag{3}$$

where A is the average of the number of viable bacteria on the control sample immediately after inoculation, B is the average of the number of viable bacteria on the control sample after 24h, and C is the average of the number of viable bacteria on the test sample after 24h. Three replicate experiments were performed for each sample and the antibacterial activity was evaluated with the following assessment: Nonsignificant ($R < 0.5$), slight ($R \geq 0.5$ and < 1), significant ($R \geq 1$ and < 3), and strong ($R \geq 3$) [34].

2.6.9   Antioxidant Measurements

The antioxidant activity of the multilayer films was determined following the DPPH assay. The film samples were stored for 1 (initial day), 3, 8, and 15 days in both open and closed systems. In each measurement, approximately 0.1 g of film was weighed in triplicate in cap vials and then an aliquot of 10 mL of a stock DPPH solution (0.05 g/L in aqueous methanol 80 vol%) was added. Vials without samples were also prepared as controls. The blank was the sample in aqueous methanol 80 vol% without DPPH. All the samples were prepared and immediately stored at room temperature for 2 h in darkness. After this, the absorbance of the solution was measured at 517 nm in the UV 4000 spectrophotometer from Dinko Instruments (Barcelona, Spain). Results were expressed as the percentage of inhibition to DPPH following Equation (4) [35] and µg equivalent of Trolox per gram of sample, employing a previously prepared calibration curve of Trolox (0–1000 µM).

$$Inhibition\ DPPH\ (\%) = \frac{A_{Control} - (A_{sample} - A_{blank})}{A_{control}} * 100 \tag{4}$$

Where $A_{control}$, A_{blank}, and A_{sample} are the absorbance values of the DPPH solution, methanol with the test sample, and the test sample, respectively.

2.6.10 Migration Tests

The specific migration test conditions were followed by the European Normative EC 13130-1:2004 [36]. For this purpose, the Inductively Coupled Plasma-Optical Emission Spectroscopy (ICP-OES) was used to determine the migration of ZnONPs particles from the active multilayer films using standardized cell (MigraCell®, FABES Forschungs-GmbH®, Munich, Germany) for overall/specific migration with an area of 0.75 dm2 in three food simulants that were sealed in clean wide-mouth jars. These simulant systems were ethanol (83.33 ml of 10 % v/v at 40 °C for 10 days), acetic acid (83.33 ml of 3% w/v at 40 °C for 10 days), and olive oil (83.33 g of 100 % wt at 10 °C for 10 days). For each formulation, the specific migration tests were carried out in triplicate. As procedural blanks, the food simulant was filled into sealed jars and stored under the same conditions to check for contamination. All results were blank subtracted. After the incubation period, the multilayer films containing OEO/ZnONPs were removed, whereas the ethanol and acetic acid simulants were evaporated on an electric hot plate (100 – 150 °C) and subsequently digested with 1.2 ml of 70 % HNO_3. After the digestion process, the samples were resuspended in 10 % acidic solution. The simulant olive oil (300 mg) was mixed with 10 mL HNO_3 (70 % vol) and 2 mL of hydrogen peroxide (30 % vol) and digested in microwave. After the digestion process, 1 mL of sample was resuspended in 2 % acidic solution. All digested sampled were introduced for metal quantification by Inductively Coupled Plasma-Optical Emission Spectrometry (ICP-OES) using a Spectrometer ICPE-9000 (Shimadzu®, Tokyo, Japan) equipped with axial torch, an ultrasonic nebulizer for higher sensitivity, and a charge-coupled device (CCD) detector. The instrumental parameters employed for ICP-OES analysis were: nebulizer gas flow (0.70 L/min Ar); auxiliary gas flow (0.60 L/min Ar); Plasma (10 L/min Ar); Ar Gas P (478.66 kPa); ICP RF power (1.20 kW); direction: axial; rotation speed (20 rpm); CCD Temp (-15 °C); vacuum level (6.9 Pa). The linearity of the calibration curve was considered acceptable for a correlation coefficient of $R^2 > 0.999$.

2.6.11 Cytotoxicity Assay

Caco-2 cells, clone HTB-37™, from human colon carcinoma, were obtained from the American Type Culture Collection (ATCC®, Manassas, Virginia, USA). Caco-2 cells (passage 25-40) were cultured in minimum essential medium (MEM), supplemented with 20 % FBS, 1 % sodium pyruvate, and 1 % penicillin/streptomycin. The cells were kept at 37 °C and 5 % CO2 in 75 cm2 flasks. For the cytotoxicity assessment, confluent cells were detached using 0.25 % trypsin-

EDTA solution, then precipitated by centrifugation at 1080 rpm for 5 min and resuspended in fresh medium MEM at a concentration of 1 x 105 cells / mL. Cells were seeded onto 96-wells plates at a density of 1×10^4 cells (100 μL of cellular suspension) per well and left adhering overnight in a humidified atmosphere of 5 % CO_2 in air at 37 °C.

The cytotoxicity was indirectly determined by CCK-8 and resazurin assays. The evaluation was performed through indirect contact with Caco-2 cells. After cells adhesion, the culture medium was removed and replaced by 200 μL of culture medium. The active multilayer films with and without CNC (28 mm²) were placed onto the top of the culture medium, above the cells surface and incubated for 24 or 48 h. At each time-point, the multilayer films were removed and replaced by the biomarker.

2.6.11.1   CCK-8 Assay

CCK-8 is a colorimetric assay, which uses a highly water-soluble tetrazolium salt, exhibiting superior detection sensitivity than other tetrazolium salts-based assays [37]. In the CCK-8 measurement, the dye WST-8 [2-(2-methoxy-4-nitrophenyl)-3-(4-nitrophenyl)-5-(2,4disulfophenyl)-2H-tetrazolium, monosodium salt] is reduced by dehydrogenase in cells to form a water-soluble orange-colored product (formazan). The amount of formazan dye produced is directly correlated with the number of living cells. 100 μL of CCK-8, diluted at 5 % (v/v) in culture medium, were added to each well. After 3h of incubation, the absorbance was measured at 450 nm using a Microplate Reader (Synergy, BioteK H1, BioTek Instruments, Winooski, VT, USA). The cell viability was expressed in percentage of absorbance in treated cells in relation to the absorbance of cells growing in MEM. A negative control was performed using cells growing in culture medium (MEM), considered as 100 % cell viability. A positive control was done using 10 % vol DMSO.

2.6.11.2   Resazurin assay

Resazurin dye is a cell permeable redox indicator that has been broadly used as an indicator of cell viability in proliferation and cytotoxicity assays [38]. Viable cells with active metabolism can reduce resazurin into the resorufin product, which is pink and fluorescent. The quantity of resorufin produced is proportional to the number of viable cells. After adhesion, the culture medium was removed and replaced by culture medium with 0.01 mg/mL resazurin. Multilayer film samples of 0.4 mm x 0.4 mm were added to each well and incubated for 24 and 48 h. A negative control was

performed using the cells growing in the culture medium (considered as 100 % cell viability) and 40 % (vol/vol) DMSO was used as a positive control (cell death).

The fluorescence intensity, which is proportional to the cell viability, was directly measured at each time point (24 and 48 h) using a Microplate Fluorescence Reader from BioTek Instruments at an excitation wavelength of 560 nm and an emission wavelength of 590 nm. The percentage of cell viability was expressed as fluorescence of treated cells compared to the fluorescence of cells growing in the culture medium as follows:

$$\% \text{ cell viability} = \frac{(F_{TC} - F_S)}{(F_C - F_{CM})} \times 100 \tag{5}$$

2.7 Statistical Analysis

The color, transparency, barrier properties, and antioxidant activity were evaluated through analysis of variance (ANOVA) with 95 % significance level ($p \leq 0.05$) and a multiple comparison test (Tukey) to identify significant differences among the treatments. Each treatment was done in triplicate. For this purpose, we used the software OriginPro8 (OriginLab Corporation, Northampton, MA, USA).

3   Results and Discussions

3.1   Morphology

The morphologies of the electrospun CW derived PHBV fibers and the multilayer films were analyzed by SEM in Figure 2. One can observe in Figure 2a that electrospinning yielded fibers with a smooth surface and free of beaded regions, having a final thickness for the layer of approximately 0.6 μm. The thickness of the multilayer films with CNC and without CNC was 140 and 131 μm, respectively. This by no means implies that the difference in thickness is accounted for by the layer of CNC, but that the substrate film used had variations along the width generated during the film blowing process. The most representative micrographs of each multilayer in their cross-sections are also shown in Figure 2. On the one hand, the multilayer film with CNC, included in Figure 2b, showed clearly the presence of the CNC coating. A higher magnification of this cross-section, shown in Figure 2c, revealed that the thickness of the resultant CNC interlayer was approximately 1 μm, and also the presence of the electrospun hot-tack active layer. It can also be observed that both interlayers were well adhered in the multilayer structure, suggesting good adhesion with the YPACK210 film. On the other hand, the active multilayer film without CNC, shown in Figure 2d, also presented a homogeneous and continuous cross-section. However, individual layers cannot be discerned, which can be attributed to the good adhesion between the electrospun hot-tack layer and YPACK210 film since both are based on PHAs. As previously researched, the electrospun interlayers have the capacity to act as a tie layer after a mild annealing post-processing step due to their high porosity and large surface-to-volume ratio, which avoid the need for adhesives or tie resins that are usually employed in conventional processes to develop multilayer systems [39,40]. Similar results were reported by Fabra et al. [41] about multilayers consisted of PHBV films obtained by both solution casting and compression molding that were coated with zein ultrathin fiber mats by electrospinning. The last ones presented a homogeneous and completely smooth surface after being annealed in a hot press. Similarly, Cherpinski et al. [42] developed multilayer films based on PHB nanopapers, showing that the multilayers presented a similar continuous structure and strong interlayer adhesion, which was attributed to the coalescence process at the fiber interphase. This annealing process, performed at temperatures well below the polymer's melting point, has been recently described and better understood by Melendez-Rodriguez et al. [43].
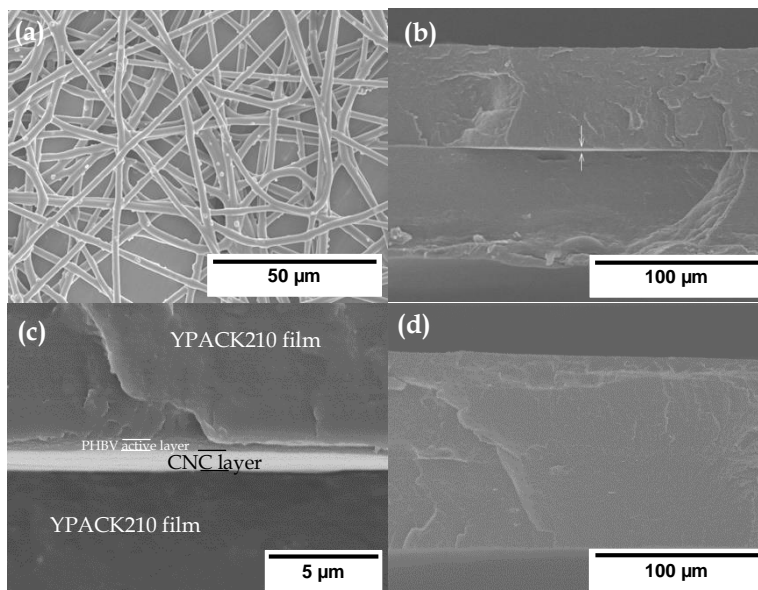
Figure 2. Scanning electron microscopy (SEM) micrographs of (**a**) the electrospun fibers of the cheese whey (CW) derived poly(3-hydroxybutyrate-co-3-hydroxyvalerate) (PHBV) containing 2.5 wt% oregano essential oil (OEO) + 2.25 wt% zinc oxide nanoparticles (ZnONPs) and of the active multilayer films (**b, c**) with cellulose nanocrystal (CNC) coating and (**d**) without CNC coating. Images taken at 800x, 500x, and 6000x show scale markers of 50, 100, and 5 μm, respectively.

3.2   Transparency and Color

Visual aspect of the active multilayer films is presented in Figure 3 and the transparency values of the films are shown in Table 1. This parameter is directly related to the surface and the internal structure of the material that is known to influence the light transmission and dispersion, thus affecting the transparency/opacity ratio [9]. The neat blown YPACK210 film, which is shown as reference in Figure 3a, presented the highest transparency value, that is, 6.83 ± 0.12. The active multilayer film with CNC showed a lower value transparency of 4.29 ± 0.15, whereas the active multilayer film without CNC presented a value of 5.94 ± 0.17. Therefore, lower transparency values were attained in the multilayer films that can ascribed to the fact that the interlayers were made of different materials that influenced on the light transmission and dispersion. In this regard, Cerqueira et al. [44] also showed that the presence of different outer layers based on PHBV and a zein interlayer with or without cinnamaldehyde led to a reduction in the transparency of the resultant multilayer films. In our previous report [24], the optical properties of similar active monolayer films based on PHBV prepared by electrospinning

presented a reduction in transparency, which was mainly ascribed to the presence of both OEO and ZnONPs. Fabra et al. [45] also reported differences in the internal transmittance values of multilayer films based on thermoplastic corn starch (TPCS) containing bacterial cellulose nanowhiskers (BCNWs) prepared by melt mixing and coated with PHB fibers by electrospinning. The reduction in transparency was attributed to the presence and different degree of dispersion of BCNW, resulting in a different refractive index. However, it is also worthy to mention that in the case of the here-developed multilayers based on CNC and electrospun PHBV interlayers, a notable transparency was still attained. Moreover, the effect of the CNC coating on the multilayer transparency was relatively low due to the low thickness and high homogeneity of this nanostructure cellulosic material. From a point of view of food preservation, the lower transparency in the multilayer films can also be positive due to their higher barrier capacity to block light, by which the photo-oxidation of organic compounds and degradation of vitamins and pigments of the food products can be reduced [46].

Figure 3. Visual aspect of: (**a**) YPACK210 film; (**b**) active multilayer films with cellulose nanocrystal (CNC) layers; (**c**) active multilayer films without cellulose nanocrystal (CNC) interlayer. Films are 5 cm × 2 cm.

The color parameters of active multilayer films were evaluated through CIELab* coordinates (L*, a*, b*), which represent the human visual color scale, and they were also reported in Table 1. It can be observed that multilayer films developed a slightly higher yellow appearance than the reference sample YPACK210 film, which probably originated by thickness doubling and also the presence of OEO since essential oils are known to increase yellow levels [21]. Accordingly, the values of a* coordinate, which represents the red and green colors, were 0.25–0.28 whereas the b* coordinate, which corresponds to yellow and blue colors, presented values of 1.31–1.42, and luminosity or brightness, represented by L*, was in the range of 89.81–89.86. Furthermore, one can also observe that the incorporation of the CNC interlayer into the active multilayer films did not show significantly differences in CIELab* coordinates. In particular, the ΔE values of the active multilayer films when referenced to the YPACK210 film were 1.88 (with CNC) and 1.84 (without CNC). In general terms, the color changes were based on a decrease in L* and an increase in the b* coordinate, which were responsible for the increase in the yellow tone of

the active multilayer films. A similar yellowing was previously observed by Melendez-Rodriguez et al. [47], who incorporated eugenol encapsulated in silica into PHBV by electrospinning. This effect was ascribed to the intrinsic eugenol color, which is a yellow oily liquid.

Table 1. Color parameters and transparency value of the neat YAPCK210 film and active multilayer films with and without cellulose nanocrystal (CNC) interlayer

Sample	a^*	b^*	L^*	ΔE	T
YPACK210 film	0.74 ± 0.02^a	-0.41 ± 0.01^a	90.44 ± 0.07^a	---	6.83 ± 0.12^a
Active multilayer with CNC	0.28 ± 0.01^b	1.31 ± 0.02^b	89.81 ± 0.17^b	1.88 ± 0.08^a	4.29 ± 0.15^b
Active multilayer without CNC	0.25 ± 0.03^b	1.42 ± 0.14^b	89.86 ± 0.22^b	1.84 ± 0.19^a	5.94 ± 0.17^c

a-c: Different superscripts within the same column indicate significant differences among samples (p < 0.05).

3.3 Barrier Properties

In general, biopolyesters show lower water barrier properties than conventional petrochemical polymers such as PET, which is detrimental for the development of packaging materials for food preservation [48]. One of the advantages of multilayer systems is the improvement of the barrier characteristics due to the use of barrier materials typically in the inner layers and protected from moisture and mechanical stress by the structural layers [49]. Permeance values in terms of water and limonene vapors, that is WVP and LP, of the active multilayer films are shown in Table 2. The WVP value (0.87×10^{-11} kg·m^{-2}·Pa^{-1}·s^{-1}) and LP value (1.36×10^{-11} kg·m^{-2}·Pa^{-1}·s^{-1}) of the active multilayer films with CNC were lower than the neat YPACK210 film modeled for similar thickness, which respectively presented a WVP value of 1.38×10^{-11} kg·m^{-2}·Pa^{-1}·s^{-1} and LP value of 1.62×10^{-11} kg·m^{-2}·Pa^{-1}·s^{-1}. Alternatively, the active multilayer film without CNC showed values of WVP and LP values of 1.32×10^{-11} kg·m^{-2}·Pa^{-1}·s^{-1} and 1.59×10^{-11} kg·m^{-2}·Pa^{-1}·s^{-1}, respectively, being also higher than those attained for the multilayer with CNC. This improvement in water and D-limonene barrier properties is ascribed primarily to the presence of the CNC thin coating, which is known to improve above all oxygen [31,42]. In addition, the presence of the active electrospun PHA layer containing OEO and ZnONPs, which are hydrophobic substances, may also contribute to block the diffusion of water molecules through the material [31]. Oxygen permeability could not be measured since the release the essential oil during the testing could alter the reading of the tester and, according to the manufacturer, could even damage the sensor. However, CNC coatings have been tested in other multilayers, yielding very strong oxygen

permeance reductions, of more than 89 % reduction when protected from moisture [42,50,51].

Other works have also reported important improvements in barrier performance by means of electrospun multilayers. For instance, Fabra et al. [52] compared the effect of adding different interlayers of electrospun whey protein isolate (WPI), pullulan and zein, to a PHA film obtained by compression molding. The addition of both electrospun zein and pullulan nanofibers improved the water vapor permeability by 28 – 35 %. In another study, Cherpinski et al. [42] improved the barrier properties of electrospun PHB and PHBV double side coatings by using cellulose nanofibrils (CNFs) and lignocellulose nanofibrils (LCNFs) interlayers. Wang et al. [53] also reported that the water vapor value of the multilayer film obtained by electrospinning with ethylcellulose nanofibers, as the outer layer, and curcumin-loaded gelatin nanofibers, as the inner one, was significantly lower (4.68×10^{-12} g·cm·cm^{-2}·s^{-1}·Pa^{-1}) than the equivalent gelatin film with or without curcumin (5.45×10^{-12} g·cm·cm^{-2}·s^{-1}·Pa^{-1}). The active multilayer films developed herein also showed slightly improved barrier properties.

Table 2. Thickness and permeance values in terms of water vapor permeance (WVP) and D-limonene permeance (LP) of the YPACK210 film and active multilayer films with and without cellulose nanocrystal (CNC) interlayer

Sample	Thickness (mm)	Permeance	
		WVP x 10^{11} (kg·m^{-2}·Pa^{-1}·s^{-1})	LP x 10^{11} (kg·m^{-2}·Pa^{-1}·s^{-1})
YPACK210 film 1 layer	0.060	3.22 ± 0.12[a]	3.78 ± 0.37[a]
YPACK210 1 layer (modeled)	0.140	1.38[b]	1.62[b]
Active multilayer with CNC*	0.140	0.87 ± 0.92[c]	1.36 ± 0.24[c]
Active multilayer with CNC**	0.140	0.89 ± 0.50[c]	1.39 ± 0.77[c]
Active multilayer without CNC	0.131	1.32 ± 0.17[b]	1.59 ± 0.38[b]

*measured by active interlayer side
**measured by CNC interlayer side
a-c: Different superscripts within the same column indicate significant differences among samples (p < 0.05).

Table 3. Mechanical properties in terms of elastic modulus (E), tensile strength at yield (σb), elongation at break (εb), and toughness (T) of the YAPCK210 film and active multilayer films with and without cellulose nanocrystal (CNC) interlayer in transversal (TD) and machine direction (MD)

Sample	Direction measure	E (MPa)	σ_b(MPa)	ε_b(%)	T (mJ/m^3)
YPACK210 film	TD	2066 ± 284[a]	23.1 ± 1.8[a]	173 ± 26[a]	40.99 ± 8.21[a]
Active multilayer with CNC		1491 ± 207[b]	20.0 ± 1.4[b]	59.1 ± 56[b]	11.95 ± 12.3[b]
Active multilayer without CNC		1446 ± 190[b]	19.2 ± 1.2[b]	51.6 ± 45[c]	10.36 ± 9.78[c]
YPACK210 film	MD	2510 ± 98[a]	29.6 ± 1.4[a]	76.3 ± 25[a]	19.17 ± 6.99[a]
Active multilayer with CNC		1828 ± 184[b]	23.5 ± 0.7[b]	45.6 ± 34[b]	9.67 ± 7.67[b]
Active multilayer without CNC		1811 ± 79[b]	22.28 ± 1.1[b]	32.3 ± 17[c]	6.87 ± 3.54[c]

a-c: Different superscripts within the same column indicate significant differences among samples (p < 0.05).

3.4 Mechanical Properties

The mechanical properties in terms of elastic modulus (E), tensile strength at break (σb), elongation at break (εb), and static toughness (T) of the YPACK210 film and active multilayer films in transversal direction (TD) and machine direction (MD) are gathered in Table 3. The YPACK210 film presented an E value of 2066 MPa (TD) and 2510 MPa (MD), a σb value of 23.1 MPa (TD) and 29.6 MPa (MD), and a εb value of 173% (TD) and 76.3% (MD). The difference in the mechanical behavior between the two directions is ascribed to the orientation of the biopolymer molecules during manufacturing of the YPACK210 film.

It can be observed that all the mechanical parameters decreased for the multilayer systems. Hence, the E values for the multilayer without CNC dropped by approximately 30% for both TD and MD samples, presenting values of 1491 MPa (TD) and 1828 MPa (MD), respectively. Similarly, the σb values of the multilayer were lower than the monolayer YPACK210 film, showing a decrease close to 20% in both tested directions. Therefore, the assembly of the multilayer system resulted in a decrease in the mechanical performance in comparison to the YPACK210 films. The lower mechanical resistance of the multilayer films can be ascribed to a delamination failure, which indicates that the interlayer adhesion was weaker than the mechanical strength of the YPACK210 film.

3.5 Antimicrobial activity

In food packaging, antimicrobial properties are indispensable to avoid or delay the microbiological reactions of the food products [54]. In this context, different natural substances, which is the case of essential oils and metallic nanoparticles, show the capacity to inhibit the growth of Gram positive (G+) and Gram negative (G–) bacteria. The antimicrobial performance of the active multilayer films with and without CNC was evaluated in an open and closed systems against *S. aureus* (+) and *E. coli* (G–) strains for 1, 3, 8, and 15 days. Table 4 shows the *S. aureus* and *E. coli* reduction values, that is, R, of the active multilayer films in an open system. The active multilayer film with CNC, measured by the active side after 15 days, showed *S. aureus* and *E. coli* reduction values of 1.33 and 1.26, respectively, which correspond to a significant reduction of the bacterial growth (R ≥ 1 and < 3). While the active multilayer film with CNC, measured by the CNC side, showed a slightly lower reduction against both bacteria, it was still significant. At 15 days, reduction value against *S. aureus* and *E. coli* of 1.08 and 1.04 were respectively attained. The slightly difference with the active multilayer film measured by the active side is due to presence of the high barrier CNC coating, which could promote a slow release of

the active compounds to the film surface. On the other hand, the active multilayer film without CNC reached, at 15 days, a slightly increase in the both bacteria reduction due to the improved release of the active compounds. The reduction of *S. aureus* was 1.35 and *E. coli* was 1.27, which corresponds to a significant reduction (R ≥ 1 and < 3). Table 5 presents the *S. aureus* and *E. coli* reduction values of the active multilayer films in the so-called closed system, which better resembles an actual packaging system. It was observed a slight difference in the reduction values reached at 15 days for the active multilayer films with CNC and without CNC against both bacteria when compared to the results obtained in the open system. This slightly increment can be associated to the release of the volatile compounds of OEO, which could accumulate in the headspace during the antimicrobial measurements and increased its concentration on the multilayer film surface. This phenomenon was observed in another research work using essential oils and natural extracts, suggesting that the use of these active volatile substances can be very relevant for food packaging [21,22]. Although the evaluated multilayer films presented a significant inhibition (R ≥ 1 and < 3), it was observed that the presence of CNC into one of the interlayers yield to sustain release of the active compounds. Besides that, in our previous study it was reported the optimization of the electrospun monolayer film containing 2.5 wt% OEO + 2.25 wt% ZnONPs [24], which showed a strong reduction (R ≥ 3) against *S. aureus* and *E. coli*., reason by which it was selected to develop the present multilayer films.

From the above, it is clearly seen that the antimicrobial activity of the monolayer films decreases in multilayer systems. However, the multilayers films obtained in this research presented a significant reduction against both G+ and G- bacteria., which enhances the application of this biodegradable active materials for food packaging applications. Other authors have also reported multilayer systems with antimicrobial performance. In this way, Lee et al. [55] developed a multilayer film based on polypropylene (PP), polyethylene terephthalate (PET), and low-density polyethylene (LDPE) containing star anise essential oil and thymol coating layers by bar coating and adhesive lamination processes. Authors concluded that the developed multilayer can show potential applicability as an active food packaging material with insect repellent and antimicrobial activities. In another study, Gherardi et al. [56] evaluated an antimicrobial packaging based on a multilayer commercial material composed of polyester, aluminum, and polyethylene joined by two adhesive layers and containing cinnamon essential oil. The resultant multilayer demonstrated a high antimicrobial activity in both inoculated culture media (in vitro) and tomato puree (in vivo) when packaged within the multilayer material against *E. coli* O157:H7 and *Saccharomyces cereviase* (*S. cereviase*) measured after 24 and 48 h, respectively. Pasqual Cerisuelo

et al. [57] also developed and successfully tested the antimicrobial activity of a multilayer material based on PP and PET coated with poly(ethylene-co-vinyl alcohol) (EVOH) that contained carvacrol, citral, marjoram essential oil or cinnamon bark essential oil through the application of a corona discharge followed by a polyethyleneimine (PEI)-based primer. In addition, Cerqueira et al. [44] studied the antimicrobial activity of multilayer films using PHBV as support and zein interlayer with or without cinnamaldehyde directly electrospun onto one side of the PHBV film and using a PHBV film as outer layer. This active multilayer system showed a greater antibacterial activity against Listeria monocytogenes (*L. monocytogenes*).

Table 4. Antibacterial activity against *Staphylococcus aureus* (*S. aureus*) and *Escherichia coli* (*E. coli*) of the active multilayer films with and without cellulose nanocrystal (CNC) interlayer in the open system for 15 days

Sample	Bacteria	Day	Control Log (CFU/mL)	Multilayer Log (CFU/mL)	R
Active multilayer with CNC*	*S. aureus*	1	6.95 ± 0.14	5.76 ± 0.09	1.19 ± 0.10
		3	6.90 ± 0.07	5.68 ± 0.08	1.22 ± 0.08
		8	6.89 ± 0.13	5.61 ± 0.15	1.28 ± 0.12
		15	6.91 ± 0.11	5.58 ± 0.12	1.33 ± 0.11
	E. coli	1	6.85 ± 0.15	5.72 ± 0.17	1.13 ± 0.16
		3	6.83 ± 0.08	5.64 ± 0.09	1.19 ± 0.07
		8	6.82 ± 0.15	5.60 ± 0.14	1.22 ± 0.13
		15	6.83 ± 0.14	5.57 ± 0.12	1.26 ± 0.11
Active multilayer with CNC**	*S. aureus*	1	6.95 ± 0.14	6.04 ± 0.12	0.91 ± 0.10
		3	6.90 ± 0.07	5.92 ± 0.08	0.98 ± 0.09
		8	6.89 ± 0.13	5.86 ± 0.11	1.03 ± 0.12
		15	6.91 ± 0.11	5.83 ± 0.09	1.08 ± 0.10
	E. coli	1	6.85 ± 0.15	5.99 ± 0.13	0.86 ± 0.13
		3	6.83 ± 0.08	5.92 ± 0.09	0.91 ± 0.08
		8	6.82 ± 0.15	5.83 ± 0.14	0.99 ± 0.12
		15	6.83 ± 0.14	5.79 ± 0.11	1.04 ± 0.13
Active multilayer without CNC	*S. aureus*	1	6.95 ± 0.14	5.74 ± 0.15	1.21 ± 0.17
		3	6.90 ± 0.07	5.66 ± 0.09	1.24 ± 0.09
		8	6.89 ± 0.13	5.59 ± 0.12	1.30 ± 0.15
		15	6.91 ± 0.11	5.56 ± 0.08	1.35 ± 0.10
	E. coli	1	6.85 ± 0.15	5.69 ± 0.12	1.16 ± 0.08
		3	6.83 ± 0.08	5.63 ± 0.09	1.20 ± 0.10
		8	6.82 ± 0.15	5.57 ± 0.13	1.25 ± 0.14
		15	6.83 ± 0.14	5.56 ± 0.11	1.27 ± 0.12

*measured by active interlayer side
**measured by CNC interlayer side

Table 5. Antibacterial activity against *Staphylococcus aureus* (*S. aureus*) and *Escherichia coli* (*E. coli*) of the active multilayer films with and without cellulose nanocrystal (CNC) interlayer in the closed system for 15 days

Sample	Bacteria	Day	Control Log (CFU/mL)	Multilayer Log (CFU/mL)	R
Active multilayer with CNC*	*S. aureus*	1	6.95 ± 0.14	5.75 ± 0.11	1.20 ± 0.09
		3	6.90 ± 0.07	5.66 ± 0.08	1.24 ± 0.07
		8	6.89 ± 0.13	5.59 ± 0.12	1.30 ± 0.11
		15	6.91 ± 0.11	5.57 ± 0.08	1.34 ± 0.07
	E. coli	1	6.85 ± 0.15	5.70 ± 0.14	1.15 ± 0.13
		3	6.83 ± 0.08	5.62 ± 0.09	1.21 ± 0.08
		8	6.82 ± 0.15	5.58 ± 0.14	1.24 ± 0.11
		15	6.83 ± 0.14	5.54 ± 0.11	1.29 ± 0.09
Active multilayer with CNC**	*S. aureus*	1	6.95 ± 0.14	6.02 ± 0.16	0.93 ± 0.15
		3	6.90 ± 0.07	5.90 ± 0.07	1.00 ± 0.08
		8	6.89 ± 0.13	5.83 ± 0.18	1.06 ± 0.16
		15	6.91 ± 0.11	5.81 ± 0.09	1.10 ± 0.09
	E. coli	1	6.85 ± 0.15	5.96 ± 0.13	0.89 ± 0.12
		3	6.83 ± 0.08	5.90 ± 0.09	0.93 ± 0.11
		8	6.82 ± 0.15	5.81 ± 0.12	1.01 ± 0.14
		15	6.83 ± 0.14	5.77 ± 0.15	1.06 ± 0.12
Active multilayer without CNC	*S. aureus*	1	6.95 ± 0.14	5.72 ± 0.09	1.23 ± 0.10
		3	6.90 ± 0.07	5.64 ± 0.08	1.26 ± 0.07
		8	6.89 ± 0.13	5.57 ± 0.11	1.32 ± 0.11
		15	6.91 ± 0.11	5.54 ± 0.10	1.37 ± 0.09
	E. coli	1	6.85 ± 0.15	5.67 ± 0.16	1.18 ± 0.18
		3	6.83 ± 0.08	5.61 ± 0.07	1.22 ± 0.08
		8	6.82 ± 0.15	5.54 ± 0.14	1.28 ± 0.14
		15	6.83 ± 0.14	5.53 ± 0.19	1.30 ± 0.17

*measured by active interlayer side
**measured by CNC interlayer side

3.6 Antioxidant activity

The antioxidant activity of the materials was studied through the DPPH free radical method, which is an antioxidant assay based on an electron-transfer that produces a violet solution in methanol. Active packaging materials with antioxidant capacity can avoid biochemical reactions caused by light that generates unpleasant aromas and flavors due to oxidation of fats and sugars [58]. Figure 4 and Table 6 show the percent inhibition and the equivalent concentration in micrograms of trolox per gram of the monolayer and multilayer (with and without CNC) films containing 2.5 wt% OEO + 2.25 wt% ZnONPs in both the open and closed systems for 15 days. As reported in a previous work [21], the antioxidant activity of OEO depends on the secondary metabolites such as, carvacrol, thymol, p-cymene, γ-terpinene, which are responsible of the high DPPH inhibition (91.96 %) with respect to other essential oils. Considering the above, the antioxidant activity of the pure OEO into PHBV multilayer and monolayer films decreased due to the low concentration into films and

the annealing process that can affect the volatile compounds stability, being sensitive to temperatures above 80 °C [59]. As expected, the active monolayer films showed the major DPPH inhibition in both systems during 15 days compared to the multilayer films, reaching a DPPH inhibition around of 12 %, that corresponds to 12.49 and 13.76 (µg eq. Trolox/g sample) for the open and closed system, respectively. The active multilayer films with CNC presented the lowest antioxidant activity of all the samples evaluated, having a DPPH percentage of 6 % after 15 days for the open and closed systems with values of 6.25 and 7.04 (µg eq. Trolox/g sample), respectively. The lower antioxidant activity attained in the multilayers could be associated with the presence of the CNC coating, which avoided the release of some volatile molecules of OEO in the aqueous medium when the test was performed. Furthermore, during the days of storage, a continuous release of the characteristic volatile compounds was produced. This behavior agrees with the antimicrobial results, where the inhibition of both bacteria was lower for the multilayer with CNC. On the other hand, the active multilayer films without CNC showed a DPPH inhibition of approximately 8.5 % at 15 days in open and closed systems with values of 9.00 and 9.29 (µg eq. Trolox/g sample) values, respectively. The DPPH percentage inhibition was significantly different with respect to the multilayer films having the CNC interlayer. This increase could be attributed to the favored release of the OEO molecules to the aqueous medium. For both multilayer films, the behavior in both storage systems (open and closed) did not show significant differences. However, in the different days of evaluation, the multilayer films presented significant differences, showing a reduction of the DPPH inhibition due to the reduced release of the active compounds that are responsible of the antioxidant activity. Similar results were reported by Wang et al. [53], who reported that t monolayer films based on curcumin-loaded gelatin prepared by electrospinning showed lower antioxidant activity compared to the pure curcumin whereas multilayer films based on ethylcellulose (EC) nanofibers, as the outer layer, and curcumin-loaded gelatin nanofibers, as the inner layer, showed lower antioxidant activity than the monolayer. Authors concluded that curcumin encapsulated in the gelatin film was well protected by the EC outer layers, which provided a physical barrier for the sustained release of curcumin. Different results were reported by Franco et al. [60] using supercritical carbon dioxide (SC-CO2) impregnation technique of α-tocopherol on monolayer and multilayer of PET/ PP films performed at 17 MPa and 40 °C. Results of percentage inhibition of the loaded films were similar to pure α-tocopherol after two hours of reaction with DPPH radical. In all cases, the antioxidant activity of the α-tocopherol was preserved after the impregnation with SC-CO_2. In this way, it is important to

point out that the functional activity of the substances and materials depends on the concentration of the active compounds and the process to obtain the materials.
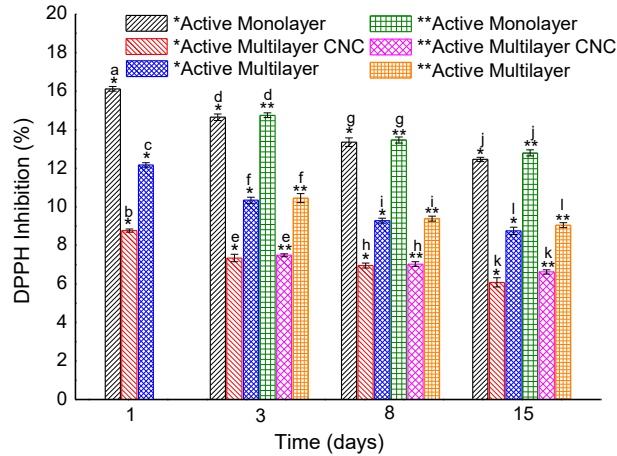
Figure 4. Inhibition percentage (%) of 2,2-diphenyl-1-picrylhydrazyl radical (DPPH) of the active multilayer films with and without cellulose nanocrystal (CNC) interlayer for 15 days. *Open system. **Closed system. a-l Different superscripts within the same column indicate significant differences among samples ($p < 0.05$).

Table 6. Concentration (µg eq. Trolox/g sample) of 2,2-diphenyl-1-picrylhydrazyl radical (DPPH) of the active multilayer films with and without cellulose nanocrystal (CNC) interlayer in the open a closed system for 15 days

Sample	Day	Open system (µg Eq. Trolox/g sample)	Closed system (µg Eq. Trolox/g sample)
Active monolayer	1	17.44 ± 0.14^{a}	---
	3	$15.94 \pm 0.10^{b,A}$	$15.98 \pm 0.19^{a,A}$
	8	$14.28 \pm 0.17^{c,B}$	$14.42 \pm 0.02^{b,B}$
	15	$12.49 \pm 0.08^{d,C}$	$13.76 \pm 0.12^{c,D}$
Active multilayer with CNC	1	9.11 ± 0.09^{e}	---
	3	$7.74 \pm 0.03^{f,E}$	$8.14 \pm 0.02^{d,F}$
	8	$7.42 \pm 0.01^{f,G}$	$7.44 \pm 0.01^{e,G}$
	15	$6.25 \pm 0.02^{g,H}$	$7.04 \pm 0.12^{e,I}$
Active multilayer without CNC	1	12.66 ± 0.12^{h}	---
	3	$10.90 \pm 0.02^{i,J}$	$11.01 \pm 0.06^{f,J}$
	8	$9.67 \pm 0.03^{j,K}$	$10.07 \pm 0.03^{g,L}$
	15	$9.00 \pm 0.09^{k,M}$	$9.29 \pm 0.04^{h,M}$

Means ± S.D
a-k: Different superscripts within the same column indicate significant differences among samples ($p < 0.05$)
A-M: Different superscripts within the same row indicate significant differences among samples ($p < 0.05$)

3.7   Migration test

Migration of nanoparticles is a competitive process that depends on their compatibility with the solid (film) and liquid (food simulant) phases during swelling of the solid phase surface as it comes into contact with the liquid phase [61]. Based on the results obtained in the three food simulants, shown in Table 7, the migration of ZnONPs from the PHA based barrier multilayer film with CNC is definitely influenced by the food simulants. The partial solubility of the biopolymers in each food simulant strongly affects the stability of the ZnONPs embedded into the PHBV matrix. The results revealed greater amounts of zinc released in the acidic solution than in the alcoholic one. Similar results were reported by EFSA [62] where the migration of zinc into 3 % acetic acid was high, up to 17.3 mg/kg, whereas in 10 % ethanol it was up to 80 µg/kg. Furthermore, Ozaki et al. [63] evaluated the migration of zinc from food contact plastics into food simulant such as distillate water, 4 % acetic acid, and 20 % ethanol, founding that zinc migration was higher in 4 % acetic acid due to the higher tendency of ionization. On the other hand, our previous research work evaluated the ZnONPs migration from electrospun active monolayer films of PHA containing 2.5 wt% OEO + 2.25 wt% ZnONPs [24], showing a migration value in acidic solution of 6.05 ± 0.81 mg/L and of 0.61 ± 0.1 mg/L in alcoholic solution. In comparison with the migration values of the here-developed active multilayer films, the ZnONPs migration was much lower than that observed for the equivalent monolayer films. These results indicate that the presence of other layers successfully hindered the ZnONPs migration through the whole multilayer. Therefore, the present active multilayer films can be used as an effective antimicrobial packaging for food preservation without affecting food safety. Contrary to the acidic and alcoholic solutions, the fatty simulant (olive oil) led to a high migration of ZnONPs into the fatty simulant. A similar behavior was observed by Heydari-Majd et al. [64], who reported that for a food simulant corresponding to fatty products (95 % ethanol), the Zn released was higher. Therefore, according to the new specific migration limit (SML) for soluble ionic Zn, that is, 5 mg/kg food or food simulant, set out by the European Plastics Regulation (EU) 2016/1416 amending [65] and correcting Regulation (EU) 10/2011, that is, 25 mg/kg food or food simulant [66] (see Annex II: Restrictions on materials and articles), all the tested multilayers are supposed to be safe for acidic and alcoholic solutions. However, in the case of the olive oil food simulant, the multilayer slightly exceeded the SML of Zn.

Table 7. Determination of the amount of zinc (Zn) migrated from the active multilayer films with cellulose nanocrystal (CNC) interlayer into different food simulants after an incubation period of 10 days at 40 °C

Sample	Food simulants					
	10% (v/v) aqueous ethanol		3 % (w/v) aqueous acetic acid		Olive Oil	
	Zn [mg/L]	Zn [mg/dm^2]	Zn [mg/L]	Zn [mg/dm^2]	Zn [mg/L]	Zn [mg/dm^2]
Active multilayer with CNC	0.051 ± 0.019	0.00089 ± 0.00021	0.185 ± 0.401	0.0032± 0.0051	26.662 ± 11.303	0.426 ± 0.142
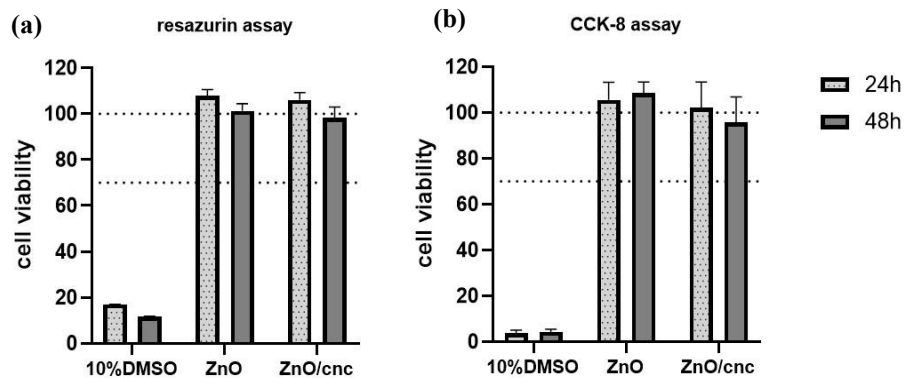
Figure 5. Cytotoxicity assay of the active multilayer films with and without cellulose nanocrystal (CNC) interlayer. Cell viability was assessed by the resazurin assay (**a**) and cell counting kit- (CCK-8) assay (**b**) on Caco-2 cells after incubation for 24 and 48h at 37 °C. Values shown Mean ± SD (N=8).

3.8 Cytotoxicity

The cytotoxicity assay studies the release of components (e.g., ZnONPs) from the material and their effect on cells viability, determining the biocompatibility and non-toxicity of biodegradable materials, which broadens its application in active food packaging design [67]. In Figure 5, the results of the cytotoxicity assay of the active multilayer films with and without CNC are shown. Cell viability was assessed by the resazurin assay (Figure 5a) and CCK-8 assay (Figure 5b) on Caco-2 cells after incubation for 24 or 48 h at 37 °C. The results showed that the cell viability was maintained close to 100 % throughout the whole experiment, demonstrating the cellular compatibility of the tested multilayer films in indirect contact with the caco-2 cells. These results show that the films and the substances eventually released from the films are non-toxic to Caco-2 cells. In this regard, Kang et al. [68] studied the cytotoxic effect of three kinds of ZnONPs on human epithelial Caco-2 cells at 24 h exposure. The report concluded that the cytotoxicity of ZnONPs was dose and time dependent and also was influenced by the size, distribution, and nanoparticles intensity. In other study, Apte et al. [69] evaluated the cytotoxicity of multilayer films based on chitosan and alginate, including subsequent cross-linking prepared by layer-by-layer (LbL) technique on viability of human dermal fibroblasts through resazurin assay. The results showed no signs of cytotoxicity in a time frame of 7 days, indicating that cross-linked films made of these biopolymers may be interesting candidates for wound dressings. Frígols et al. [70] also evaluated the cytotoxicity of zinc and graphene oxide (GO) into alginate films cross-linked with Ca^{2+} cations on human keratinocyte HaCaT cells. The results showed that the Zn and GO particles were not cytotoxic for the cell line tested and it was highlighted that zinc release and water sorption/diffusion depended significantly on the type of alginate utilized. In another research work, Ma et al. [71] fabricated poly(ether urethane) (PEU, Biospan®) films by the casting method for the controlled sustained release of the gallium (Ga) or Zn complexes, using poly(ethylene glycol) (PEG) as pore-forming agent. Cell viability of mouse NIH-3 T3 fibroblasts evaluated by alamarBlue™ assay demonstrated no cytotoxicity responses of the Ga- or Zn-complex releasing PEU films. According to the reports mentioned above, it is worthy to highlight that the cytotoxicity of the metallic nanoparticles and other substances does not only depends on their physical and chemical characteristics, but also on the matrix where they are entrapped.

4 Conclusions

In response to the constantly evolving food packaging industry requirements, novel research studies are currently focused on the development of environmentally friendly materials with active and barrier properties that are able to extend food shelf life. Active multilayer films with and without CNC have been successfully developed in this work, presenting a homogeneous and continuous surface with thickness ranging from 130 to 150 μm. Also, they showed high contact transparency with a slightly yellow appearance. The water vapor and limonene barrier properties of the active multilayer films with the CNC coating were higher than the active multilayer without CNC, due to the nanocellulose interlayer. The multilayer films presented significant inhibition ($R \geq 1$ and < 3) against *S. aureus* and *E. coli* in both storage systems, that is, closed and open, after 15 days. The antioxidant activity tested after 15 days, which is attributed to the presence of OEO, was significantly lower in the active multilayer films with the CNC coating also due to its barrier effect. The migration tests performed on the active multilayer film with CNC revealed that the ZnONPs migration values were much lower compared with the monolayer films, being for all food simulants below the SML for Zn, except for olive oil. Lastly, the cytotoxicity assay showed that the cell viability was maintained nearly at 100 %, demonstrating the cellular compatibility of the tested active multilayer films in indirect contact with Caco-2 cells.

The novel active multilayer films developed in this study can be regarded as potential candidates for use in the design of sustainable active food packaging. The active and barrier properties of these materials are certainly positive attributes and can be advantageous for food preservation. Since the developed multilayers are based on PHAs they can be applied as compostable or even biodegradable packaging articles, such as food trays or lids. Furthermore, they are partially obtained through the valorization of food waste, contributing to the Circular Bioeconomy progress. Future studies will be focused on analyzing their biodisintegration in both industrial conditions and natural environments as well as their in vivo performance to preserve different foods.

5   References

1. Chen, G.Q.; Wu, Q.; Jung, Y.K.; Lee, S.Y. 3.21 - PHA/PHB. In *Comprehensive Biotechnology (Second Edition)*, Moo-Young, M., Ed. Academic Press: Burlington, 2011; https://doi.org/10.1016/B978-0-08-088504-9.00179-3pp. 217-227.

2. Sudesh, K.; Abe, H.; Doi, Y. Synthesis, structure and properties of polyhydroxyalkanoates: biological polyesters. *Progress in Polymer Science* **2000**, *25*, 1503-1555, doi:https://doi.org/10.1016/S0079-6700(00)00035-6.

3. Park, S.J.; Kim, T.W.; Kim, M.K.; Lee, S.Y.; Lim, S.C. Advanced bacterial polyhydroxyalkanoates: towards a versatile and sustainable platform for unnatural tailor-made polyesters. *Biotechnology advances* **2012**, *30*, 1196-1206, doi:10.1016/j.biotechadv.2011.11.007.

4. Masood, F. Chapter 8—Polyhydroxyalkanoates in the Food Packaging Industry. In *Nanotechnology Applications in Food*; Oprea, A.E., Grumezescu, A.M., Eds.; Academic Press: Massachusetts, Cambridge, **2017**; pp. 153–177, doi:10.1016/B978-0-12-811942-6.00008-X.

5. Rivera-Briso, A.L.; Serrano-Aroca, Á. Poly(3-Hydroxybutyrate-co-3-Hydroxyvalerate): Enhancement Strategies for Advanced Applications. *Polymers (Basel)* **2018**, *10*, 732, doi:10.3390/polym10070732.

6. Tampau, A.; González-Martínez, C.; Chiralt, A. Biodegradability and disintegration of multilayer starch films with electrospun PCL fibres encapsulating carvacrol. *Polymer Degradation and Stability* **2020**, *173*, 109100, doi: https://doi.org/10.1016/j.polymdegradstab.2020.109100.

7. Fang, J.M.; Fowler, P.A.; Escrig, C.; Gonzalez, R.; Costa, J.A.; Chamudis, L. Development of biodegradable laminate films derived from naturally occurring carbohydrate polymers. *Carbohydrate Polymers* **2005**, *60*, 39-42, doi:https://doi.org/10.1016/j.carbpol.2004.11.018.

8. Heidemann, H.M.; Dotto, M.E.R.; Laurindo, J.B.; Carciofi, B.A.M.; Costa, C. Cold plasma treatment to improve the adhesion of cassava starch films onto PCL and PLA surface. *Colloids and Surfaces A: Physicochemical and Engineering Aspects* **2019**, *580*, 123739, doi:https://doi.org/10.1016/j.colsurfa.2019.123739.

9. Fabra, M.J.; Sánchez, G.; López-Rubio, A.; Lagaron, J.M. Microbiological and ageing performance of polyhydroxyalkanoate-based multilayer structures of interest in food packaging. *LWT - Food Science and Technology* **2014**, *59*, 760-767, doi:https://doi.org/10.1016/j.lwt.2014.07.021.

10. Benetto, E.; Jury, C.; Igos, E.; Carton, J.; Hild, P.; Vergne, C.; Di Martino, J. Using atmospheric plasma to design multilayer film from polylactic acid and thermoplastic starch: a screening Life Cycle Assessment. *Journal of Cleaner Production* **2015**, *87*, 953-960, doi:https://doi.org/10.1016/j.jclepro.2014.10.056.

11. Martucci, J.F.; Ruseckaite, R.A. Biodegradation behavior of three-layer sheets based on gelatin and poly (lactic acid) buried under indoor soil conditions. *Polymer Degradation and Stability* **2015**, *116*, 36-44, doi:https://doi.org/10.1016/j.polymdegradstab.2015.03.005.

12. Figueroa-Lopez, K.J.; Castro-Mayorga, J.L.; Andrade-Mahecha, M.M.; Cabedo, L.; Lagaron, J.M. Antibacterial and Barrier Properties of Gelatin Coated by Electrospun Polycaprolactone Ultrathin Fibers Containing Black Pepper Oleoresin of Interest in Active Food Biopackaging Applications. *Nanomaterials* **2018**, *8*, 199.

13. Jin, K.; Tang, Y.; Zhu, X.; Zhou, Y. Polylactic acid based biocomposite films reinforced with silanized nanocrystalline cellulose. *International Journal of Biological Macromolecules* **2020**, *162*, 1109-1117, doi:https://doi.org/10.1016/j.ijbiomac.2020.06.201.

14. Chen, J.; Wu, D.; Tam, K.C.; Pan, K.; Zheng, Z. Effect of surface modification of cellulose nanocrystal on nonisothermal crystallization of poly(β-hydroxybutyrate) composites. *Carbohydrate Polymers* **2017**, *157*, 1821-1829, doi:https://doi.org/10.1016/j.carbpol.2016.11.071.

15. de Carvalho, K.C.C.; Montoro, S.R.; Cioffi, M.O.H.; Voorwald, H.J.C. Chapter 13 - Polyhydroxyalkanoates and Their Nanobiocomposites With Cellulose Nanocrystals. In *Design and Applications of Nanostructured Polymer Blends and Nanocomposite Systems*, Thomas, S., Shanks, R., Chandrasekharakurup, S., Eds. William Andrew Publishing: Boston, 2016; https://doi.org/10.1016/B978-0-323-39408-6.00012-1pp. 261-285.

16. Dasan, Y.K.; Bhat, A.H.; Ahmad, F. Polymer blend of PLA/PHBV based bionanocomposites reinforced with nanocrystalline cellulose for potential application as packaging material. *Carbohydrate Polymers* **2017**, *157*, 1323-1332, doi:https://doi.org/10.1016/j.carbpol.2016.11.012.

17. Thomas, P.; Duolikun, T.; Rumjit, N.P.; Moosavi, S.; Lai, C.W.; Bin Johan, M.R.; Fen, L.B. Comprehensive review on nanocellulose: Recent developments, challenges and future prospects. *Journal of the Mechanical Behavior of Biomedical Materials* **2020**, *110*, 103884, doi:https://doi.org/10.1016/j.jmbbm.2020.103884.

18. Bao, C.; Chen, X.; Liu, C.; Liao, Y.; Huang, Y.; Hao, L.; Yan, H.; Lin, Q. Extraction of cellulose nanocrystals from microcrystalline cellulose for the stabilization of cetyltrimethylammonium bromide-enhanced Pickering emulsions. *Colloids and Surfaces A: Physicochemical and Engineering Aspects* **2021**, *608*, 125442, doi:https://doi.org/10.1016/j.colsurfa.2020.125442.

19. da Rocha Neto, A.C.; Beaudry, R.; Maraschin, M.; Di Piero, R.M.; Almenar, E. Double-bottom antimicrobial packaging for apple shelf-life extension. *Food Chemistry* **2019**, *279*, 379-388, doi:https://doi.org/10.1016/j.foodchem.2018.12.021.

20. Espitia, P.J.P.; Soares, N.d.F.F.; Coimbra, J.S.d.R.; de Andrade, N.J.; Cruz, R.S.; Medeiros, E.A.A. Zinc Oxide Nanoparticles: Synthesis, Antimicrobial Activity and Food Packaging Applications. *Food and Bioprocess Technology* **2012**, *5*, 1447-1464, doi:10.1007/s11947-012-0797-6.

21. Figueroa-Lopez, K.J.; Vicente, A.A.; Reis, M.A.M.; Torres-Giner, S.; Lagaron, J.M. Antimicrobial and Antioxidant Performance of Various Essential Oils and Natural Extracts and Their Incorporation into Biowaste Derived Poly(3-hydroxybutyrate-co-3-hydroxyvalerate) Layers Made from Electrospun Ultrathin Fibers. *Nanomaterials* **2019**, *9*, doi:10.3390/nano9020144.

22. Figueroa-Lopez, K.J.; Enescu, D.; Torres-Giner, S.; Cabedo, L.; Cerqueira, M.A.; Pastrana, L.; Fuciños, P.; Lagaron, J.M. Development of electrospun active films of poly(3-hydroxybutyrate-co-3-hydroxyvalerate) by the incorporation of cyclodextrin inclusion complexes containing oregano essential oil. *Food Hydrocolloids* **2020**, *108*, 106013, doi:https://doi.org/10.1016/j.foodhyd.2020.106013.

23. Moezzi, A.; McDonagh, A.M.; Cortie, M.B. Zinc oxide particles: Synthesis, properties and applications. *Chemical Engineering Journal* **2012**, *185-186*, 1-22, doi:https://doi.org/10.1016/j.cej.2012.01.076.

24. Figueroa-Lopez, K.J.; Torres-Giner, S.; Enescu, D.; Cabedo, L.; Cerqueira, M.A.; Pastrana, L.M.; Lagaron, J.M. Electrospun Active Biopapers of Food Waste Derived Poly(3-hydroxybutyrate-co-3-hydroxyvalerate) with Short-Term and Long-Term Antimicrobial Performance. *Nanomaterials* **2020**, *10*, 506.

25. Mo, Z.; Lin, J.; Zhang, X.; Fan, Y.; Xu, X.; Xue, Y.; Liu, D.; Li, J.; Hu, L.; Tang, C. Morphology controlled synthesis zinc oxide and reinforcement in polyhydroxyalkanoates composites. *Polymer Composites* **2014**, *35*, 1701-1706, doi:10.1002/pc.22823.

26. Heydari-Majd, M.; Ghanbarzadeh, B.; Shahidi-Noghabi, M.; Najafi, M.A.; Hosseini, M. A new active nanocomposite film based on PLA/ZnO nanoparticle/essential oils for the preservation of refrigerated Otolithes ruber fillets. *Food Packaging and Shelf Life* **2019**, *19*, 94-103, doi:https://doi.org/10.1016/j.fpsl.2018.12.002.

27. Castro-Mayorga, J.L.; Fabra, M.J.; Pourrahimi, A.M.; Olsson, R.T.; Lagaron, J.M. The impact of zinc oxide particle morphology as an antimicrobial and when incorporated in poly(3-hydroxybutyrate-co-3-hydroxyvalerate) films for food packaging and food contact surfaces applications. *Food and Bioproducts Processing* **2017**, *101*, 32-44, doi:https://doi.org/10.1016/j.fbp.2016.10.007.

28. Zhang, C.; Li, Y.; Wang, P.; Zhang, H. Electrospinning of nanofibers: Potentials and perspectives for active food packaging. *Comprehensive Reviews in Food Science and Food Safety* **2020**, *19*, 479-502, doi:10.1111/1541-4337.12536.

29. Topuz, F.; Uyar, T. Antioxidant, antibacterial and antifungal electrospun nanofibers for food packaging applications. *Food Research International* **2020**, *130*, 108927, doi:https://doi.org/10.1016/j.foodres.2019.108927.

30. Zhao, L.; Duan, G.; Zhang, G.; Yang, H.; He, S.; Jiang, S. Electrospun Functional Materials toward Food Packaging Applications: A Review. *Nanomaterials (Basel, Switzerland)* **2020**, *10*, doi:10.3390/nano10010150.

31. Figueroa-Lopez, K.J.; Cabedo, L.; Lagaron, J.M.; Torres-Giner, S. Development of Electrospun Poly(3-hydroxybutyrate-co-3-hydroxyvalerate) Monolayers Containing Eugenol and Their Application in Multilayer Antimicrobial Food Packaging. *Frontiers in Nutrition* **2020**, *7*, doi:10.3389/fnut.2020.00140.

32. Cruz, M.V.; Freitas, F.; Paiva, A.; Mano, F.; Dionísio, M.; Ramos, A.M.; Reis, M.A.M. Valorization of fatty acids-containing wastes and byproducts into short- and medium-chain length polyhydroxyalkanoates. *New Biotechnology* **2016**, *33*, 206-215, doi:https://doi.org/10.1016/j.nbt.2015.05.005.

33. Lanham, A.B.; Ricardo, A.R.; Albuquerque, M.G.E.; Pardelha, F.; Carvalheira, M.; Coma, M.; Fradinho, J.; Carvalho, G.; Oehmen, A.; Reis, M.A.M. Determination of the extraction kinetics for the quantification of polyhydroxyalkanoate monomers in mixed microbial systems. *Process Biochemistry* **2013**, *48*, 1626-1634, doi:https://doi.org/10.1016/j.procbio.2013.07.023.

34. Torres-Giner, S.; Torres, A.; Ferrándiz, M.; Fombuena, V.; Balart, R. Antimicrobial activity of metal cation-exchanged zeolites and their evaluation on injection-molded pieces of bio-based high-density polyethylene. *Journal of Food Safety* **2017**, *37*, e12348, doi:10.1111/jfs.12348.

35. Busolo, M.A.; Lagaron, J.M. Antioxidant polyethylene films based on a resveratrol containing Clay of Interest in Food Packaging Applications. *Food Packaging and Shelf Life* **2015**, *6*, 30-41, doi:https://doi.org/10.1016/j.fpsl.2015.08.004.

36. European Standard, EN:13130-1:2004. Materials and articles in contact with foodstuffs - Plastics substances subject to limitation - Part 1: Guide to test methods for the specific migration of substances from plastics to foods and food simulants and the determination of substances in plastic; European Committee for Standardization: Brussels, Belgium, **2004**.

37. Chamchoy, K.; Pakotiprapha, D.; Pumirat, P.; Leartsakulpanich, U.; Boonyuen, U. Application of WST-8 based colorimetric NAD(P)H detection for quantitative dehydrogenase assays. *BMC Biochemistry* **2019**, *20*, 4, doi:10.1186/s12858-019-0108-1.

38. Nociari, M.M.; Shalev, A.; Benias, P.; Russo, C. A novel one-step, highly sensitive fluorometric assay to evaluate cell-mediated cytotoxicity. *Journal of Immunological Methods* **1998**, *213*, 157-167, doi:https://doi.org/10.1016/S0022-1759(98)00028-3.

39. Quiles-Carrillo, L.; Montanes, N.; Lagaron, J.M.; Balart, R.; Torres-Giner, S. Bioactive Multilayer Polylactide Films with Controlled Release Capacity of Gallic Acid Accomplished by Incorporating Electrospun Nanostructured Coatings and Interlayers. *Applied Sciences* **2019**, *9*, 533.

40. Cerqueira, M.A.; Torres-Giner, S.; Lagaron, J.M. Chapter 6—Nanostructured Multilayer Films. In *Nanomaterials for Food Packaging*; Cerqueira, M.Â.P.R., Lagaron, J.M., Pastrana Castro, L.M., de Oliveira Soares Vicente, A.A.M., Eds.; Elsevier: Amsterdam, Netherlands, **2018**; pp. 147–171, doi:10.1016/B978-0-323-51271-8.00006-1.

41. Fabra, M.J.; Lopez-Rubio, A.; Lagaron, J.M. High barrier polyhydroxyalcanoate food packaging film by means of nanostructured electrospun interlayers of zein. *Food Hydrocolloids* **2013**, *32*, 106-114, doi:https://doi.org/10.1016/j.foodhyd.2012.12.007.

42. Cherpinski, A.; Torres-Giner, S.; Vartiainen, J.; Peresin, M.S.; Lahtinen, P.; Lagaron, J.M. Improving the water resistance of nanocellulose-based films with polyhydroxyalkanoates processed by the electrospinning coating technique. *Cellulose* **2018**, *25*, 1291-1307, doi:10.1007/s10570-018-1648-z.

43. Melendez-Rodriguez, B.; Torres-Giner, S.; Lorini, L.; Valentino, F.; Sammon, C.; Cabedo, L.; Lagaron, J.M. Valorization of Municipal Biowaste into Electrospun Poly(3-hydroxybutyrate-co-3-hydroxyvalerate) Biopapers for Food Packaging Applications. *ACS Applied Bio Materials* **2020**, *3*, 6110-6123, doi:10.1021/acsabm.0c00698.

44. Cerqueira, M.A.; Fabra, M.J.; Castro-Mayorga, J.L.; Bourbon, A.I.; Pastrana, L.M.; Vicente, A.A.; Lagaron, J.M. Use of Electrospinning to Develop Antimicrobial Biodegradable Multilayer Systems: Encapsulation of Cinnamaldehyde and Their Physicochemical Characterization. *Food and Bioprocess Technology* **2016**, *9*, 1874-1884, doi:10.1007/s11947-016-1772-4.

45. Fabra, M.J.; López-Rubio, A.; Ambrosio-Martín, J.; Lagaron, J.M. Improving the barrier properties of thermoplastic corn starch-based films containing bacterial cellulose nanowhiskers by means of PHA electrospun coatings of interest in food packaging. *Food Hydrocolloids* **2016**, *61*, 261-268, doi:https://doi.org/10.1016/j.foodhyd.2016.05.025.

46. Figueroa-Lopez, K.J.; Andrade-Mahecha, M.M.; Torres-Vargas, O.L. Development of Antimicrobial Biocomposite Films to Preserve the Quality of Bread. *Molecules* **2018**, *23*, 212.

47. Melendez-Rodriguez, B.; Figueroa-Lopez, K.J.; Bernardos, A.; Martínez-Máñez, R.; Cabedo, L.; Torres-Giner, S.; M. Lagaron, J. Electrospun Antimicrobial Films of Poly(3-hydroxybutyrate-co-3-hydroxyvalerate) Containing Eugenol Essential Oil Encapsulated in Mesoporous Silica Nanoparticles. *Nanomaterials* **2019**, *9*, 227.

48. Cava, D.; Giménez, E.; Gavara, R.; Lagaron, J.M. Comparative Performance and Barrier Properties of Biodegradable Thermoplastics and Nanobiocomposites versus PET for Food Packaging Applications. *Journal of Plastic Film & Sheeting* **2006**, *22*, 265-274, doi:10.1177/8756087906071354.

49. Fabra, M.J.; Lopez-Rubio, A.; Lagaron, J.M. Nanostructured interlayers of zein to improve the barrier properties of high barrier polyhydroxyalkanoates and other polyesters. *Journal of Food Engineering* **2014**, *127*, 1-9, doi:https://doi.org/10.1016/j.jfoodeng.2013.11.022.

50. Zhang, J.; Ozturk, S.; Singh, R.K.; Kong, F. Effect of cellulose nanofiber-based coating with chitosan and trans-cinnamaldehyde on the microbiological safety and quality of cantaloupe rind and fresh-cut pulp. Part 1: Microbial safety. *LWT* **2020**, *134*, 109972, doi:https://doi.org/10.1016/j.lwt.2020.109972.

51. Wang, L.; Chen, C.; Wang, J.; Gardner, D.J.; Tajvidi, M. Cellulose nanofibrils versus cellulose nanocrystals: Comparison of performance in flexible multilayer films for packaging applications. *Food Packaging and Shelf Life* **2020**, *23*, 100464, doi:https://doi.org/10.1016/j.fpsl.2020.100464.

52. Fabra, M.J.; López-Rubio, A.; Lagaron, J.M. On the use of different hydrocolloids as electrospun adhesive interlayers to enhance the barrier properties of polyhydroxyalkanoates of interest in fully renewable food

packaging concepts. *Food Hydrocolloids* **2014**, *39*, 77-84, doi:https://doi.org/10.1016/j.foodhyd.2013.12.023.

53. Wang, P.; Li, Y.; Zhang, C.; Feng, F.; Zhang, H. Sequential electrospinning of multilayer ethylcellulose/gelatin/ethylcellulose nanofibrous film for sustained release of curcumin. *Food Chemistry* **2020**, *308*, 125599, doi:https://doi.org/10.1016/j.foodchem.2019.125599.

54. Figueroa-Lopez, K.J.; Andrade-Mahecha, M.M.; Torres-Vargas, O.L. Spice oleoresins containing antimicrobial agents improve the potential use of bio-composite films based on gelatin. *Food Packaging and Shelf Life* **2018**, *17*, 50-56, doi:https://doi.org/10.1016/j.fpsl.2018.05.005.

55. Lee, J.S.; Park, M.A.; Yoon, C.S.; Na, J.H.; Han, J. Characterization and Preservation Performance of Multilayer Film with Insect Repellent and Antimicrobial Activities for Sliced Wheat Bread Packaging. *Journal of food science* **2019**, *84*, 3194-3203, doi:10.1111/1750-3841.14823.

56. Gherardi, R.; Becerril, R.; Nerin, C.; Bosetti, O. Development of a multilayer antimicrobial packaging material for tomato puree using an innovative technology. *LWT - Food Science and Technology* **2016**, *72*, 361-367, doi:https://doi.org/10.1016/j.lwt.2016.04.063.

57. Cerisuelo, J.P.; Gavara, R.; Hernández-Muñoz, P. Natural Antimicrobial – Containing EVOH Coatings on PP and PET Films: Functional and Active Property Characterization. *Packaging Technology and Science* **2014**, *27*, 901-920, doi:10.1002/pts.2078.

58. Moghadam, M.; Salami, M.; Mohammadian, M.; Khodadadi, M.; Emam-Djomeh, Z. Development of antioxidant edible films based on mung bean protein enriched with pomegranate peel. *Food Hydrocolloids* **2020**, *104*, 105735, doi:https://doi.org/10.1016/j.foodhyd.2020.105735.

59. Pavoni, L.; Perinelli, D.R.; Bonacucina, G.; Cespi, M.; Palmieri, G.F. An Overview of Micro- and Nanoemulsions as Vehicles for Essential Oils: Formulation, Preparation and Stability. *Nanomaterials (Basel, Switzerland)* **2020**, *10*, 135, doi:10.3390/nano10010135.

60. Franco, P.; Incarnato, L.; De Marco, I. Supercritical CO2 impregnation of α-tocopherol into PET/PP films for active packaging applications. *Journal of CO2 Utilization* **2019**, *34*, 266-273, doi:https://doi.org/10.1016/j.jcou.2019.06.012.

61. Lin, Q.-B.; Li, H.; Zhong, H.-N.; Zhao, Q.; Xiao, D.-H.; Wang, Z.-W. Migration of Ti from nano-TiO2-polyethylene composite packaging into food simulants. *Food Additives & Contaminants: Part A* **2014**, *31*, 1284-1290, doi:10.1080/19440049.2014.907505.

62. EFSA Panel on Food Contact Materials, E., Flavourings; Aids, P. Scientific Opinion on the safety evaluation of the substance zinc oxide, nanoparticles, uncoated and coated with [3-(methacryloxy)propyl] trimethoxysilane, for use in food contact materials. *EFSA Journal* **2015**, *13*, 4063, doi:10.2903/j.efsa.2015.4063.

63. Ozaki, A.; Kishi, E.; Ooshima, T.; Hase, A.; Kawamura, Y. Contents of Ag and other metals in food-contact plastics with nanosilver or Ag ion and their migration into food simulants. *Food Additives & Contaminants: Part A* **2016**, *33*, 1490-1498, doi:10.1080/19440049.2016.1217067.

64. Heydari-Majd, M.; Ghanbarzadeh, B.; Shahidi-Noghabi, M.; Najafi, M.A.; Adun, P.; Ostadrahimid, A. Kinetic release study of zinc from polylactic acid based nanocomposite into food simulants. *Polymer Testing* **2019**, *76*, 254-260, doi:https://doi.org/10.1016/j.polymertesting.2019.03.040.

65. (EU), E.C. Amending and correcting Regulation on plastic materials and articles intended to come into contact with food. *Official Journal of the European Union* **2016**, *1416*, 230.

66. (EU), E.C. Commission recommendation on the definition of nanomaterial. Annex II: Restrictions on materials and articles. *Official Journal European Union* **2011**, *696*, 38–40.

67. Mahamuni-Badiger, P.P.; Patil, P.M.; Patel, P.R.; Dhanavade, M.J.; Badiger, M.V.; Marathe, Y.N.; Bohara, R.A. Electrospun poly(3-hydroxybutyrate-co-3-hydroxyvalerate)/polyethylene oxide (PEO) microfibers reinforced with ZnO nanocrystals for antibacterial and antibiofilm wound dressing applications. *New Journal of Chemistry* **2020**, *44*, 9754-9766, doi:10.1039/D0NJ01384F.

68. Kang, T.; Guan, R.; Chen, X.; Song, Y.; Jiang, H.; Zhao, J. In vitro toxicity of different-sized ZnO nanoparticles in Caco-2 cells. *Nanoscale research letters* **2013**, *8*, 496, doi:10.1186/1556-276x-8-496.

69. Apte, G.; Repanas, A.; Willems, C.; Mujtaba, A.; Schmelzer, C.E.H.; Raichur, A.; Syrowatka, F.; Groth, T. Effect of Different Crosslinking Strategies on Physical Properties and Biocompatibility of Freestanding Multilayer Films Made of Alginate and Chitosan. *Macromolecular Bioscience* **2019**, *19*, 1900181, doi:10.1002/mabi.201900181.

70. Frígols, B.; Martí, M.; Salesa, B.; Hernández-Oliver, C.; Aarstad, O.; Teialeret Ulset, A.S.; Inger Sætrom, G.; Aachmann, F.L.; Serrano-Aroca, Á. Graphene oxide in zinc alginate films: Antibacterial activity, cytotoxicity, zinc release, water sorption/diffusion, wettability and opacity. *PloS one* **2019**, *14*, e0212819, doi:10.1371/journal.pone.0212819.

71. Ma, H.; Darmawan, E.T.; Zhang, M.; Zhang, L.; Bryers, J.D. Development of a poly(ether urethane) system for the controlled release of two novel anti-biofilm agents based on gallium or zinc and its efficacy to prevent bacterial biofilm formation. *Journal of controlled release : official journal of the Controlled Release Society* **2013**, *172*, 1035-1044, doi:10.1016/j.jconrel.2013.10.005.
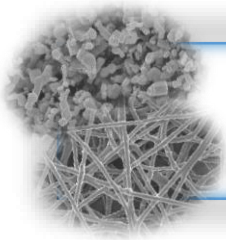
IV. GENERAL DISCUSSION

General Discussion

Due to increasing consumer concern about foodborne diseases, food waste, and climate change, the research and development of new materials obtained from renewable resources with similar properties to petrochemical materials has drastically increased in recent years. Likewise, the study of natural substances with active properties, such as antimicrobial and antioxidant activities, has also motivated the development of active biodegradable food packaging materials to extend the shelf life and maintain the quality of foodstuff. Packaging is one of the most important and well-known methods to achieve food preservation, storage, and transportation. Therefore, new materials, methodologies, and processing methods have been found to develop functional and active food packaging. In this context, this PhD thesis deals with the development of active multilayer systems based on polyhydroxyalkanoates (PHAs) containing essential oils and metallic nanoparticles processed by the electrospinning technique for food packaging applications.

Polyhydroxyalkanoates (PHAs) are promising renewable and biodegradable polymers obtained from bacteria fed with organic sources such as glucose or fatty acids [1]. They have interesting properties, similar to fossil derived polyolefins, such as polyethylene (PE) and polypropylene (PP), which meet the current requirements for food packaging materials [2]. In this way, these biopolymers have many advantages for developing different types of materials, depending on the final application. They can be processed by different techniques such as extrusion, injection molding, thermoforming, film blowing, and electrospinning [3]. The versatility of these polymers allows the inclusion of different organic and inorganic substances to improve and confer active and functional properties, such as antimicrobial, antioxidant, mechanical, and barrier oxygen and water and aroma vapor properties. Active food packaging is an important tool for enhancing food shelf life and safety. In the last decade, consumers have increased their interest in products and methods that are eco-friendly and health promoting. In this context, the use of essential oils (EOs) has increased in the food industry as preservatives due to the interesting aroma, flavor, and antimicrobial and antioxidant properties [4]. These activities are conferred by secondary metabolites that have multiple constituents, oscillating from 20 to 200 active compounds, such as terpenes, phenylpropanoids, organic acids, aldehydes, phenols, ketones, and sulfur-containing compounds [5]. EOs obtained from oregano and their main active compounds (thymol and carvacrol) are the most studied for their high antioxidant and antimicrobial activities against a wide variety of gram positive (G+) and gram negative (G-) bacteria [6]. As it is well known, EOs have high volatility and they can decompose or oxidize during

formulation, processing, and storage due to exposure to heat, pressure, light, or oxygen that results in an activity loss [7]. These problems can be reduced using encapsulation processes in different systems (e.g., films, capsules, or inclusion complexes such as cyclodextrins). The encapsulation method allows the protection of volatile compounds, while enhancing stability and maintaining bioactivity [8]. Other substances with high antimicrobial activity are metallic nanoparticles. They have been widely used in the pharmaceutical and cosmetic industry, whereas they have recently been applied in the food packaging industry to develop antimicrobial materials due to their ease of processing and high thermal stability [9,10]. The inclusion of EOs and metallic nanoparticles (MNPs) within PHAs by electrospinning technique has been originally studied. This technique operates at room temperature, allowing the processing of substances sensitive to high temperatures (e.g., EOs) and avoids activity loss [11]. Therefore, the development of active monolayer materials by electrospinning and their characterization in terms of morphological, thermal, mechanical, and active properties allows the design of active multilayer systems with mechanical, barrier, and active properties and improves the shelf life of foodstuff, while maintaining their microbiological and physicochemical quality throughout the supply chain.

In the first chapter, we studied the antimicrobial and antioxidant activities of oregano essential oil (OEO), extracts of green tea (GTE), and rosemary (RE). The preliminary selection of these active substances was based on their commercial availability and economies of scale. Among the three natural substances, OEO was the active substance that presented the highest antioxidant and antimicrobial activities against *S. aureus* and *E. coli*. Furthermore, all the active substances presented a good compatibility and processability with the technique and it was possible to achieve the homogenous fiber formation with uniform diameters. The attained fiber morphology allowed optimal film formation by the application of a thermal post-treatment, obtaining active continuous films. The active PHBV films containing OEO, RE, and GTE showed thermal stability of up to 200 °C. The films containing OEO presented the highest reduction values against the two foodborne bacterial strains and the highest antioxidant activity.

Since OEO was the substance with the highest antimicrobial and antioxidant activities, the second chapter focused on the development of compression-molded green composite sheets made of PHBV reinforced with coconut fibers (CFs) impregnated with OEO. The incorporation of CFs into PHBV generated green composite sheets with similar thermal stability, good fiber distribution, and average fiber length. The green composites presented a slightly higher rigidity but lower ductility. The CFs improved the water, limonene, and oxygen barrier properties.

Moreover, the resultant green composites showed a bacteriostatic effect against *S. aureus* for up to 15 days.

With the objective to further develop active films for food packaging, and after having studied the antimicrobial and antioxidant properties of OEO, the third chapter of this thesis was devoted to the study of MNPs as an antimicrobial agent. Therefore, hybrid fibers of PHBV containing varying amounts of OEO and zinc oxide nanoparticles (ZnONPs) were developed by electrospinning followed by annealing to produce active films with short- and long-term antimicrobial properties. The resultant active films presented improved the thermal properties, ductility, and toughness. The OEO-containing PHBV films showed a strong inhibition for the first 15 days of storage (short-term inhibition). Whereas the electrospun PHBV biopapers containing ZnONPs showed a high and slightly increased antimicrobial activity for 48 days (long-term inhibition). The electrospun hybrid PHBV biopapers, containing 2.5 wt% OEO + 2.25 wt% ZnONPs, yielded the highest antimicrobial properties in the short term and also high performance in the long term. The migration test showed that the values complied with regulations and European directives, demonstrating that these materials can be utilized in the food packaging industry [12].

The use of carriers such as cyclodextrins (CDs) to protect the volatile compounds from degradation or from losses by evaporation and for controlled release has been proposed to maintain the active properties of EOs. Also, it has been shown that the antimicrobial potential of EOs can be reduced in foods with lower water activity and it is influenced by the presence of macro- and micronutrients, pH, storage temperature, and the amount of oxygen within the packaging [13]. In this context, the fourth chapter dealt with the encapsulation of OEO in two cyclodextrins types (α-CD and γ-CD). These inclusion complexes were incorporated into PHBV fibers by electrospinning and, subsequently, annealed for film formation. The films containing the CD:OEO inclusion complexes showed higher mechanical and thermal properties. Moreover, the antimicrobial and antioxidant activities for the γ-CD:OEO and α-CD:OEO inclusion complexes were higher than the pure OEO, maintaining the activity for up to 15 days in both open and closed systems.

The fifth chapter presented the development of an active multilayer based on an electrospun interlayer of commercial PHBV containing eugenol with a cast-extruded PHB sheet and a food contact layer as the external layers. The newly prepared active multilayers showed high hydrophobicity, good interlayer adhesion, and mechanical and barrier (water vapor and limonene) properties. Also, the resultant active multilayers showed a significant growth reduction of *S. aureus* and *E. coli* in both open and closed systems for up to 15 days.

Finally, in the sisth and last chapter, an active and barrier multilayer film was developed. Once the PHBV monolayer films containing active substances (OEO and ZnONPs) were evaluated in terms of their antimicrobial, antioxidant, thermal, migratory, and morphological properties, they were incorporated as a monolayer. The multilayer structure consisted of the electrospun active layer (2.5 wt% OEO + 2.25 wt% ZnONPs) and a CNC coating, both as interlayers, and a blown film of a commercial PHA-based resin in the external layers. The active multilayer film presented a homogeneous, continuous surface, and good contact transparency. The use of the CNC interlayer provided the films with enhanced water vapor and limonene barrier properties. The multilayers also showed high antimicrobial activity, presenting a significant inhibition against *S. aureus* and *E. coli* after 15 days due to the presence of the electrospun active interlayer. The migration test performed on the active multilayer films revealed that the ZnONPs migration values were significantly lower compared to the monolayer films. Likewise, the active multilayer films also presented cellular compatibility (non-toxicity).

Based on the above, the present doctoral thesis demonstrates the advantages of using active substances (OEO, eugenol, ZnONPs) and the high versatility of the electrospinning technique to incorporate them and develop active monolayer and multilayer films based on PHA for active food packaging applications. The here-attained novel multilayers show good mechanical properties that provide resistance to puncture, tensile strength to prevent stretching or snapping impact and tear. Also, they can offer high barrier properties to water vapor, limonene, and oxygen to protect the food from external influences that could cause deterioration in food quality. Likewise, they can also achieve protection against the both visible and ultraviolet (UV) light to prevent light-induced changes in flavor or nutritional quality. Additionally, these multilayers present antimicrobial and antioxidant properties, which can respectively protect food against foodborne bacteria and oxidative reactions. All these characteristics can thus allow the novel design of novel active packaging systems with the capability to extend the shelf life of food products and also increase food safety.

References

1. Adeleye, A.T.; Odoh, C.K.; Enudi, O.C.; Banjoko, O.O.; Osiboye, O.O.; Toluwalope Odediran, E.; Louis, H. Sustainable synthesis and applications of polyhydroxyalkanoates (PHAs) from biomass. *Process Biochemistry* **2020**, *96*, 174-193.
2. Zikmanis, P.; Kolesovs, S.; Semjonovs, P. Production of biodegradable microbial polymers from whey. *Bioresources and Bioprocessing* **2020**, *7*, 36.
3. Keshavarz, T.; Roy, I. Polyhydroxyalkanoates: bioplastics with a green agenda. *Current Opinion in Microbiology* **2010**, *13*, 321-326.
4. Tajkarimi, M.M.; Ibrahim, S.A.; Cliver, D.O. Antimicrobial herb and spice compounds in food. *Food Control* **2010**, *21*, 1199-1218.
5. Pereira, L.P.L.A.; Ribeiro, E.C.G.; Brito, M.C.A.; Silveira, D.P.B.; Araruna, F.O.S.; Araruna, F.B.; Leite, J.A.C.; Dias, A.A.S.; Firmo, W.d.C.A.; Borges, M.O.d.R., et al. Essential oils as molluscicidal agents against schistosomiasis transmitting snails - a review. *Acta Tropica* **2020**, *209*, 105489.
6. Bhavaniramya, S.; Vishnupriya, S.; Al-Aboody, M.S.; Vijayakumar, R.; Baskaran, D. Role of essential oils in food safety: Antimicrobial and antioxidant applications. *Grain & Oil Science and Technology* **2019**, *2*, 49-55.
7. Figueroa-Lopez, K.J.; Enescu, D.; Torres-Giner, S.; Cabedo, L.; Cerqueira, M.A.; Pastrana, L.; Fuciños, P.; Lagaron, J.M. Development of electrospun active films of poly(3-hydroxybutyrate-co-3-hydroxyvalerate) by the incorporation of cyclodextrin inclusion complexes containing oregano essential oil. *Food Hydrocolloids* **2020**, *108*, 106013.
8. Sagiri, S.S.; Anis, A.; Pal, K. Review on Encapsulation of Vegetable Oils: Strategies, Preparation Methods, and Applications. *Polymer-Plastics Technology and Engineering* **2016**, *55*, 291-311, doi:10.1080/03602559.2015.1050521.
9. SIMBINE, E.O.; RODRIGUES, L.d.C.; LAPA-GUIMARÃES, J.; KAMIMURA, E.S.; CORASSIN, C.H.; OLIVEIRA, C.A.F.d. Application of silver nanoparticles in food packages: a review. *Food Science and Technology* **2019**, *39*, 793-802.
10. Polat, S.; Ağçam, E.; Dündar, B.; Akyildiz, A. Nanoparticles in Food Packaging: Opportunities and Challenges. In *Health and Safety Aspects of Food Processing Technologies*, Malik, A., Erginkaya, Z., Erten, H., Eds. Springer International Publishing: Cham, 2019; 10.1007/978-3-030-24903-8_21pp. 577-611.
11. Figueroa-Lopez, K.J.; Vicente, A.A.; Reis, M.A.M.; Torres-Giner, S.; Lagaron, J.M. Antimicrobial and Antioxidant Performance of Various Essential Oils and Natural Extracts and Their Incorporation into Biowaste Derived Poly(3-hydroxybutyrate-co-3-hydroxyvalerate) Layers Made from Electrospun Ultrathin Fibers. *Nanomaterials* **2019**, *9*, 144.
12. Souza, V.G.L.; Fernando, A.L. Nanoparticles in food packaging: Biodegradability and potential migration to food—A review. *Food Packaging and Shelf Life* **2016**, *8*, 63-70.
13. Dini, I. Chapter 14 - Use of Essential Oils in Food Packaging. In *Essential Oils in Food Preservation, Flavor and Safety*, Preedy, V.R., Ed. Academic Press: San Diego, 2016; 139-147.

Holistic Impact of the PhD

The research activities carried out during this PhD thesis has put forward work to contribute, from a global perspective, to the reduction of food loss and waste, while increasing resource efficiency and environmental protection, which are related to the United Nations Sustainable Development Goals, i.e. goal 3 (Zero Hunger), goal 12 (Responsible Consumption and Production) and goal 13 (Climate Action) [1]. In this regard, the here-developed food sustainable and high-performance packaging materials are considered to play a crucial role in reducing food waste by both upcycling food waste and protecting foodstuffs better, reducing losses by prolonging shelf-life. The active monolayers and multilayers developed, both based on PHAs and obtained by electrospinning, have proven the potential of this innovative processing technology for food packaging. As demonstrated during the research, one of the main advantages of electrospinning is its high versatility to develop at room conditions internal or external layers with active properties, that is, antimicrobial and antioxidant capacities, which can be conferred by natural substances, such as essential oils, and nanoparticles. The novel multilayers prepared during this thesis have also shown improved performances in terms of mechanical, thermal, and barrier properties (water vapor, limonene, and oxygen). All of the developed active mono and multilayer packaging features are expected to help to extend shelf-life of foodstuffs, and hence improve food quality and safety. Furthermore, these novel packaging materials are totally aligned with the so-called Circular Bioeconomy strategy, that intends to valorize biowastes and bring the organic carbon back to the soil.

References

1.   Sustainable Development Goals. Food and Agriculture Organization of the United Nations (FAO). 2015. http://www.fao.org/sustainable-development-goals/es/ [Accessed April 26, 2021].
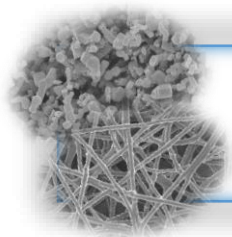
V. CONCLUSIONS

Conclusions

1. Oregano essential oil (OEO) presented the highest antimicrobial activity against *S. aureus* and *E. coli* and antioxidant properties among the tested essential oils (EOs) and natural extracts (NEs).

2. The incorporation of OEO into poly(3-hydroxybutyrate-*co*-3-hydroxyvalerate) (PHBV) was successfully achieved by electrospinning, obtaining homogenous and continues films with strong reduction (R ≥ 3) of the food-borne *S. aureus* ad *E. coli* bacteria in both open and closed system for up to 15 days.

3. Optimal incorporation of coconut fibers (CFs) into PHBV was achieved by melt compounding at 150 rpm and residence time of the order of 100 s, these processing conditions delivered the most balanced properties in terms of fiber distribution and average fiber length. OEO-containing green composite sheets with enhanced physical performance were produced, which also showed bacteriostatic effect against *S. aureus* for a period of at least 15 days.

4. The kneading method was the most efficient for the encapsulation of OEO in α- and γ-cyclodextrins (α- and γ-CD). The contents of α-CD:OEO and γ-CD:OEO inclusion complexes were optimal at 15 and 25 wt%, respectively. Higher active properties were attained for the electrospun PHBV films incorporating γ-CD:OEO due to their greater encapsulation efficiency, showing high antimicrobial and antioxidant activities for up to 15 days.

5. Hybrid fibers of PHBV containing 2.5 wt% OEO + 2.25 wt% ZnONPs (zinc oxide nanoparticles) were successfully developed by electrospinning. The dual incorporation of OEO and ZnONPs decreased the tensile modulus but increased the ductility and toughness of the PHBV films.

6. Monolayer films based on electrospun PHBV containing 2.5 wt% OEO + 2.25 wt% ZnONPs showed a high antimicrobial activity against *S. aureus* ad *E. coli* strains in both open and closed systems in the short term (15 days) and long term (48 days).

7. Active multilayer films based on an electrospun interlayer of commercial PHBV containing eugenol (15 wt.%) and cast-extruded PHB sheets and food contact layer as the external layers was developed. The multilayer presented high hydrophobicity, sufficient interlayer adhesion, good mechanical performance,

sufficient thermal stability, improved barrier properties against water and aroma vapors, and high antibacterial properties against *S. aureus* and *E. coli*.

8. Active multilayer films based on the electrospun active layer (2.5 wt% OEO + 2.25 wt% ZnONPs) and a CNC coating, as interlayers, and a biodegradable blown film in the external layers were developed. These multilayer showed good physical properties, such as contact transparency, water vapor and limonene barrier properties as well as significant antimicrobial activity (R≥1 and <3) against *S. aureus* and *E. coli* in both storage systems after 15 days and antioxidant activity.

9. Active multilayer films containing 2.5 wt% OEO + 2.25 wt% ZnONPs showed a cell viability nearly at 100%, demonstrating the cellular biocompatibility and non-toxicity of multilayer films in indirect contact with Caco-2 cells.

10. Monolayer films containing 2.5 wt.% OEO + 2.25. wt% ZnONPs in the ethanol aqueous food simulants were under the current specific migration limit (SML) values. In the case of multilayer films containing 2.5 wt.% OEO + 2.25. wt% ZnONPs, acceptable SML values were achieved for the acidic and alcoholic solutions. These results suggest that the monolayer and multilayer films can be used as food packaging for alcoholic and acidic solutions without impairing food safety.

VI. ANNEXES

nanomaterials

MDPI
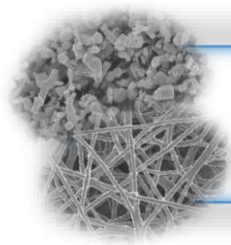
Article

Antimicrobial and Antioxidant Performance of Various Essential Oils and Natural Extracts and Their Incorporation into Biowaste Derived Poly(3-hydroxybutyrate-*co*-3-hydroxyvalerate) Layers Made from Electrospun Ultrathin Fibers

Kelly J. Figueroa-Lopez [1], António A. Vicente [2], Maria A. M. Reis [3], Sergio Torres-Giner [1] and Jose M. Lagaron [1,*]

[1] Novel Materials and Nanotechnology Group, Institute of Agrochemistry and Food Technology (IATA), Spanish National Research Council (CSIC), Calle Catedrático Agustín Escardino Benlloch 7, Paterna, 46980 Valencia, Spain; kjfigueroal@iata.csic.es (K.J.F.-L.); storresginer@iata.csic.es (S.T.-G.)
[2] Centre of Biological Engineering, University of Minho, Campus Gualtar, 4710-057 Braga, Portugal; avicente@deb.uminho.pt
[3] UCIBIO-REQUIMTE, Departamento de Química, Faculdade de Ciências e Tecnologia, Universidade Nova de Lisboa, Campus de Caparica, 2829-516 Caparica, Portugal; amr@fct.unl.pt
*   Correspondence: lagaron@iata.csic.es

check for updates

Abstract: In this research, the antibacterial and antioxidant properties of oregano essential oil (OEO), rosemary extract (RE), and green tea extract (GTE) were evaluated. These active substances were encapsulated into ultrathin fibers of poly(3-hydroxybutyrate-*co*-3-hydroxyvalerate) (PHBV) derived from fruit waste using solution electrospinning, and the resultant electrospun mats were annealed to produce continuous films. The incorporation of the active substances resulted in PHBV films with a relatively high contact transparency, but it also induced a slightly yellow appearance and increased the films opacity. Whereas OEO significantly reduced the onset of thermal degradation of PHBV, both the RE and GTE-containing PHBV films showed a thermal stability profile that was similar to the neat PHBV film. In any case, all the active PHBV films were stable up to approximately 200 °C. The incorporation of the active substances also resulted in a significant decrease in hydrophobicity. The antimicrobial and antioxidant activity of the films were finally evaluated in both open and closed systems for up to 15 days in order to anticipate the real packaging conditions. The results showed that the electrospun OEO-containing PHBV films presented the highest antimicrobial activity against two strains of food-borne bacteria, as well as the most significant antioxidant performance, ascribed to the films high content in carvacrol and thymol. Therefore, the PHBV films developed in this study presented high antimicrobial and antioxidant properties, and they can be applied as active layers to prolong the shelf life of the foods in biopackaging applications.

Keywords: PHBV; oregano; rosemary; green tea; electrospun nanofibers; antibacterial; antioxidant

1. Introduction

The packaging industry requires the development of new plastic materials with active properties, based on the demand by consumers for safer and more nutritive food [1]. Moreover, the growing concern over the environmental problems caused by petroleum-derived materials has led to the search for new renewable raw materials for the development of compostable packaging [2,3]. Polyhydroxyalkanoates (PHAs) are amongst the most promising biopolymers,

Melt processability, characterization, and antibacterial activity of compression-molded green composite sheets made of poly(3-hydroxybutyrate-*co*-3-hydroxyvalerate) reinforced with coconut fibers impregnated with oregano essential oil

S. Torres-Giner[a,*], L. Hilliou[b], B. Melendez-Rodriguez[a], K.J. Figueroa-Lopez[a], D. Madalena[c], L. Cabedo[d], J.A. Covas[b], A.A. Vicente[c], J.M. Lagaron[a]

[a] *Novel Materials and Nanotechnology Group, Institute of Agrochemistry and Food Technology (IATA), Spanish Council for Scientific Research (CSIC), Paterna, Spain*
[b] *Institute for Polymers and Composites/I3N, University of Minho, Guimarães, Portugal*
[c] *CEB - Centre of Biological Engineering, University of Minho, Braga, Portugal*
[d] *Polymers and Advanced Materials Group (PIMA), Universitat Jaume I (UJI), Castellón, Spain*

ABSTRACT

New packaging materials based on green composite sheets consisting of poly(3-hydroxybutyrate-*co*-3-hydroxyvalerate) (PHBV) and coconut fibers (CFs) were obtained by twin-screw extrusion (TSE) followed by compression molding. The effect of varying the CF weight content, *i.e.* 1, 3, 5, and 10 wt.-%, and the screw speed during melt processing, *i.e.* 75, 150, and 225 rpm, on both the aspect ratio and dispersion of the fibers was analyzed and related to the properties of the compression-molded sheets. Finally, the CFs were impregnated with oregano essential oil (OEO) by an innovative spray coating methodology and then incorporated into PHBV at the optimal processing conditions. The functionalized green composite sheets presented bacteriostatic effect against *Staphylococcus aureus* from fiber contents as low as 3 wt.-%. Therefore, the here-prepared CFs can be successfully applied as natural vehicles to entrap extracts and develop green composites of high interest in active food packaging to provide protection and shelf life extension.

1. Introduction

The use of agro-food residues for the preparation of polymer composites is gaining a significant attention due to their huge availability and low price, being at the same time a highly sustainable strategy for waste valorization. Natural fibers (NFs), particularly those obtained from plants, represent an environmentally friendly and unique choice to reinforce bioplastic matrices due to their relative high strength and stiffness (Yang, Kim, Park, Lee, & Hwang, 2006). The substitution of oil-derived polymers with bio-based polymers as the matrix component results in the term "green composites" (Zini & Scandola, 2011), which indicates that the composite as a whole, *i.e.* both matrix and reinforcement, originates from renewable resources. In this regard, the incorporation of NFs such as jute, sisal, flax, hemp, and bamboo fibers into biopolymers has been recently intensified (Bogoeva-Gaceva et al., 2007). Resultant green composites do not only offer environmental advantages over traditional polymer composites, such as reduced dependence on non-renewable energy/material sources, lower

greenhouse gas and pollutant emissions, improved energy recovery, and end-of-life biodegradability of components (Joshi, Drzal, Mohanty, & Arora, 2004), but also a potential reduction of both product density and energy requirements for processing (Faruk, Bledzki, Fink, & Sain, 2014).

Polyhydroxyalkanoates (PHAs) comprise a family of biodegradable aliphatic polyesters produced by microorganisms. PHAs show the highest potential to replace polyolefins in a wide range of applications, including packaging, due to their high mechanical strength and water resistance (Bugnicourt, Cinelli, Lazzeri, & Alvarez, 2014). Among PHAs, poly(3-hydroxybutyrate) (PHB) and its copolymer with 3-hydroxyvalerate (HV), *i.e.* poly(3-hydroxybutyrate-*co*-3-hydroxyvalerate) (PHBV), have so far received the greatest attention in terms of pathway characterization and industrial-scale production. The use of PHA copolymers presents certain advantages since they have a lower melting point and higher flexibility than their homopolymers, which improves melt stability and broadens their processing window (Torres-Giner, Montanes, Boronat, Quiles-Carrillo, & Balart, 2016). Furthermore, the

* Corresponding author.
E-mail address: storresginer@iata.csic.es (S. Torres-Giner).

Article

Electrospun Active Biopapers of Food Waste Derived Poly(3-hydroxybutyrate-*co*-3-hydroxyvalerate) with Short-Term and Long-Term Antimicrobial Performance

Kelly J. Figueroa-Lopez [1] , **Sergio Torres-Giner** [1,*] , **Daniela Enescu** [2] , **Luis Cabedo** [3] , **Miguel A. Cerqueira** [2] , **Lorenzo M. Pastrana** [2] and **Jose M. Lagaron** [1,*]

[1]   Novel Materials and Nanotechnology Group, Institute of Agrochemistry and Food Technology (IATA), Spanish National Research Council (CSIC), Calle Catedrático Agustín Escardino Benlloch 7, 46980 Paterna, Spain; kjfigueroal@iata.csic.es
[2]   International Iberian Nanotechnology Laboratory (INL), Avenida Mestre José Veiga, 4715-330 Braga, Portugal; danielamenescu@gmail.com (D.E.); miguel.cerqueira@inl.int (M.A.C.); lorenzo.pastrana@inl.int (L.M.P.)
[3]   Polymers and Advanced Materials Group (PIMA), Universitat Jaume I (UJI), Avenida de Vicent Sos Baynat s/n, 12071 Castellón, Spain; lcabedo@uji.es
*   Correspondence: storresginer@iata.csic.es (S.T.-G.); lagaron@iata.csic.es (J.M.L.); Tel.: +34-963-900-022 (S.T.-G.); +34-963-900-022 (J.M.L.)

Abstract: This research reports about the development by electrospinning of fiber-based films made of poly(3-hydroxybutyrate-*co*-3-hydroxyvalerate) (PHBV) derived from fermented fruit waste, so-called bio-papers, with enhanced antimicrobial performance. To this end, different combinations of oregano essential oil (OEO) and zinc oxide nanoparticles (ZnONPs) were added to PHBV solutions and electrospun into mats that were, thereafter, converted into homogeneous and continuous films of ~130 μm. The morphology, optical, thermal, mechanical properties, crystallinity, and migration into food simulants of the resultant PHBV-based bio-papers were evaluated and their antimicrobial properties were assessed against *Staphylococcus aureus* (*S. aureus*) and *Escherichia coli* (*E. coli*) in both open and closed systems. It was observed that the antimicrobial activity decreased after 15 days due to the release of the volatile compounds, whereas the bio-papers filled with ZnONPs showed high antimicrobial activity for up to 48 days. The electrospun PHBV biopapers containing 2.5 wt% OEO + 2.25 wt% ZnONPs successfully provided the most optimal activity for short and long periods against both bacteria.

Keywords: PHBV; essential oils; inorganic nanoparticles; biopapers; electrospinning; migration; active packaging

---

1. Introduction

The packaging industry has increased the demand of active materials obtained from renewable resources due to the environmental concerns related to the extensive use of conventional plastics and also to the consumer requests for safer, more nutritious, and high-quality food [1]. Polyhydroxyalkanoates (PHAs) are bio-based and biodegradable aliphatic polyesters of high potential to replace polyolefins in packaging applications [2]. PHAs are synthesized in the mitochondria of a wide range of Gram-negative (G−) and Gram-positive (G+) microorganisms [3]. They can be divided into short chain length (scl-PHAs) with monomers with three to five carbon atoms and medium chain length (mcl-PHAs) with monomers with more than six carbons [4]. Among them, scl-PHAs are the most

Development of electrospun active films of poly (3-hydroxybutyrate-*co*-3-hydroxyvalerate) by the incorporation of cyclodextrin inclusion complexes containing oregano essential oil

K.J. Figueroa-Lopez [a,*], D. Enescu [b,**], S. Torres-Giner [a], L. Cabedo [c], M.A. Cerqueira [b], L. Pastrana [b], P. Fuciños [b], J.M. Lagaron [a,***]

[a] *Novel Materials and Nanotechnology Group, Institute of Agrochemistry and Food Technology (IATA), Spanish National Research Council (CSIC), Calle Catedrático Agustín Escardino Benlloch 7, 46980, Paterna, Spain*
[b] *Department Life Sciences, Nano4Food/Food Processing Research Unit, International Iberian Nanotechnology Laboratory (INL), Av. Mestre José Veiga s/n, 4715-330 Braga, Portugal*
[c] *Polymers and Advanced Materials Group (PIMA), Universitat Jaume I (UJI), Avenida de Vicent Sos Baynat s/n, 12071, Castellón, Spain*

ABSTRACT

This paper reports the development of biodegradable active packaging films of poly(3-hydroxybutyrate-*co*-3-hydroxyvalerate) (PHBV) by the incorporation of alpha- and gamma-cyclodextrins (α-CD andγ-CDs) containing oregano essential oil (OEO). Herein, both the kneading method (KM) and freeze-drying method (FDM) were first explored for the preparation of α-CD:OEO andγ-CD:OEO inclusion complexes at host:guest ratios of 80:20 wt/wt and 85:15 wt/wt, respectively. The results showed that KM was the most efficient method for the encapsulation of OEO in the CDs cavity in terms of simplicity and rapidity, while it was also yielded the inclusion complexes with the highest antimicrobial and antioxidant performance. The α-CD:OEO andγ-CD:OEO inclusion complexes obtained by KM were thereafter incorporated at 10, 15, 20, 25, and 30 wt% into PHBV fibres by electrospinning and annealed at 160 °C to produce contact transparent films. It was observed that the optimal concentration of α-CD:OEO andγ-CD:OEO inclusion complexes for homogeneous and continuous film formation was attained at contents of 15 and 25 wt%, respectively. Higher antimicrobial and antioxidant activities were obtained for the γ-CD:OEO inclusion complexes due to the greater encapsulation efficiency of OEO in γ-CD, resulting in PHBV films with good performance for up to 15 days. This aspect, together with their improved thermal stability and mechanical strength, give interesting applications to these biopolymer films in the design of active-releasing packaging materials to maintain the physical, chemical, and microbiological characteristics of food products.

1. Introduction

Essential oils (EOs) are mixtures of volatile organic compounds obtained from aromatic plants that are well known for their fragrant properties. They are also used in food preservation and as antimicrobial, analgesic, sedative, anti-inflammatory, spasmolytic, and locally anaesthetic remedies (Bakkali, Averbeck, Averbeck, & Idaomar, 2008; Ribeiro-Santos, Andrade, Melo, & Sanches-Silva, 2017). Their mechanisms of active action, particularly at the antimicrobial level, have been well reported (Owen & Laird, 2018; Sharifi-Rad et al., 2017). The global

market of EOs was 226.9 kton/year in 2018 (Research, 2018) while approximately 160 ones are considered as Generally Recognized as Safe (GRAS) by the U.S. Food and Drug Administration (FDA, 2016). Therefore, their application is currently growing in the food and beverage, personal care & cosmetics, aromatherapy, and pharmaceutical industries (Bakhtiary, Sayevand, Khaneghah, Haslberger, & Hosseini, 2018; Prakash, Kedia, Mishra, & Dubey, 2015; Prakash, Singh, Kedia, & Dubey, 2012; Raut & Karuppayil, 2014).

Among EOs, oregano essential oil (OEO) is one of the most interesting since it is FDA approved and it is also included by the Council of

---

* Corresponding author.
** Corresponding author.
*** Corresponding author.
E-mail addresses: kjfigueroal@iata.csic.es (K.J. Figueroa-Lopez), danielaenescuu@gmail.com (D. Enescu), lagaron@iata.csic.es (J.M. Lagaron).

Development of Electrospun Poly(3-hydroxybutyrate-*co*-3-hydroxyvalerate) Monolayers Containing Eugenol and Their Application in Multilayer Antimicrobial Food Packaging

Kelly J. Figueroa-Lopez[1], Luis Cabedo[2], Jose M. Lagaron[1]* and Sergio Torres-Giner[1]*

[1] Novel Materials and Nanotechnology Group, Institute of Agrochemistry and Food Technology (IATA), Spanish National Research Council (CSIC), Paterna, Spain, [2] Polymers and Advanced Materials Group (PIMA), Universitat Jaume I (UJI), Castellón de la Plana, Spain

In this research, different contents of eugenol in the 2.5–25 wt.% range were first incorporated into ultrathin fibers of poly(3-hydroxybutyrate-*co*-3-hydroxyvalerate) (PHBV) by electrospinning and then subjected to annealing to obtain antimicrobial monolayers. The most optimal concentration of eugenol in the PHBV monolayer was 15 wt.% since it showed high electrospinnability and thermal stability and also yielded the highest bacterial reduction against *Staphylococcus aureus* (*S. aureus*) and *Escherichia coli* (*E. coli*). This eugenol-containing monolayer was then selected to be applied as an interlayer between a structural layer made of a cast-extruded poly(3-hydroxybutyrate) (PHB) sheet and a commercial PHBV film as the food contact layer. The whole system was, thereafter, annealed at 160°C for 10 s to develop a novel multilayer active packaging material. The resultant multilayer showed high hydrophobicity, strong adhesion and mechanical resistance, and improved barrier properties against water vapor and limonene vapors. The antimicrobial activity of the multilayer structure was also evaluated in both open and closed systems for up to 15 days, showing significant reductions ($R \geq 1$ and < 3) for the two strains of food-borne bacteria. Higher inhibition values were particularly attained against *S. aureus* due to the higher activity of eugenol against the cell membrane of Gram positive (G+) bacteria. The multilayer also provided the highest antimicrobial activity for the closed system, which better resembles the actual packaging and it was related to the headspace accumulation of the volatile compounds. Hence, the here-developed multilayer fully based on polyhydroxyalkanoates (PHAs) shows a great deal of potential for antimicrobial packaging applications using biodegradable materials to increase both quality and safety of food products.

Keywords: PHA, essential oils, multilayer, antimicrobial activity, electrospinning

285

Article

Development of Active Barrier Multilayer Films Based on Electrospun Antimicrobial Hot-Tack Food Waste Derived Poly(3-hydroxybutyrate-*co*-3-hydroxyvalerate) and Cellulose Nanocrystal Interlayers

Kelly J. Figueroa-Lopez [1], Sergio Torres-Giner [1,†], Inmaculada Angulo [2], Maria Pardo-Figuerez [1,3], Jose Manuel Escuin [4], Ana Isabel Bourbon [5], Luis Cabedo [6], Yuval Nevo [7], Miguel A. Cerqueira [5] and Jose M. Lagaron [1,*]

[1] Novel Materials and Nanotechnology Group, Institute of Agrochemistry and Food Technology (IATA), CSIC, Calle Catedrático Agustín Escardino Benllonch 7, 46980 Valencia, Spain; kjfigueroal@iata.csic.es (K.J.F.-L.); storresginer@upv.es (S.T.-G.); mpardo@iata.csic.es (M.P.-F.)
[2] Gaiker Technological Centre, Department of Plastics and Composites, Parque Tecnológico Edificio 202, 48170 Zamudio, Spain; angulo@gaiker.es
[3] Bioinicia R&D, Bioinicia S.L., Calle Algepser 65, Nave 3, 46980 Paterna, Valencia, Spain
[4] Tecnopackaging S.L., Poligono Industrial Empresarium, Calle Romero 12, 50720 Zaragoza, Spain; josemanuel.escuin@aitiip.co
[5] Food Processing and Nutrition Group, International Iberian Nanotechnology Laboratory (INL), Av. Mestre José Veiga s/n, 4715-330 Braga, Portugal; ana.bourbon@inl.int (A.I.B.); miguel.cerqueira@inl.int (M.A.C.)
[6] Polymers and Advanced Materials Group (PIMA), School of Technology and Experimental Sciences, Universitat Jaume I (UJI), Avenida de Vicent Sos Baynat s/n, 12071 Castellón, Spain; lcabedo@uji.es
[7] Melodea Bio-Based Solutions, Faculty of Agriculture-Hebrew University, Rehovot 76100, Israel; yuval@melodea.eu
* Correspondence: lagaron@iata.csic.es; Tel.: +34-963-900-022
† Current Address: Research Institute of Food Engineering for Development (IIAD), Universitat Politècnica de València (UPV), Camino de Vera s/n, 46022 Valencia, Spain.

Abstract: Active multilayer films based on polyhydroxyalkanoates (PHAs) with and without high barrier coatings of cellulose nanocrystals (CNCs) were herein successfully developed. To this end, an electrospun antimicrobial hot-tack layer made of poly(3-hydroxybutyrate-*co*-3-hydroxyvalerate) (PHBV) derived from cheese whey, a by-product from the dairy industry, was deposited on a previously manufactured blown film of commercial food contact PHA-based resin. A hybrid combination of oregano essential oil (OEO) and zinc oxide nanoparticles (ZnONPs) were incorporated during the electrospinning process into the PHBV nanofibers at 2.5 and 2.25 wt%, respectively, in order to provide antimicrobial properties. A barrier CNC coating was also applied by casting from an aqueous solution of nanocellulose at 2 wt% using a rod at 1m/min. The whole multilayer structure was thereafter assembled in a pilot roll-to-roll laminating system, where the blown PHA-based film was located as the outer layers while the electrospun antimicrobial hot-tack PHBV layer and the barrier CNC coating were placed as interlayers. The resultant multilayer films, having a final thickness in the 130–150 μm range, were characterized to ascertain their potential in biodegradable food packaging. The multilayers showed contact transparency, interlayer adhesion, improved barrier to water and limonene vapors, and intermediate mechanical performance. Moreover, the films presented high antimicrobial and antioxidant activities in both open and closed systems for up to 15 days. Finally, the food safety of the multilayers was assessed by migration and cytotoxicity tests, demonstrating that the films are safe to use in both alcoholic and acid food simulants and they are also not cytotoxic for Caco-2 cells.

nanomaterials

MDPI

Article

Antibacterial and Barrier Properties of Gelatin Coated by Electrospun Polycaprolactone Ultrathin Fibers Containing Black Pepper Oleoresin of Interest in Active Food Biopackaging Applications

Kelly Johana Figueroa-Lopez [1,2], Jinneth Lorena Castro-Mayorga [3], Margarita María Andrade-Mahecha [4], Luis Cabedo [5] and Jose Maria Lagaron [2,*]

[1] Optoelectronics Group, Interdisciplinary Science Institute, Faculty of Basic Science and Technologies, Universidad del Quindío, Carrera 15 Calle 12 Norte, 630004 Armenia, Colombia; kjfigueroal@iata.csic.es

[2] Novel Materials and Nanotechnology Group, Instituto de Agroquímica y Tecnología de Alimentos (IATA), Calle Catedrático Agustín Escardino Benlloch 7, 46980 Valencia, Spain

[3] Nanobiotechnology and Applied Microbiology (NANOBIOT), Universidad de los Andes, 11711 Bogotá, Colombia; jincasma@iata.csic.es

[4] Group of Research on Agroindustrial Processes (GIPA), Universidad Nacional de Colombia, 763533 Palmira, Colombia; mmandradem@unal.edu.co

[5] Polymers and Advanced Materials Group (PIMA), Universitat Jaume I (UJI), Avenida de Vicent Sos Baynat s/n, 12071 Castellón, Spain; lcabedo@uji.es

* Correspondence: lagaron@iata.csic.es

check for updates

Abstract: The present study evaluated the effect of using electrospun polycaprolactone (PCL) as a barrier coating and black pepper oleoresin (OR) as a natural extract on the morphology, thermal, mechanical, antimicrobial, oxygen, and water vapor barrier properties of solvent cast gelatin (GEL). The antimicrobial activity of the developed multilayer system obtained by the so-called electrospinning coating technique was also evaluated against *Staphylococcus aureus* strains for 10 days. The results showed that the multilayer system containing PCL and OR increased the thermal resistance, elongated the GEL film, and significantly diminished its permeance to water vapor. Active multilayer systems stored in hermetically closed bottles increased their antimicrobial activity after 10 days by inhibiting the growth of *Staphylococcus aureus*. This study demonstrates that addition of electrospun PCL ultrathin fibers and OR improved the properties of GEL films, which promoted its potential use in active food packaging applications.

Keywords: nanofibers; electrospinning coating technique; gelatin; polycaprolactone; antimicrobials

1. Introduction

The environmental issues generated by the slow degradation rate of the plastics once discarded after use have fostered the study and development of biodegradable polymers to obtain continuous matrices for the production of biodegradable packaging [1]. Among the bio-based biodegradable polymers, gelatin is one of the proteins with the greatest industrial applications due to its gelling properties, ability to form and stabilize emulsions, its adhesive properties, and dissolution behavior [2]. This biopolymer has a unique sequence of amino acids with a high content of proline, glycine, and hydroxyproline, which help in the formation of flexible films [3] and presents a good barrier against oxygen and carbon dioxide. For these reasons, gelatin is a very promising candidate for new bio-based and biodegradable packaging formulations. However, gelatin is very sensitive to moisture and,

Article

Electrospun Antimicrobial Films of Poly(3-hydroxybutyrate-*co*-3-hydroxyvalerate) Containing Eugenol Essential Oil Encapsulated in Mesoporous Silica Nanoparticles

Beatriz Melendez-Rodriguez [1], Kelly J. Figueroa-Lopez [1], Andrea Bernardos [2,3,4,5], Ramón Martínez-Máñez [2,3,4,5], Luis Cabedo [6], Sergio Torres-Giner [1] and Jose M. Lagaron [1,*]

[1] Novel Materials and Nanotechnology Group, Institute of Agrochemistry and Food Technology (IATA), Spanish Council for Scientific Research (CSIC), Calle Catedrático Agustín Escardino Benlloch 7, 46980 Paterna, Spain; beatriz.melendez@iata.csic.es (B.M.-R.); kjfigueroal@iata.csic.es (K.J.F.-L.); storresginer@iata.csic.es (S.T.-G.)

[2] Instituto Interuniversitario de Investigación de Reconocimiento Molecular y Desarrollo Tecnológico (IDM), Universitat Politècnica de València (UPV), Universitat de València (UV), camí de Vera s/n, 46022 Valencia, Spain; anberba@upv.es (A.B.); rmaez@qim.upv.es (R.M.-M.)

[3] CIBER de Bioingeniería, Biomateriales y Nanomedicina (CIBER-BBN), Camino de Vera s/n, 46022 Valencia, Spain

[4] Unidad Mixta de Investigación en Nanomedicina y Sensores, Universitat Politècnica de València (UPV), Instituto de Investigación Sanitaria La Fe, 46026 Valencia, Spain

[5] Unidad Mixta UPV-CIPF de Investigación en Mecanismos de Enfermedades y Nanomedicina, Universitat Politècnica de València (UPV), Centro de Investigación Príncipe Felipe, 46012 Valencia, Spain

[6] Polymers and Advanced Materials Group (PIMA), Universitat Jaume I, 12071 Castellón, Spain; lcabedo@uji.es

* Correspondence: lagaron@iata.csic.es

Abstract: The main goal of this study was to develop poly(3-hydroxybutyrate-*co*-3-hydroxyvalerate) (PHBV) films with long-term antimicrobial capacity of interest in food packaging applications. To this end, eugenol was first highly efficiently encapsulated at 50 wt.-% in the pores of mesoporous silica nanoparticles by vapor adsorption. The eugenol-containing nanoparticles were then loaded in the 2.5–20 wt.-% range into PHBV by electrospinning and the resultant electrospun composite fibers were annealed at 155 °C to produce continuous films. The characterization showed that the PHBV films filled with mesoporous silica nanoparticles containing eugenol present sufficient thermal resistance and enhanced mechanical strength and barrier performance to water vapor and limonene. The antimicrobial activity of the films was also evaluated against foodborne bacteria for 15 days in open vs. closed conditions in order to simulate real packaging conditions. The electrospun PHBV films with loadings above 10 wt.-% of mesoporous silica nanoparticles containing eugenol successfully inhibited the bacterial growth, whereas the active films stored in hermetically closed systems increased their antimicrobial activity after 15 days due to the volatile portion accumulated in the system's headspace and the sustained release capacity of the films. The resultant biopolymer films are, therefore, potential candidates to be applied in active food packaging applications to provide shelf life extension and food safety.

Keywords: PHBV; MCM-41; eugenol; antimicrobial properties; active packaging

The impact of electrospun films of poly(ε-caprolactone) filled with nanostructured zeolite and silica microparticles on *in vitro* histamine formation by *Staphylococcus aureus* and *Salmonella* Paratyphi A

Esen Alp-Erbay[a], Kelly J. Figueroa-Lopez[b], José M. Lagaron[b], Emre Çağlak[c], Sergio Torres-Giner[b,*]

[a] Central Fisheries Research Institute (SUMAE), Food Technology Department, Vali Adil Yazar Ave. 14, Kaşüstü, Yomra, 61250, Trabzon, Turkey
[b] Novel Materials and Nanotechnology Group, Institute of Agrochemistry and Food Technology (IATA), Spanish National Research Council (CSIC), Calle Catedrático Agustín Escardino Benlloch 7, 46980, Paterna, Spain
[c] Recep Tayyip Erdoğan University, Faculty of Fisheries, Department of Processing Technology, Su Ürünleri Fakültesi Zihni Derin Yerleşkesi, 53100, Rize, Turkey

ARTICLE INFO

ABSTRACT

This research study originally reports the preparation and characterization of electrospun films based on poly(ε-caprolactone) (PCL) with high histamine-binding capacity. To this end, submicron PCL fibers filled with nanostructured zeolite or silica (SiO$_2$) microparticles in the 5–20 wt% range were first prepared by solution electrospinning. The resultant electrospun composite fiber mats were thereafter thermally post-treated at 55 °C to successfully develop contact-transparent films with reduced porosity and improved mechanical strength. The capacity of the developed composite films to entrap histamine was evaluated *in vitro* by the culture media method using *Staphylococcus aureus* (*S. aureus*) and *Salmonella* Paratyphi A (*S. Paratyphi A*) foodborne bacteria. Both electrospun zeolite- and SiO$_2$-containing PCL films exhibited high histamine-binding capacity, being more effective for *S. aureus*. The histamine entrapment performance was significantly higher for the PCL films filled with zeolite due to the enhanced porous structure and more optimal adsorption selectivity of this inorganic filler. The here-developed electrospun composite films can be applied as novel active-scavenging packaging materials to entrap heat-stable histamine and other biogenic amines released from fish and fishery products.

1. Introduction

Amines are basic nitrogenous compounds in which one, two or three atoms of hydrogen in ammonia are replaced by alkyl or aryl groups. Amines are designated "biogenic" when they are produced by the action of living organisms through the decarboxylation process of amino acids (Shalaby, 1996). One of the most important biogenic amines occurring in fish and fishery products is histamine. High levels of histamine are usually formed during decomposition or spoilage process of fish, involving formation of free amino acids through proteolysis together with bacterial production and action of amino acid decarboxylases (Visciano, Schirone, Tofalo, & Suzzi, 2012). Fish of the families *Scombridae* and *Scomberesocideae*, which include mackerel, tunas, saury, bonito, seerfish, and butterfly kingfish, are commonly involved in incidents of histamine poisoning (Taylor & Eitenmiller, 1986). Non-scombroid fish such as sardine, pilchards, anchovies, herring and marlin, has also been reported to be implicated (Taylor, Smith, & Calaby, 1985). These species of fish have the naturally occurring amino acid histidine in their flesh and some spoilage bacteria rich in the enzyme histidine decarboxylase can proliferate and produce histamine (Hungerford, 2010; Kimura, Konagaya, & Fujii, 2001; Kung et al., 2009; Laganà et al., 2015; López-Sabater, Rodríguez-Jerez, Roig-Sagués, & Teresa Mora-Ventura, 1994). Gram-positive (G+) histamine-producing bacteria typically belong to the *Staphylococcus* strain (Chang, Kung, Chen, Lin, & Tsai, 2008; Kuley & Özogul, 2011; Simon & Sanjeev, 2007; Zarei, Maktabi, & Ghorbanpour, 2012), which can be isolated from fresh fish and shrimp (Lakshmanan, Shakila, & Jeyasekaran, 2002), fermented foods such as wine, cheese and fish sauce (Satomi, 2016), salted fish (Hernández-Herrero, Roig-Sagués, Rodríguez-Jerez, & Mora-Ventura, 1999), and other fishery products (Gokdogan et al., 2012; Özogul, Kacar, & Hamed, 2015). *Salmonella* Gram-negative (G-) bacteria of *Enterobacteriaceae* family have also been reported to be a histamine producer strain (Geornaras, Dykes, & Holy, 1995; Gokdogan et al., 2012; Kuley et al., 2017; Özogul et al., 2015).

---

* Corresponding author.
E-mail address: storresginer@iata.csic.es (S. Torres-Giner).

1

Emerging Trends in Biopolymers for Food Packaging

Sergio Torres-Giner, Kelly J. Figueroa-Lopez, Beatriz Melendez-Rodriguez, Cristina Prieto, Maria Pardo-Figuerez, and Jose M. Lagaron

Novel Materials and Nanotechnology Group, Food Safety and Preservation Department, Institute of Agrochemistry and Food Technology (IATA), Spanish Council for Scientific Research (CSIC), Calle Catedrático Agustin Escardino Benlloch 7, Paterna 46980, Spain

1.1 Introduction to Polymers in Packaging

According to the Food and Agriculture Organization of the United Nations (FAO), approximately one-third of all food produced globally is lost or wasted [1]. Food waste is produced throughout the whole food value chain, from the household to manufacturing, distribution, retail, and food service activities. Taking into consideration the limited natural resources available, it is more effective to reduce food waste than to increase food production. For this reason, several efforts have been put for the development of more effective food packaging strategies [2, 3]. Packaging items have become essential to protect food from different environmental conditions. Depending on the type of food, the packaging article can be customized to prevent or inhibit microbial growth, avoid food decomposition by removing the entrance of light, oxygen, and moisture, or even to prevent spoilage from small insects. Additionally, novel packaging items can be monitored to give information about the quality of the packaged food, ultimately diminishing food waste during distribution and transport [4].

Common materials utilized for food packaging include glass, paper, metal, and plastic. The latter are nowadays more frequently used since they have a large availability at a relatively low cost and can display good characteristics for packaging items, such as mechanical strength, barrier properties, and transparency [4, 5]. The most commonly used petrochemical materials for packaging applications can be divided into various families:

- Polyolefins and substitutes of olefins, such as low-density polyethylene (LDPE) and linear low-density polyethylene (LLDPE), polypropylene (PP), polystyrene (PS), oriented polystyrene (OPS), polyvinyl alcohol (PVOH), polyvinyl chloride (PVC), and polyvinylidene chloride (PVDC). Polyolefins are frequently used in reusable bags, paper cups, and stand-up pouches, while substitutes of olefins such as PVC are popularly used in cling films and in some prepackaged meals.